Cyclometallated platinum and palladium complexes with N^C^N-coordinating terdentate ligands: synthesis, luminescence and catalytic properties.

Rochester, David Lee

Cyclometallated platinum and palladium complexes with N^C^N-coordinating terdentate ligands: synthesis, luminescence and catalytic properties

by David Lee Rochester

Ph.D. Chemistry

Supervised by Dr. J. A. G. Williams

Durham University, Department of Chemistry

2007

Abstract

A series of cyclometallated platinum and palladium(II) complexes based on the N^C^N coordinating terdentate ligand 1,3-di(2-pyridyl)benzene, HL1, have shown that cyclometalation at C2 of the central ring affords many advantages to square-planar d8-metal complexes. The cyclometalating bond is notably shorter than that observed in many related cyclometallated complexes, e.g. 6-phenyl-2,2'-bipyridine platinum/palladium(II) chloride and 2-phenylpyridine derivatives. The luminescent properties of the complexes reported herein have been investigated. All complexes are intensely luminescent, in their own right, with quantum yields of luminescence significantly higher than those reported for related complexes. In the solid-state and at high concentrations, intermolecular interactions create new emissive species, such as self-quenching accompanied by excimeric emission observed in solution, $\lambda_{em} \approx 700$ nm, and multi-centred excited-states in solid samples, $\lambda_{em} = 610–700$ nm. Modification of both N^C^N and ancillary ligands is shown to manipulate the electronic properties of the d^8-metal complexes. Excited-state emission energies have been tuned from 469 nm (blue), $L^{26}PtCl$, to 588 nm (red), $L^{16}PtCl$, in the platinum(II) complexes, and from 466 nm (blue), $L^{1}PdCl$, to 530 nm (orange), $L^{16}PdCl$, in the palladium complexes. Incorporation of steric incumberance into the ligands can attenuate the excimer emission compared to $L^{1}PtCl$. Electron-rich pendant ligands encourage the accessibility of charge-transfer excited-states, which adds to the diversity of the photophysical properties, but when coupled with functional groups can give rise to potential in sensory applications. The high quantum yields and special oxygen sensitivity of the platinum complexes have allowed their incorporation into optoelectronic devices.

The palladium complexes are of particular interest owing to the limited attention previously paid to palladium complexes as emissive species, particularly, excimeric behaviour is even rarer. Additionally, the electronic tuning which is manifested in the luminescent properties of these complexes has allowed studies into catalytic behaviour of these complexes, revealing some surprising results relating activity to structure.

Declaration

The work herein was carried out in the Department of Chemistry, University of Durham between October 2003 and September 2006. All the work is my own unless otherwise stated and no part of it has been submitted for a degree at this or any other university.

Statement of Copyright

Acknowledgements

My most sincre thanks to the following:

First and foremost I would like to thank Dr. J. A. Gareth Williams for encouragement, support and unwavering patience....I told you it would be finished by January.

The EPSRC for funding.

Dr. Amber Thompson for many crystal structure determinations and pretty pictures, that's what it's really all about; Dr. Alan Kenwright, Catherine Heffernan and Ian McKeag for NMR spectroscopy, it's easy to forget how vital it is when it's always available; Dr. Mike Jones and Lara Turner for mass spectrometry it's easy to forget how vital it is when it's always available; Jarka Dorstal and Judith Magee for CH&N analysis which always fit with the right solvent additions.

Dr. P. Steel and Dr. A. Beeby for the use of some of your stuff, I'm sure Gareth will reimburse you for the cost of everything I took.

All of the members of CG001 past, present and future; Kathryn Arm/Knuckey for help and support and teaching me not to always be an idiot; Andy Wilkinson for help and trustworthy chemistry advice; Victoria for teaching me that it is best to be organised (I have finally learned); Will for teaching me circus tricks; Marie for a fantastic effort in helping me finish and lending me 20 pence when the coke machine ripped me off; Aileen for all the gossip, even about people I didn't know; Tom hehhh!; Pete; Chris; Amel; Nick; Dunwell; Lisa; Jonathon; Stephanie; Jean-Luc; Marc; Olivier; the 4^{th} years and many more.

All the staff at the chemistry department, it was a very enjoyable place to work. Paricularly, to Miriam, your weekly visits and kind heart will make fond memories.

My family for all their support and letting me hang around and make a mess far longer than I needed to.

Shelley, final love and thanks go to you for all the support and patience you've given me through the more difficult times.

Abbreviations

Acac	acetylacetone
AlQ_3	tris(8-hydroxyquinolate)aluminium
B_2neo_2	bis(neopentylglycolato)diboron
B_2pin_2	bis(pinacolato)diboron
Bn	benzene
Bpy	2,2'-bipyridine
CCD	charge-coupled device
C^N^C	a terdentate ligand coordinating *via* one C, one N and by one C atoms
COSY	correlation spectroscopy
Cy	cyclohexyl
d	days
dba	dibenzylideneacetone
DCM	dichloromethane
DFT	density functional theory
DMAP	4-N,N-dimethylaminopyridine
DMF	dimethylformamide
DME	dimethoxyethane
DMSO	dimethylsulfoxide
dppf	1,1'-bis(diphenylphosphino)ferrocene
ε	extinction coefficient (L mol^{-1} cm^{-1})
EI	electron ionisation
E_{em}	emission energy
E^{ox}	energy of oxidation
EPA	diethyl ether:isopropane:ethanol (2:2:1 v/v)
equiv	equivalents
ES+	positive ion electrospray ionisation
ET	electron transfer
Fc	ferrocene
h	hour
HOMO	highest occupied molecular orbital
HRMS	high resolution mass spectrometry
HSQC	heteronuclear single quantum correlation
Hz	Hertz

IC	internal conversion
ILCT	intraligand charge transfer
ISC	intersystem crossing
ITO	indium tin oxide
k_0	self-quenching rate constant at infinite dilution
k_q	quenching rate constant
λ_{em}	emission wavelength
LC	ligand-centred
LCD	liquid crystal display
LUMO	lowest unoccupied molecular orbital
MC	metal centred
Me	methyl
MeCN	acetonitrile
MeOH	methanol
MLCT	metal-to-ligand charge transfer
MO	molecular orbital
MS	mass spectrometry
n	non bonding orbital
NBS	N-bromosuccinimide
N^C	a bidentate ligand coordinating *via* one N and one C atom
N^C^N	a terdentate ligand coordinating *via* one N, one C and followed by one N atoms
NMR	nuclear magnetic resonance
N^N	a bidentate ligand coordinating *via* two N atoms
N^N^C	a terdentate ligand coordinating *via* two N atoms and one C atom
NOESY	nuclear Overhauser effect spectroscopy
OAc	acetate
OLED	organic light emitting diode
ORTEP	Oak Ridge Thermal Elipsoid Plot
p	para-substituted
PET	photoinduced electron transfer
phbpy	6-phenyl-2:2'-bipyridine
ppm	parts per million
ppy	2-phenylpyridine
Pt(OEP)	platinum(II) octaethylporphyrin
py	pyridine

Φ	quantum yield
[Q]	quencher concentration
R_f	retention function
S_0	ground singlet state
S_n	nth excited singlet state
τ	lifetime
τ_{obs}	observed lifetime in the presence of quencher
τ_0	observed lifetime in the absence of quencher
tbb	1,3,5-tribromobenzene
terpy	2,2':6',2''-terpyridine
TFA	trifluoroacetic acid
THF	tetrahydrofuran
tlc	thin layer chromatography
T_n	nth triplet excited state
TOF	turn over number (moles of product formed per mole of catalyst)
TON	turn over frequency (moles of product formed per unit time)
UV	ultra violet
v/v	volume ratio between two solvents

CHAPTER 1

INTRODUCTION

1. Introduction

Square-planar platinum(II) and palladium(II) complexes hold the possibility of ground- and excited-state interactions that are not possible in octahedral and tetrahedral metal-complexes,[1] and as such, display a wide range of intriguing properties.[2,3] Examples of the axial interactions which make these classes of complexes intriguing include excimer and exciplex formation,[1,4] concentration related effects of aggregation (that can induce excited-state switching),[2] as well as chemical and photochemical reactivity.[5,6,7] Ultimately, photoactive coordinatively unsaturated complexes are attractive for many applications, including solar energy conversion, photocatalysis,[5,8] vapochromism,[9,10,11] mesogenic materials for applications in liquid crystal displays (LCDs)[12] and bio-molecular agents[13,14,15,16,17] such as DNA intercalators and probes, and chemotherapeutic drugs.[18, 19,20]

An area of considerable interest for a large number of research groups is in the development of new triplet-emissive materials for use as dopant molecules in organic light emitting diodes (OLEDs).[21,22,23] OLEDs are considered by many to be the next important development within the field of display-screen technology, due to their high levels of performance and efficiency, as well as their relative ease of manufacture into flexible, wafer-thin films *via* ink-jet printing type methods, compared with more rigid liquid-crystal or plasma displays.[24] Square-planar d^8-metal complexes are of considerable interest to this field due to their applications as dopants to increase luminescence efficiency of the emissive layer of the devices. The triplet nature of the luminescence observed from certain transition metal complexes, a process commonly known as phosphorescence, renders the more emissive compounds as potential triplet-harvesting agents which can dramatically increase device efficiency. The high spin-orbit coupling constant, induced by the presence of the heavy metal-ion, is the key feature which allows their successful application in this field.[25,26] Consequently, there is considerable growth in research focused on the development of neutral, efficiently luminescent heavy-metal complexes as candidates for incorporation into OLED systems.[27] Due to this high demand for novel compounds with properties applicable to this field, exploration of high efficiency phosphorescent emitters has represented one of the major research aims of the work discussed here. Further details on OLEDs, their mode of operation, and how transition-metal complexes are used to enhance device performance are discussed later in this introduction.

1.1. Platinum(II) complexes

1.1.1. N^N^N and N^N polypyridyl coordinated complexes

Initiated by the remarkable photochemistry of the d^6 complex of $[Ru(bpy)_3]^{2+}$ and its derivatives,[28,29,] a large number of transition-metal complexes containing polypyridyl ligand systems have been developed.[2,4] However, square-planar d^8-complexes composed of mono- and bi-dentate ligands are unstable with respect to a D_{2d} distortion in the excited-state.[3] The process of exciting an electron into higher energy d-d levels of the complex can unbalance the square-planar configuration and induce large structural changes in the metal coordination geometry, which normally results in non-radiative decay of the excited-state, Figure 1.[30,31,32] If the lowest energy excited-state lies too close in energy to the metal-centred excited-states, the two can thermally equilibrate, quenching the emission through fast radiationless decay. Therefore, the energy gap between the d-d states and the lowest energy excited-state may be considered to be one of the limiting factors for emission efficiency (*i.e.* a small energy gap between these states leads to low quantum yields).[3]

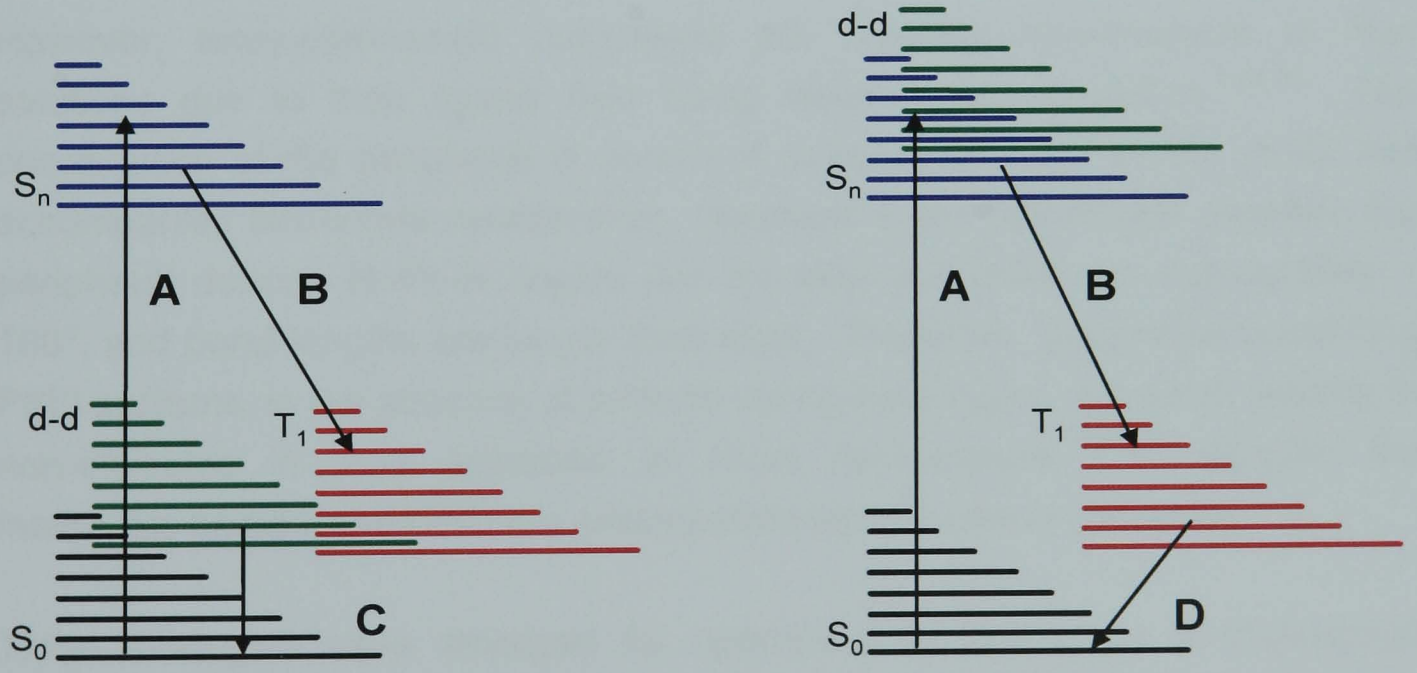

Figure 1: Jablonski-type diagram illustrative of the fate of excited-states for square-planar d^8-metal complexes. A: Absorption of a photon, resulting in generation of a S_n excited-state molecule. B: Rapid relaxation to the lowest energy excited-state, in this case a triplet state, T_1. C: If the d-d excited-states are low enough in energy then the excited-states can relax non-radiatively back down to the ground state, S_0. D: By removing the d-d states from thermal accessibility, the T_1-state can then become radiatively active and relax via the emissive process of phosphorescence.

As a result, simple platinum(II) complexes of polypyridyl ligands, *e.g.* 2,2'-bipyridine (bpy) based complexes (this and similar systems are often denoted as N^N referring to the chelating bis-nitrogen donors of the ligands, examples shown in Figure 2), are typically non-emissive in fluid solutions at room temperature.[33,34] In fact, it is quite rare for platinum(II) and palladium(II) N^N systems to be emissive.[35] Many researchers have therefore diverted their attention to the ligand 2,2':6',2''-terpyridine (terpy), Figure 2, which shows a strong preference for maintaining a planar geometry.[3,36,37,38,39] The chelated ring-strain of the two fused metallocycles formed upon terdentate coordination to the metal atom restricts vibrational motion, limiting distortion as an efficient deactivation pathway for excited-states.

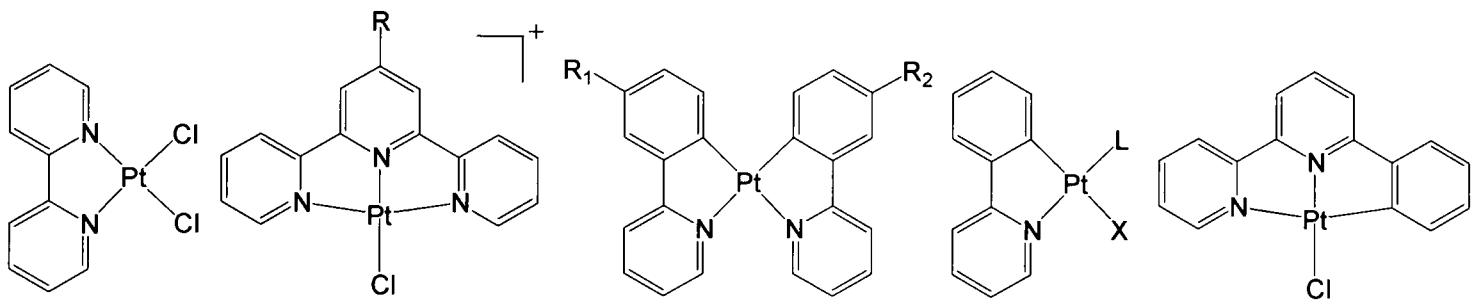

Figure 2: Examples of bpy N^N,[1,33] terpy N^N^N[3,5,36] (R = location for 4'-substitution), ppy N^C ($R_1 = R_2$ homoleptic; $R_1 \neq R_2$ heteroleptic),[6] phbpy N^N^C based systems.[40,41]

However, terpy-platinum(II) complexes are typically non-emissive in fluid solutions due to their ligand field being weaker than expected.[3,36,39] The coordination of the peripheral N donors is severely affected by the strain that accompanies terdentate coordination, observed in the bite angles between the peripheral donors: N–Pt–N angles (for the later pyridines) are substantially < 180°, and bond lengths are longer than ideal. Therefore, terpyridine containing Pt(II) systems, in the absence of a fourth strong-field ligand, are either weakly or non-emissive in fluid solutions at room temperature,[38,42,43] despite the molecules being locked into the ground-state square-planar geometry.

Three strategies have emerged for optimising luminescence of platinum(II) complexes. Firstly, introduction of an aryl-substituent at the 4-position of a terpy ligand can lead to complexes that are emissive in fluid solutions at room temperature.[38] The influence of the pendant substituent is most pronounced for the most electron-rich appendages. McMillin and co-workers have interpreted a similar effect from polycyclic aromatic substituents as a switch from the usual ^{3}MLCT excited-state to a lower energy ^{3}ILCT excited-state. When the ^{3}ILCT state is sufficiently low in energy the d–d states are thought to be relatively too high to promote non-radiative decay. Consequently, luminescence lifetimes as

long as 64 μs and quantum yields *ca.* Φ = 0.05 have been observed.[42] Alternatively, increasing the ligand-field strength at the metal centre can be used to manipulate the deactivating d–d excited-states, raising their energy and hence reducing their influence as a deactivation pathway, as is pictorially represented in Figure 1. This can be achieved through replacing the weak-field chloride ligands found in many systems, with strong ligand-field alternatives, such as acetylide groups.[1,5,44] This has been successful in generating a number of platinum(II) polypyridyl complexes that are emissive in solution at room temperature, such as platinum diimine bis(acetylide) complexes.[45] The ligand field can also be increased by replacing the polypyridyl ligand with a cyclometalating analogue. The cyclometalating carbanion has a very strong ligand-field and again increases the energy of the d–d states. This strategy has led to a variety of classes of compounds employing terdentate ligands, which are discussed below.

1.1.2. N^C and N^N^C coordinated complexes

The simplest cyclometallated Pt(II) complexes are based on bidentate ligands such as 2-phenylpyridine (ppy) and 2-(2-thienyl)pyridine.[6] As binding centres they are isoelectronic with the previously discussed polypyridyl ligand 2,2'-bipyridine; examples are shown in Figure 2. The photophysics of some of these complexes revealed low-lying ^{3}MLCT excited-states with interesting photochemical properties.[6,46] Examples include homoleptic complexes, $Pt(N^C)_2$,[47,48] heteroleptic complexes, Pt(N^C)(N^C'),[48,49] and complexes with a single cyclometalating ligand (N^C) and non-cyclometalating ancillary ligands (L and/or X),[46] Figure 2. However, while increasing the ligand-field strength compared to their polypyridyl analogues does successfully induce the desired destabilisation of the deactivating d–d excited states, these complexes remain susceptible to deactivation through distortion of the coordination sphere, and again the luminescence efficiencies of these systems are often far from impressive.[50]

Ligands such as 6-phenyl-2,2'-bipyridine (phbpy), containing an N^N^C coordinating geometry, have been designed to counter the excited-state distortion effect through the rigid binding mode favoured by terdentate systems such as terpy, whilst still employing a carbanion binding site for cyclometallation as utilized in ppy. By incorporating features of both cyclometallation and terdentate binding, N^N^C complexes currently display superior emissive properties compared to N^N^N and C^N^C congeners (discussed below,

Section 1.1.3).[40,51,52,53,54] As a result, the N^N^C-bound complexes have been extensively investigated with derivatisation of these systems having proved to be extremely popular.[55] However, despite the additive effects of chelation restricting vibration, and the increase in ligand-field strength, the complexes typically have only quite moderate quantum yields of phosphorescence, *e.g.* Φ = 0.025,[53] which has limited their application as emissive species for incorporation in OLED systems. Further development through replacement of the chloride in the fourth coordination site by other ligands has led to new highly luminescent species (Section 1.1.5).

1.1.3. C^N^C coordinated complexes

Relatively uncommon, examples of doubly cyclometallated species that give complexes with terdentate C^N^C donor sets have been limited. This type of coordination arises when two cyclometallated bonds from the same ligand are formed *via* two C–H activations by the same metal, Equation 1.[12,56] Complexes of this type were first reported by von Zelewsky and co-workers.[57,58] However, only recently have the first high yield syntheses of terdentate C^N^C complexes of platinum been reported.[56,59,60] The presence of two strongly donating carbanion groups is thought to create a highly stable complex,[61] and despite having two mutually *trans*-metallating donors there is little structural difference in the binding mode of this terdentate ligand compared with neutral donors, N^N^N, and mono-anionic systems, N^N^C, for example similar values are observed for bite angles and bond lengths around the central metal-ion.[59]

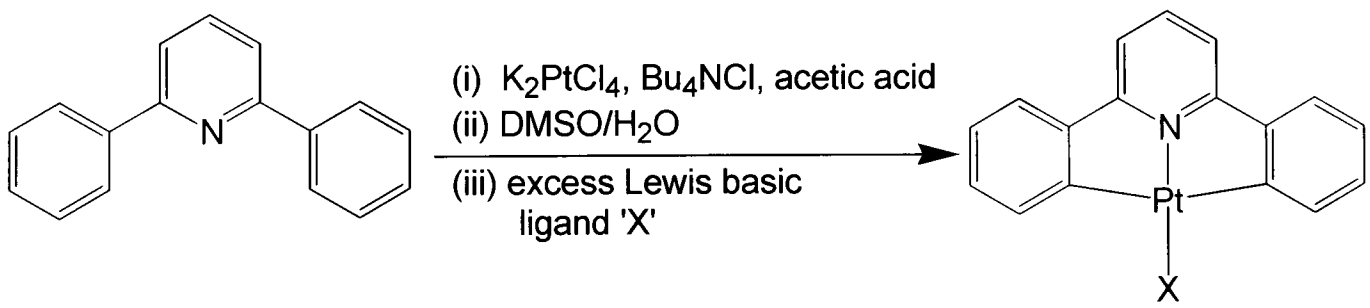

Equation 1: Recently discovered, high yielding synthesis of bis-carbanion terdentate platinum complexes.[56,60]

The double cyclometalation feature of these complexes would be expected to further destabilise the metal-centred states and in turn unlock high quantum yields. However, bis-cyclometallated C^N^C coordinated platinum(II) complexes are rarely emissive in fluid solutions at room temperature.[56] Although some have been shown to display emission from a ^{3}LC state, there is no improvement in the quantum yields achieved for these compounds over

those previously discussed. The mutually *trans*-cyclometallated fragments are slightly distorted from ideal square planar geometry, reducing the overall electron-donating effect of the cyclometalating bonds in this case.[57] Additionally, the Pt–C bonds are slightly elongated, for example, Pt–C distances of 2.069(9) Å are longer than typical due to their mutually opposing *trans*-influence.[60]

1.1.4. N^C^N coordinated complexes

The first organometallic complexes containing terdentate monoanionic ligands were reported in the late 1970s. Compounds of this sort have a general structure of a 1,3-disubstituted phenyl ring, Figure 3, and the common name "pincer" ligand is given because the monoanionic carbon donor group is flanked on both sides by neutral two-electron donors. The neutral donors in pincer ligands can be a variety of atoms such as N, S, P or even O, which give the ligand an overall coordination motif of η^3-E^C^E (where E represents one of the aforementioned types of donor atoms).[62,63,64] Isoelectronic with previously discussed systems N^N^N and N^N^C ligands, N^C^N systems also act as six-electron donors to the metal. Chelation of all of the donating atoms to the same metal centre leads to the formation of a bis-metallacyclic species containing the desirable two fused five-membered rings. Each chelate ring incorporates the metal-carbon bond and one of the two *ortho*-substituted neutral donor-groups, providing rigid terdentate binding. The ligand also provides substantial stabilisation of the M–C σ–bond, which, as will become apparent, is a key feature of these complexes. Bonds observed between platinum(II) and carbanions without the aid of chelation, *e.g.* *trans*-[PtH(C_6H_4F-*p*)(PPh_3)$_2$] 2.066(23) Å,[65] and *trans*-[Pt(CO)(C_6H_4Cl-*p*)(PEt_3)$_2$]PF_6 2.06(4) Å, are consistently longer than such bonds incorporated into cyclometalating ligands.

The stabilising effect of the metallacycles can be easily followed. The cyclometalating bonds of C^N^C ligands are similar to those of non-chelated systems, *e.g.* (C^N^C)Pt(CO) 2.057(9) Å.[59] The above mentioned N^C and N^N^C complexes contain mono-cyclometallated bonds that are shorter, *e.g.* $Pt(bpy)_2$ 1.99 Å[47] and (phbpy)PtCl 2.067(3) Å.[41] However, in the case of biscyclometallated N^C^N pincer systems the Pt–C bond length is substantially reduced, typically in the range 1.90–1.94 Å,[66] therefore, the ligand-field strength experienced by the metal centre is substantially increased.

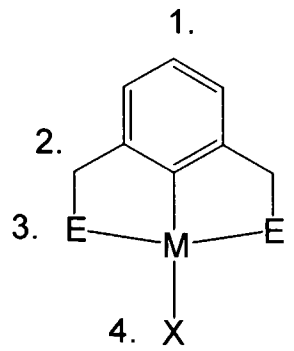

1. Remote electronic modulations
   Anchoring site
2. Site for chiral/steric modification
   Electronic modulation *i.e.* extension of aromaticity
3. Variable donor atoms
   Expansion of chiral/steric constraints
4. Ligand substitution: tunable electronics

Figure 3: Basic structure associated with pincer ligand systems and sites of possible variation that may influence the electronic environment around the metal centre and so have a bearing on the nature of luminescence.[67]

"Pincer ligands" have been the focus of extensive research for groups targeting catalytic metal complexes,[68,69,70] but investigations into phosphorescent platinum(II) complexes based upon this type of structure have been limited. However, low-energy metal-centred emission at 77 K has been observed by Connick and co-workers in platinum(II) N^C^N pincer complexes with coordinated alkyl-amine arms.[71,72] Importantly, however, pincer systems have a large number of possible modifications available which influence the overall properties of the metal complex, Figure 3. Clearly some of these modifications will have electronic consequences, so fine tuning of the electronic properties of these complexes can be easily achieved,[67] a feature which has been utilised for probing catalytic reactions.[73]

The area of work discussed in this thesis has been centred around the core structure of the ligand 1,3-di(2-pyridyl)benzene, HL^1, which follows this "pincer" binding motif abbreviated as N^C^N, Figure 4. It is observed for this system that while incorporating the high ligand-field strength of this coordination mode, the extended π-conjugation afforded by the pyridine donors reduces the energies of the excited-states associated with the N^C^N ligand, thus, further removing them from the influence of the d-d states.[3]

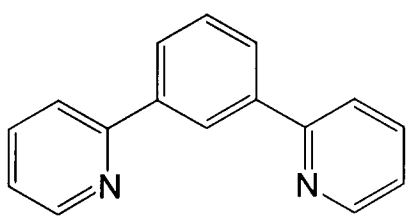

HL^1

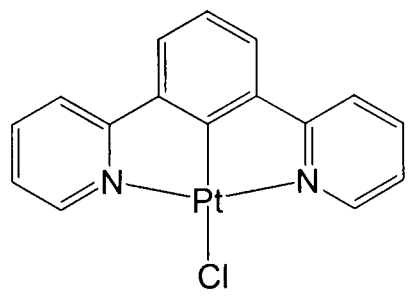

L^1PtCl

Figure 4: Core ligand 1,3-di(2-pyridyl)benzene, HL^1, and N^C^N coordinated platinum complex, 1,3-di(2-pyridyl)benzene-2-platinum(II) chloride, L^1PtCl.

It has previously been established that platinum(II) chloride complexes of HL^1 are easily prepared under inert atmosphere conditions.[66] Simple derivatives incorporating alkyl or ester substituents at the 5-position of the central benzene ring displayed red and blue shifts in the luminescence properties repectively, when compared with the parent complex, L^1PtCl.[74] Importantly, luminescent quantum yields (Φ = 0.58–0.68) and excited-state lifetimes (τ = 7.0–8.0 μs) were not affected greatly by the presence of the substituent and are still over an order of magnitude greater than those for analogous N^N^C complexes, *e.g.* (phbpy)PtCl (Φ = 0.025).[53] Overall this massive enhancement in photophysical properties is attributed to a combination of the very short Pt–C bond increasing the ligand-field experienced by the metal, the rigidity of the N^C^N coordinating mode reducing the deactivating nature of the d-d states, and the large conjugated aromatic system making ligand-centred excited-states accessible.

1.1.5. Ancillary ligands

Platinum(II) complexes with polypyridyl ligands and their cyclometallated analogues are normally prepared with chloride in the remaining coordination sites (*e.g.* those discussed in previous sections). However, the photoluminescence from platinum(II) complexes can arise from a variety of excited-states, and the nature of a complex's emissive state is sensitive not only to the properties of the polypyridyl based ligand but to those of the ancillary ligand as well.[1,35,38,45,53] Different ancillary ligands can influence the orbital parentage and relative energies, intensities and lifetimes of the excited-states in platinum complexes according to the differences in the extent of their electronic interaction with the metal centre.[3,36] Additionally, the ability to vary the nature of the fourth coordination site affords the possibility of studying a series of related complexes without affecting the chosen polydentate binding core.[45]

There are a number of options available for the identity of the ancillary ligand, such as neutral nitrogen, sulfur or phosphorus donors,[54,75] examples shown in Figure 5. However, there has been particular interest in platinum(II) σ-alkynyl complexes, with applications including nonlinear optics, liquid crystals, low-dimension conductors, photovoltaic devices, and luminescent sensor applications reported thus far.[5,44,76] The wide range of applications for this class of compounds has been attributed to their chemical and structural stability.[77,78] Also, as previously mentioned (Section 1.1.1), acetylide ligands can induce large ligand-field effects on the metal centre. Many platinum(II) complexes with aromatic ligands, *e.g.* terpy and ppy, incorporating acetylene units as ancillary

ligands have been found to be strongly luminescent at room temperature in contrast to their chloro parents.[5,79] Furthermore, acetylides generating new low-energy transitions in platinum(II) complexes have demonstrated that judicious selection of the acetylide group may be used to tune the emission wavelength across the visible spectrum.[55] For example, Eisenberg and co-workers have investigated the excited-state properties of a series of platinum acetylide complexes,[45,80] where some of the complexes feature low-lying triplet charge-transfer excited-states which derive from transitions involving the acetylide π-system. Consequently, as a combination of increased quantum yields and the ability to tune their emission, acetylide complexes have also shown excellent results as materials in OLED fabrications.[44,81]

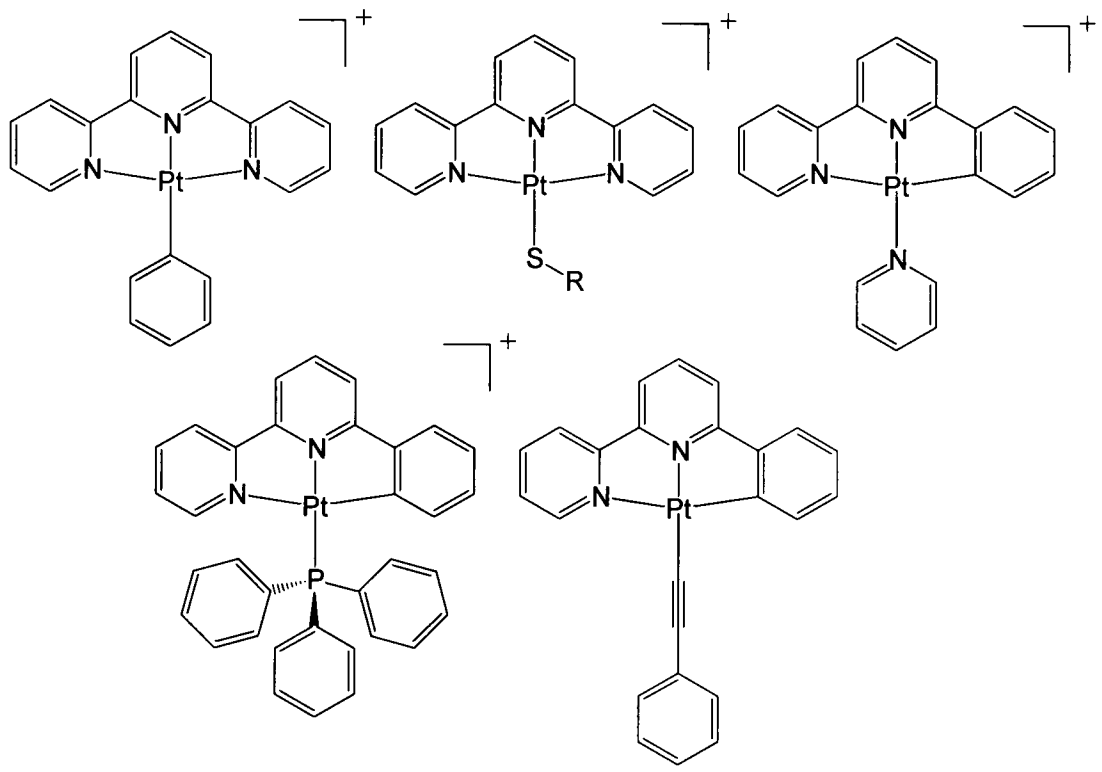

Figure 5: Variation of ancillary ligand offers a versatile means of fine tuning properties. $[(terpy)PtPh]^+$,[36] $[(terpy)PtSR]^+$,[82] $[(N^N^C)Ptpy]^+$,[54] $[(N^N^C)PtPPh_3]^+$,[40] (N^N^C)PtCCPh.[81]

Apart from acetylides, other ancillary ligands have been investigated. The substitutional lability of the chloride ligand allows facile exploration of series of related complexes. Other donors, shown in Figure 5, include carbanions and thiolates which possess a formal negative charge, and neutral pyridine and phosphorus donor groups. While the effect the new ancillary ligand will have on the system is reliant on the polypyridyl platinum complex it is attached to, there are some generalisations that can be made. Eisenberg and coworkers have discovered that certain thiolate complexes will be luminescent in fluid solution at room temperature from CT transitions.[35,83] Ancillary ligands such as thiolates and carbanions are good electron-donating ligands and can lower the energy of previously inaccessible ^{3}MLCT and ^{3}LLCT transitions. Weaker electron-donors,

such as chloride, pyridine and phosphorus ligands are known to influence the MLCT transitions observed in the UV-Vis spectra, however, these complexes are typically emissive from ^{3}LC states located on the polpyridyl ligand[40] and therefore ancillary ligand substitution will only influence the emissive state when more electron-donating species are employed, *e.g.* (phbpy)Pt(2-dimethylamino-pyridine).[54]

1.1.6. Effect of intermolecular interactions on luminescence

All of the above sections and discussions have been concerned with obtaining highly efficient luminescent materials from isolated monomeric species. However, the coordinative unsaturation of square-planar complexes allows interactions between metal centres and between π-conjugated systems of near neighbouring molecules, *i.e.* metal-metal and π-π bonding interactions,[34] that can generate new excited-states in complexes that are otherwise non-emissive at room temperature. Many platinum and palladium(II)-polypyridine complexes have the ability to form these types of interactions in the solid state when contacts between metal and conjugated ligand systems are sufficiently close.[2] The metal centres are known to have the ability to act as a two-electron donor[84] and can generate weak bonding interactions between neighbouring molecules that can be energetically favourable. Weak bonding metal-metal and/or π-π interactions are the driving force for forming dimers or extended chains of interacting complexes in the solid-state.[33,34,85,86] These weak interactions are also responsible for solution-state aggregation phenomena, such as the oligomerisation observed in some terpyridyl complexes,[2,39] as well as excimer and/or exciplex formation.[1]

Generally these types of interactions lead to significantly red-shifted emission compared with the isolated monomers. The $5d_{z^2}$ and p_z orbitals of adjacent Pt atoms can give rise to bonding, dσ, and antibonding, dσ*, orbitals and the red-shifted electronic behaviour is assigned to dσ*→π* transitions, represented in Figure 6.[33,39,40,85] Ligand manipulation can be effective in controlling multinuclear interactions, see Figure 6,[86] through influencing the electronics and/or sterics of the metal-centre and the conjugated ligand system. The intermolecular distance can be somewhat controlled, and therefore, the strength of the metal/ligand bonding interactions.[4,45]

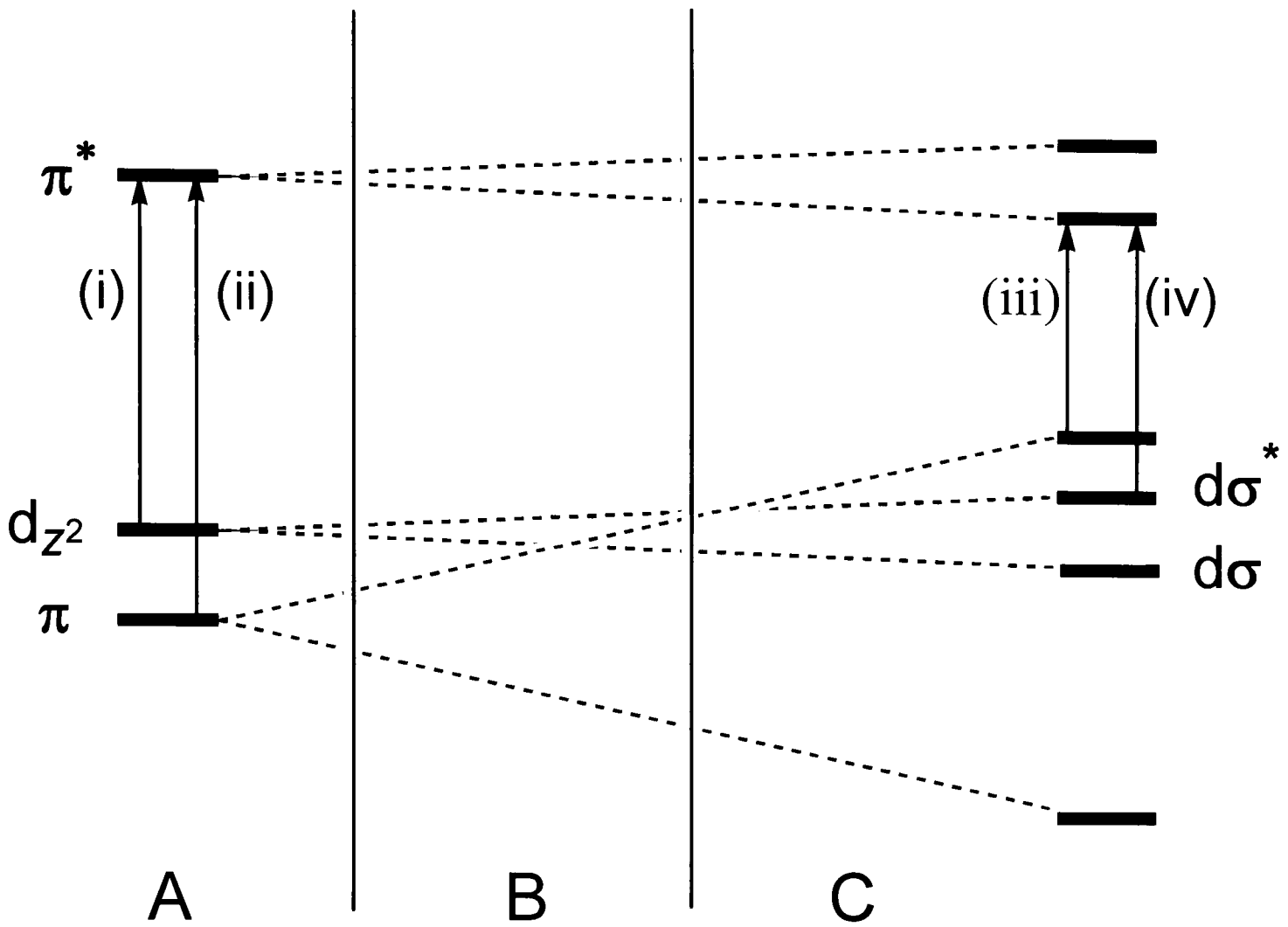

Figure 6: MO level diagram representative of metal-metal and π-π interactions in dimerisation.[55,86] Domain A: representative of monomeric type behaviour where the intermolecular contacts aren't sufficient to generate new excited-states. Domain B: due to the fact that the upper limits for interactions between ligand π-systems are larger than metal interactions, domain B is representative of intermolecular ligand-ligand excited states being the lowest energy transitions. Domain C is representative of significant intermolecular metal-metal interactions, where dσ/dσ* intermolecular orbitals are generated. Transitions of the type (i), (ii), (iii) and (iv) are LC, MLCT, π→π* and dσ*→π* according to the nature of the electronic origins and destination.

1.1.7. Luminescent sensors

Sensitive and selective luminescent probes are important for monitoring *in vivo* and *in vitro* biological events,[15,87,88] including the study of physiological roles of metal ions. Many luminescent probes have been successfully developed and are of interest for many environmental effects, such as the presence of cations including protons,[89,90] alkali and alkaline earth metals, zinc[91,92,93] and other metal ions,[94,95] (for a review see de Silva *et al.*[96]). Transition metal complexes have many advantages as luminescent sensor compounds,[29] including large spectral shifts between the excitation and emission energies, which reduces self absorption effects. Moreover, they can possess a variety of energetically accessible excited states that can have different probing effects.[97]

Chromophores such as $Ru(bpy)_3^{2+}$ and tricarbonyl Re(I) polypyridyl complexes have been the most commonly used signalling centres in supramolecular assembly sensors, because of their well documented photophysics.[98] However, metal complexes based on platinum have recently shown promise in sensor development.[99]

There are several strategies used in luminescence based detection. The first approach and one of the most commonly exploited is often termed "inclusion" or "host-guest" chemistry. A luminophore with the ability to selectively interact with a host molecule to yield a new species with different luminescent properties can sometimes provide quantitative analysis of the luminophore's environment. pH or small ion sensing are good examples.[91,96,98,99] 'Selectively' is a key word from the above sentence: sensors need to discriminate between their target and additional influences or species that may be present, demonstrated in Figure 7. Therefore, molecular recognition components capable of binding one particular species among a mixture are employed. To this end, host-guest chemistry based on polyether donor units has attracted much attention since the pioneering work by Pedersen,[100,101] Lehn,[102] and Cram[103] on the synthesis of crown-ethers, cryptands, spherands and macrocyclic polyether chains, that can selectively bind guest cations that "fit" correctly into their cavity and optimally interact with the Lewis-basic donor atoms. Subsequently, binding motifs for metal ions such as crown-ethers, cryptands, cyclophanes, calixarenes and specific multidentate ligands, which are all able to unambiguously sequester ions and/or molecules, have been extensively used in molecular recognition studies for the conversion of discrete, stoichiometric interaction events into luminescent signals.[104,105,106,107,108,109]

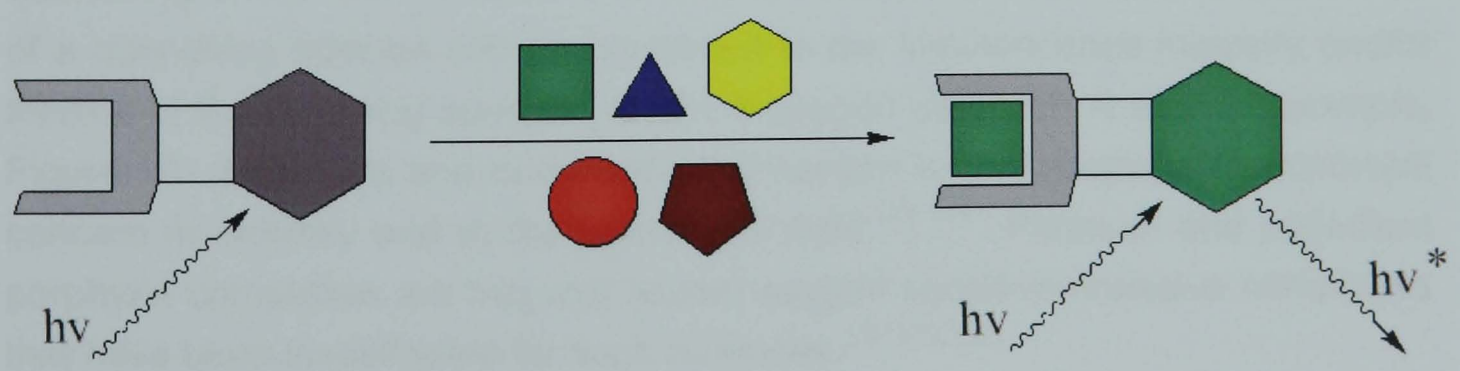

Figure 7: Schematic representation of a selective supramolecular sensor. The device is built of three separate components, from left to right: the recognition centre capable of selectively binding with desired analytes; the linker group; and the reporter group, in this case represented by the hexagon as an 'off-on' luminescent centre.

Generally, however, the recognition centres cannot themselves generate sufficient changes in their physical properties through complexation and so the binding act is usually indicated by a molecular signalling centre, a responsive fragment capable of producing a distinct signal change immediately after the binding act. Building a sensor molecule therefore requires the use of components with specific functions, shown schematically in Figure 7. Typically, a sensor will require a recognition site, discussed above; a luminophoric group, capable of responding to guest binding and a linker unit, which connects the recognition site to the luminescent segment.[96] The latter can be represented through as little as one bond between the other two fragments, or in some case may be extended conjugated systems; some examples are shown in Figure 8.[110] The overall idea is to build a composite molecule that has a luminescent beacon, which is covalently attached to a binding site, which can modulate the beacon signal upon host-guest interaction.

Host-guest sensing, based on luminescence signalling, is common amongst organic emitters, with a large area devoted to research with photo-induced electron transfer (PET) systems, Figure 9.[96,111] In contrast, the use of transition metal complexes as luminescent cation sensors has not been as extensively explored.[110,112] However, examples of platinum complexes for signalling centres,[99,113,114] and crown-ether based inclusion systems have recently been reported.[96,115,116]

The sensory role of many luminescent compounds can be expanded from host-guest interactions to other processes since their emission can often be influenced by environmental stimuli.[15,16] Sensors based on bimolecular quenching of the excited-state molecule are possible, where the concentration of a quenching species can be correlated to the luminescence intensity and/or lifetime of the reporting species, of which oxygen detection is a good example, Figure 10. Detection and quantisation of oxygen is an exceptionally important concern in industry and in the biomedical field.[117,118] Platinum and palladium porphyrin complexes are two well known oxygen-sensitive emissive complexes that have been investigated for such purposes.[117,119,120]

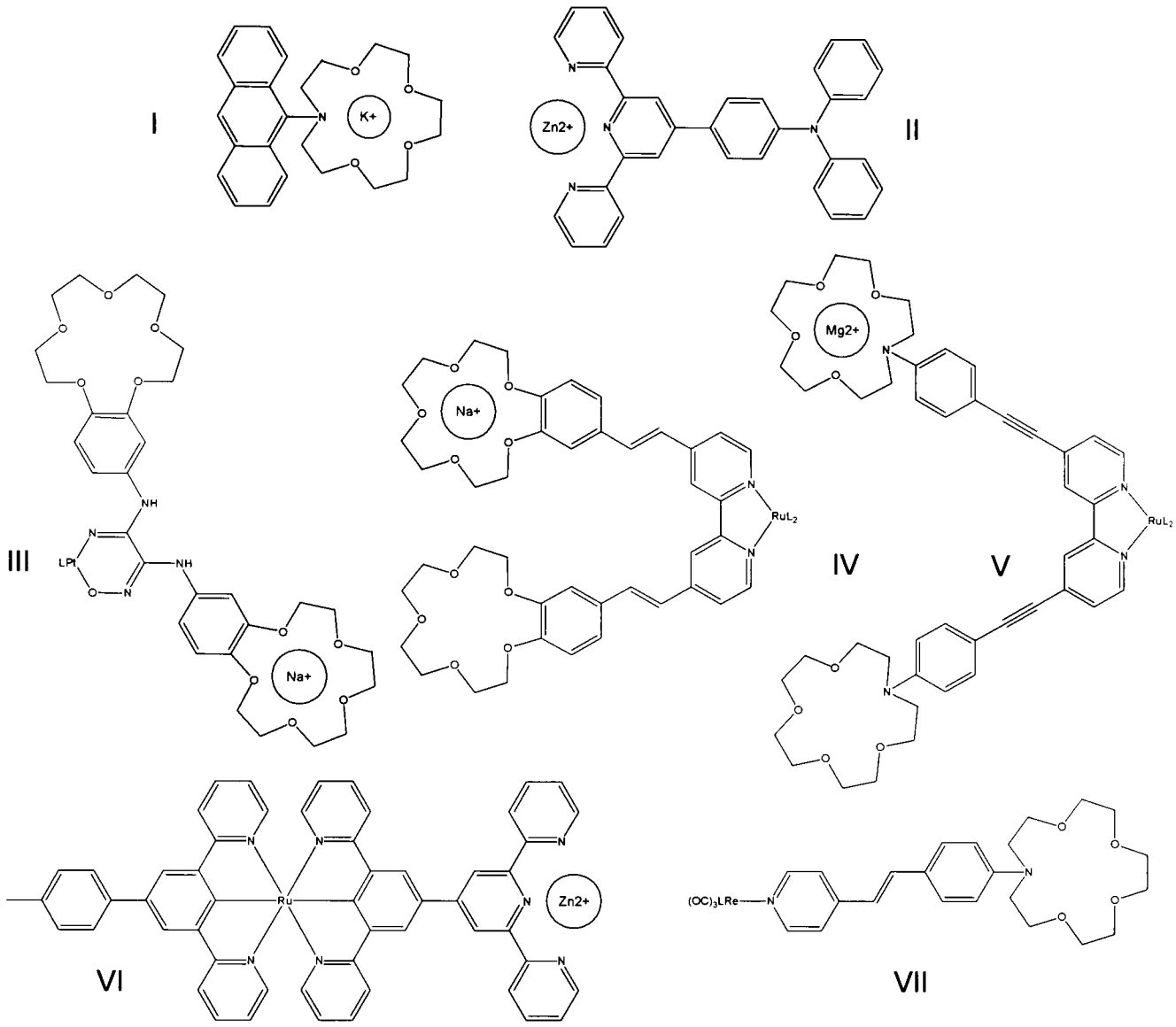

Figure 8: Examples of supramolecular 'host-guest' luminescent sensors, including organic and inorganic systems with different extents of linker group communication; *i.e.* single bond, (I); double (IV and VII), triple (V) and aromatic (II, III and VI) bonded electronic conjugation.[91,96,110,115,121]

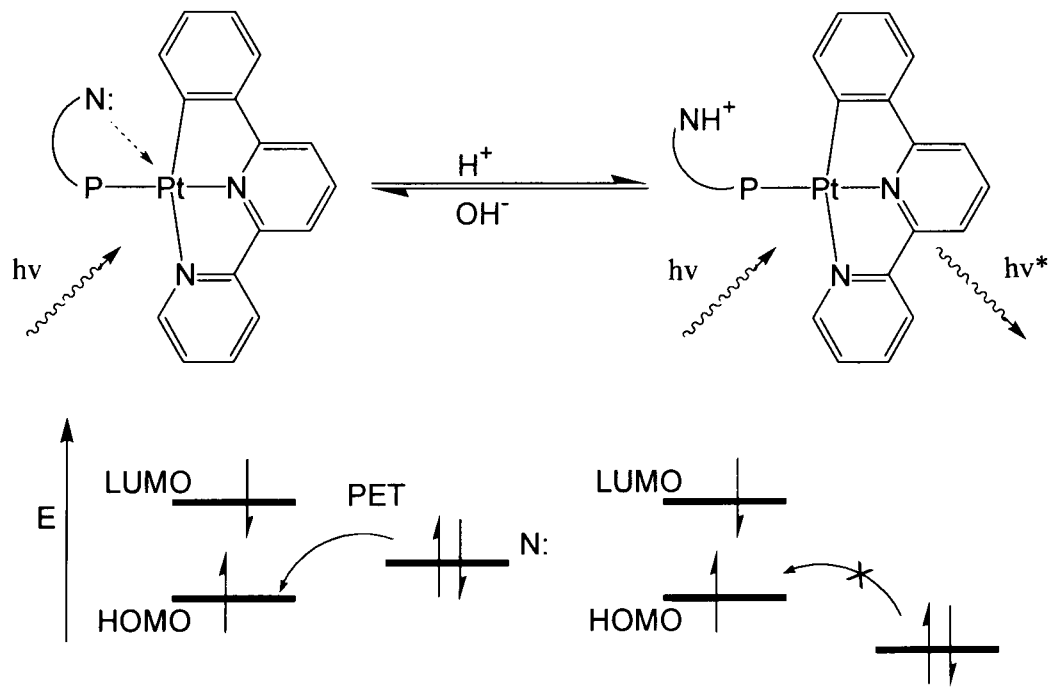

Figure 9: Platinum complex example of PET sensor and MO diagram representing electron transfer (ET) processes involved in the excited state quenching leading to an 'off-on' luminescence response.[122]

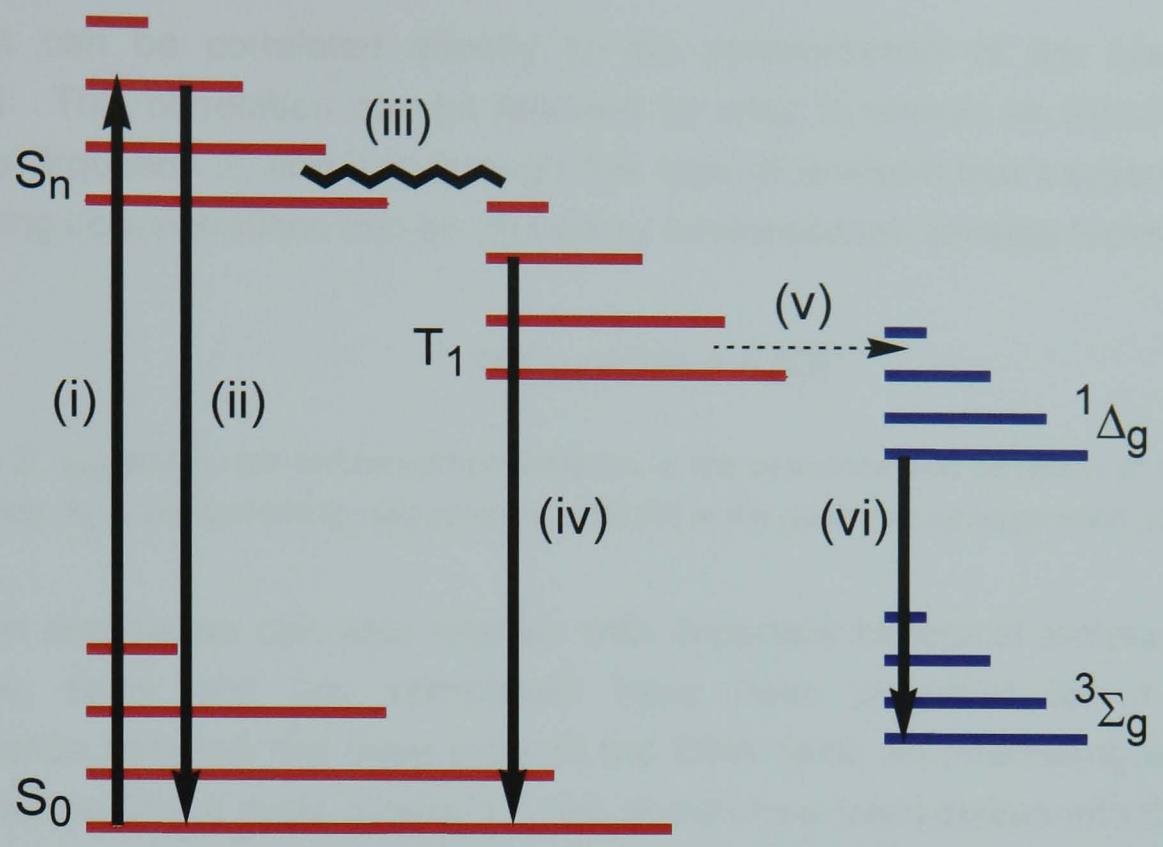

Figure 10: Oxygen sensing *via* bimolecular quenching of excited-state molecules. Collision controlled energy transfer (v) is observed between an excited-state molecule and triplet oxygen, ($^3\Sigma_g$), recreating the ground state molecule and higher energy singlet ($^1\Delta_g$) oxygen. For oxygen quenching of excited states to occur the energy of the emissive transition must be sufficient to activate the excitation of triplet oxygen, 7900 cm^{-1}. The net result is a decrease in the observed emission intensity, and luminescence lifetime, when compared with values recorded in the absence of the oxygen. Key: (i) absorption; (ii) fluorescence or internal conversion; (iii) intersystem crossing (ISC); phosphorescence or internal conversion; (iv) phosphorescence (v) energy transfer; (vi) phosphorescence or internal conversion of the excited oxygen molecule.

Oxygen is not the only quenching agent known to cause deactivation of luminescence from transition-metal complexes. The quenching species can be anything capable of affecting the luminescence intensity and lifetime of the luminophore. For example, it was discussed at the beginning of this report that square-planar platinum(II) and palladium(II) complexes hold the possibility of ground- and excited-state interactions, such as formation of excimers and exciplexes.[1,45,74] Formation of excimers, short excited-state dimers, is another form of luminescence quenching which also leads to changes in the monomeric emission intensity and lifetime. The process involves a ground-state molecule colliding with the excited-state molecule and forming the excimer, which has a different excited-state, and therefore photophysical properties, to that of the parent complex.

As with oxygen and excimer quenching, bimolecular quenching processes of this type are diffusion controlled, simply by the two species happening upon one another at the correct moment in time. Therefore, the emission intensities and

lifetimes can be correlated directly to the concentration of the quenching species. This correlation can be followed by what is known as Stern-Volmer analysis, Equation 2, and it is through this type of analysis that oxygen and/or quenching concentrations can be probed by luminescence sensing techniques.

$$1/\tau_{obs} = 1/\tau_0 + k_q[Q]$$

Equation 2: τ_{obs} and τ_0 are luminescence lifetimes in the presence and absence of quencher respectively, k_q is the quenching rate constant, and [Q] is the quencher concentration, mol dm^{-3}.

Platinum complexes can also interact with important biological molecules; for example, terpy and bpy complexes have been prepared for π-system intercalation between the base pairs of the DNA helix; an interesting example based on the ligand dppz, Figure 11, has shown how intercalation into the DNA helix can shield the molecule from water-induced bimolecular quenching,[123] and thus generate a switching-on of the luminescent signal. Modulation of aggregation effects of square-planar platinum complexes has also been exploited in systems designed for probing environmental stimuli such as temperature, pressure, and concentration of organic solvents and vapours.[2,9] Also, some transitions within transition-metal complexes are highly dependent on solvent polarity and/or rigidity. Specifically, CT transitions are altered energetically through relative ground/excited-state stabilisation by the solvent and the related reorientation timescales, a phenomenon that can be probed spectrophotometrically, known as rigidochromism.[96]

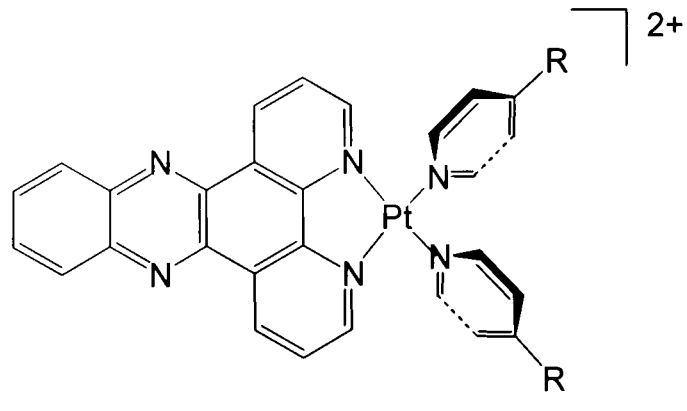

Figure 11: Planar ligand dppz readily intercalates into DNA, causing distinctive changes in luminescent properties of the complex, R = H,[123] R = NH_2.[97]

1.1.8. Optoelectronics

One of the key areas of interest for investigations into novel luminescent compounds is for their successful application as luminous materials in energy efficient lighting and display screen technology. In the development of superior

compounds for these applications, heavy-metal complexes are finding special advantages making them of particular interest in many applications.[25,26,27,124] As one such field of interest, OLEDs are emerging as the leading technology for the new generation of full-colour flat-screen displays and are already in use for mobile phones and digital cameras.[125,126] One of the many attractive features of OLEDs is that no backlighting is required, allowing them to be thinner, lighter and more efficient than liquid crystal displays (LCDs). As a result, OLED research is expanding both academically and industrially towards the development of new materials capable of displaying economically viable performances.[26,127,128,129,130]

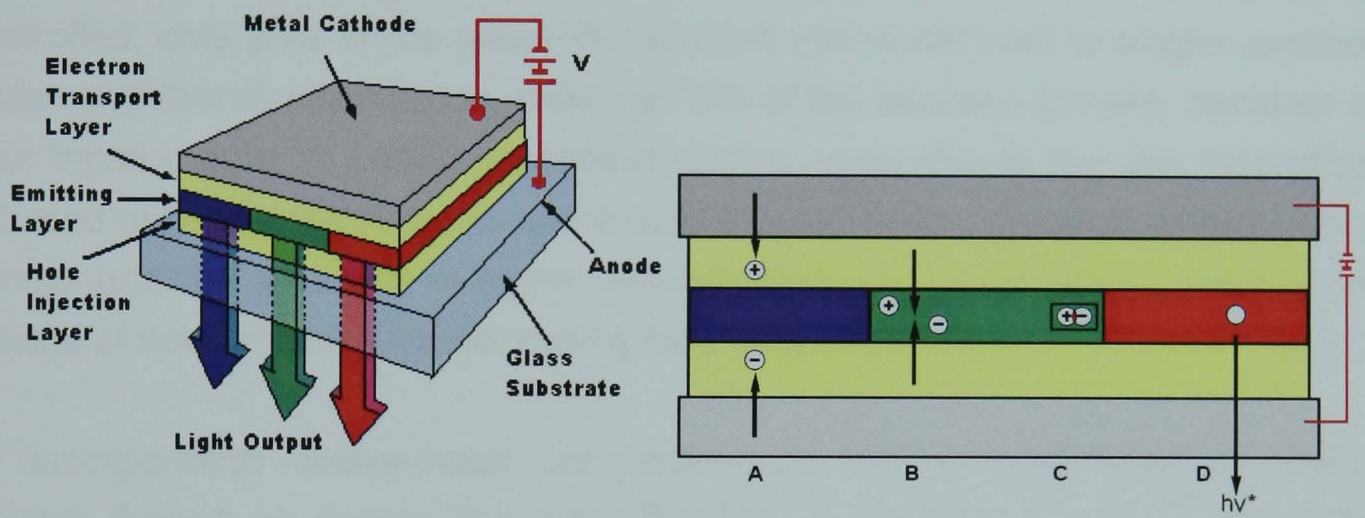

Figure 12: Basic structure of OLEDs (left), designed for conversion of electrical charge into light energy. Schematic representation of the working process involved in OLEDs (right); A: charge carrier insertion, B: charge migration, C: charge carrier recombination, and D: exciton formation leading to electroluminescence from the device.

The basic structure of a typical OLED consists of a multilayered arrangement of thin organic films sandwiched between two electrodes, shown in Figure 12. The two electrodes are usually an Indium Tin Oxide (ITO) anode and a metallic cathode, *e.g.* aluminium. The ITO layer is a transparent solid,[126] thus allowing the light generated from the device to be effectively displayed. The organic layers, as labelled in Figure 12, normally consist of a hole injection layer, an electron transport layer, in state of the art devices an exciton blocking layer (not shown), [128,130] and the all-important emissive layer. The emissive layer usually consists of an emissive charge-transport material, typically tris(8-hydroxyquinolate)aluminium (AlQ_3) or an organic polymer. The electrodes generate an applied voltage across the device from where electrons and holes are inserted into organic layers. These charges migrate towards opposite poles of the device and combine in the emissive layer, generating an electrically induced excited-state molecule or "exciton", Figure 12. It is the radiative

relaxation of the excited states in the emissive material that generate the luminescence observed from the device; hence the crucial importance of optimising this process with respect to the applied electric charge. Early OLEDs utilised organic fluorophores as their emissive material, however, a purely organic emitting-layer will be restricted in its upper limit of quantum efficiency.[125,129] The upper limit of efficiency is governed by spin statistics relating to how electroluminescent excited-states are generated,[131] represented schematically in Figure 13. Under electrical excitation these excitons are generated in both singlet and triplet states in a theoretical 1:3 ratio, respectively. However, radiative decay from triplet states is typically forbidden in organic molecules and only fluorescence, singlet emission, can contribute to device performance. If recombination of charge carriers to form excitons is statistically controlled, only 25% of the generated excited states will lead to singlet excited-states and therefore emission, wasting 75% of the excitons formed, because of their triplet nature.[132] Although recent studies have shown that the theoretical 1:3 ratio may be attenuated to some extent when there is a large singlet–triplet energy gap, for example in some polymer systems, nevertheless, there is an excess of non-emissive triplets during electroluminescence.

By incorporating heavy-metal complexes into the emitting layer of OLED devices (known as doping, the metal complex in question is referred to as the dopant) the electrically generated triplet excitons can be accessed by the spin-orbit coupling of the metal centre, and triplet-state phosphorescence can then contribute to the efficiency of the device. Either the heavy-metal complex can emit light directly, or it can transfer the harvested energy to a fluorophore. Therefore, unlike their organic predecessors, transition-metal doped emissive layers will facilitate triplet-based phosphorescence from the device, theoretically harvesting all of the previously wasted triplet excitons. Efficient S→T intersystem crossing, also induced by spin-orbit coupling, allows conversion of all singlet excitons to the lower energy triplet species, so all the luminescence observed can be isoenergetic, and uniform. Overall this approach of incorporating heavy metals into emitting systems has been dubbed "triplet harvesting" because, by employing triplet-based phosphors as the emitting species, the theoretical maximum internal quantum efficiency is increased from 25 to 100%.[25,133,134]

The three most important features when considering transition-metal complexes as luminescent materials for OLEDs are emission wavelength (λ_{em}), excited-state lifetime (τ) and quantum yield (Φ). The emission wavelength determines

the colour generated by the fabricated device. Long emission lifetimes severely decrease device efficiency, *e.g.* if a molecule remains in the excited state for too long then either non-radiative T–T annihilation occurs or conversion of electrical energy into photon energy is inhibited by ground-state depopulation.[131,133] Therefore, it is thought that luminescent materials should ideally exhibit a phosphorescent lifetime in the region of 100 ns – 1 μs at operating temperature, 298 K.[135] Overall, OLED efficiency is fundamentally governed by the quantum yield of the luminescent material, therefore, the dopant molecule should ideally have a quantum yield of luminescence approaching unity at 298 K. It is generally agreed that the minimum quantum yield acceptable for emitting materials is 0.25.

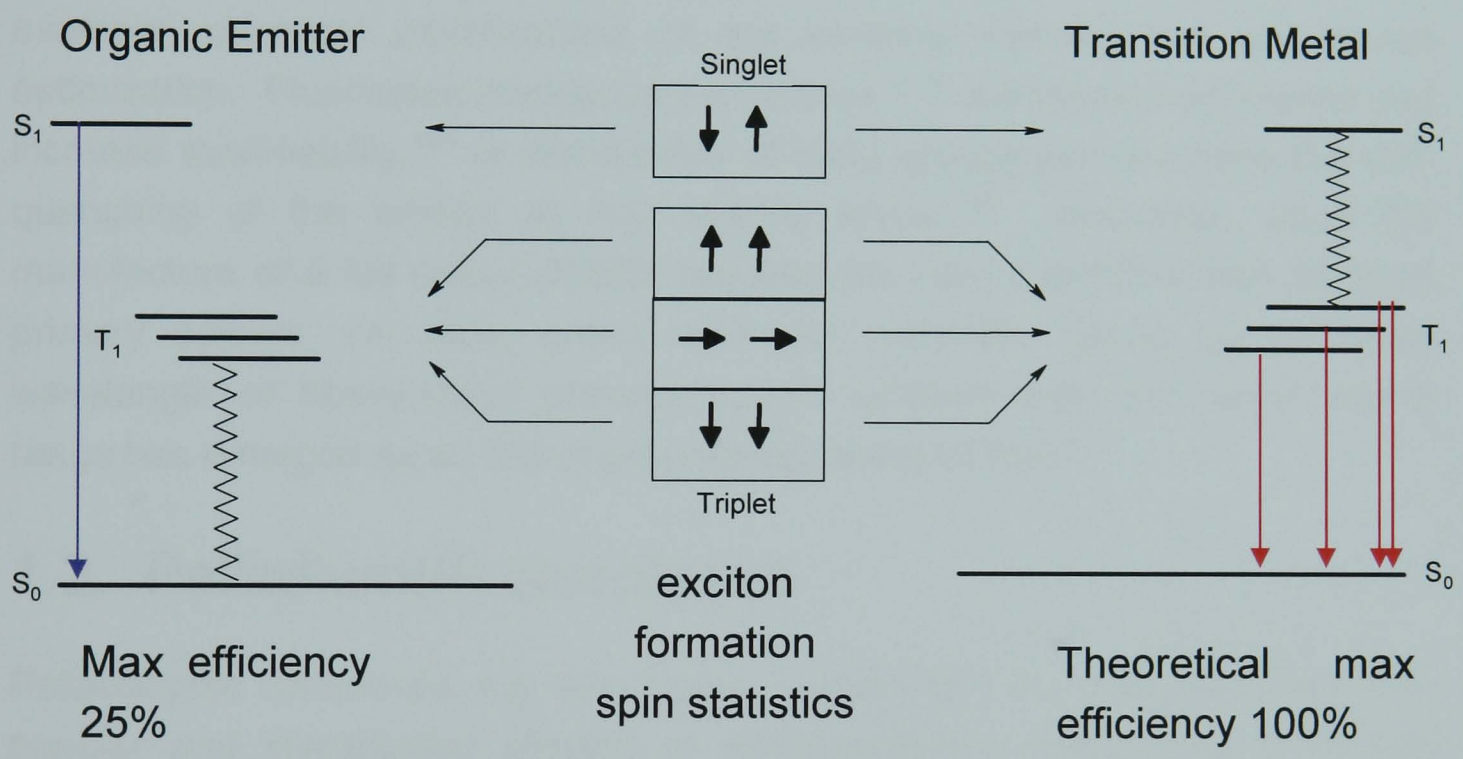

Figure 13: Spin statistics predict electroluminescence yielding singlet and triplet excitons in a 1:3 ratio. Spin-orbit coupling from heavy-metal doping allows intersystem crossing between singlet, S_1, and triplet excited-states, T_1. Additionally, spin orbit coupling will allow phosphorescence from triplet states, previously forbidden in organic molecules. Coloured direct arrows indicate radiative processes and zigzag lines represent non-radiative deactivation of excited states.

In addition to the above criteria, potential applicants must be easily fabricated into potential devices, usually through sublimation for vacuum deposition onto the ITO layer,[129,131,133] requiring compounds with good thermal stability. Charge neutrality is also important since it aids uniform deposition of the emissive material, whereas salts have a tendency to form crystalline layers which are detrimental to device performance *via* higher turn-on voltages, as well as

migration of ionic materials to electrodes which leads to a build-up of compounds along the interface. Finally, compounds are also required to possess longevity through reversible redox activity and photochemical stability, so that fabricated devices will have a suitable working life.

Most studies have been centred around iridium(III) complexes containing cyclometallated ligands such as ppy and its derivatives.[25,26,124,125] The use of cyclometallated ligands, apart from promoting emission, also allows the formation of neutral complexes.[133] Organometallic compounds, including platinum(II) complexes,[55] represent a new class of electroluminescent materials and have been successful as luminescent centres in many organic light emitting diodes (OLEDs)[25,64,136,137,138] Research is often aimed at creating novel compounds suitable for furthering applications and device performance. For example, chemical modifications of the emitting material can aid device optimisation. Fluorinated analogues can reduce T-T annihilation processes and increase sublimability,[139] or introduction of bulky groups can decrease the self-quenching of the emitter at high doping levels.[140] Moreover, since the manufacture of a full colour display requires the use of emitters with all three primary colours, *i.e.* blue, green, and red, rationally tuning the emission wavelength of heavy-metal phosphorescent emitters over the entire visible range has emerged as an important ongoing research task.[55]

1.2. Palladium(II) complexes

Palladacyclic complexes, *e.g.* see Figure 3 where M = Pd, are one of the most popular and investigated classes of cyclometallated compounds in current research, owing to the very high stability associated with such system.[67,68] Fine tuning the steric and electronic properties of the metal centre through ligand modulation has resulted in a vast array of applications,[73,141] such as amorphous films of photoconducting materials, as well as bioactive molecules.[142] The application of palladacycles has mainly been focused on catalytic processes[143,144,145,146] and only recently have examples of luminescent complexes begun to emerge.[52,57,147,148,149,150,151,152]

1.2.1. N^C^N palladium complexes

Direct cyclometalation is a particularly attractive method for the formation of a new M–C bond since it does not require prefunctionalisation of the ligand in order to achieve regioselective metalation. However, long reaction-times and high temperatures are usually required for this approach, and while formation of

pincer complexes is relatively straightforward for P^C^P and S^C^S donor sets,[64,153,154] difficulties are associated with N^C^N-coordinating ligands as they can adopt a variety of binding modes shown in Figure 14. Additionally, this feature is more dramatic for palladium than observed for platinum complexation,[66] therefore, special procedures are often required to induce regiospecific binding for N^C^N ligands, particularly with palladium.[68,69]

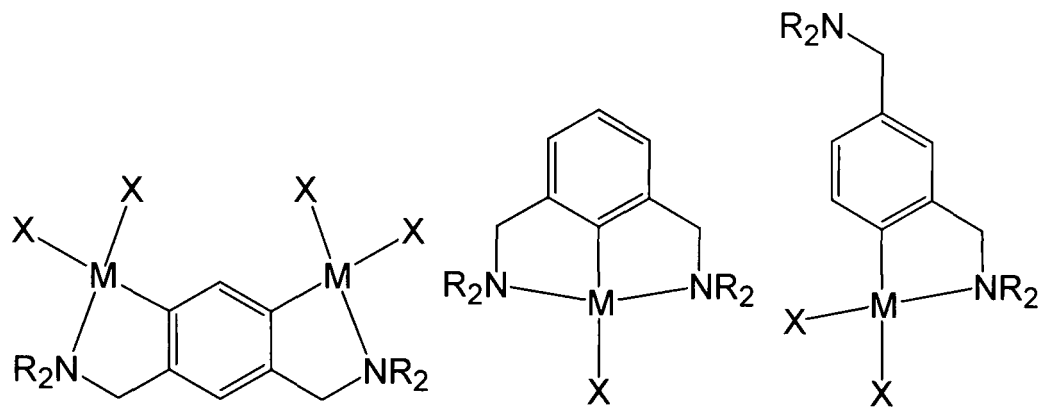

Figure 14: Variable binding modes associated with N^C^N donor ligands. Two individual metallacycles are formed on the same benzene ring (left), terdentate binding forming a bis-metallacyclic product (middle) and monocyclometallated yet *para* to the other potentially coordinating arm (right).[66] (M = Pt/Pd(II); X = halogen)

Cyclopalladation is generally considered as a two-step process which involves the prerequisite initial coordination of at least one ligating neutral donor holding the metal centre close to a C–H bond, and subsequent closure of the ring *via* the formation of a new metal-carbon bond. Whilst relatively straightforward for unsymmetric N^N^C ligands,[151,155] where the metal centre can be tightly held in position by the chelate effect of the mutually *cis*-nitrogen donors (a bpy fragment), the linear *trans*-donors of pincer moieties makes the direct cyclometalation route less reliable. The reduced tendency of bicyclic-cyclometallation in these species is thought to be a result of the relatively low bond strength of the M–N bond compared to alternative neutral donor species; the topic has been reviewed in 1998.[156] The lack of binding affinity of the two *trans*-nitrogens can lead to kinetically controlled products. Consequently, double metalated products with each N coordinated to a different metal atom have been observed,[66,67] Figure 14a). Various methods have been developed for regioselective cyclometalation of N^C^N pincer ligands,[67] Scheme 1, such as oxidative addition to carbon-halogen bonds,[15,68,157] transmetalation,[69] and even transcyclometalation.[63,84] These methods, however, require prefunctionalisation of ligands or prior coordination to a labile metal-ion before substitution can take place. All of these approaches have added difficulties in their application, and therefore, are utilised only when direct metalation has been proved ineffective.

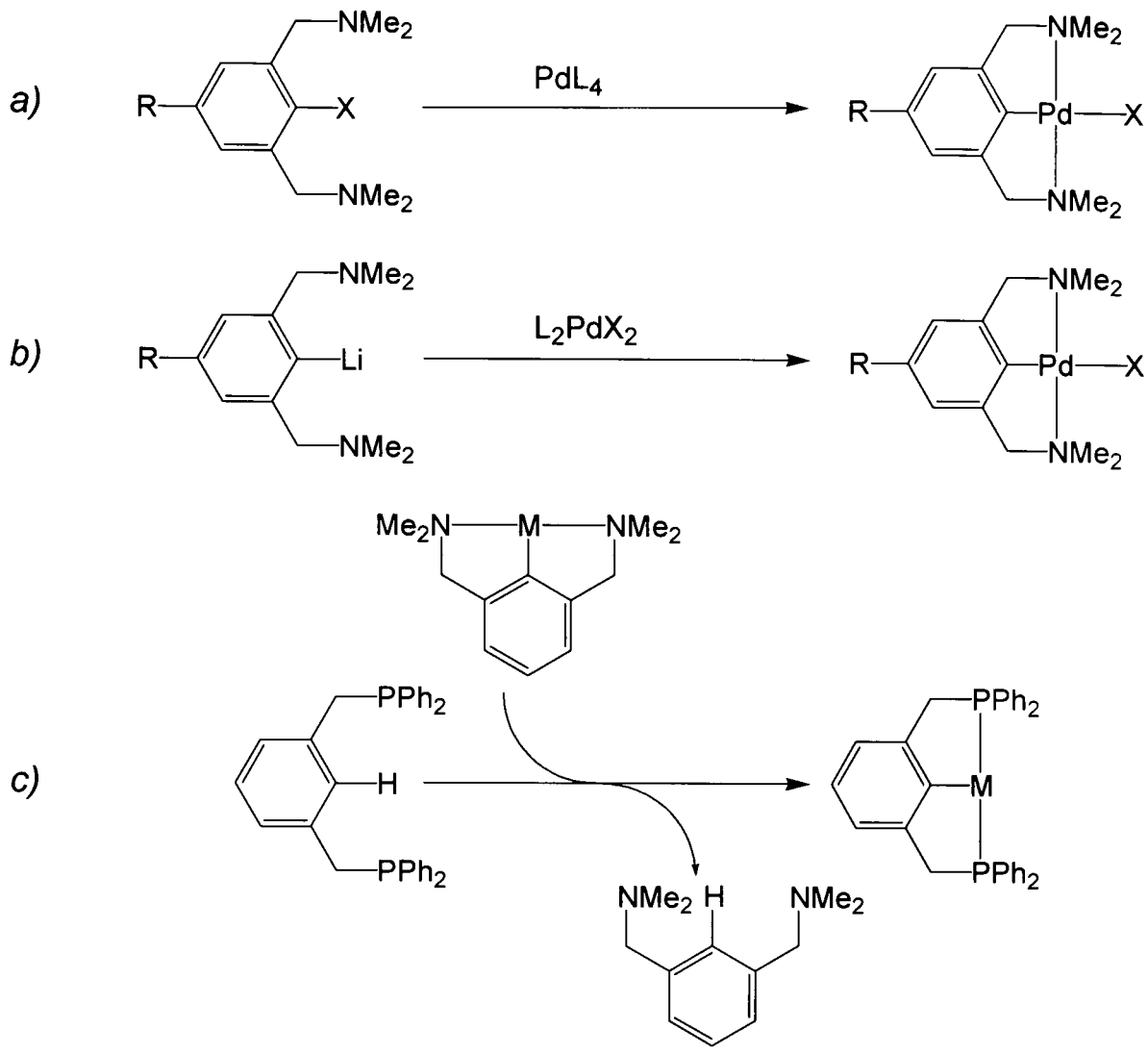

Scheme 1: Regioselective cyclometalation can be induced through either oxidative addition of a carbon–halogen bond (top),[15] metathesis of a regiospecific labile metal ion, such as lithium, known as transmetalation,[69] or transcyclometalation which involves substitution of a cyclometallated metal ion from one ligand system to a more strongly binding system (X = halogen).[63]

1.2.2. Photochemistry

Although luminescent palladium complexes have been proposed for a number of different purposes including OLEDs and mesogenic materials,.[75,141,152,155,158,159] luminescent studies involving palladium(II) complexes, particularly in solution at room temperature, are exceedingly rare.[75,147,148] Examples are largely restricted to frozen samples and the solid state.[152] Most palladium compounds suffer from excited-state deactivation *via* thermally accessible metal-centred excited-states similar to those observed in platinum analogues, Section 1.1.1.[160,161] Indeed the problem is normally worse in Pd(II) than Pt(II) for a given type of ligand,[162] since the ligand-field splitting is smaller for the second row element. The deleterious effect can be attenuated by reducing the ability to thermally populate these deactivating states either by judicious choice of the types of ligands employed[163] or by inhibiting the population of the metal states in frozen glass samples at 77 K[154,164] or in a rigid host matrix to disfavour geometrical distortion.[165,166,167]

Alternatively, luminescence can be achieved in palladium complexes through the generation of intermolecular excited-states (aggregate states) arising from pairing interactions at either high concentrations or in crystal packing where intermolecular contacts are of the appropriate distance.[150,151] However, such contacts behaviour is again less frequently observed for palladium complexes than for their platinum analogues.[152] Additionally, regardless of the approach taken, luminescence is often very weak.

While cyclometallated platinum(II) complexes have represented an important class of luminescent complexes as dopants in OLEDs, the heavy-atom effect exerted by the palladium(II) metal-centre is much weaker. However, luminescent cyclopalladated complexes do display properties making them applicable as potential candidates in this field[154,166] and the optimisation of photogeneration could be very important for such exploitation.

1.2.3. Catalysis

The development of new catalysts is a major topic of interest for research groups working on palladium complexes.[168,169,170] Two important organic transformations catalysed by palladium species are the Suzuki[171] and Heck[172] cross-coupling reactions, Scheme 2 and Scheme 3, respectively.

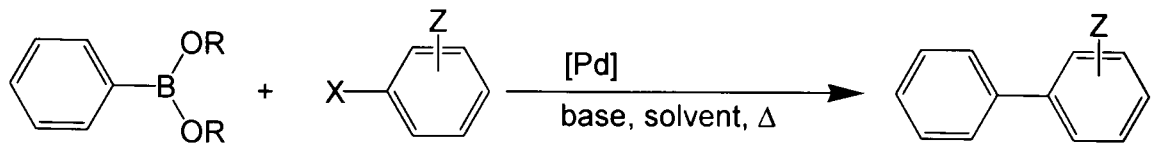

Scheme 2: The Suzuki reaction is a palladium catalysed cross-coupling reaction between organo-electrophiles and organoboranes for the formation of new carbon-carbon bonds.[171]

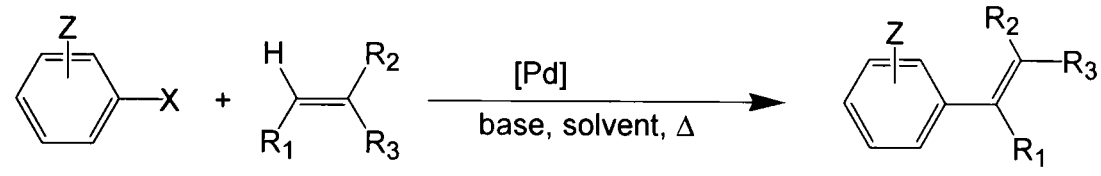

Scheme 3: Heck reaction: palladium catalysed cross-coupling reaction between aryl-halide and an unsaturated alkene for the formation of a new carbon-carbon bond.[172]

The Suzuki reaction is a well developed reaction that offers a powerful and general methodology for forming carbon-carbon bonds, with a well understood reaction mechanism, shown in Scheme 4.[171] The Heck reaction, while also a very useful synthetic method for the generation of carbon-carbon bonds that has found many applications,[173,174,175] still remains clouded with issues that require resolution before it can be exploited to its full potential. Both reactions are still current topics of interest in research, with a view to improving reaction performance such as catalytic activation of aryl-chlorides[175,176] (which, while being relatively unreactive, are the cheapest and most readily available of the aryl halides), the cross-coupling between sp^3-based partners,[171,177] and eventual aims to C–H bond activation. Other interests include making these reactions more economical and practical, such as lower catalyst loadings, lower temperatures and shorter reaction times, to ultimately move them from the academic laboratory into industrial applications.

The Heck reaction, which involves olefination of aryl halides or sulfonates, Scheme 3, is an important reaction in many synthetic protocols.[173] Homogeneous catalysis, whilst being more active than heterogeneous systems, is fraught with disadvantages. Firstly, the high costs associated with palladium catalysts, of both the precious metal and synthesising the complex ligands currently employed, means that the consumption of large quantities of a catalyst is not economically viable. Secondly, contamination of reaction products by the catalyst and by-products thereof need to be tightly controlled. Both are features which make homogeneous catalysis an unattractive process when compared with heterogeneous systems, which allow catalysts to be recovered and recycled after the completion of the reaction.

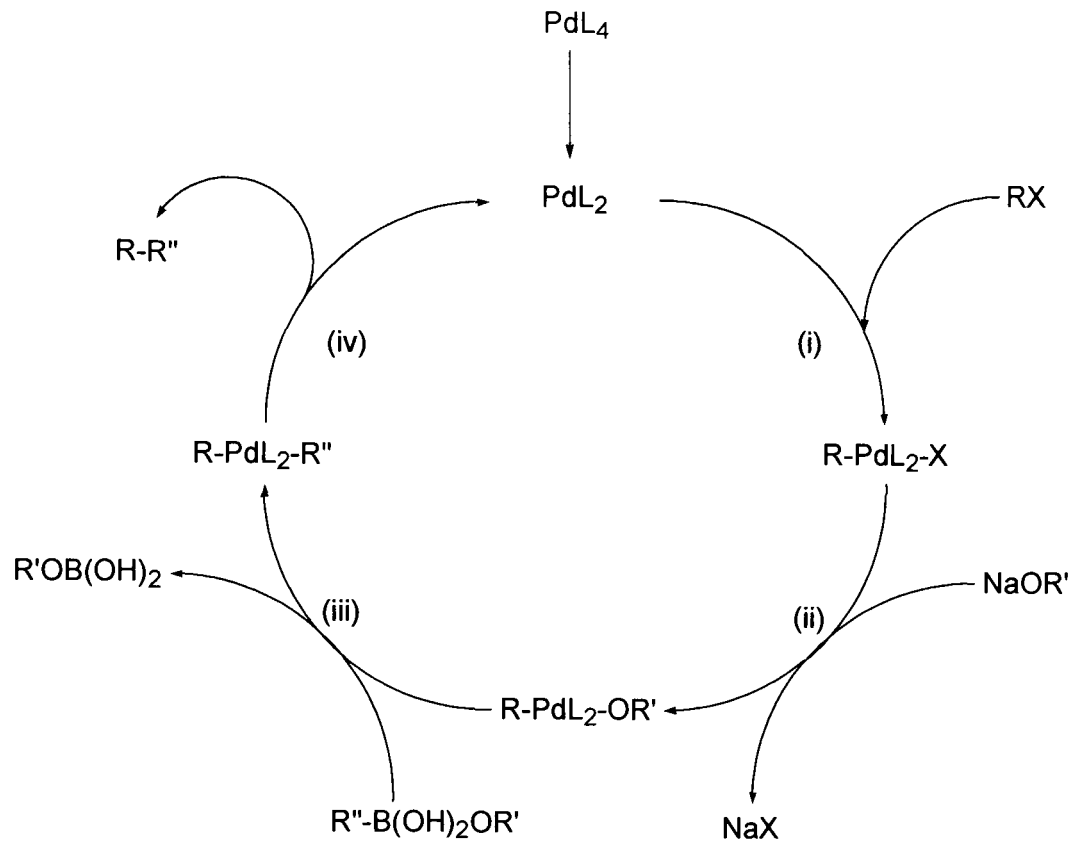

Scheme 4: Suzuki cross-coupling reaction mechanism; (i) oxidative addition; (ii) base mediated metathesis; (iii) transmetalation; (iv) reductive elimination[171]

Development of new, highly-active homogeneous catalysts, that possess high stability and can operate in exceedingly low concentrations, can be seen to massively reduce the costs and contamination issues. However, the factors which control overall rates and stability of catalysts do not appear to be well understood, and literature seems mainly focused on listing new catalysts and attempting to demonstrate their turnover numbers (TON, number of moles of product that can be produced per mole of catalyst employed) and turnover frequencies (TOF, number of moles of product which can be produced per unit time). A major area of contention with current Heck catalysis research is the exact nature of the reaction mechanism, particularly the role the palladium metal plays in the C–C bond forming process.[178] Three distinct systems, or theories, have emerged as potential modes of catalytic activity for the palladium species. One of the areas with a lot of focus and attention is aimed around discrete complexes as catalytic centres; this is the route most popular with advocates of the palladacycle.[145,168] Since 1995, when Herrmann *et al.* announced the use of the first palladacycle in the catalysis of Heck couplings,[179] the activity of many palladacycles has been explored for catalysis research, both extensively and successfully for a number of organic transformations.[180] Additionally, investigations into the ability to catalyse Heck, Suzuki, and other cross-coupling processes by complexes based around terdentate ligands containing M–C bonds, particularly the field of "pincer" ligands, have been rewarded with many species displaying high degrees of catalytic activity.[181] It is

keenly thought that through ligand modification, tuning the properties of the metal centre can influence activity (TONs and TOFs) of the system employed.[67] This approach has developed a wide range of palladacyclic structures, with many different binding motifs and geometries, with little rhyme or reason to activities of specific entities.[182]

The second approach can be thought of as dissociative ligand systems, such as the "traditional" catalytic systems *i.e.* $Pd(OAc)_2$ plus PPh_3.[172,183] A four-coordinate metal centre is used, or created *in situ*, and the presence of labile ligands is based around the need for metal-centre stabilisation.

The final approach has been termed "ligandless" catalysis which is based on *in situ* generation of palladium colloids.[184,185] Researchers advocating these systems take the approach of believing that all ligands simply retard catalysis and should be avoided completely.[186,187] Ligandless colloid systems have been shown to display high activity, but are known to suffer from a lack of stability through ready decomposition to palladium black, a relatively inert, inactive form of palladium.

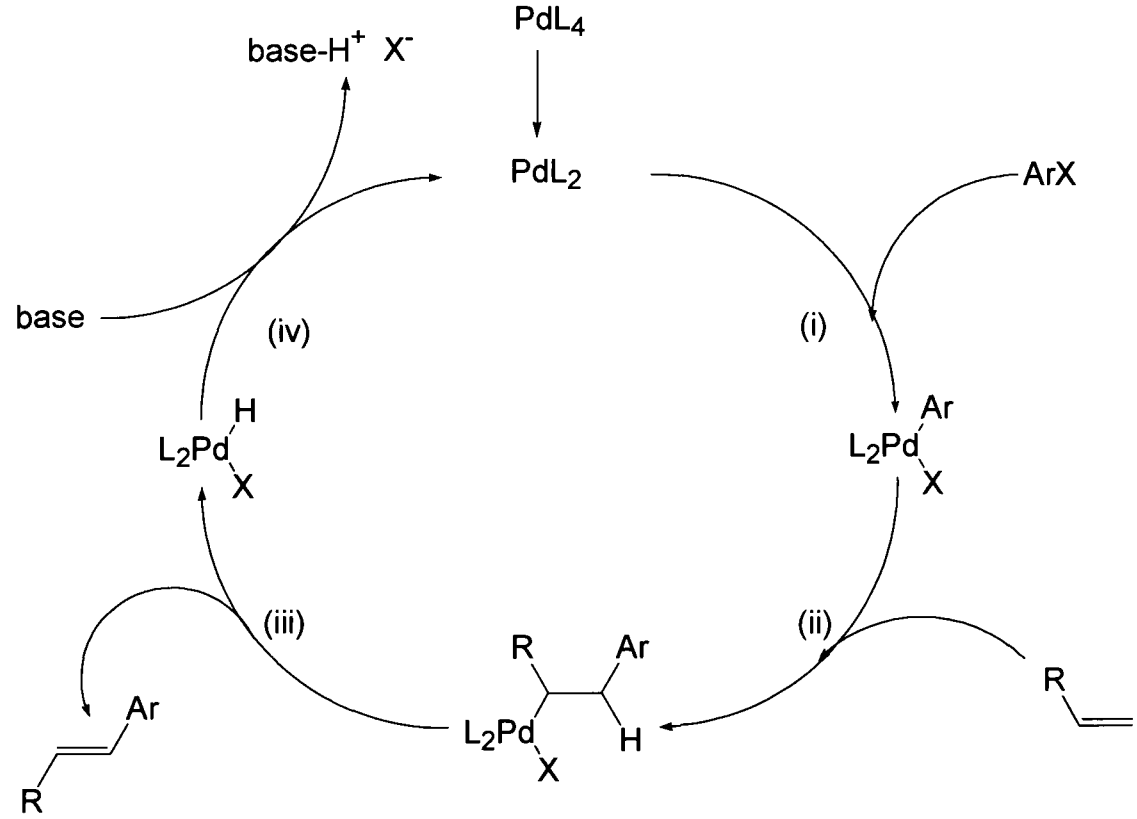

Scheme 5: Dissociative mechanism commonly associated with palladium Heck cross-coupling reactions. Typically the palladium source will be palladium salt coordinated with either phosphines or acetates. (i); oxidative addition, (ii); olefin insertion, (iii); β-hydride elimination, (iv); catalytic reduction completing catalytic cycle.

Traditional palladium catalytic systems for the Heck reaction have been thought to proceed *via* a Pd(0)/Pd(II) cyclic mechanism, shown in Scheme 5, involving

the *in situ* generation of a Pd(0) species, which undergoes oxidative addition of the aryl-halide bond yielding a Pd(II)-aryl intermediate. Coordination of the olefin and its migratory insertion into the Pd-aryl bond leads to a Pd(II)-alkyl complex. β-Hydride elimination affords the arylated olefin and a Pd–H species, which, through reductive elimination, regenerates the Pd(0) catalytically active species. However, since the discovery of the catalytic activity of palladacycles, the intermediary of a Pd(IV) species in a Pd(II)/Pd(IV) cycle has been invoked,[179,188] leading to the possibility of different modes of action possible depending on the type of palladium source employed. There are many voices of unrest against the existence of the Pd(II)/Pd(IV) cycle, refuting its legitimacy.[178]

Recent evidence elucidating that the active species in the Heck reaction can be metallic palladium[189] has opened up the field of colloidal based systems, and many studies have highlighted possible modes of decomposition and leaching of palladium from palladacycles, yielding an active Pd(0) species with particular focus on Herrmann's original complex.[190] Such attention has led to authors citing the use of palladacycles in catalysis as simple "precursors" for the gradual formation of low levels of Pd(0) colloids, and as such, are simply bystanders that play little or no role in the catalytic process.[189] This slow leaching of palladium as colloids from palladacycles is thought to account for induction periods associated with many of these systems, and it is also thought to account for controlling the levels of colloidal palladium in solution. At high concentrations, such as those presented by the use of simple palladium salts, such as $Pd(OAc)_2$, palladium is released quickly into solution and the formation of inactive palladium black is a consequence of Pd(0) aggregation. This has led to the belief that the relatively high turnover numbers of palladcycles can be attributed to this very slow leaching, and not a consequence of chelation generating a highly stable active system. Although high palladium concentrations are often observed to induce a reduction in activity associated with Pd(0) aggregation, it has also been interpreted as an increase in complex aggregation inhibiting axial interactions required for the catalytic process. Neither argument has concrete evidence for its individual mechanistic views.[191,192,193] Furthermore, contrary to what has been discussed above, certain complexes have shown an absence of an induction period, consistent with there being no slow initial catalyst reduction step associated with the Pd(0) mechanism.[61,146] Such findings, coupled with a number of compounds remaining active during the mercury drop test,[194] (showing no reduction in activity from addition of elemental mercury, which is known to selectively poison

heterogeneous catalysts such as colloids)[61] support evidence for these species behaving homogeneously.

Authors citing activity in the presence of oxygen as evidence of the Pd(II)/Pd(IV) cycle, have been rebuffed by the known activity of colloids in systems open to air, and added them to the high temperatures required for palladacycles to become active. These high temperatures can be attributed to either the temperature required to induce decomposition of the pincer systems compared to simpler palladium species,[61,189] or simply the energy of activation required to induce the high coordinate intermediates, such as those observed after MeI insertion into both palladium and platinum(II) complexes,[195] shown in Figure 15.

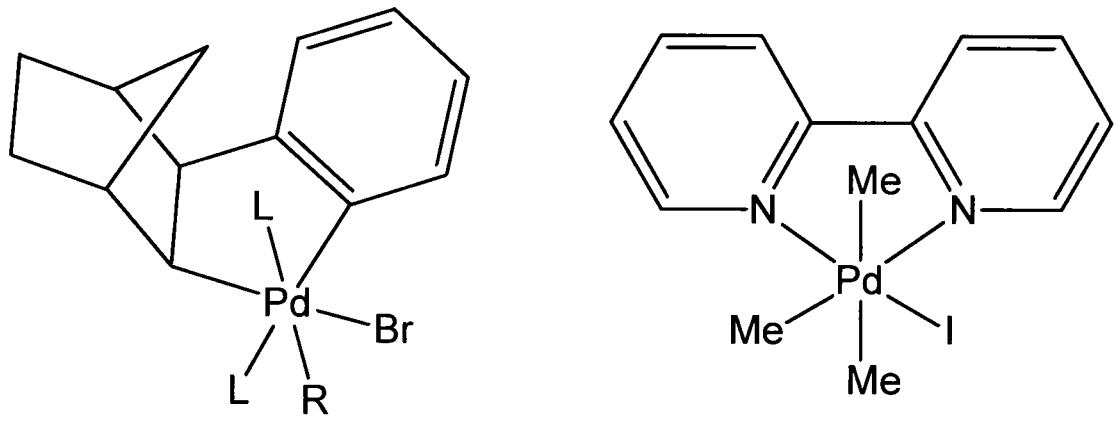

Figure 15: Two identified Pd(IV) species that could give clues to the mode of action of the Pd(II)/Pd(IV) cycle; (left) L = PPh_3, R = Ph; (right).

It has been postulated that the most important factor in controlling catalyst lifetime is the need to strongly stabilise the palladium centre to prevent decomposition, thus preventing metal aggregation. This is evidently achieved in palladacyclic systems as the metal centre is tightly coordinated. Additionally, impressive conversion numbers have been observed for P^C^P systems[196] (showing no presence of colloidal palladium) with catalyst recovery after heating under extreme conditions indicating that the Pd–C bond can be conserved throughout catalysis. Pincer complexes are known to have increased stability and are less likely to decompose under reaction conditions when compared to simpler palladacycles.[146] These features point to a catalytic cycle involving Pd(0) intermediates being highly unlikely, especially since metal reduction is thought to require Pd–C bond fission.[196] The absence of any evidence for Pd–C bond cleavage and concomitant Pd(0) formation is a strong indication, but clearly not yet proof, of the operation of a Pd(II)/Pd(IV)/Pd(II) cycle.

Decomposition of the palladium colloid systems can be controlled somewhat by tetraalkylammonium halide salts, and therefore the increase in activity

associated with its addition to catalysis involving palladacycles has also been noted as further evidence that colloidal chemistry is the true reaction mechanism.[187] However, the use of these salts has been hypothesized to aid stability of one of the key intermediates in the Pd(II)/Pd(IV) cycle and therefore there is still no conclusive support for either mechanism. Dispite its advantages, NBu_4Br is an added expense and achieving high TONs without this additive is desirable regardless of the system employed.[187]

There are many advantages that can be discerned from a Pd(II)/Pd(IV) cycle. The stabilisation of the metal centre afforded by the M–C σ-bond is assumed to efficiently prevent metal leaching, removing the contamination problem common to catalysts containing exclusively heteroatom-coordinated metals. The stability of the metallocyclic rings is the reason motivating several mechanistic investigations of catalytic processes through the many ligand modifications available to this class of complex, Figure 3.[67,196] The electronic properties of the metal centres are thought to be highly sensitive towards modifications in the donor array, therefore, electronic fine tuning through variation of substituents on the benzene ring, as well as chiral or steric modifications around the catalytic site, may allow the metal to discriminate against some substrates, or to create a pocket for asymmetric catalysis of chiral products.[197] As a result, some attention has been paid to the development of new ways of enantioselective synthesis through palladium catalysis.[198,199]

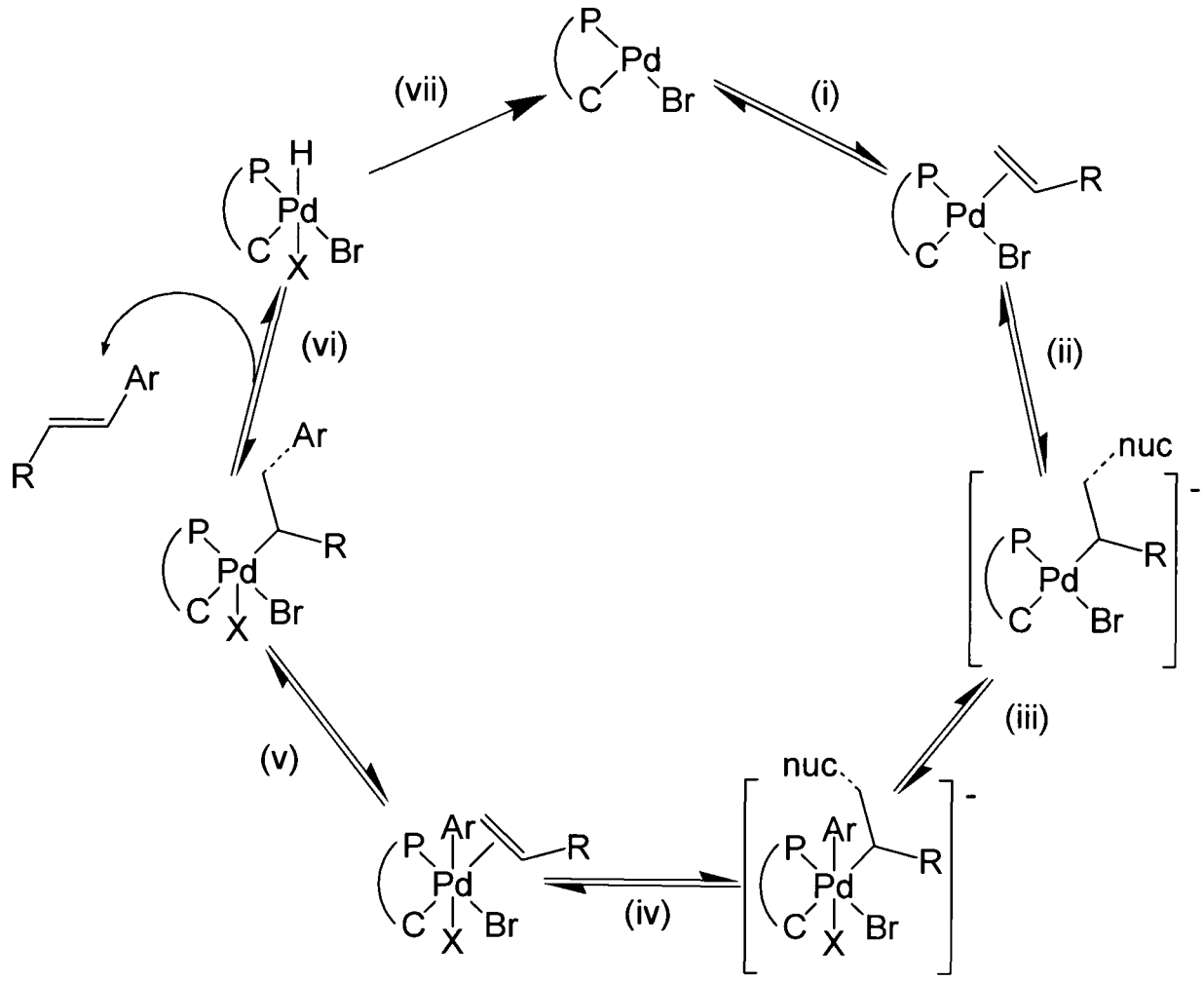

Scheme 6: Shaw's proposed mechanism for the much debated Pd(II)/Pd(IV) cycle.[195] Key steps; (i) CH_2=CHR addition; (ii) reversible attack by nucleophile (e.g. OAc^-, Br^-, OH^-), shown at the terminal carbon, but which could alternatively occur at the internal carbon atom; (iii) oxidative addition of aryl halide; (iv) loss of nucleophile; (v) aryl migration; (vi) β-hydride elimination; (vii) base mediated removal of HX (X = Br).

The mechanism proposed by Shaw involving the Pd(II)/Pd(IV) cycle, shown in Scheme 6,[195,200] starts with the alkene coordinating to the Pd(II) and being reversibly attacked by a nucleophile to give a negatively charged alkyl species. The Pd(II) centre is now electron rich and oxidatively adds ArX. Loss of nucleophile regenerates the coordinated alkene which can undergo migratory insertion of the aryl group. Finally, β-hydride elimination gives the product, and removal of HBr by the base regenerates the Pd(II) catalysts. Whether the initial step of the Heck reaction is coordination of the alkene or the oxidative addition of the aryl-halide bond is therefore in some debate.[195,196] Specifically in the presence of allyl-ancillary coordination, the terdentate ligand is known to be able to dissociate the peripheral nitrogen donors readily in solution, so that a dynamic equilibrium between η^3 and η^2 coordination is observed even at room temperature, Scheme 7.[201,202]

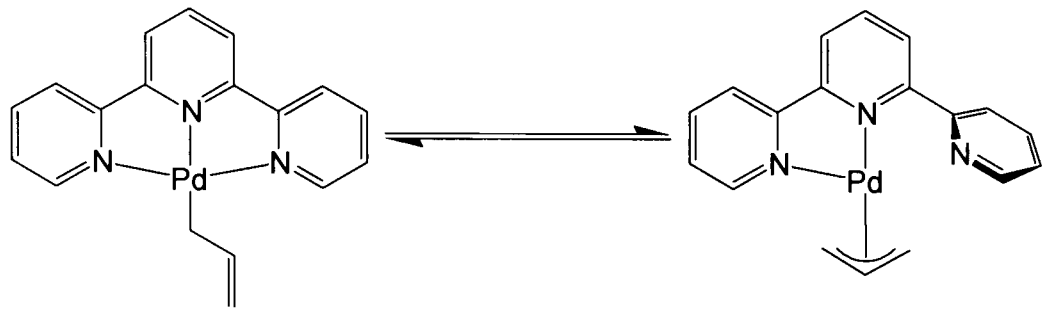

Scheme 7: Both η^1/η^3 allyl-coordination is observed even at low temperature, which in turn creates a tridentate (arm-on) and bidentate (arm-off) coordination of the terpy.[201,202]

In conclusion, the major aim is in developing catalysts with sufficient activity (*e.g.* coupling aryl-chlorides), selectivity (minimising side products), and of sufficient throughput (linking not only high TON but also high TOF). However, many decomposition pathways have been elucidated for palladium catalysts,[203] and it is known that for simple coupling reactions, such as the Heck couplings with aryl-iodides and acrylates, or Suzuki couplings of activated aryl-bromides with phenylboronic acid, virtually any palladium source is capable of producing high TONs,[178] making it hard for researchers to know which is the best route to pursue. Contradictory reports have been published on the legitimacy of both discrete and colloidal reaction systems, such as publications citing higher activities of supposedly "precatalytic" palladacycles over colloidal systems, citations claiming proof of inactivity until induced metal leaching, reports regarding the catalytic activity of palladcycles in the presence of colloidal poisoning mercury, and other selected reports are hard to explain. As such, the only thing that is clear is that no clear explanation for the activity of the palladium centre is at hand.[180]

1.3. Concluding remarks and research aims

The N^C^N coordinating motif of 1,3-di(2-pyridyl)benzene has already been identified as possessing many attractive features when bound to d^8-metal ions.[74] Particularly when used to create platinum(II) complexes, this ligand and its simple 5-position benzene-ring substituted adaptations, produce complexes with impressive photophysical properties compared to terdentate platinum(II) complexes with N^N^N or N^N^C ligands.

The first aims of this research were focused upon expanding the current library of 5-substituted complexes, and investigating the effects such modifications will have upon the photophysical properties of the complexes. Further exploitation of the 1,3-di(2-pyridyl)benzene structure was also addressed through incorporation of a number of functional groups into HL^1. Specific aims of each

variation are addressed in the opening comments of each section, including, for example, exploitation of host-guest chemistry of polyether chains to create potential selective luminescence-based metal-ion sensors.

Platinum(II) complexes of HL^1, due to the square-planar geometry adopted by the system, are also known to have the ability to interact with one another in solution-state self-quenching of excited-state molecules.[1,7,74] Modifications of the 5-position of the benzene ring are thought to influence this phenomenon, and investigations into the crystal structures of many of the complexes formed were used to give some insight to spectroscopic data obtained from both solution and solid-state investigations.

Investigations into substitution of the ancillary chloride ligand in 1,3-di(2-pyridyl)benzene-2-platinum(II) chloride were undertaken, producing a number of derivatives including those with neutral nitrogen and phosphorus donors. Due to intense recent interest in acetylide systems,[5] acetylides as co-ligands were also explored. Investigations were then made into the physical and photophysical properties of the complexes formed from these reactions.

It has previously been established that the palladium(II) complexes of HL^1 are not easily formed from direct cyclometalation with a variety of palladium sources.[66] Through the use of ligand modification, N^C^N palladium complexes were targeted with a view to investigating their photophysical properties. Room temperature phosphorescence is rarely observed from palladium(II) complexes, and with the impressive photophysical properties of the platinum analogues in mind, the palladium counterparts were clearly worthy of investigation.

Palladacyclic pincer complexes are somewhat of a hot topic in current catalytic chemistry. The N^C^N palladium(II) complexes formed were expected to be catalytically active in a number of palladium-catalysed organic transformations. It is also hypothesised that the subtle changes in electronic environment of the metal centre, available through ligand modification, may also have a significant influence upon the catalytic activity of the palladium complexes. With this in mind, the palladium species formed were investigated in attempts to correlate activity in Heck reactions with electronic subtleties of the metal centre.

CHAPTER 2

PLATINUM(II) COMPLEXES OF 5-SUBSTITUTED 1,3-DI(2-PYRIDYL)BENZENE LIGANDS

2. Platinum(II) complexes of 1,3-di(2-pyridyl)-benzene ligands

The primary synthetic target of this part of the work was aimed at expanding the current catalogue of 5-substituted 1,3-di(2-pyridyl)benzene ligands. The high-efficiency luminescent materials of N^C^N coordinated platinum(II) compounds were already known to be tuneable with respect to their emission energy, but only three examples had been reported at the outset of this work.[74] Therefore, a series of synthetic targets with varying donor strength were designed, retrosynthetic analysis of which highlighted C–C bond forming coupling reactions as an effective synthetic protocol.

2.1. Synthesis of ligands

2.1.1. Stille cross-coupling reactions

The 1,3-di(2-pyridyl)benzene motif, HL^1, was prepared throughout *via* a Stille cross-coupling reaction,[204,205,206] Equation 2. The Stille reaction is a palladium-catalysed reaction for coupling an organotin compound with an sp^2-hybridised organo-halide. Trimethylstannyl or tributylstannyl compounds are commonly used, and, although trimethylstannyl compounds show higher reactivity compared with the butyl derivatives, the toxicity of the former is *ca.* 1,000 times higher than that of the latter. Therefore, the less toxic 2-tri-*n*-butylstannnylpyridine was used, typically 1.25 equivalents per aryl-halide bond, due to competitive formation of homo-coupling products. While N^C^N binding ligands have been prepared by other methods in the literature, including Kronke pyridine synthesis[197] and cobalt catalysed ring closure between nitrile and acetylene,[207] the Stille reaction was the chosen approach because the desired products could readily be synthesised through one reaction with commercially available starting materials, diversification of products could easily be achieved through simple modification of the benzene ring prior to, or after the use of the Stille reaction, and the reaction possessed none of the risks associated with alternative cyclotrimerisation reactions that involve large quantities of acetylene gas.[208]

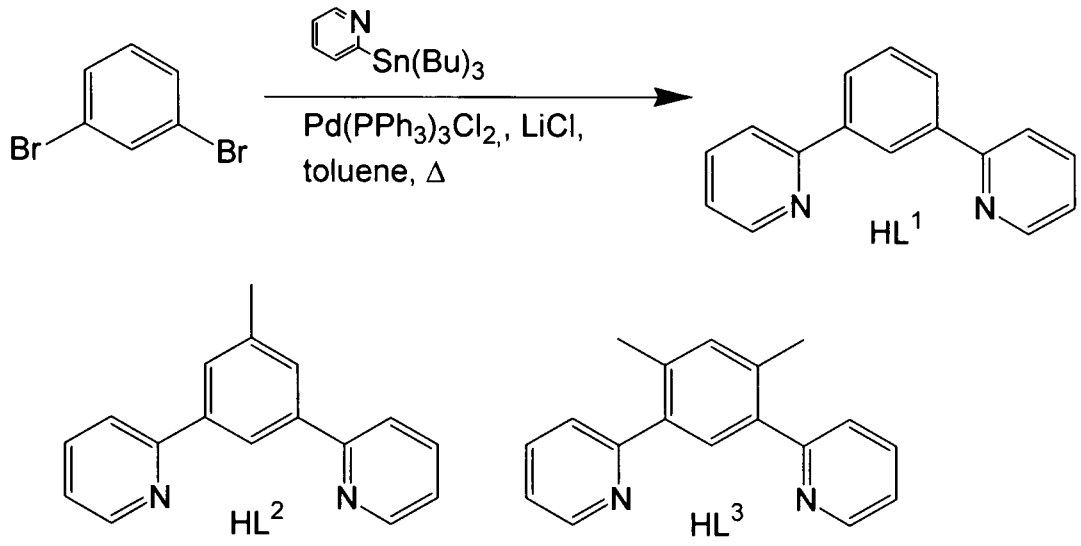

Equation 2: Stille cross-coupling reaction used to synthesise the 1,3-di(2-pyridyl)benzene unit, HL^1, and variations thereof; including 1,3-di(2-pyridyl)-5-methylbenzene, HL^2, from 1,3-dibromo-5-methylbenzene and 1,3-di(2-pyridyl)-4,6-dimethylbenzene, HL^3, from 4,6-dibromo-m-xylene.

All of the precursors were produced from a starting material containing a *meta*-dibromo substituted aromatic ring; for example 1,3-dibromobenzene, to prepare HL^1 in Equation 2. The 5-position on the benzene ring can be modified to achieve a series of related compounds. The substituted ligands examined in this work can be split into 2 sub-groups, (i) those where the benzene ring is substituted with non-aromatic functionalities (*e.g.* 5-position substitution = Me) and (ii) those which contain aromatic substituents.

The core structure, HL^1, was produced in 60% yield, whilst 1,3-di(2-pyridyl)-5-methylbenzene, HL^2, and 1,3-di(2-pyridyl)-4,6-dimethylbenzene, HL^3, were prepared from their respective dibromo-functionalised starting materials. Similarly, the 5-hydroxy and 5-methoxy ligands HL^4 and HL^5, were synthesised from 3,5-dibromophenol as shown in Scheme 8. 3,5-Dibromophenol was converted to the methoxy substituted intermediate, 3,5-dibromoanisole, through deprotonation in acetonitrile followed by treatment with iodomethane at room temperature. The Stille reaction proceeded in substantially higher yield for HL^5 compared to the phenolic analogue, HL^4. A number of subsequent reactions have confirmed that yields are consistently poor for substrates with unprotected hydroxyl groups.

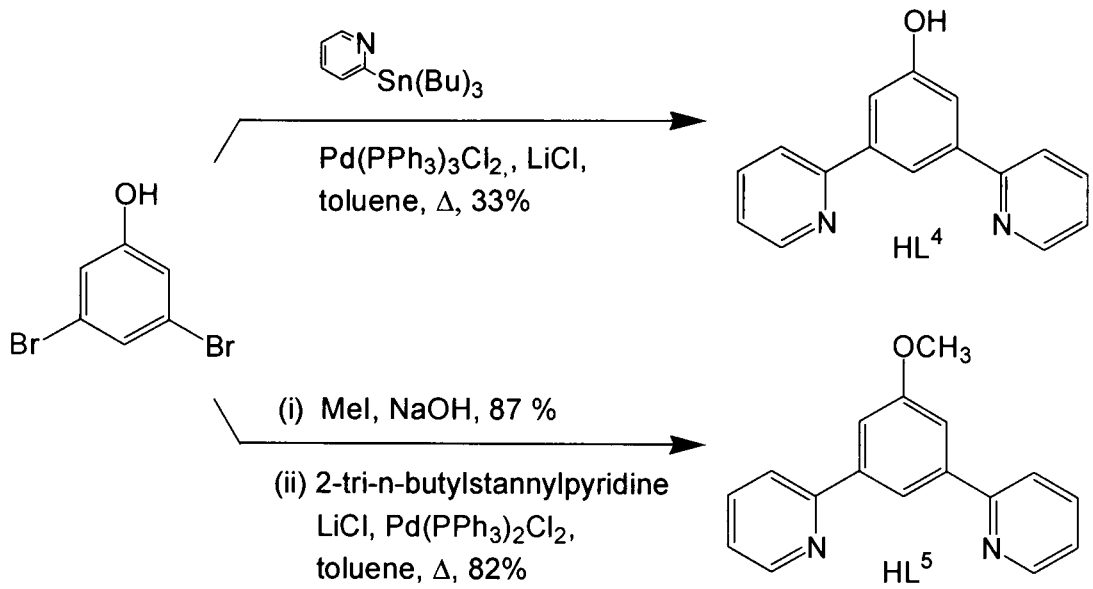

Scheme 8: Use of the Stille coupling reaction to create 5-OR substituted N^C^N ligands. R = H or CH_3, HL^4 or HL^5 respectively.

The 5-aryl-substituted ligands, HL^7–HL^{13}, and HL^{16}–HL^{21} were synthesised by a combination of coupling reactions *via* one of four routes, outlined in Scheme 9. The ligand 1,3,5-tri(2-pyridyl)benzene, HL^7, was also directly prepared in one step by the Stille reaction, Scheme 9: Route A: reaction between 1,3,5-tribromobenzene (tbb) and an excess of 2-(tri-*n*-butylstannyl)pyridine afforded the C_3-symmetric ligand in 40% yield. All of the other ligands in this section contain 2-fold symmetry and required the selective substitution of 2 from 3 bromine atoms of the starting material tbb with the 2-pyridyl functionality. The third bromine was used to substitute with the appropriate aryl group, affording the desired ligands, Scheme 9: Routes B, C and D.

The Stille cross-coupling reaction of tbb with a reduced quantity of stannyl reagent (2.2 equivalents) was found to yield a key intermediate for further ligand modification, 1,3-di(2-pyridyl)-5-bromobenzene, HL^6. The bromo-functionalised compound could be reacted to produce a variety of 5-substituted ligand systems, Scheme 9: Routes C and D. Previous work on the synthesis of 5-functionalised-1,3-di(2-pyridyl)benzene derivatives has proceeded *via* this intermediate, obtained by either Stille reaction or a related organozinc species prepared *in situ* (Negishi-type coupling).[209,210] Previous synthesis of this compound by Stille coupling reported yields of 35%.[211] However, it was noted during the present work that this compound is susceptible to competitive hydro-debromination under Stille conditions, as well as further reaction towards the tripyridyl compound HL^7. The optimal reaction time for HL^6 was found to be around 20–24 h, leading to yields of 50–55%. Significant quantities of side products 1,3-di(2-pyridyl)benzene, HL^1, and 1,3,5-tri(2-pyridyl)benzene, HL^7, were isolated when longer reaction times were employed. Once HL^6 had been

successfully isolated the remaining bromine was then available for further cross-coupling to introduce the requisite aryl group. This strategy was explored for the synthesis of a number of ligands outlined in Scheme 9: Routes C and D.

2.1.2. Suzuki cross-coupling reactions

The Suzuki cross-coupling reaction has become established as a powerful tool in C–C bond formation from arylboronates or boronic acids, with aryl halides or triflates.[171] A general reaction equation for the Suzuki-coupling is shown earlier in this report Section 1.2.3; Scheme 4. The reaction has a number of attractive features; for example, it proceeds under mild conditions, tolerates a broad array of functional groups, and yields non-toxic by-products, whilst starting materials such as aryl-boron reagents and aryl-halides are readily accessible substrates, and reactions can even proceed in the presence of oxygen and water when specialist catalysts are used.[212]

From the key intermediate HL^6, the substitution of the final bromine atom on the benzene ring could readily be achieved through Suzuki cross-coupling reactions, Scheme 9: Route C, to generate ligands HL^8, HL^{11-13}, and HL^{16} using commercially available boronic acids. An alternative approach of mono-substituting the tbb starting material with the requisite aryl-group by Suzuki coupling, prior to reaction with stannylpyridine, was also investigated and shown to be a viable option, Scheme 9: Route B. The Suzuki couplings were found to go readily, and after purification by chromatography to remove any disubstituted material and unreacted tbb, the isolated dibromophenyl compound was subjected to the Stille reaction to introduce the required pyridyl functionalities. This method was employed for the production of ligand precursors HL^{8-10} and HL^{17}. The *p*-tolyl-substituted ligand HL^8 was prepared by synthetic Routes B and C, Scheme 10. Although this compound appears to slightly favour Route C, there is little to choose between the two procedures without optimisation of any of the specific reactions involved.

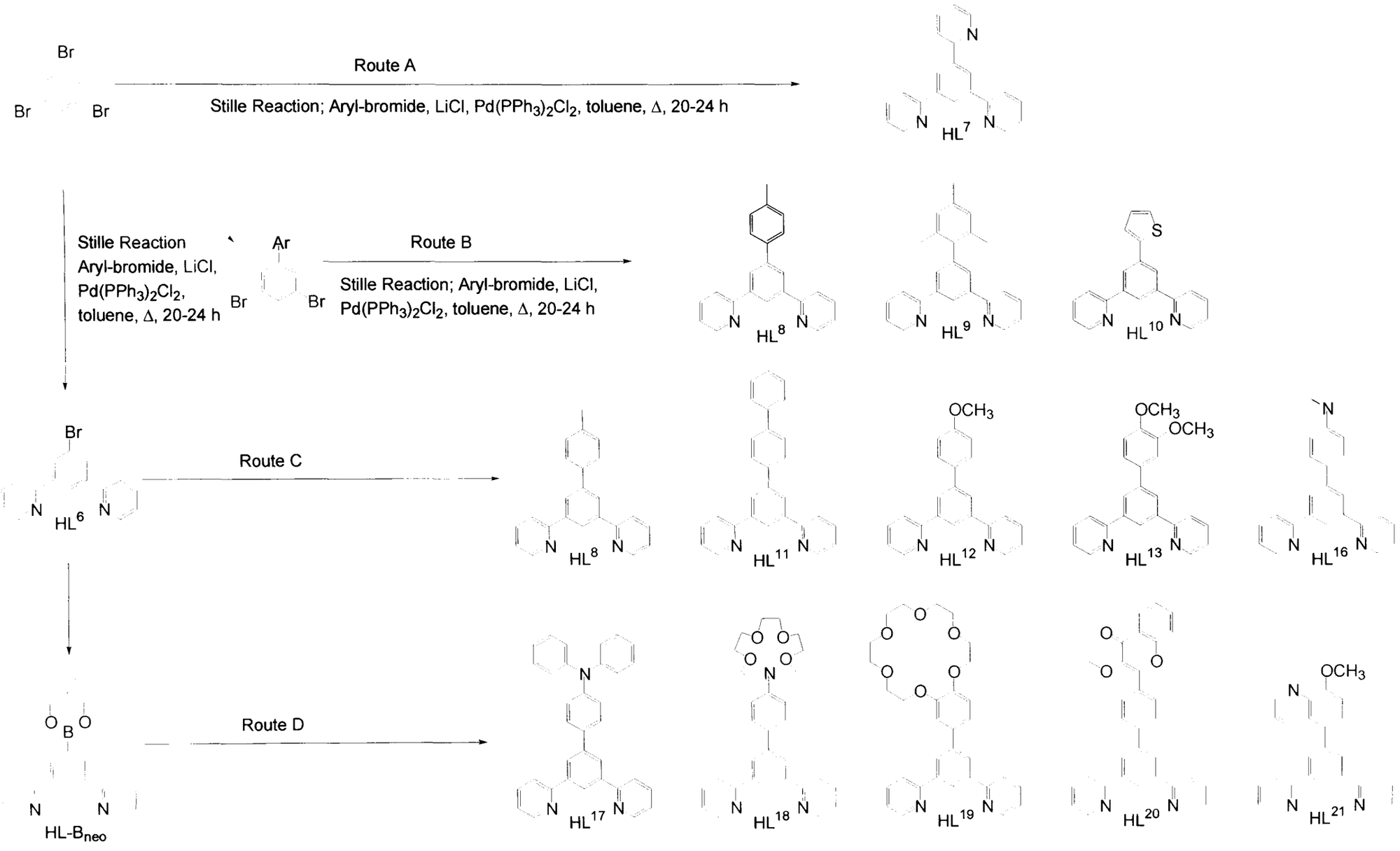

Scheme 9: Synthesis of N^C^N coordinating ligands HL^n (n = 7–13, 16–21). Synthetic routes used a combination of Stille, Suzuki and Miyaura couplings.

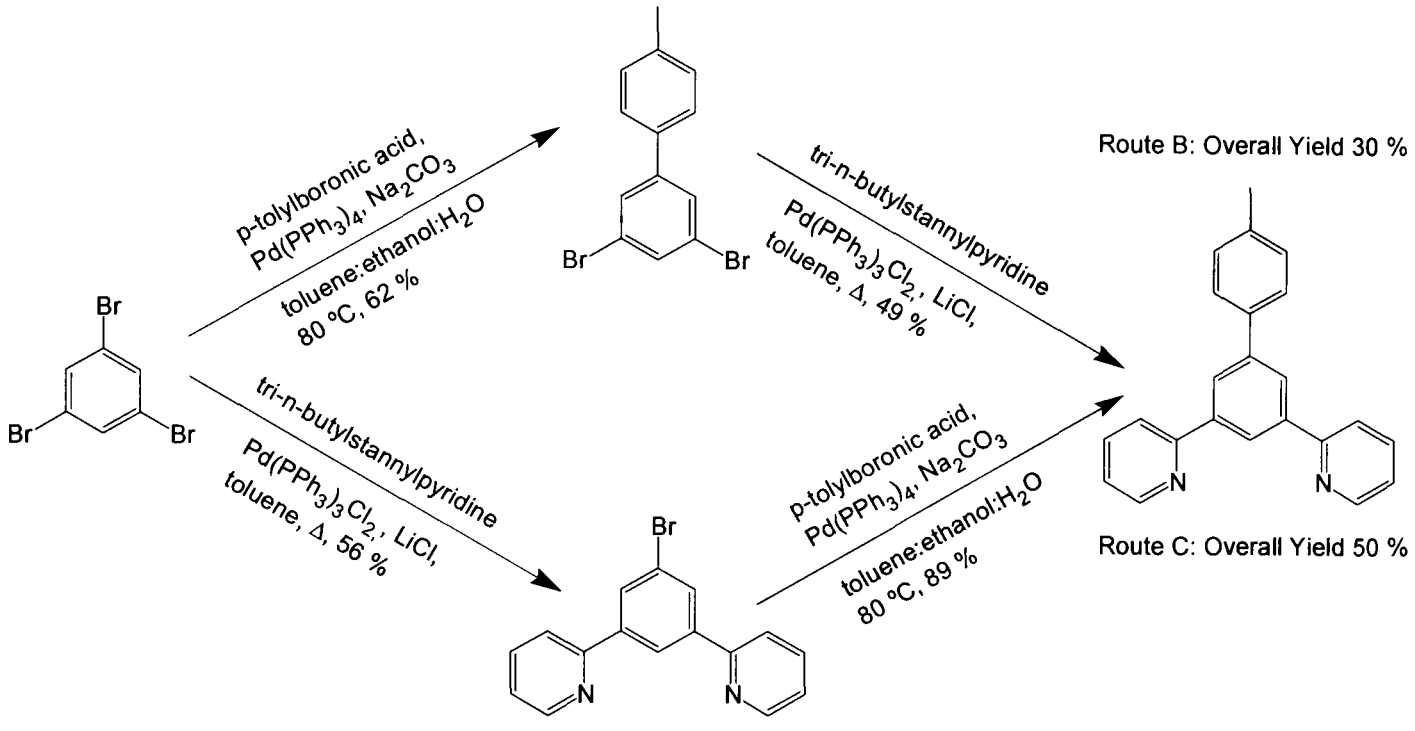

Scheme 10: Two synthetic routes through alternative Stille and Suzuki couplings for the production of HL^8.

For 1,3-dibromo-5-mesityl-benzene the general procedure for the Suzuki coupling was found to be ineffective at coupling tbb and mesitylboronic acid. The lack of reactivity is due to the steric hindrance of the di*ortho*-substituted boronic acid, a well known issue for Suzuki couplings.[171,212] Procedures outlined by Suzuki *et al*[213] have identified that Na_2CO_3 is not an effective base for the coupling of mesitylboronic acid. Addition of a stronger base, *e.g.* barium hydroxide, exerts a remarkable effect on the reaction, and, in the present instance, led to coupling to give the desired product in 54% yield.[213]

The Suzuki coupling of HL^6 was also employed to build multi-site ligand precursors, HL^{14} and HL^{15}, Scheme 11. The coupling of two equivalents of HL^6 through a nickel(0) controlled homocoupling reaction previously reported[211] proved ineffective. The use of the Suzuki reaction in heterocoupling of HL^6 with boronate ester, $HL\text{-}B_{neo,}$ was somewhat more successful. Reaction of HL^6 with commercially available benzene-1,4-diboronic acid was straightforward and yielded the desired ligand, HL^{15}, in 70% yield.

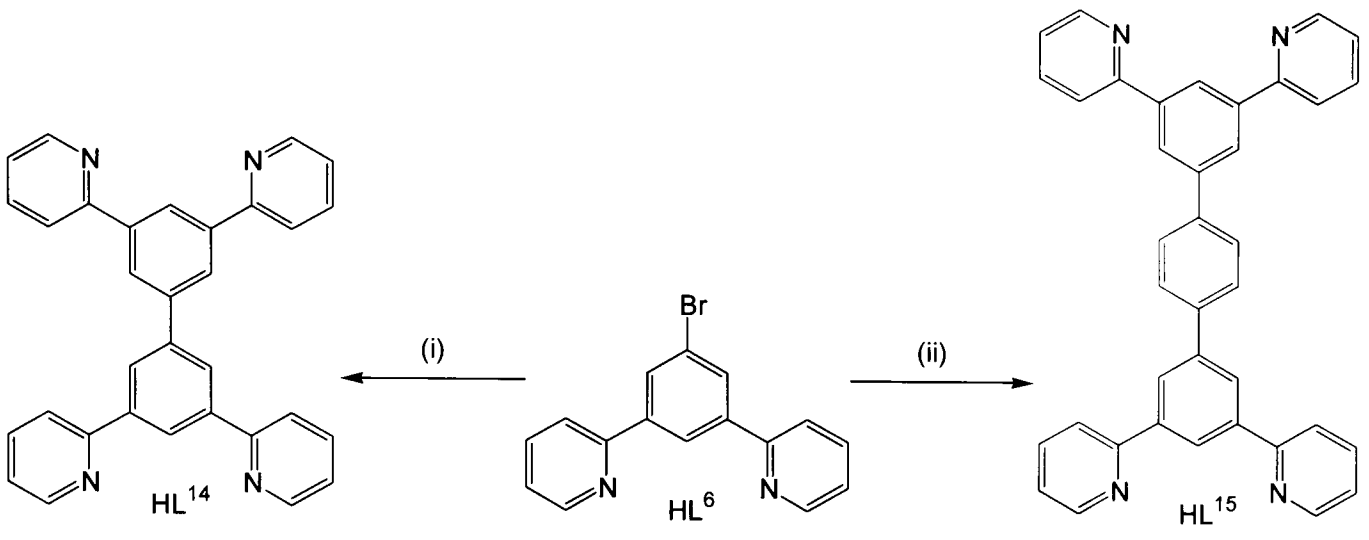

Scheme 11: Suzuki couplings between HL^6 and suitable boronic acids to produce multidentate ligands, HL^{14} and HL^{15}. (i) HL-$_{Bneo}$, Na_2CO_3, $Pd(PPh_3)_4$, toluene:ethanol:H_2O (3:3:1 mL respectively), 80 °C, 2 d; (ii) 1,4-benzene diboronic acid, Na_2CO_3, $Pd(PPh_3)_4$, toluene:ethanol:H_2O (6:6:2 mL respectively), 80°C, 1 d.

2.1.3. Miyaura cross-coupling reactions: boronate substituted intermediates

The palladium-catalysed cross-coupling reactions of the neopentyl or pinacol esters of diboronic acids, $[Me_2C(CH_2O)_2]B–B[(CH_2O)_2CMe_2]$ and $(Me_4C_2O_2)B–B(O_2C_2Me_4)$ respectively, with haloarenes give a direct procedure for the synthesis of arylboronic esters from aryl-halides. The reaction is catalysed by $Pd(dppf)Cl_2$ (3 mol%) at 80°C in the presence of KOAc in DMSO. The reaction is tolerant of many functional groups with yields typically > 50%. The procedure provides a facile route to a large number of synthons capable of expanding the scope of the aforementioned Suzuki cross-coupling reaction, Section 2.1.2.

The ligands already discussed in above sections, with the exception of HL^{14}, were synthesised through cross-coupling methodologies using commercially available boronic acids. The Suzuki reaction has become such a powerful tool in synthetic chemistry, in part, because of the ease with which aryl-halides can now be converted into boron intermediates *via* the Miyaura cross-coupling reaction, which is widely accepted as an important synthetic route to many biaryl species.[214]

The bromo-functionalised intermediate, HL^6, was chosen as the ideal candidate for the Miyaura reaction, and both boronate esters, $HL\text{-}B_{neo}$ and $HL\text{-}B_{pin}$, were synthesised using the appropriate diboron source, Equation 3. The palladium-catalysed process, as reported by Miyaura,[215] proceeded well for both compounds.

However, solvent quality was found to be an important feature of this reaction. Reactions performed in freshly distilled DMSO appeared to yield a high purity product nearing stochiometric conversions, while reactions attempted after the solvent had been stored for some time led to competitive formation of large quantities of HL^1, probably *in situ* protonation of the boronate product. However, the presence of this ligand appeared not to have any detrimental effects upon the subsequent Suzuki coupling reaction, allowing purification to be performed at a later stage.

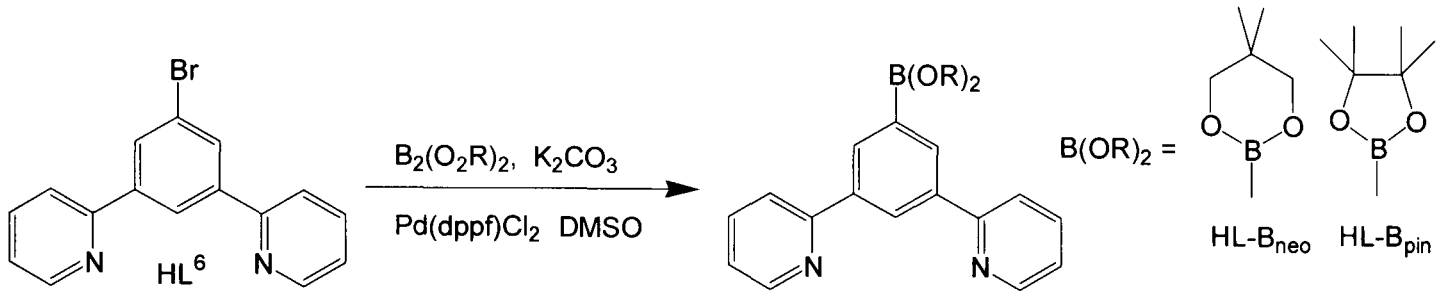

Equation 3: Miyaura cross-coupling reaction used to access the second key intermediates, namely the neopentyl and pinacol esters of 1,3-di(2-pyridyl)-5-phenylboronic acid, HL-B_{neo} and HL-B_{pin}. Corresponding boron sources were $B_2(O_2R)_2$ = bis(neopentyl glycolato)diboron, B_2neo_2, and bis(pinacolato)diboron, B_2pin_2, respectively.

The synthesis of the diphenylaniline pendent ligand, HL^{17}, outlined in Scheme 12, required the formation of boron intermediates for subsequent Suzuki couplings. The precursor 4-bromo-N,N-diphenylaniline was first synthesised by literature methods[92] involving the coupling of N,N-diphenylamine and 4-iodo-bromobenzene, *via* a copper catalysed Ullmann-type coupling in the presence of 1,10-phenanthroline. From this point the substitution of the bromine by the N^C^N unit could be achieved *via* one of two routes. The first route, Scheme 12 Route B similar to that used in literature,[92] involved the conversion of the bromine functionality on the tertiary amine precursor to a neopentyl boronate *via* the Miyaura reaction. Once formed, the boronate then allowed the use of the Suzuki reaction with tbb to generate the dibromobenzene-functionalised compound. Using an excess of tbb in the Suzuki coupling for this type of reaction aids in reducing twice-coupled reaction by-products, *e.g.* bis-(4-N,N-diphenylaniline)-(5-bromobenzene). However, in this particular synthetic route, the Stille coupling of 4-(3,5-dibromophenyl)-N,N-diphenylaniline with py-$SnBu_3$ proved disappointing, yielding an impure product in poor yield, 8%. The second route shown in Scheme 12 was centred on the use of the boronate ester intermediate HL-B_{neo}. The Suzuki

coupling between 4-bromo-(N,N-phenylaniline) and the boronate HL-B_{neo} proved more successful and purified in much greater yield, 31%.

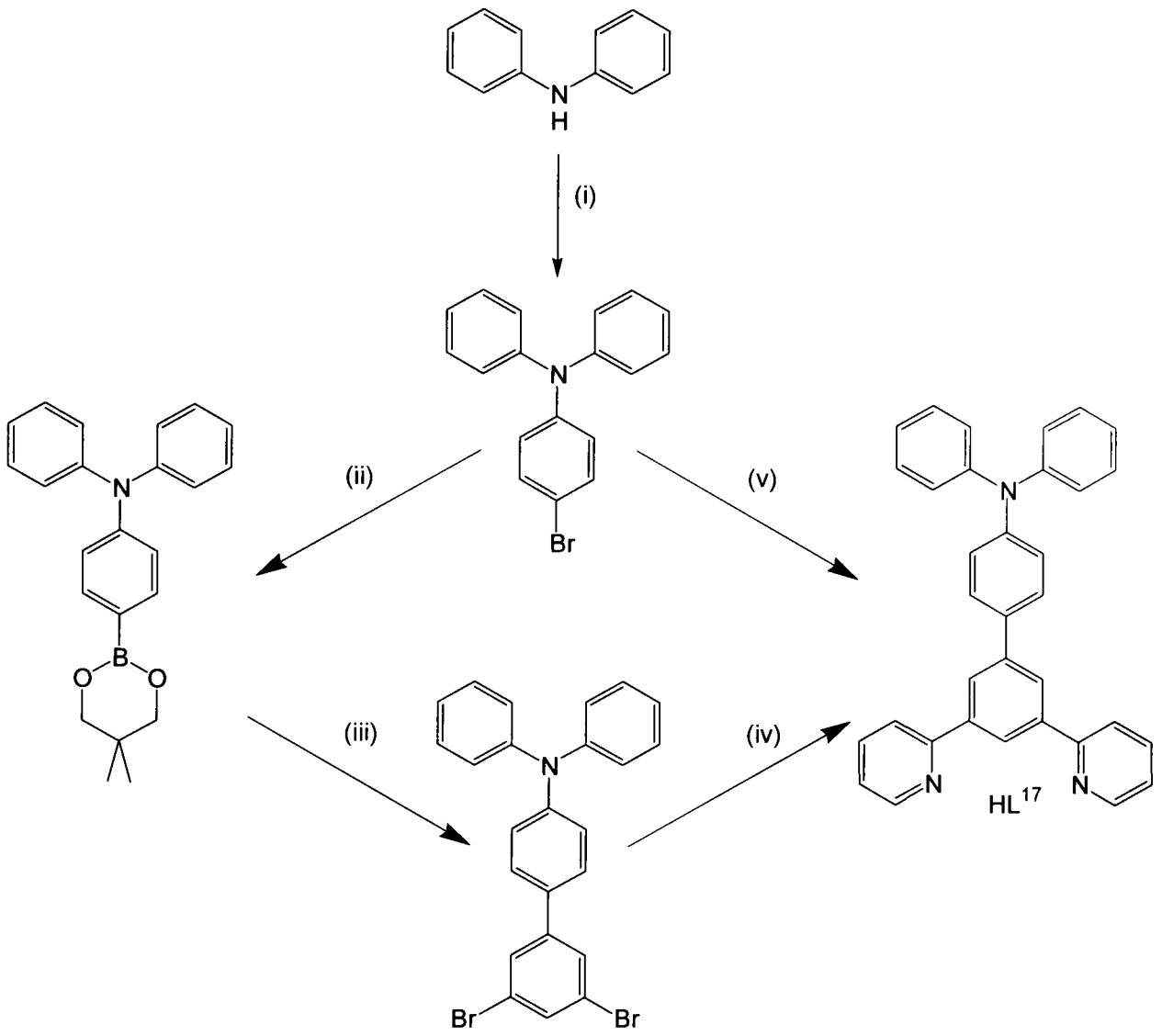

Scheme 12: Synthesis of diphenylaniline pendent N^C^N ligand. (i) Ullmann coupling: 4-iodo-bromobenzene, CuI, xylene, KOH, 1,10-phenanthroline. (ii) Miyaura coupling: $Pd(dppf)Cl_2$, B_2neo_2, KOAc, DMSO. (iii) Suzuki coupling: tbb, Na_2CO_3, $Pd(PPh_3)_4$, DEME. (iv) Stille coupling: tri-n-butylstannylpyridine, $Pd(PPh_3)_2Cl_2$, LiCl, toluene. (v) Suzuki coupling: HL-B_{neo}, Na_2CO_3, $Pd(PPh_3)_4$, toluene:ethanol:water.

Similar to the synthesis of ligand precursor HL^{17}, functional pendant compounds $HL^{18\text{-}20}$ were synthesised *via* the Suzuki-Miyaura coupling methodology, all involving the synthesis of boronate esters. Compounds HL^{19}, and HL^{20} were synthesised from bromo-functionalised aryl components, shown in Figure 16, obtained commercially and from the research group of Dr. J.-L. Fillaut,[216] respectively.

The synthesis of the aza-crown functionalised ligand, HL^{18}, required the intermediate 4-bromophenyl-N-monoaza-15-crown-5, Figure 16 R = Br, and so this intermediate was the first synthetic target for this molecule.

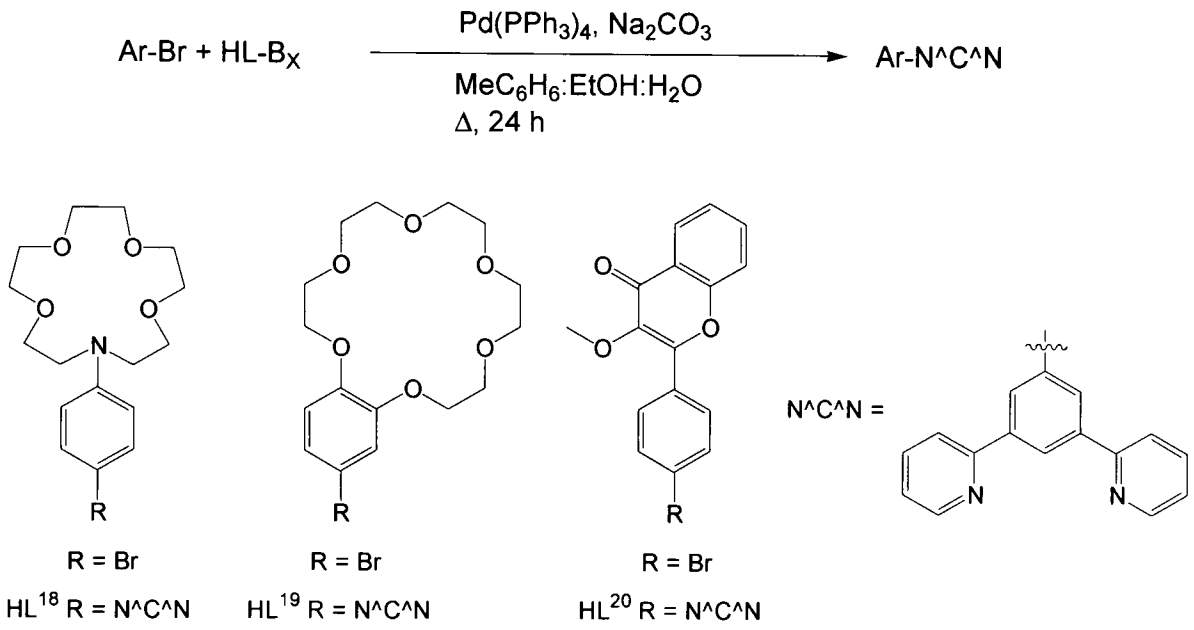

Figure 16: Functional 5-pendant N^C^N ligands prepared by the Stille-Suzuki-Miyaura cross-coupling methodology. HL-B_X represents HL-B_{neo} for $HL^{18\text{-}19}$ and HL-B_{pin} for HL^{20}.

Initial efforts, focused on the coupling of monoaza-15-crown-5 to 4-iodo-bromobenzene through palladium(0) amination reaction,[121,217,218] Equation 4, were found to yield only trace quantities of product, with starting material by far the most significant component. Changes in palladium source to one more electron-rich supporting ligand (PCy_3, PPh_3) failed to prevent premature termination of the reaction.[121]

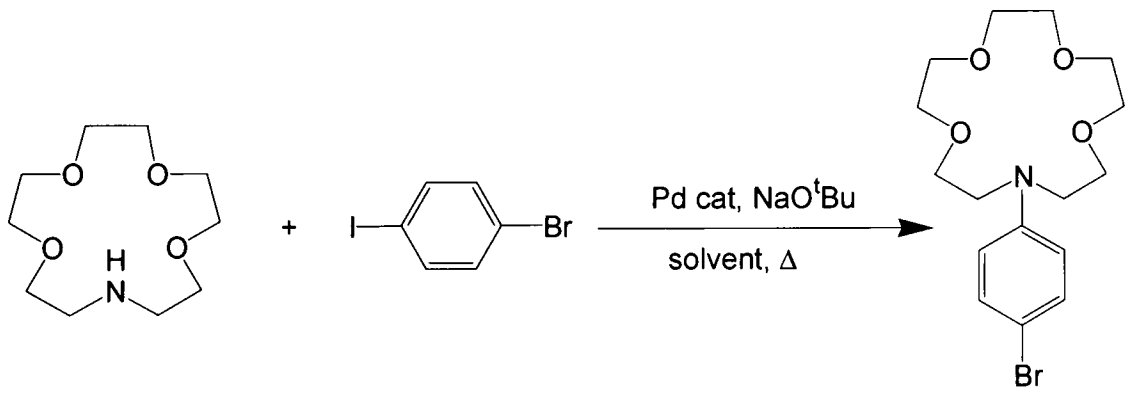

Equation 4: Palladium catalysed amination of aryl-iodide, which failed to yield sufficient quantities of desired product. Modification of Pd catalyst from $Pd(PPh_3)_4$ to $Pd_2(dba)_3/PCy_3$ failed to induce satisfactory conversions.

Synthesis of the 4-bromophenyl-N-monoaza-15-crown-5 unit was performed by a procedure which had previously been reported in the literature[116] from the readily available starting materials, 4-bromo-aniline and triethylene glycol, Scheme 13. First, 4-bromo-aniline refluxed in neat 2-chloroethanol in the presence of base gave the dialcohol intermediate in 37% yield. A substantial quantity of mono-substituted amine was isolated as a by-product which could easily be converted to the dialcohol product by returning to the reaction under similar conditions.[219] Tri-ethylene glycol was converted to (ethylene glycol) di-*p*-toluenesulfonate by reacting with *p*-tolylsulfonylchloride in aqueous base/THF mixture below 0ºC.[220] Purification through chromatography, although achieving pure quantities of the ditosylate, was found to be detrimental to the final yield, plummeting from 77% to < 10% when compared with drying the crude product over $CaCl_2$ (although the $CaCl_2$ method failed to remove all traces of starting material and mono-substituted ether). The ring-closing reaction required the tosylates to react as good S_N2 leaving groups in the reaction with the dialcohol-amine produced from 4-bromoaniline. Strict moisture control was required for ring closure to increase yield and prevent hydrolysis of the tosylate groups, while dilute conditions were employed to encourage ring closure of the ether system and prevent formation of polymeric type materials.[221]

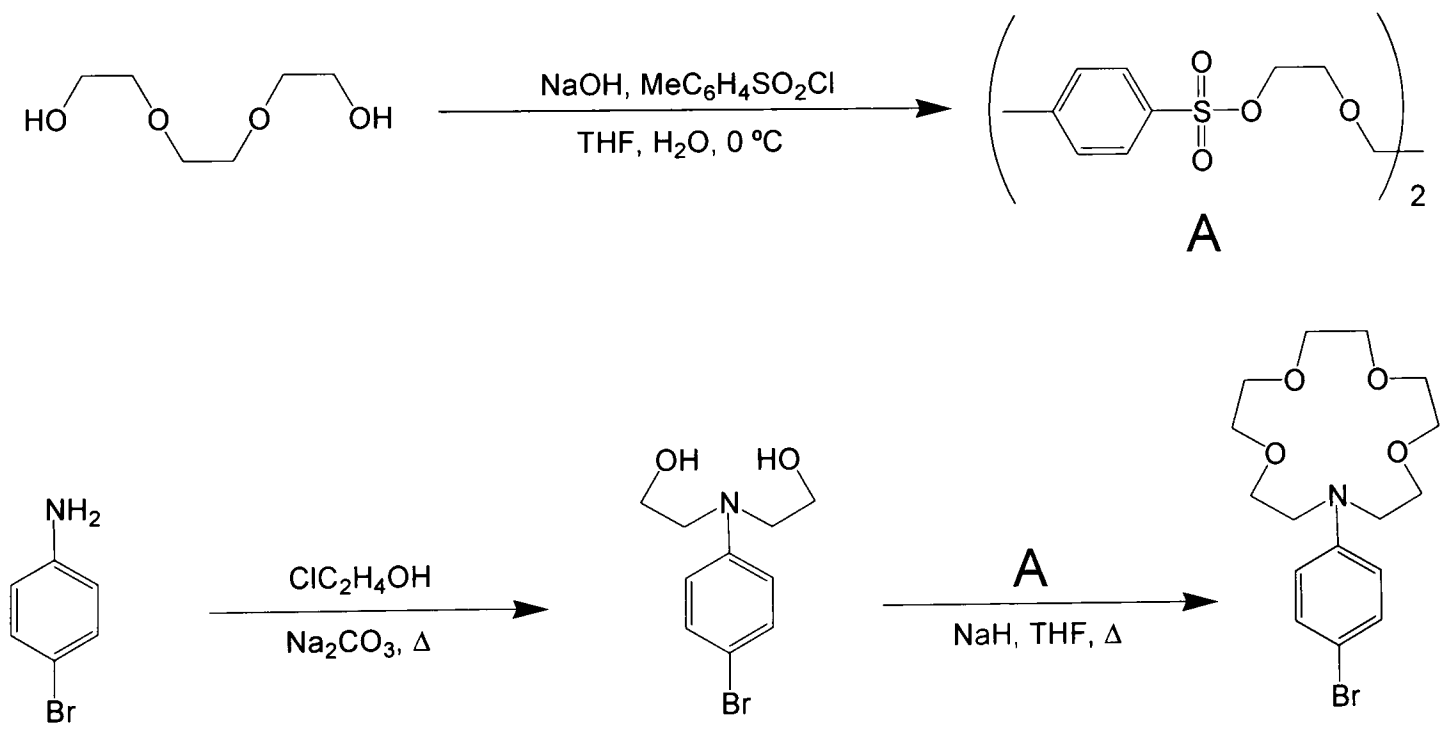

Scheme 13: Synthetic route to 4-bromo-N-monoaza-15-crown-5 *via* N,N-di(hydroxyethyl)aniline and (ethylene glycol) di-*p*-toluenesulfonate.

The final compound, HL[18], was synthesised *via* the Suzuki coupling with boronate ester HL-B_{neo} under standard conditions, with purification on aluminium oxide,

88%. Alternative attempts to synthesise the boronate ester or boronic acid derivative of phenyl-N-monoaza-15-crown-5 through the Miyauara reaction proved ineffective, possibly due to protonation of the boronic acid product.

2.1.4. Spectroscopic characterisation

The ligands HL^n (n = 1–21) were fully characterised by 2-D ^1H and ^{13}C NMR spectroscopy and mass spectrometry. Complete assignment of ^1H NMR spectra was possible using ^1H–^1H NOESY experiments, which crucially allows the resonances on the pendent ring to be assigned on the basis of through-space coupling of, typically, H^4-bn with H^2-ph, Figure 17: (showing H^4-bn with H^3-th of HL^{10}). ^1H NMR spectra display the following predictable order of signals for the N^C^N coordination motif, in order of decreasing frequency, H^6-py > H^2-bn > H^4-bn > H^3-py ≥ H^4-py > H^5-py for a typical numbering system shown in Figure 17:. Mass spectrometry, particularly positive electrospray ionisation, was used to further confirm product formation. Typically, acquired signals were from corresponding mono-cationic singly-protonated species of the parent compound, while the crown-ether pendent compounds showed signals from the sodium-bound monocations.

Single crystals suitable for X-ray diffraction analysis for ligand HL^7 and key intermediate HL^6 were obtained by slow evaporation of saturated DCM solutions of the appropriate compound. A study of HL9 obtained at the same time by another member of the group will be considered along with the samples obtained through this body of work.[222]

The ORTEP diagrams representing structures of the three compounds are displayed in Figure 18 and pertinent bond angles listed in Table 1. All three compounds displayed a head-to-tail orientation of the pyridyl rings. This configuration may be adopted to minimise unfavourable electrostatic interactions between the nitrogen lone-pairs within the molecule and resembles a similar configuration found in the crystal structures of 2,2':6',2''-terpyridines.[223,224,225] However, the nitrogen atoms are noticed to participate in weak intermolecular hydrogen bonding C-H···N interactions, *ca.* 3.5 Å, which may also influence configuration. The aromatic rings are not coplanar in any of the compounds. Angles are displayed in Table 1; a compromise between increasing conjugation, molecular stacking and sterics probably accounts for the observed angles. The only other feature of significant note is that in compound HL^9, the mesityl

substituent is almost orthogonal with respect to the central benzene ring, 80.53(4)°. This feature is expected for such a system, where the need to minimise destabilising steric interactions takes precedence over the desire to increase the π-conjugation of the system.[225]

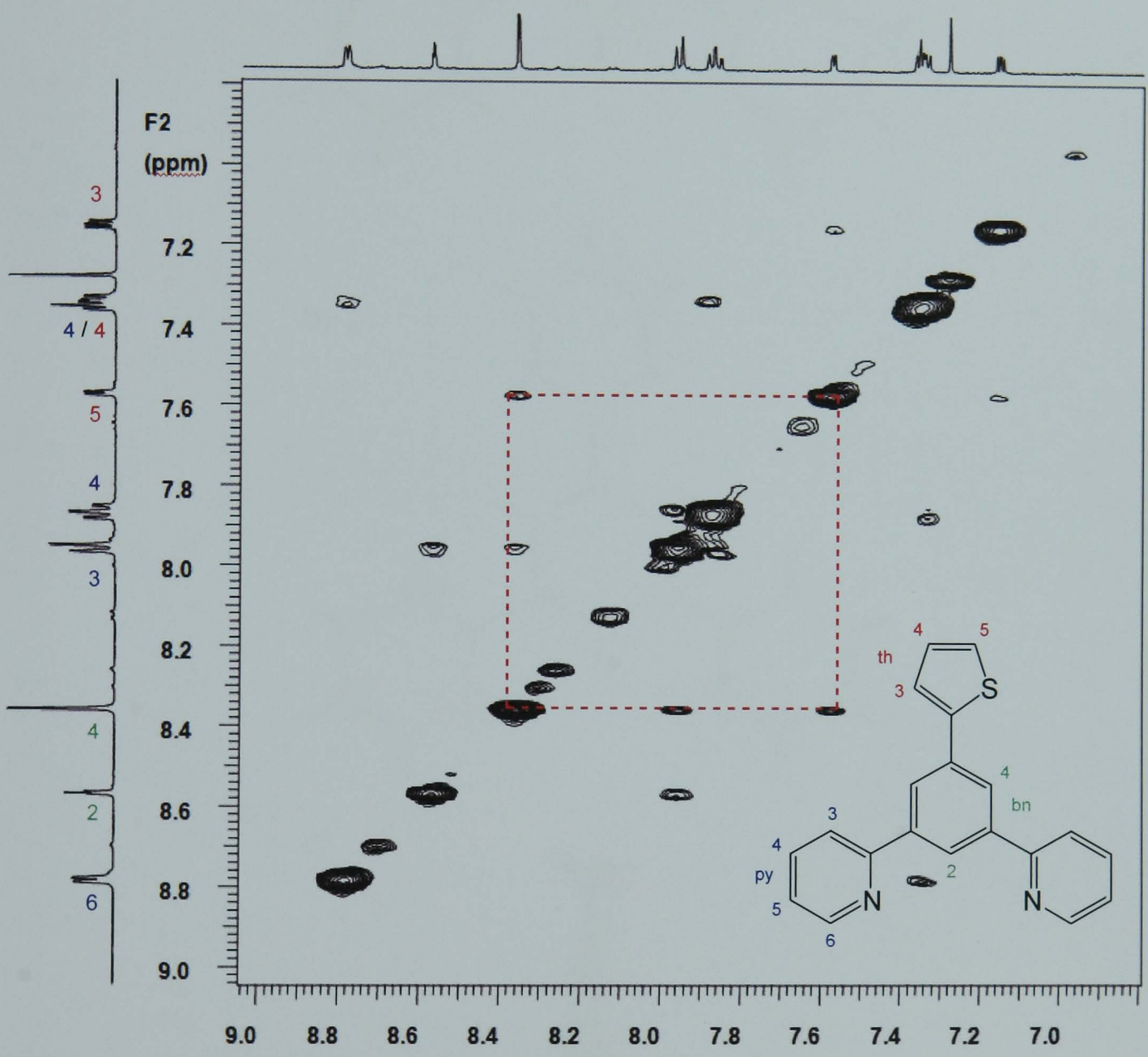

Figure 17:: 1H–1H NMR NOESY Correlations between H4-bn and H3-th (----). Numbering system typical of ligands synthesised in this section.

HL[6]	Angle °	HL[7]	Angle °	HL[9]	Angle °
C36–C11	8.34(11)	C42–C15	15.99(7)	C32–C15	34.64(6)
C32–C21	26.35(8)	C46–C25	24.58(6)	C36–C25	30.06(6)
		C44–C35	18.91(6)	C34–C41	80.53(4)

Table 1: HL[6]; HL[7]; and HL[9] angles observed between planes of benzene ring and peripheral aromatics connected by bond described.

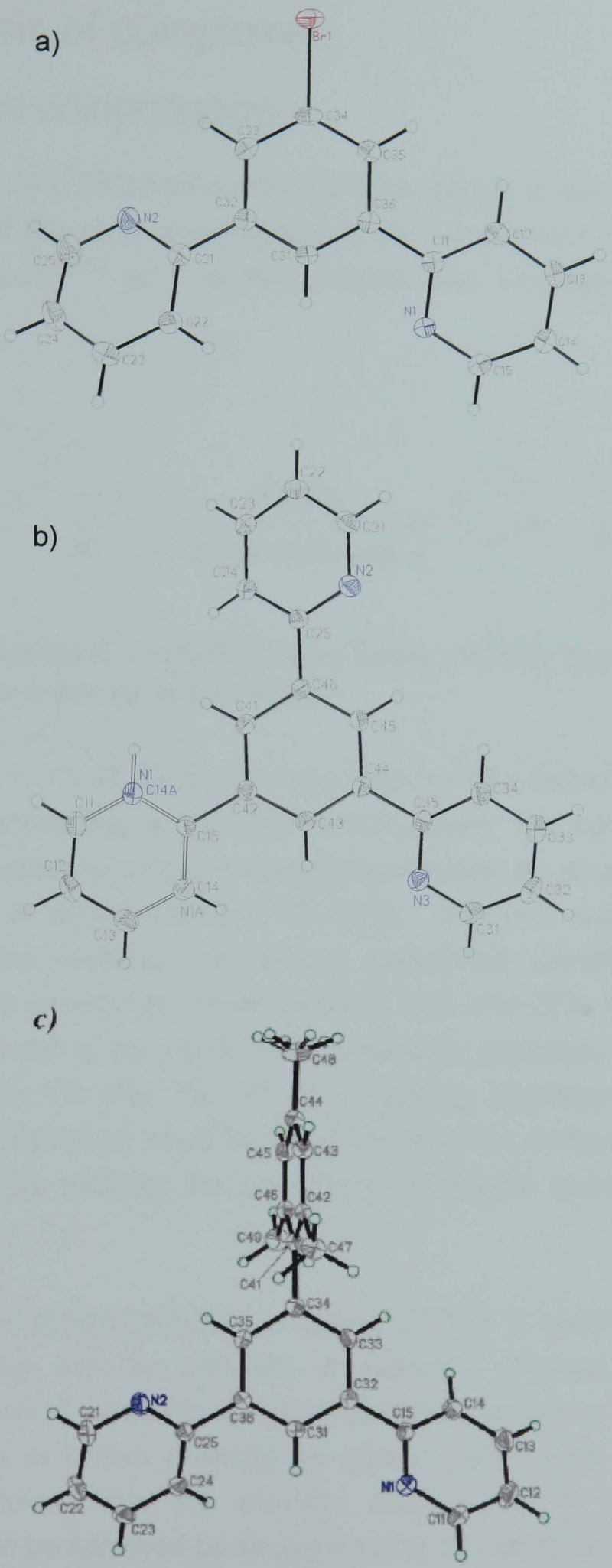

Figure 18: ORTEP diagrams for (a) key intermediate HL[6] (b) C_3-symmetric HL[7] and (c) HL[9]. A suitable crystal for X-ray diffraction studies obtained by S. J. Farley previously published.[222]

2.2. Synthesis of complexes

2.2.1. Ligand complexation

The core structure of L^1PtCl had previously been shown to be accessible through direct metalation of the corresponding ligand, HL^1, under inert refluxing conditions in glacial acetic acid,[66,74] and so this method was employed here, shown in Equation 5.

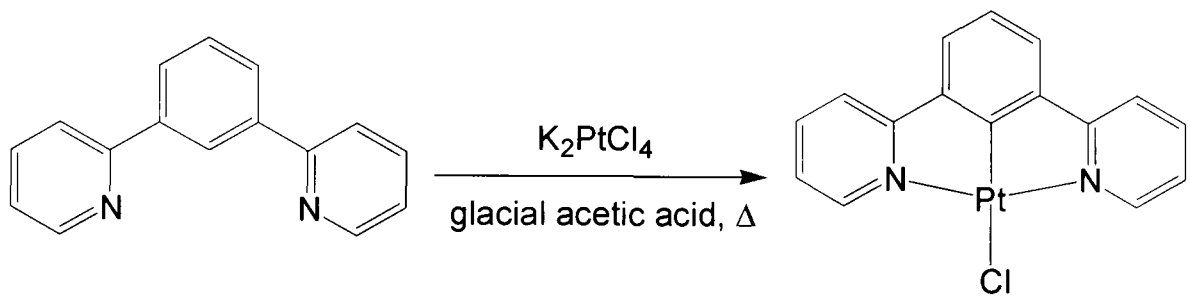

Equation 5: Direct metalation of N^C^N coordinating ligands. Typically refluxed for 3 d in solvent, either glacial acetic acid or acetonitrile/water mixture.

Complexes L^nPtCl (n = 1–3, 5–13, 17) were found to be accessible by the reaction between the corresponding ligand and K_2PtCl_4 under the same conditions. A simple purification procedure (see Experimental Section 8.1.4) allows the isolation of the complexes in typical yields of 60–80%. The only exceptions were the complexation of the methoxy and thienyl substituted complexes, L^5PtCl and $L^{10}PtCl$, which were isolated in poorer yields of 30% and 22%, respectively. Both complexes were found to be significantly soluble in methanol, so much so, that yields of as little as 1% after the standard washing procedures were obtained. Further quantities of product could be extracted from the methanol washings, with careful purification by washing the complex with minimal quantities of methanol and diethyl ether.

In the case of the pyridyl pendent complex, L^7PtCl, a second potential N^C-coordinating binding site for platinum is present, although no evidence of competitive formation of dimetallic complex was observed, even in the presence of excess K_2PtCl_4, as is known possible for similar compounds.[166] However, the complex was isolated from the reaction mixture as its N-protonated salt. Deprotonation could be achieved by simply treating the initial concentrated reaction mixture with aqueous base prior to the typical purification procedure, described fully in the experimental section.

Several of the platinum complexes investigated in this work have also been shown to be accessible through direct complexation in an acetonitrile/water solvent mixture,[74] see Experimental 8.1.4.2. The methyl substituted complex L^2PtCl was synthesised under both solvent conditions with yields found to be favoured by the glacial acetic acid route, 75% *vs* 52%. However, specific ligands were found to be unsuitable for complexation in acetic acid, such as the amine pendant systems HL^{16} and HL^{18}, yielding impure mixtures from which the desired product was inseparable. Unless otherwise required, complexes were synthesised under acetic acid conditions, but systems displaying exposed functionalities, such as the amine systems, were synthesised in the acetonitrile/water solvent mix.

2.2.2. Spectroscopic characterisation

Some general statements can be made regarding the changes in ^1H NMR resonances that accompanied ligand complexation to platinum(II). (i) A shift to higher frequency of the H^6-py resonance, $\Delta\delta$ 0.5–0.6 ppm, accompanied by the appearance of well defined ^{195}Pt satellites (I = ½, relative abundance 33.8%) about this signal (^3J typically *ca.* 40 Hz). (ii) A shift to lower frequency of H^4-bn, $\Delta\delta$ 0.6–0.8 ppm, was observed, occasionally accompanied by the appearance of resolvable ^{195}Pt satellites (^4J *ca.* 6 Hz). (iii) A small shift to a higher frequency of H^4-py, $\Delta\delta$ 0.1–0.2 ppm, accompanied by a comparable shift of H^3-py to a lower frequency, the combined effect of which leads to a reversal in the ordering of these two signals when compared to that of the free ligand. (iv) The disappearance of the H^2-bn signal, due to the cyclometalation to the metal ion - the key feature for confirmation of cyclometalation through ^1H NMR analysis. The chemical shifts of resonances in the pendent aryl groups were not greatly affected upon coordination. An example NMR of the free ligand HL^{13} and complex $L^{13}PtCl$ are shown in Figure 19.

2.2.3. Crystal structures

Single crystals suitable for X-ray diffraction analysis of complexes L^2PtCl and $L^{11}PtCl$ were obtained by slow evaporation of saturated chloroform solutions, L^9PtCl and $L^{18}PtCl$ crystals were obtained from very slow solvent evaporation of saturated acetonitrile solutions, whilst suitable crystals of $L^{17}PtCl$ were obtained from slow vapour diffusion of diethyl ether into a concentrated solution of the complex in DCM.

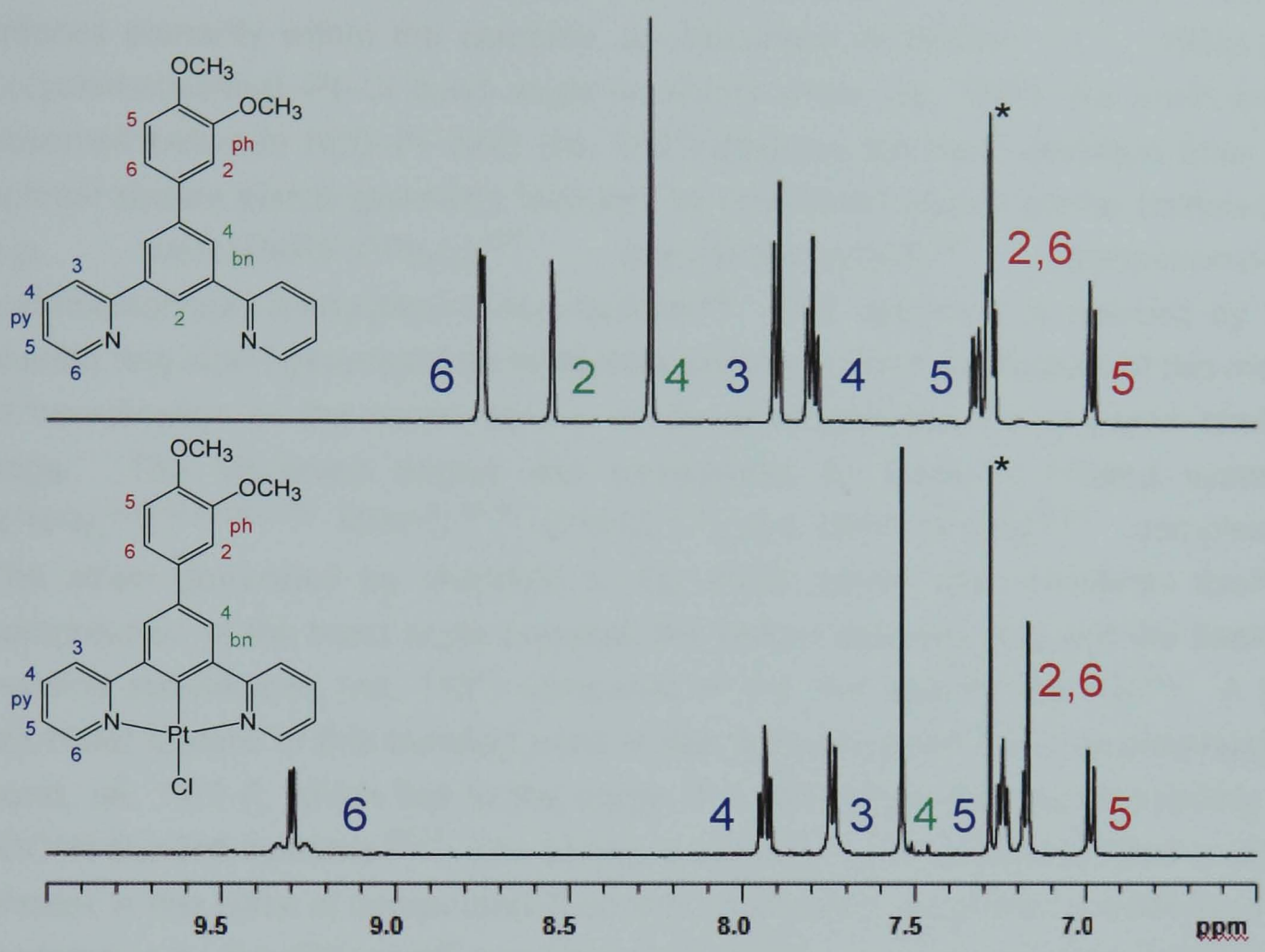

Figure 19: ^{1}H NMR of HL^{13} and $L^{13}PtCl$ (* = $CHCl_3$ residual solvent peak), the most dramatic changes observed for H^6-py accompanied by the appearance of ^{195}Pt (I = ½) signals. Also noteworthy is the position switch of signals H^3/H^4-py. Additionally, the increase in electron density in the central ring that accompanied cyclometallation can be seen in the dramatic shift to lower frequency of H^4-bn.

2.2.3.1. General points common to all structures

X-ray diffraction studies confirm the proposed binding mode of the N^C^N terdentate unit. All the complexes are essentially isostructural with respect to the platinum coordination geometry, and consistent with previously published results for L^1PtCl[66] and 3,5-di(2-pyridyl)methyl-benzoate-2-platinum(II) chloride.[74] The platinum(II) centres are in a distorted square-planar environment, each coordinated to the N^C^N donor atoms of the terdentate ligands and the fourth coordination sites are occupied by a chloride ligand located *trans* to the cyclometalating carbon. The coordination plane is almost completely flat where deviations from best plane through the platinum and the coordinating atoms display a maximum displacement of 0.0079 Å of any one atom away from the ideal position, recorded in L^2PtCl. The

presence of the fused rings formed by cyclometalation to the platinum centre induces planarity within the complex, as discussed in Section 1.1.1. While the C(cyclometalating)–Pt–Cl bond angle is almost linear (*ca.* 180°), the bond angle observed between N(1)–Pt–N(2) (*ca.* 160°) displays the most deviation from the optimal square planar geometry favoured by unstrained square planar complexes, *e.g.* *trans*-[PhPtF(PPh_3)$_2$],[226] trans-[PtPh(py)$_2$Cl],[227] *trans*-bromo-(5-methoxynorticycl-3-enyl)dipyridinepalladium.[228] The distortion is induced by the chelate ring strain generated by terdentate binding, a common feature of this mode of coordination to the metal centre, which generates two 5-membered chelate rings. The observed angles are comparable to those in related systems N^N^N,[3,38,43,82,229,230] N^N^C,[54,55] C^N^C[12,56] and other N^C^N[66,74] complexes. The strain generated by chelation to the metal centre also manifests itself in compression of the bond angle between the central benzene ring and the flanking pyridine substituents (*ca.* 112°) compared to the free ligands (*ca.* 120°). A key structural feature of this bonding motif is the relatively short Pt–C cyclometalation bond, *ca.* 1.91 Å, which lies in the range of 1.90–1.94 Å observed previously for N^C^N bonded systems.[66,74] The strong σ-donating cyclometalating bond is much shorter in this class of compounds than that of platinum complexes containing N^C systems, e.g. (ppy)Pt(acac)[46] and Pt(ppy)$_2$[47] N^N^C chelating ligands,[54] and non-chelating, e.g. [PtH(C_6H_4F-*p*)(PPh_3)$_2$] 2.066(23) Å;[65] Pt–C bonds[231] A second key feature is that the Pt–N peripheral bonds, *ca.* 2.04 Å, are shorter than their equivalent bonds in N^N^C systems, *e.g.* [(phbpy)Ptpy]$^+$ 2.092(6) Å.[54] The net effect is the tighter binding of the platinum atom within the terdentate "cage".

2.2.3.2. L^2PtCl Methyl-substituted complex

The complex L^2PtCl in the crystallographic unit cell contains two independent molecules with essentially identical structures. An ORTEP diagram representing the complex is shown in Figure 20 along with relevant bond lengths and angles.

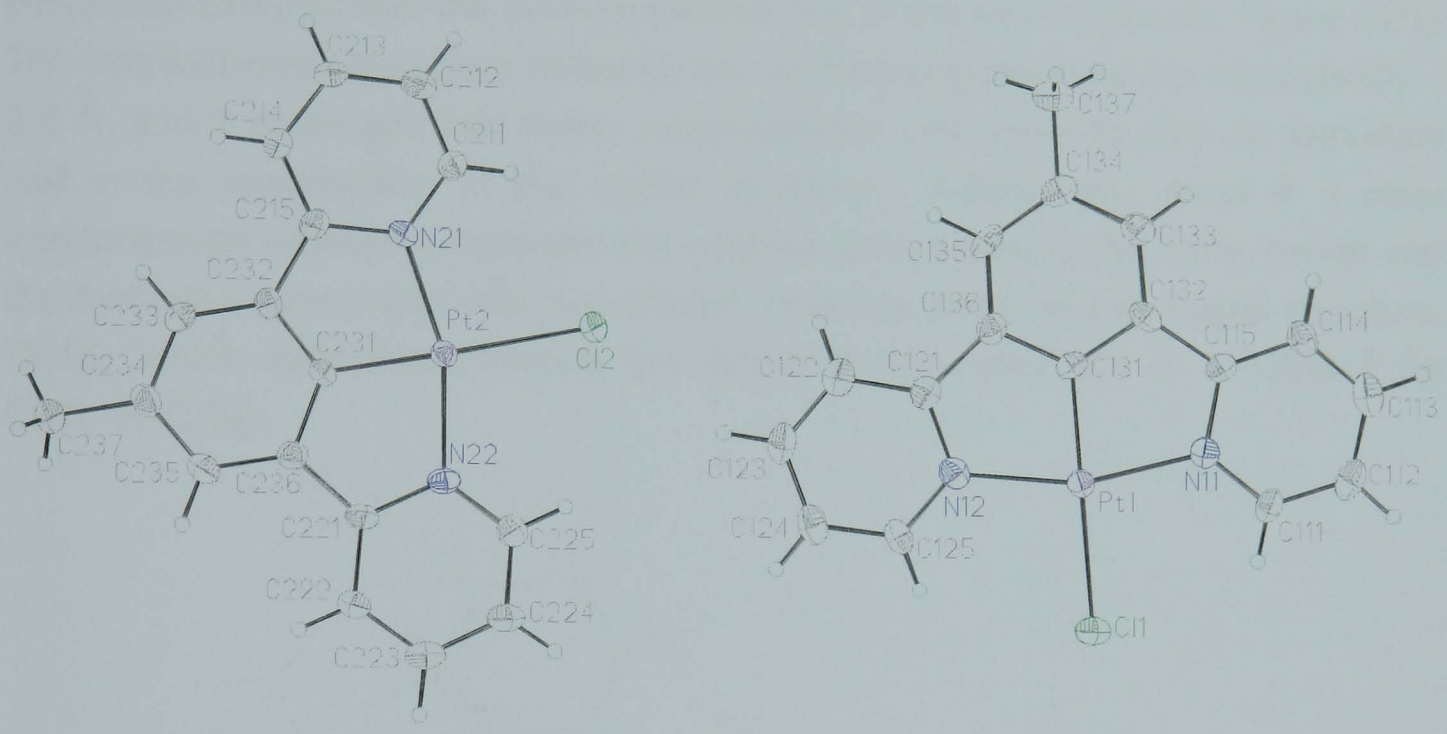

Figure 20: ORTEP diagram representative of the complex L^2PtCl, confirming the terdentate, N^C^N "pincer"-type binding mode of the ligand system with platinum. Pt(1)-C(131) 1.908(6), Pt(1)-N(11) 2.044(5), Pt(1)-N(12) 2.033(6), Pt(1)-Cl(1) 2.4060(16) Å; C(131)-Pt(1)-N(11) 80.9(2), C(131)-Pt(1)-N(12) 80.5(7), N(11)-Pt(1)-N(12) 161.4(2), C(131)-Pt(1)-Cl(1) 179.15(18), C(131)-C(132)-C(115) 112.8(6)º.

2.2.3.3. $L^{11}PtCl$ Biphenyl-substituted complex

An ORTEP diagram representing the biphenyl substituted complex is shown in Figure 21 along with relevant bond lengths and angles. The molecule lies on a crystallographic 2-fold axis that passes through the metal ion, the chloride ligand and the cyclometallated carbon. The angle between the plane of the cyclometallated benzene ring and that of the first ring of the biphenyl pendant is 29.63(16)°, while the angle between the constituent rings of the biphenyl unit is 26.99(19)° in the opposite direction, such that the cyclometallated ring and the terminal ring are almost coplanar at 2.6(2)°, Figure 22a). Apparently, there is a balance between the desire to maximise conjugation with the attached phenyl rings favoured by coplanarity, and the steric repulsion between neighbouring H atoms attached to those rings that would accompany the coplanar conformation. The angles observed are in the expected range of 20–40° for *ortho*-H biphenyl

compounds.[157] This feature has similarly been observed by Alcock and co-workers for a series of biphenyl-substituted terpyridine complexes.[232] In the structure of $L^{11}PtCl$ the molecules stack flat in an offset head-to-tail arrangement, similar to the type-B stacking reported by Alcock for $[Cd(biptpy)_2](PF_6)_2$. However, in the present case, the molecules are laterally further apart, so that the pyridine rings are positioned partially over the cyclometallated ring of the next molecule, Figure 22b). The intermolecular distances between the overlaid ring systems are consistently < 3.8 Å, and it is thought that these intermolecular π-π contacts play an important role in the organisation of the crystal structure. Additionally, there is a clear intermolecular interaction between the chlorine atom bound to the metal centre and the hydrogen associated with the solvent molecule found in the crystal structure, $CHCl_3$, which may also influence the overall configuration ($Cl\cdots C$ = 3.505 Å for $Cl(1)\cdots H–CCl_3$).

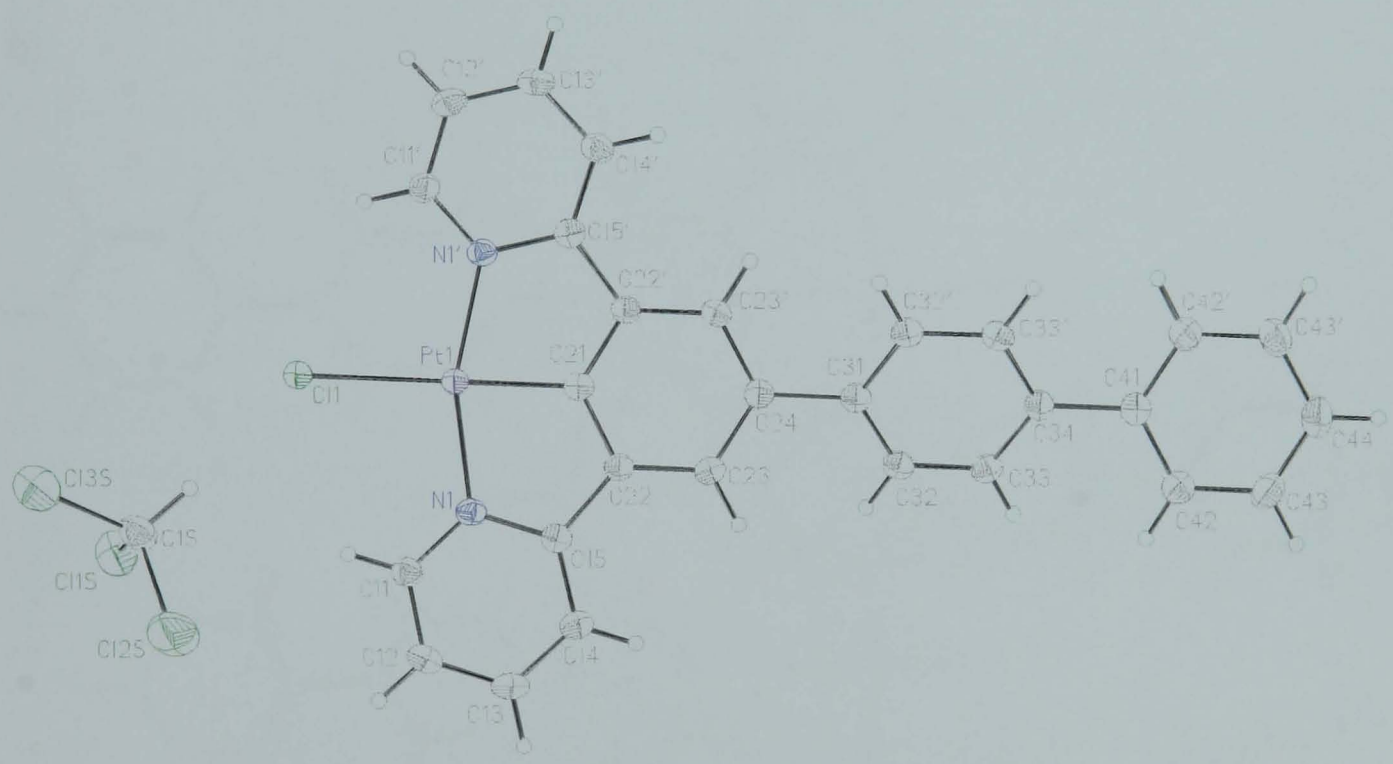

Figure 21: ORTEP diagram representative of the complex $L^{11}PtCl$, confirming the terdentate, N^C^N "pincer"-type binding mode of the ligand system with platinum. Pt(1)-C(21) 1.912(3), Pt(1)-N(1) 2.0445(19), Pt(1)-N(1') 2.0445(19), Pt(1)-Cl(1) 2.4421(8) Å; C(21)-Pt(1)-N(1) 80.57(5), C(21)-Pt(1)-N(1') 80.57(5), N(1)-Pt(1)-N(1') 161.13(11), C(21)-Pt(1)-Cl(1) 180.0, C(21)-C(22)-C(15) 112.6(2), aromatic planes between C(24)-C(31) 29.63(16) and C(34)-C(41) 26.99(19)°.

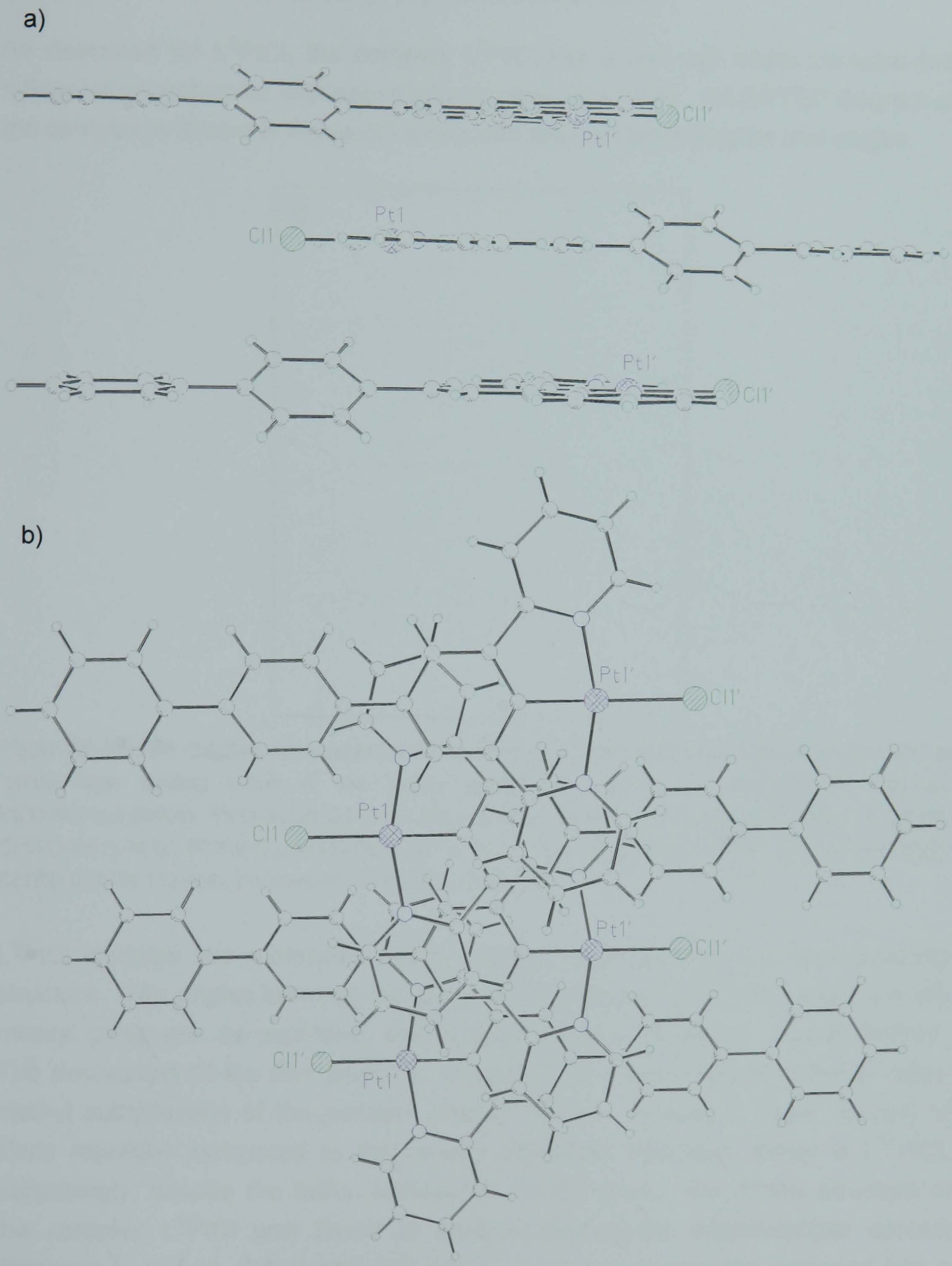

Figure 22: Crystal packing in $L^{11}PtCl$ showing packing interactions in planes (a) parallel and (b) perpendicular to the N^C^N-Pt-Cl plane. The complex is clearly shown to possess remarkable planarity which aids aromatic π-orbital overlap.

2.2.3.4. L^9PtCl Mesityl-substituted complex

As described for L^2PtCl, the complex L^9PtCl has a unit cell which contains two independent molecules with essentially identical structures. An ORTEP diagram of the complex is shown in Figure 23 along with relevant bond lengths and angles.

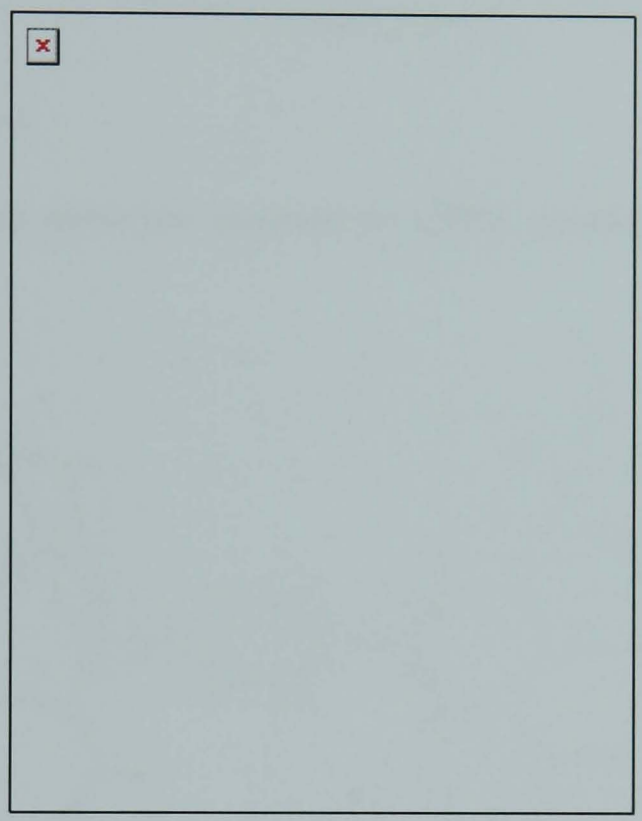

Figure 23: ORTEP diagram representative of the complex L^9PtCl, confirming the terdentate, N^C^N "pincer"-type binding mode of the ligand system with platinum. Pt(1)-C(131) 1.913(4), Pt(1)-N(11) 2.033(4), Pt(1)-N(12) 2.040(4), Pt(1)-Cl(1) 2.4139(11) Å; C(131)-Pt(1)-N(1) 80.74(17), C(131)-Pt(1)-N(12) 80.53(17), N(11)-Pt(1)-N(12) 161.27(15), C(131)-Pt(1)-Cl(1) 176.11(13), C(131)-C(132)-C(115) 112.4(4), pendent-N^C^N plane 87.36(14)°.

L^9PtCl contains two molecules which possess slight variations in the observed structure. The angles between the plane of the platinum coordination site and the mesityl group are, as expected, almost perpendicular, 84.89(13)° and 87.36(14)°. The decoupling of the two aromatic π-systems is a direct result of the di-*ortho*-methyl substitutions of the pendant mesityl system, creating a larger amount of steric repulsion compared to the closely orientated hydrogen atoms in $L^{11}PtCl$. Surprisingly, despite the bulky, orthogonal mesityl group, the crystal structure of the complex L^9PtCl was found to contain appreciable intermolecular contact distances.[2] In fact, the crystal unit cell contains two complexes arranged into a head-to-tail dimeric structure. The pair appear to interdigitate, with the platinum coordination planes in close contact, *ca.* 3.4 Å, while the orthogonal mesityl units seem to "cap" the ends of the opposing molecule, Figure 24.

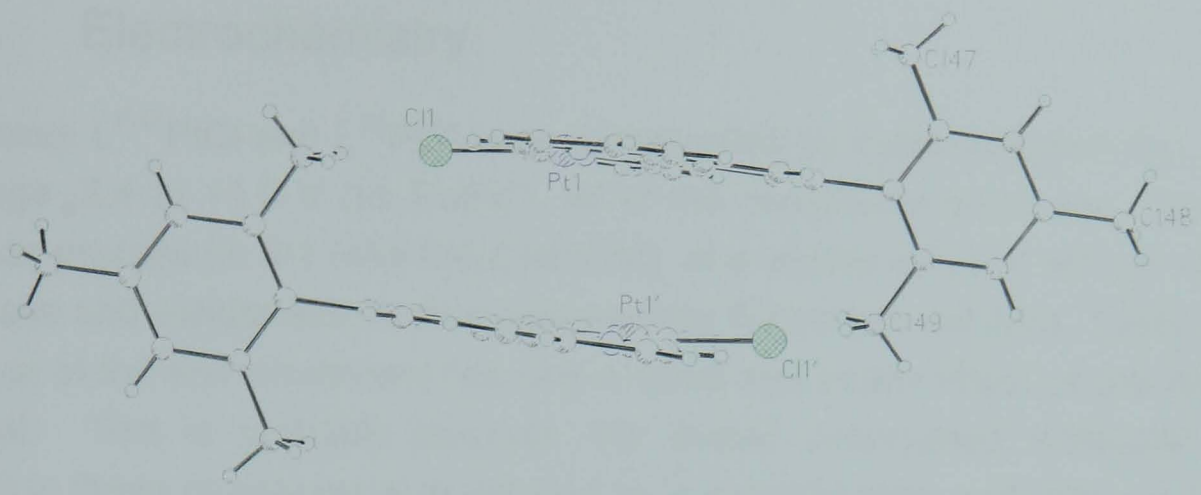

Figure 24: Dimeric packing behaviour observed in $L^{9}PtCl$, creating short π-π intermolecular contacts, 3.4225 Å.

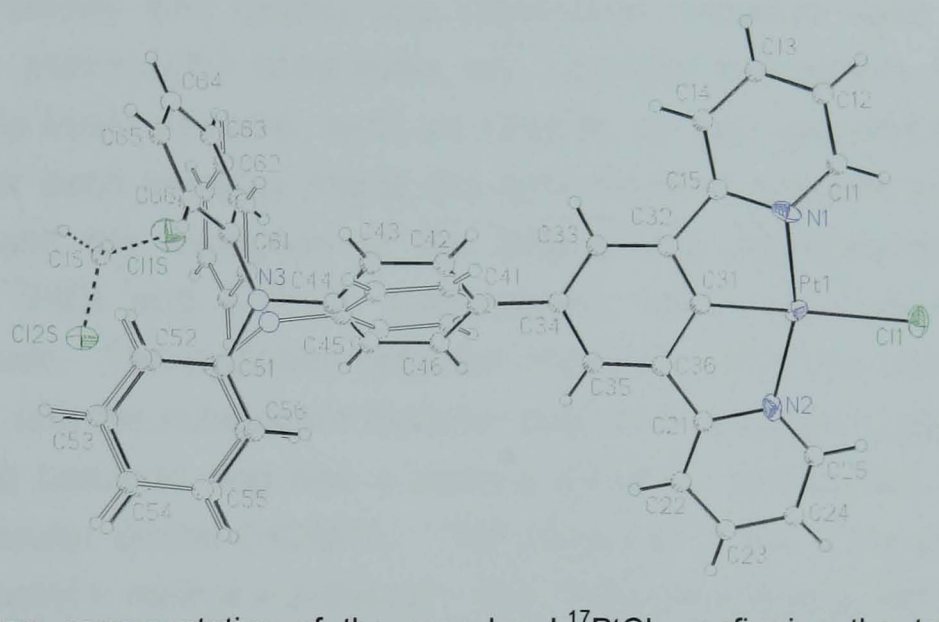

Figure 25: Diagram representative of the complex $L^{17}PtCl$, confirming the terdentate, N^C^N binding. The ligand pendant group is disordered creating a void which is alternatively filled with a DCM molecule.

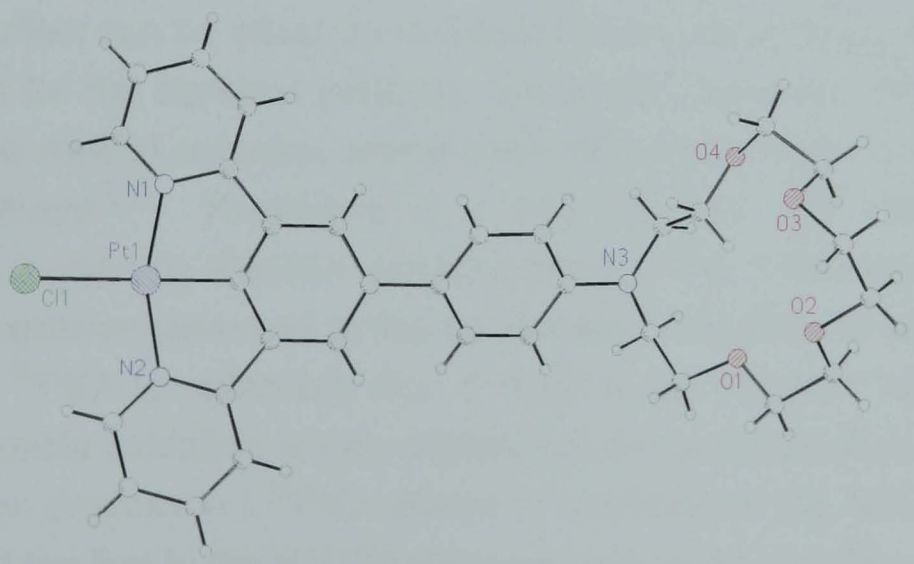

Figure 26: Diagram representative of the complex $L^{18}PtCl$ confirming the N^C^N binding and the aza-crown pendant. Although the crystal structure data are not of sufficient quality for publication, single X-ray diffraction data indicate the structure is correct.

2.2.4. Electrochemistry

Complexes $L^{7\text{-}11}PtCl$ and $L^{16}PtCl$ were investigated by cyclic voltammetry. Within the range -2.4 to +1.0 V (*vs* Fc/Fc^{+}), all of the complexes show one irreversible reduction process [in 9:1 (v/v) CH_3CN/DCM], at a similar value of around -2.0 V in each case and comparable to that observed for the parent complex, Table 2. The presence of the aryl substituent has only a small and erratic effect on the reduction potential. This is probably because the lowest unoccupied molecular orbital (LUMO) in these complexes is dominated by the pyridyl rings, with little contribution expected from the formally anionic cyclometalating ring or its pendant substituent.

All of the complexes also display one irreversible oxidation wave in this region. Square-planar platinum(III) complexes are normally susceptible to nucleophilic attack by Lewis basic solvents, such as CH_3CN, so that irreversible behaviour is the norm.[4] For each complex this is the only oxidation process within the range investigated, with the exception of the thienyl and dimethylaniline substituted complexes, $L^{10}PtCl$ and $L^{16}PtCl$, respectively, which both display a second oxidation process. The oxidation potential present in all of the complexes shows more variation with the substituent than the reduction potential, suggesting that the cyclometalating benzene ring has a more substantial contribution to the highest occupied molecular orbital (HOMO). The observed order, mesityl > 2-pyridyl > 4-tolyl > 4-biphenyl > methyl > 2-thienyl > 4-N,N-dimethylaniline can be rationalised with respect to the electron-donating ability of the substituents. In terms of σ-bonding, the simple aryl substituents are electron-withdrawing relative to methyl, accounting for the higher E_{ox} values exhibited by the first four complexes in the list. However, this effect can be offset by π-donation from the aromatic pendants. This is most evident for the biphenyl complex, the most conjugated of the complexes, and least for the mesityl complex, where steric effects disfavour co-planarity of the pendent substituent.[225] Thiophene is a very electron rich heterocycle, while dimethylaniline is strongly electron donating through the π-framework, accounting for the lowest oxidation potentials of the complexes. The second oxidation process observed for $L^{16}PtCl$ is reversible $E_{1/2}$ = 0.29 V, as the free ligand HL^{16} also displays a reversible oxidation at only slightly smaller potential ($E_{1/2}$ = 0.24 V). The second oxidation process in $L^{16}PtCl$ relates to oxidation of the N,N-dimethylaniline substitutent and the first to the N^C^N platinum core of the complex.

Complex Substituent	Absorbance λ_{max}/nm (ε/L mol^{-1} cm^{-1})	Emission λ_{max}/nm	τ_0/µs[a]	Φ_{lum} degassed (aerated)	k_q (self- quenching) / 10^9 M^{-1} s^{-1}	k_q (O_2 Quenching)/ 10^8 M^{-1} s^{-1}	E^{red}/ V	E^{ox}/V
L^1PtCl H	332 (6510), 380 (8690), 401 (7010), 454 (270), 485 (240)	491, 524, 562	7.2	0.60 (0.039)	5.3	9.1	-2.03	0.43
- Methylester	329 (7560), 380 (9990), 397 (7880), 446 (180), 478 (200)	481, 513, 550	8.0	0.58 (0.067)	3.6	4.4	-1.93	0.47
L^2PtCl Methyl	335 (5710), 381 (6900), 412 (6780), 460 (190), 495 (130)	505, 539, 578	7.8	0.68 (0.024)	3.3	16	-2.02	0.37
L^5PtCl Methoxy	361 (2545), 376 (3700), 418 (4420), 432 (4591)	554, 587	12.7	0.37 (0.011)	0.3	12.3		
L^6PtCl Bromo	326 sh (4150), 362 sh (3372), 378 (4210), 418 (4450), 492 (100)	500, 537, 574	8.2	0.39 (0.040)	4.8	7.0		
L^7PtCl Pyridine	364 sh (4700), 382 (7510), 412 (7540), 493 (120)	506, 538, 580 sh	9.2	0.57 (0.043)	4.4	5.7	-2.00	0.53
L^8PtCl Tolyl	332 sh (4750), 362 sh (3090), 381 (4670), 418 (5020), 496 (140)	516, 544 sh	9.2	0.59 (0.035)	2.5	7.8	-2.00	0.43
L^9PtCl Mesityl	332 sh (5640), 363 (3850), 381 (5410), 410 (5210), 492 (130)	501, 534, 574 sh	7.9	0.62 (0.045)	1.0	7.4	-1.99	0.58
L^{10}PtCl	363 sh (3270), 380 (4690), 426 (5080)	548, 584, 641 sh	20.5	0.54 (0.015)	1.1	7.8	-1.93	0.23, 0.61

Thienyl								
$L^{11}PtCl$ Biphenyl	364 sh (7520), 381 (11500), 418 (12400), 496 (230)	522, 551 sh	11.5	0.65 (0.035)	6.1	6.9	-1.84	0.40
$L^{12}PtCl$ Methoxyphenyl	364 (4070), 381 (6300), 420 (7200), 497 (120)	528, 555 sh	9.6	0.44 (0.017)	2.7	13		
$L^{13}PtCl$ Dimethoxyphenyl	334 (4780), 362 (2668), 381 (4200), 422 (4970), 497 (< 100)	533, 560 sh	11.2	0.49 (0.015)	4.5	16		
$L^{16}PtCl$ Dimethylaniline	380 (6410), 431 (8880)	588	12.4	0.46 (0.007)	0.12	24	-2.06	0.19, 0.29[b]
$[L^{16}PtCl]H^{+}$ [Dimethylaniline]H^{+}	331 sh (8070), 362 (5560), 381 (7720), 410 (7310)	482, 514, 547	5.8	0.40 (0.041)	1.5	6.8		
$L^{17}PtCl$ Diphenylaniline	380 sh (7200), 424 (7160), 495 (110)	557	9.0	0.29 (0.005)	0.29	21		
$L^{18}PtCl$ Aza-15-crown-5	360 (7260), 379 (4930), 433 (5710)	618						
$L^{19}PtCl$ 18-crown-6	333 (5570), 363 (2980), 381 (4130), 420 (4400), 498 (120)	529, 560 sh	10.5	0.37 (0.015)	2.5	14		

Table 2: Photophysical data in dichloromethane at 295 K, except where stated otherwise. [a]Lifetime at infinite dilution. Electrochemistry measured in CH_3CN/CH_2Cl_2 [9:1 (v/v)], in the presence of 0.1 M $[Bu_4N][BF_4]$ as the supporting electrolyte; scan rate 300 mV s^{-1}; all processes were chemically irreversible, except that indicated with a footnote[b]; $E_p^{ox/red}$ = peak potential of chemically irreversible oxidation/reduction; values are reported *vs* Fc^{+}/Fc ($E_{1/2}$ = +0.42 V vs SCE). [b]Chemically reversible process; anodic-to-cathodic peak separation, ΔE = 90 mV; the quoted value is the half-wave potential. For HL^{16} $E_{1/2}$ = 0.26 V and ΔE = 70 mV.

2.3. Photophysical properties

Complete photophysical data for the 5-pendant complexes are listed below in Table 2, including absorption and emission wavelengths, luminescent quantum yields, lifetimes, quenching rate constants and redox potentials, where applicable. Values for the complexes previously reported are also listed for comparative purposes.[74] The photochemistry of the complexes, on the whole, will be discussed together, however, the functional complexes, HL^{18}, HL^{19} and HL^{21} will be discussed separately with their own unique features.

2.3.1. Absorbance

Absorption spectra showing the lowest energy transitions of the complexes L^nPtCl (n = 1, 5, 7–13, 16, 17) recorded at 295 K in DCM are shown below in Figure 27. All of these complexes display very intense absorption bands ≤ 300 nm, assigned to π-π* transitions localised on the aromatic ligand (ε > 20,000 L mol^{-1} cm^{-1}). These transitions are followed by a second set of intense bands in the region 350–450 nm (typically ε = 4,000–10,000 L mol^{-1} cm^{-1}). This second set of transitions consists of at least three bands, of which one, *ca.* 380 nm, is invariant within this series, and thus apparently independent of the 5-position substituent. The component of the lowest energy in this particular set of transitions is increasingly red shifted through the range of complexes from 401–431 nm. In each complex, this low energy component exhibits strong negative solvatochromic behaviour, typically increasing in energy by around 1500 cm^{-1} on going from the least polar solvent investigated, CCl_4, to the most polar solvent, CH_3CN. Strong solvatochromism is typical of transitions with an appreciable degree of charge transfer character, whilst the negative shift implies an excited-state with a lower dipole moment than the ground-state,[7] illustrated in Figure 28.

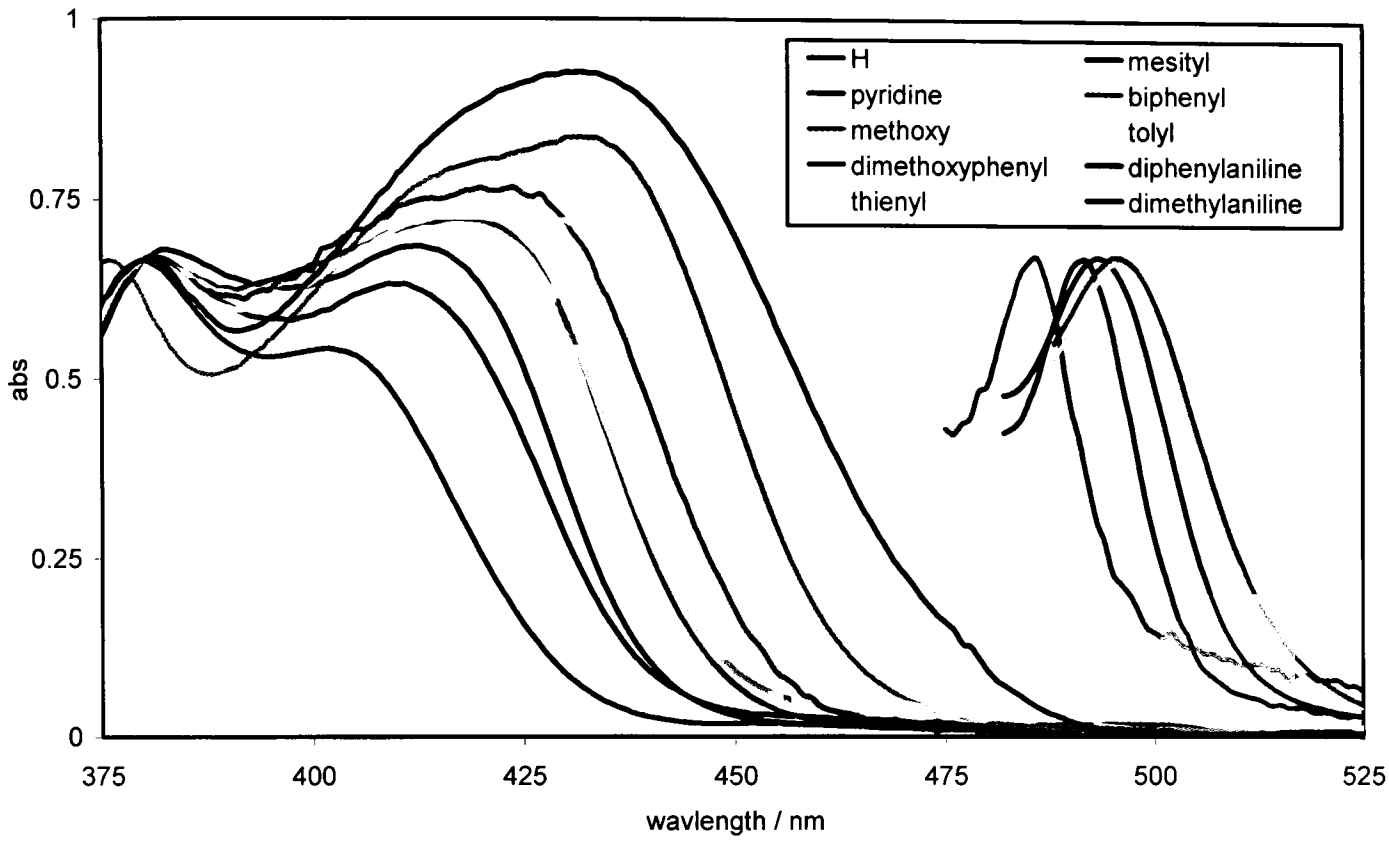

Figure 27: UV-vis absorption spectra of the platinum(II) complexes L^nPtCl (n = 1, 5, 7-13, 16, 17) in DCM at 295 K, normalised at 380 nm for comparison (extinction coefficients are provided in Table 2). An expansion of the low energy regions is also presented (< 475 nm, ca. 30 fold), normalised at relative λ_{max}, for the complexes LnPtCl (n = 1, 7–11) to show the weak bands attributed to direct population of ^{3}LC excited states.

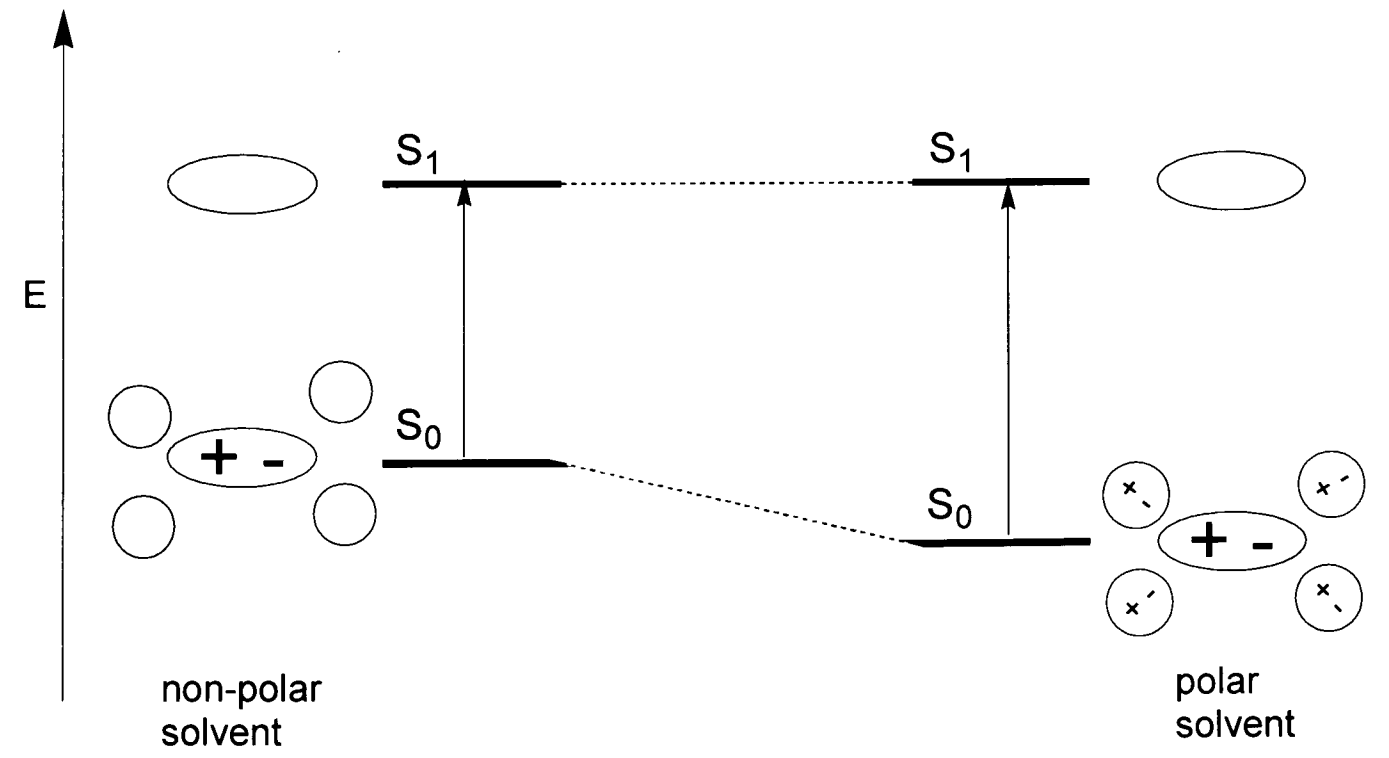

Figure 28: Diagram illustrates the solvent effect on the absorption transitions of a molecule with a larger dipole moment in its ground than excited-state.[96] Hence, the transition on the right is higher in energy in polar media, observed as negative solvatochromism, due to the relative stabilisation effect of the solvent of the molecule's ground state.

The non-aromatic pendent complexes previously reported,[74] together with the methoxy-substituted complex, L^5PtCl, display this red-shift in the order ester < H < methyl << methoxy, clearly related to the electron-donating ability of the 5-pendant functionality. The aromatic pendent complexes also display this increasing red shift in the lowest energy transition, in the order H < mesityl < 2-pyridyl < 4-tolyl < 4-biphenyl < methoxyphenyl < dimethoxyphenyl < N,N-diphenylaniline < thienyl < dimethylaniline and this, in turn, correlates with the decreasing order of oxidation potentials for this set of complexes discussed above, Section 2.2.4, Table 2, and Figure 29. The two sets of complexes however do not correlate well with one another. This can be rationalised through close examination of the complexes L^2PtCl and L^7PtCl. While the electron-donating effects of the methyl group directly lead to a red shift in the ^{1}MLCT and a concomitant reduction in the oxidation potential when compared to the core structure L^1PtCl, this is primarily attributed to the effect this substitutent has upon the HOMO of this transition. However, the pyridyl-substituted complex, while displaying a higher metal-centred oxidation potential than L^2PtCl, has the same ^{1}MLCT energy. This has been attributed to a lowering of the ^{1}MLCT LUMO through extended π-conjugation of the N^C^N acceptor unit in L^7PtCl. The net effect of lowering the energy of both HOMO and LUMO energies in L^7PtCl has a less significant effect upon the ^{1}MLCT transition than upon E^{ox}.

A much weaker band ($\varepsilon \leq 200$ L mol^{-1} cm^{-1}) is observed at lower energy than the 350–450 nm envelope, Figure 27. This band is not observed for the most red shifted of complexes, *e.g.* $L^{10}PtCl$ and $L^{16}PtCl$ respectively, where it is most likely masked by the tail of the ^{1}MLCT transition. The wavelength of this band is red shifted by 10 nm for the non-aromatic substituted complexes, from 485 nm in L^1PtCl to 495 nm in L^2PtCl, in keeping with the electron donating character of the pendant group.[74] However, this band remains fairly consistent in the aryl-substituted systems, *ca.* 495 nm. The band displays a much weaker degree of solvatochromism than the ^{1}MLCT band detailed above, and so is attributed to direct population of excited-states predominantly ^{3}LC in character, made weakly allowed by the high spin-orbit coupling associated with the platinum(II) ion, but is clearly dwarfed by the spin allowed singlet transitions.

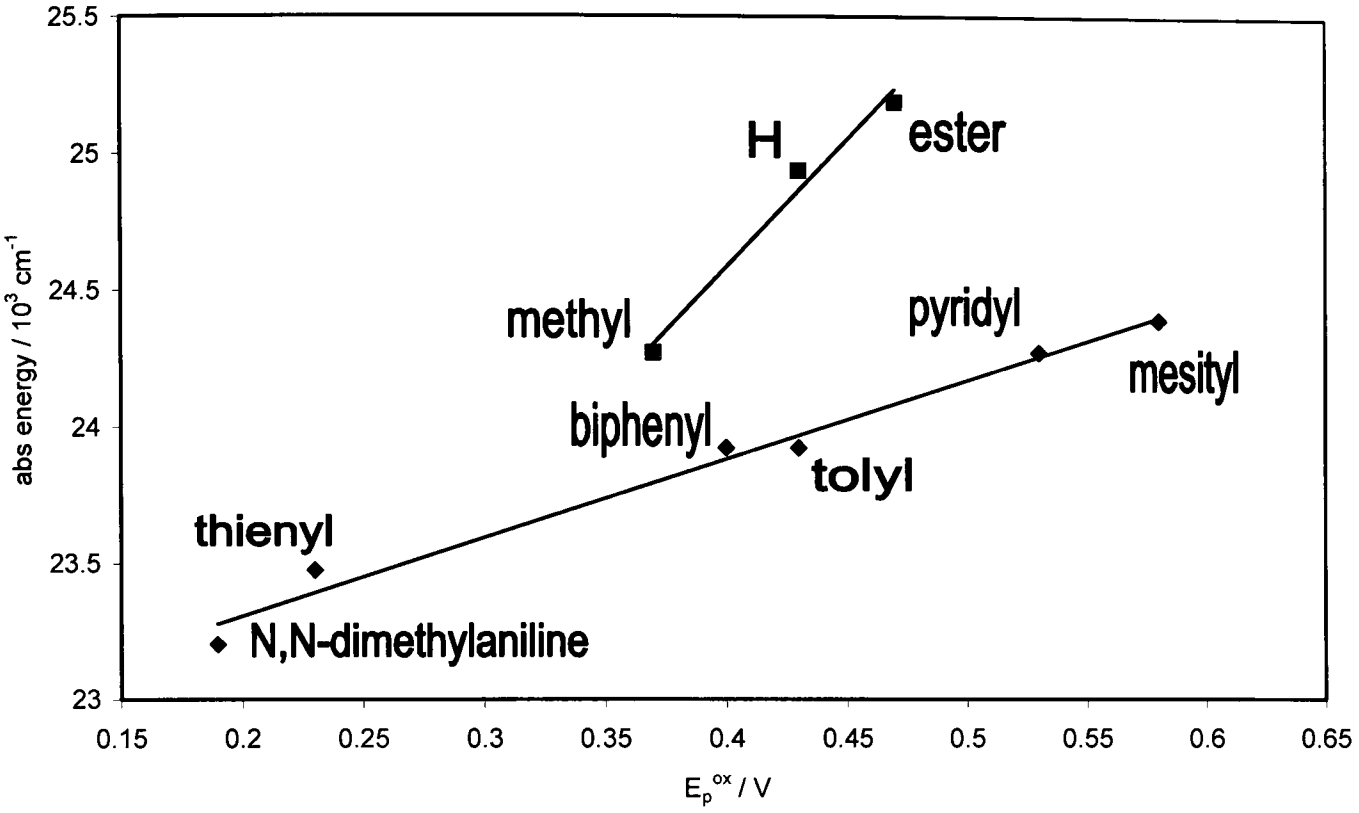

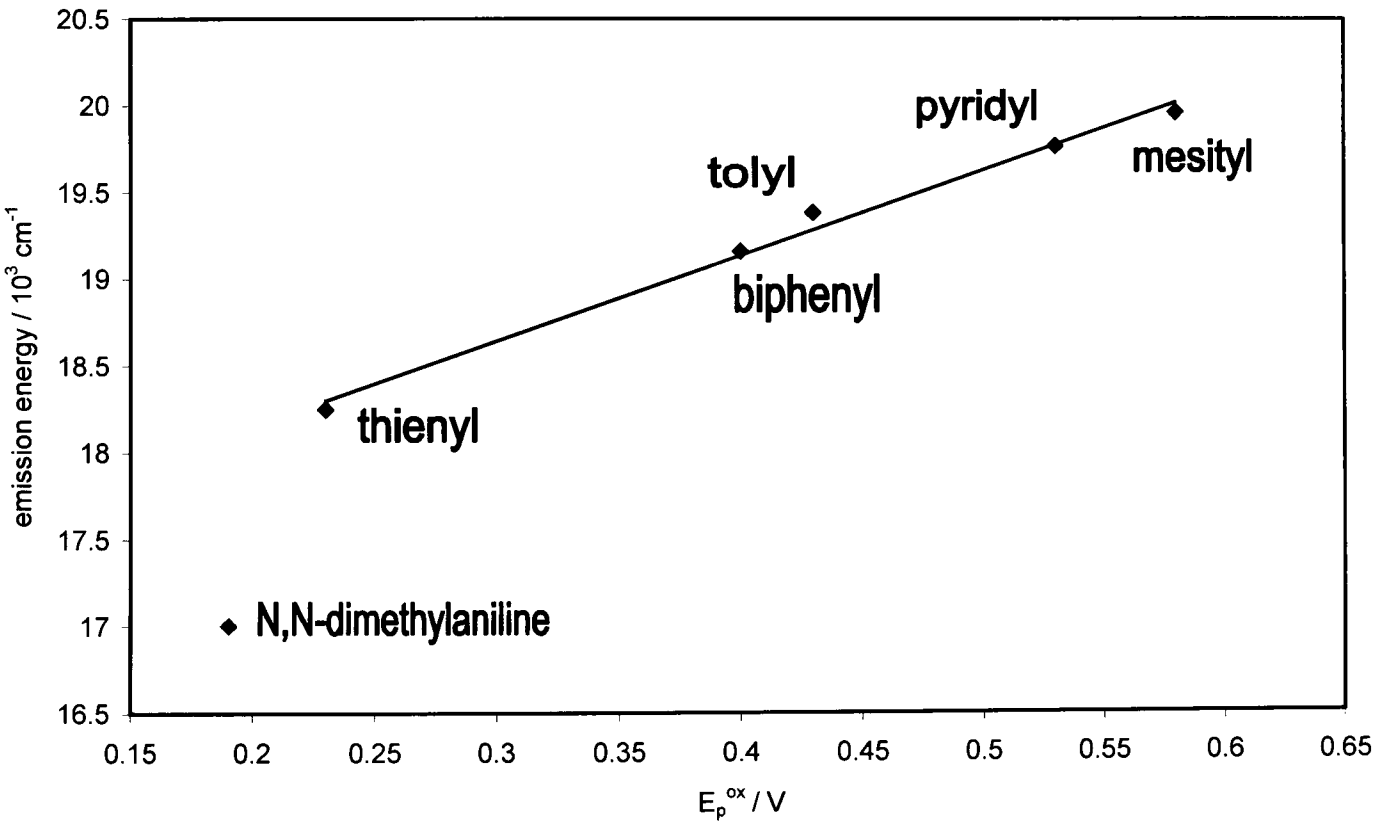

Figure 29: Correlation between oxidation potentials and absorbance energy of maxima from the lowest energy intense transition, $\varepsilon > 1{,}000$ L mol^{-1} cm^{-1} (top). The correlation between the oxidation potentials and emission maxima of L^{n}PtCl complexes (n = 7–11, 16) (bottom). Note L^{16}PtCl does not correlate well in the emission energies due to the different nature of the lowest energy excited-state.

2.3.2. Emission

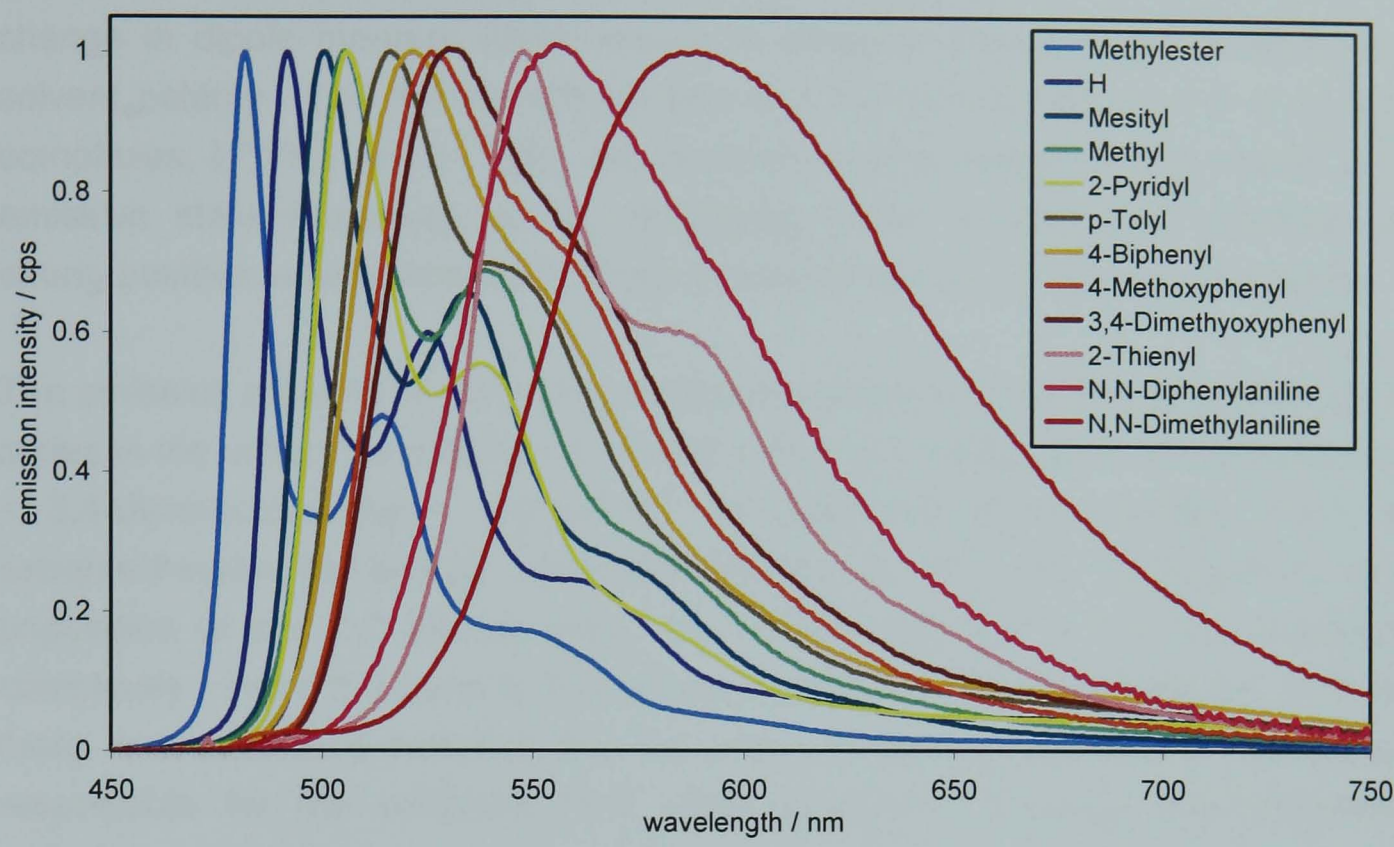

Figure 30: Emission spectra of the complexes L^nPtCl (n = 1, 2, 7–13, 16, and 17) in a dilute dichloromethane solution (ca. 10^{-5} M) at 295 K (λ_{ex} = 400 nm; band-passes of 1.0 nm).

The complexes described are intensely luminescent in solution at room temperature, Figure 30 and Table 2. The quantum yields of luminescence in degassed DCM solution are *ca.* 0.45–0.60, which are particularly high when compared to other cyclometalating platinum(II) complexes.[48,50,52,53] By shortening the platinum-carbon cyclometalating bond, whilst employing a rigid ligand framework, radiationless decay of excited states is minimised. Similarly, this approach has led to high quantum efficiencies in polypyridyl iridium complexes.[233, 234] The emission spectra of the complexes are on the whole highly structured, typical of luminescence of ^{3}LC character, therefore ^{3}MLCT transition is too high in energy and not the lowest energy triplet transition, in contrast to that observed in the singlet processes (UV-vis). The component of highest intensity is the one of highest energy (*i.e.* 0–0 transition), indicating a minimal difference between ground- and excited-state geometry, and lifetimes are of the order of microseconds. Long excited-state lifetimes are consistent with a phosphorescent spin-forbidden process, promoted by the presence of the heavy-metal atom. The spectra show minimal effect of solvatochromism, *e.g.* shifting by only *ca.* 200 cm^{-1}, which is again a feature typical of emission predominantly from a ligand-centred

excited-state, where the polarity change accompanying this transition is localised toward the outer pyridine units. Such transitions are expected to display a minimal change in dipole moment which results in emission being largely unaffected by solvent polarity. The N,N-dimethylaniline and the N,N-diphenylaniline substituted complexes, $L^{16}PtCl$ and $L^{17}PtCl$, are anomalous with respect to the nature of the emissive state discussed above, displaying broad structureless emission and strong positive solvatochromism. Their behaviour will be discussed separately.

The emission maxima of the aryl-substituted complexes are red shifted through the series in the order H < mesityl < 2-pyridyl < 4-tolyl < 4-biphenyl < 4-methoxyphenyl < 3,4-dimethoxyphenyl < 2-thienyl. As described above Section 2.3.1, the extremely-weak low-energy absorption bands at 495 nm, attributed to direct population of the ^{3}LC excited state, are roughly invariant in the aryl substituted complexes. From the trend in the emission energy of these complexes, it is clear there is a difference between the ^{3}LC state excited in absorption and the one responsible for the emission from each complex. Through low-temperature emission spectroscopy in a rigid glass matrix at 77 K [2:2:1 (v/v) ether/isopentane/ethanol] this difference in energy was identified as arising from the need for torsional rearrangement in the complex whilst in this excited state. For maximal conjugation with the N^C^N core after light absorption, the molecule will need to optimise the π-π overlap between the planar coordination motif and the aromatic substituent. By reducing the dihedral angle observed between the two planes in the ground-state, *i.e. ca.* 30° from X-ray studies of $L^{11}PtCl$, Figure 22, the LUMO is reduced in energy *via* the extended conjugation, furthermore the energy of the HOMO associated with this transition may be increased in energy by the increase in sterics. The net effect is a decrease of the HOMO-LUMO energy gap. For example, there is little difference between emission energies at 295 and 77 K for the sterically hindered mesityl-substituted complex, where the difference in the rigid matrix and the hindered rotation in fluid solution is only slight, since coplanarity under either condition is strongly disfavoured. Larger energy changes in emission at the two temperatures are observed for compounds where torsional rearrangement in fluid solutions is more pronounced, such as the biphenyl-substituted complex, $L^{11}PtCl$, where a significant red shift is observed associated with the aligning of two additional π-conjugated centres, a feature not possible in the frozen rigid matrix. Increasing aromaticity is well known to induce a red shift in the emission observed from luminescent metal complexes.[225, 233]

The emission energies of the complexes correlate with rough linearity with the oxidation potentials, in line with the substituents' influence on the HOMO of each complex. However, compared to the absorbance spectra, the variation in energy with E_{ox} is steeper, Figure 29, at 4,900 cm^{-1} V^{-1}. This behaviour is consistent with the different nature of the emissive state compared to that formed initially upon excitation into the solvatochromic absorption band, previously observed in the ^{3}LC emission of 4'-substituted terpyridine iridium(III) complexes.[225] It has also been demonstrated through DFT calculations on N^C coordinated ppy complexes that a large amount of electron density in the HOMO is centred on the 5-position of the phenyl ring.[46] Therefore, it has been no surprise that electronic transitions involved between the frontier orbitals are pronounced in these complexes when the ligand is functionalised at the postion *para* to the cyclometalating carbon.

The non-aryl-substituted complexes also display a red shift in emission maxima in the order: ester < H < methyl << methoxy. Again, the emission spectra are highly structured and assigned to ^{3}LC states. The red shift in this case is also mimicked in the weak ^{3}LC absorption band (not visible in L^5PtCl), which is most likely a direct consequence of electron-donation raising the energy of the HOMO. On closer inspection of the methoxy-subtituted complexes, L^5PtCl and $L^{12\text{-}13}$PtCl, details can be discerned about the effect the phenyl group has on electron delocalisation, and interaction with the metal centre. Firstly, both absorption and emission maxima of L^5PtCl are significantly red shifted compared to L^{12}PtCl. Therefore, the phenyl spacer is observed to reduce the electron-donating effect of the methoxy-functionality. Additionally, the emission spectrum of L^5PtCl displays more vibrational structure than L^{12}PtCl, Figure 31, suggesting that the latter has a higher degree of MLCT character in the emissive excited state, as well as the influence of the different conformations possible for aryl-substituted systems.

2.3.2.1. Concentration dependence

For the complexes L^nPtCl (n = 1, 2, 5-13), increasing concentration leads to the appearance of a new, broad, structureless emission band centred at 690–700 nm, the progressive growth of which is accompanied by a concomitant reduction in the intensity of the aforementioned ^{3}LC emission. No significant differences were observed in the position or spectral profile of this low-energy band formed by the different substituted complexes. This behaviour is characteristic of excimer formation and emission, common to square-planar platinum(II) complexes.[1,74] A

typical result is the corrected luminescence spectra of L^1PtCl in DCM solution at two different concentrations, shown in Figure 32.

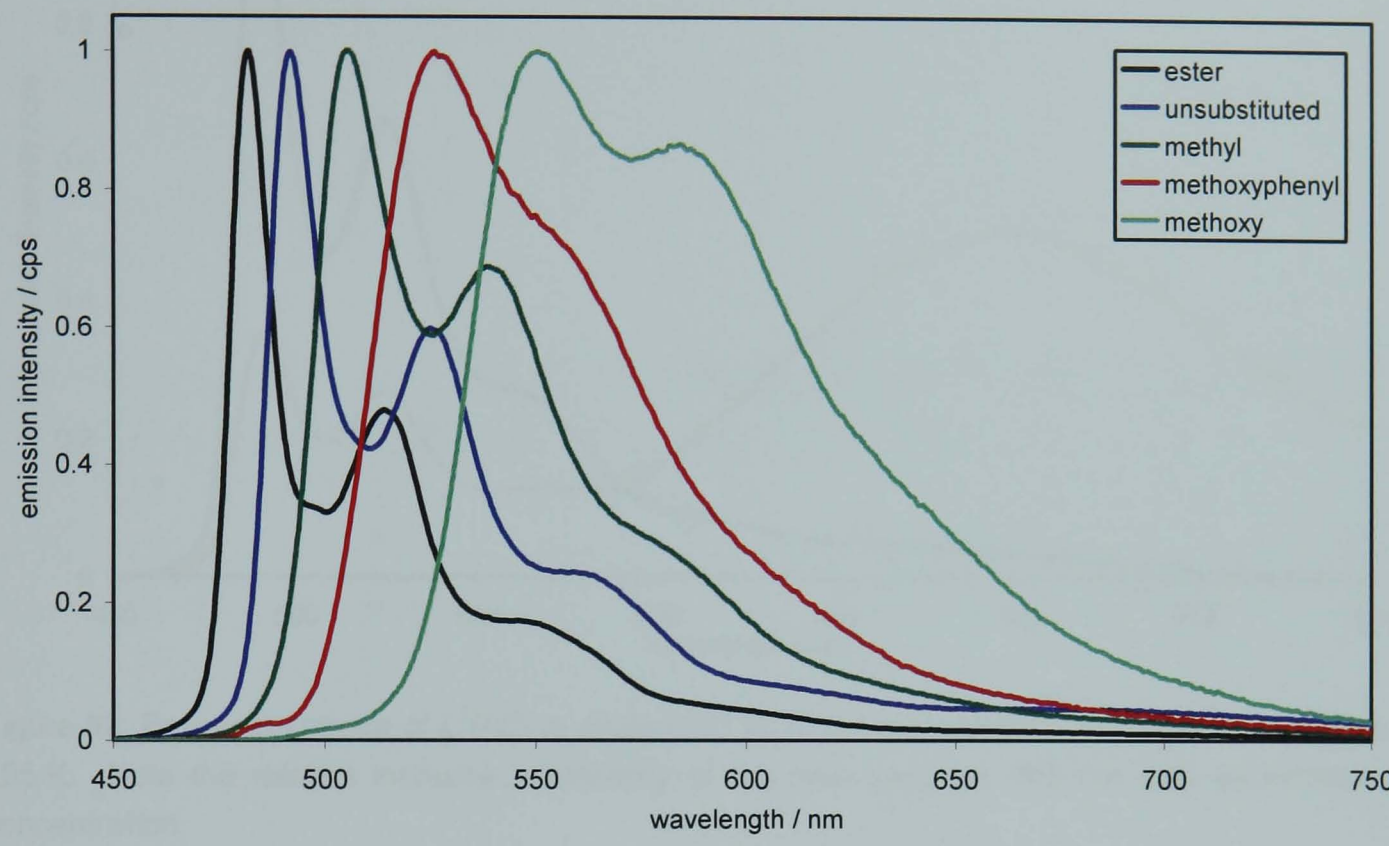

Figure 31: Inspection of features specific to methoxy-substituted complex, L^5PtCl, shows more pronounced vibrational structure compared to the 4-methoxyphenyl-substituted complex, $L^{12}LPtCl$, due to the latter containing rotational freedom in the C–C bond connecting the N^C^N binding motif and the pendant substituent.

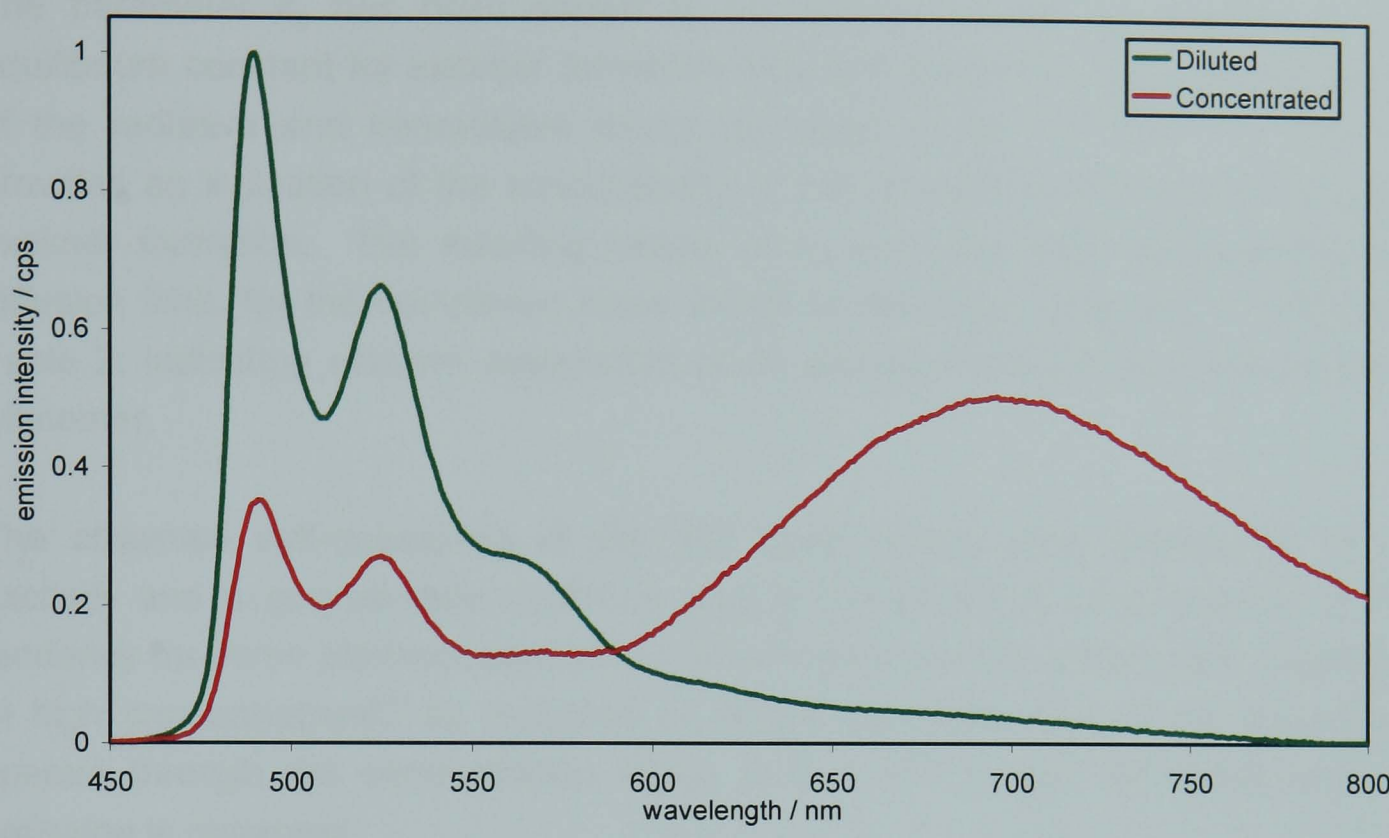

Figure 32: Emission spectra of L^1PtCl in dilute (10^{-7} M) and concentrated (10^{-3} M) DCM solutions at 295 K. Note the relative increase in intensity of the new band ca. 700 nm with an increase in concentration.

The temporal decay of the emission registered in the region of monomer luminescence (480–550 nm), where no contribution from the excimer is anticipated, remains monoexponential over the whole range of concentrations studied (7.5×10^{-6}–1.5×10^{-4} M). In contrast, the emission kinetic trace registered at 680 nm shows a monoexponential growth of the emission intensity ($k_{obs} \approx 10^6\ s^{-1}$) as the excimer responsible for the emission at this wavelength is formed from the monomer in a bimolecular process, Scheme 14. This is followed by monoexponential decay of the excimer emission with the same rate constant as that of the monomer. The observed emission decay rate constants ($k_{obs} = 1/\tau_{obs}$) increase linearly with the concentration, and are well modelled by a Stern-Volmer expression[1] shown in Equation 6.

$$k_{obs} = k_0 + k_q[Pt]$$

Equation 6: Stern-Volmer equation used to determine the rate constants for quenching process; where k_{obs} is the observed rate of emission decay, [Pt] is the platinum complex concentration, k_0 is the emission rate constant at infinite dilution and k_q is the apparent rate constant of self-quenching.

The parameter k_q has been shown to be determined by the product of the equilibrium constant for excimer formation (K_E) and the sum of the rate constants of the radiative and nonradiatve decay pathways of the excimer.[235] Thus, k_q provides an indication of the susceptibility of the complex to self-quench through excimer formation. The resulting values of k_q are quite high, approaching the diffusion limit, for the complexes more prone to self-quenching, *e.g.* $L^{11}PtCl$ see Table 2, indicating efficient association of an excited-monomer and ground-state monomer.

The observed self-quenching of the ^3LC band results from association of an excited- and a ground-state molecule and is *not* simply a consequence of the tendency for some platinum complexes to form ground-state dimers and oligomers at high concentrations,[2] as indicated by Beers Law behaviour of the absorption spectra through the concentration range of 5×10^{-6} to 10^{-4} M where excimer emission is observed.

Square-planar platinum complexes are well known to self-quench, however, only in some cases is excimer emission detectable, for example in $[Pt(diimine)(CN)_2]$.[236,237] It is clear that the rate of self-quenching of these complexes can be attenuated by steric mediation, a feature previously highlighted for related coordinatively unsaturated platinum(II) complexes.[1] An increase in steric bulk significantly lowers excimer response, as shown by the lower value of k_q for L^9PtCl Table 2, due to shielding of the d_{z^2} orbital of the metal centre involved in the most relevant interactions.[238] Therefore, introduction of the mesityl group into the system has a detrimental effect of the rate of excimer formation, despite dimeric species observed in the crystal studies of L^9PtCl, Figure 24. Bulky, sterically demanding systems, such as mesityl and *tert*-butyl groups are known to minimise solid-state intermolecular interactions between neighbouring planes of platinum complexes.[55] It is clear that intermolecular interactions here cannot be completely disrupted by this simplistic approach, however, with these interactions becoming antagonistic in the solid state, so they are disfavoured in dynamic fluid solutions.

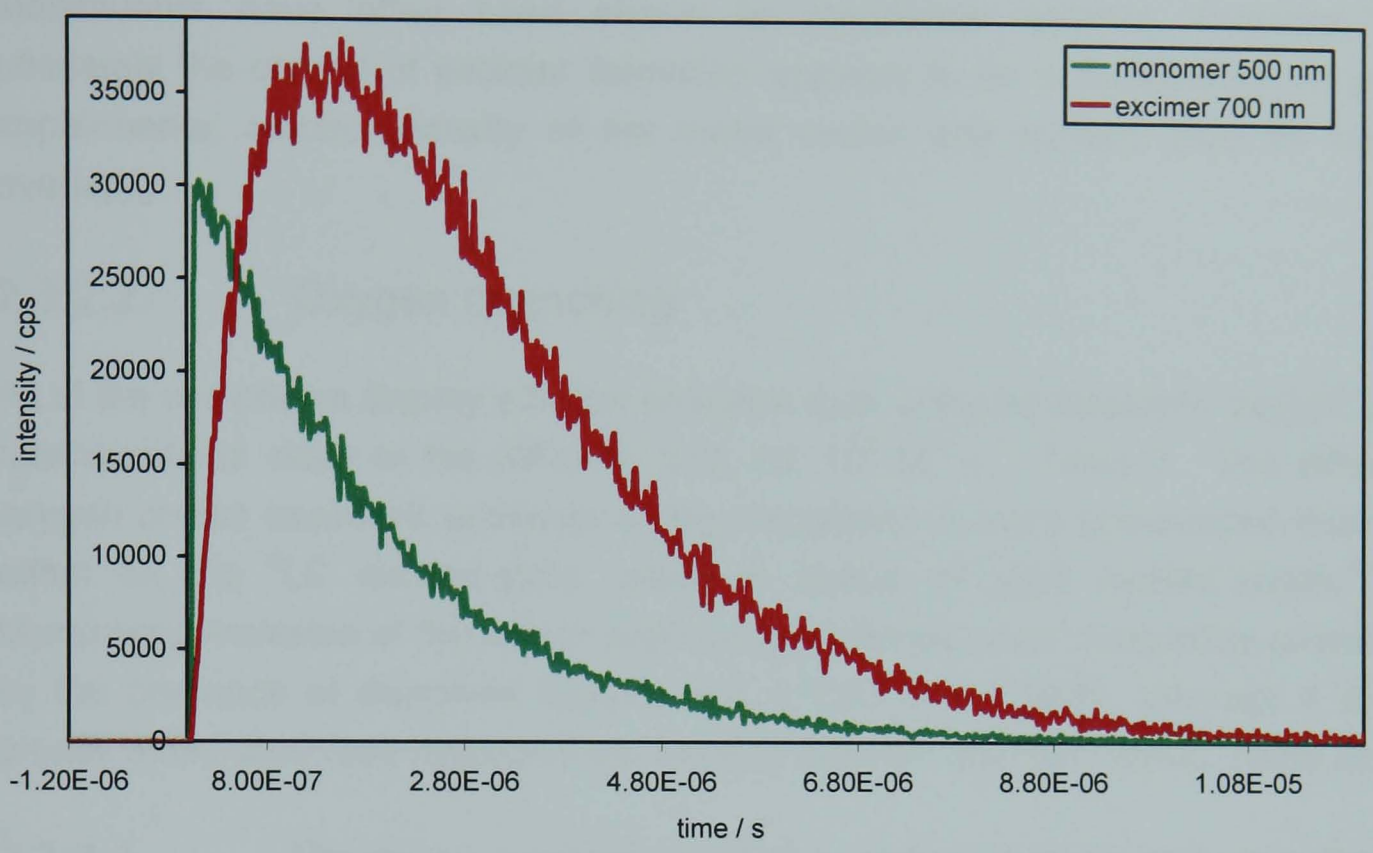

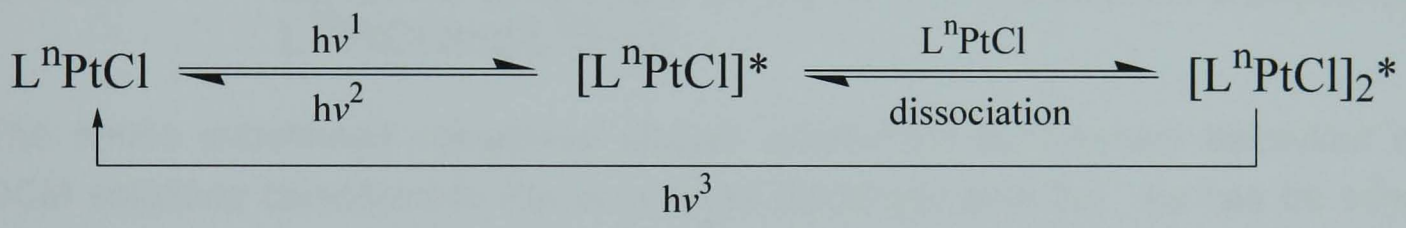

Scheme 14: Scheme shows the process of excited-state generation, excimer formation and the fates of the excited-state species. The generation of an excited-state complex, $[L^nPtCl]^*$, through the absorption of a photon, hv^1, can either lead to emission from the monomeric species, hv^2, or association with another ground state molecule, L^nPtCl, to form an excited-state dimer, $[L^nPtCl]_2^*$. The excimer species can then relax back down to the ground-state species through emission, hv^3, seen as long wavelength excimer band in Figure 32.

Additionally, the methoxy-substituted complex, L^5PtCl, was observed to display a significant reduction in its tendency to form excimers, k_q = 0.3 x 10^9 M^{-1} s^{-1}, approaching 20 times smaller than the core structure L^1PtCl k_q = 5.3 x 10^9 M^{-1} s^{-1}. Obviously this cannot be symptomatic of reduced contacts induced by steric repulsion, as displayed by L^9PtCl. Therefore, it is believed this behaviour is related to some sort of electronic effect. For example, it is plausible that a donor-acceptor interaction may be required to promote the association of the excited- and ground-state species. However, in the case of L^5PtCl and the thienyl substituted $L^{10}PtCl$, these complexes are expected to be electron-rich compared to the other complexes discussed here, and both appear to be less willing to interact in this fashion, possibly because they are not sufficiently Lewis acidic. While methoxy

substituents have often been shown to destabilise excimer formation,[81,151] ultimately the control of excimer formation appears to be a combination of steric impairments, electron-density of the metal centre and surface area for orbital overlap.

2.3.2.2. Oxygen quenching

All of the complexes display efficient emission quenching by dissolved oxygen, with rate constants close to the diffusion limit, *ca.* 10^9 M^{-1} s^{-1}, Table 2. The effect of oxygen on the excimeric emission of the complexes is more pronounced than the effect on the ^{3}LC excited-state, which is typical of such excited-states.[239,240] Monomeric emission of the above platinum complexes is not completely quenched by the presence of dissolved oxygen, *e.g.* L^1PtCl Φ = 0.0039, although it is still greatly attenuated (see degassed *vs.* aerated solution quantum yields, Table 2).

2.3.2.3. Emission properties of the amino-substituted complexes $L^{16}PtCl$ and $L^{17}PtCl$

The amino substituted complexes display anomalous luminescent behaviour in DCM solutions compared to the complexes discussed thus far. As can be seen from Figure 30, the emission bands are broad and unstructured (fwhm = 120 and 80 nm, $L^{16}PtCl$ and $L^{17}PtCl$ respectively). The emission maxima are significantly red shifted compared to the other complexes, particularly the emission maximum of the dimethylaniline complex which has an emission maximum displaced by *ca.* 100 nm from that of the core structure, L^1PtCl. The position of the dimethylamino complex in the plot of E_{em} vs E_{ox} is anomalous Figure 29, the complexes are subject to very little self-quenching, $k_q = 0.12 \times 10^9$ M^{-1} s^{-1} $L^{16}PtCl$ and 0.29×10^9 M^{-1} s^{-1} $L^{17}PtCl$, and both are considerably more susceptible to oxygen quenching, $k_q = 24 \times 10^8$ M^{-1} s^{-1} $L^{16}PtCl$ and 21×10^8 M^{-1} s^{-1} $L^{17}PtCl$, compared to L^1PtCl (k_q = 5.3×10^9 M^{-1} s^{-1} and 9.1×10^8 M^{-1} s^{-1} respectively).

These differences suggest a different type of excited state compared to the ^{3}LC state displayed by the other complexes. The broad structureless profiles of the emission spectra and relatively small self-quenching rate constants are typical of complexes with emissive charge transfer transitions, and it is hypothesised that the introduction of the strong electron-donating amine fragments generate molecular orbitals localised predominantly on the amino groups of these molecules, an ^{3}ILCT

$\pi_{R_2N\text{-}Ar}$–$\pi^*_{N^C^N}$ transition is thought to arise. A similar effect has already been discussed in the introduction regarding the use of electron rich aromatic units to generate new, low lying excited-states in platinum terpyridine complexes,[42] and this effect is well known for other amino substituted systems, such as 4'-(1-naphthyl)-2,2':6',2''-terpyridine-N'-platinum chloride and 4'-(9-phenanthrenyl)-2,2':6',2''-terpyridine-N'-platinum chloride.[42,91,241] Notably however, the change in emissive-state has little effect on the radiative processes of the complexes, and quantum yields are still high (Φ = 0.29–0.46), despite the low energy of the excited-state.

Further evidence in support of the involvement of charge-transfer excited-states in DCM solution is provided by the positive solvatochromism in the emission spectrum of these complexes. For example, the emission energy is almost 4,000 cm^{-1} lower in acetonitrile than in carbon tetrachloride for $L^{16}PtCl$. Interestingly, the spectrum of $L^{16}PtCl$ recorded in the least polar solvent, CCl_4, resembles that of the ^3LC emission from the complexes previously discussed. The new emission maximum is similar to that observed for the pyridyl-substituted complex, L^7PtCl, and shows well defined vibrational structure. Thus, the ^3LC and ^3ILCT excited-states are close in energy for $L^{16}PtCl$ and $L^{17}PtCl$. In polar solvents the charge-transfer states are stabilised due to the high degree of charge separation, however, in non-polar solvents the ^3ILCT state is no longer stabilised by the solvent and increases in energy, shown in Scheme 15. This effect can be quite dramatic, so much so that the ^3LC excited-state dominates the radiative decay processes under non-polar conditions, shown in Figure 33. This effect is less pronounced in the delocalised diphenylaniline pendant complex, ΔE = *ca.* 400 cm^{-1} between the peak maximum for emission in CCl_4 and CH_3CN. It is believed that the excited state of this complex is more accurately described as an admixture of the ^3LC and ^3ILCT excited-states, displaying features of both types of excited-state.

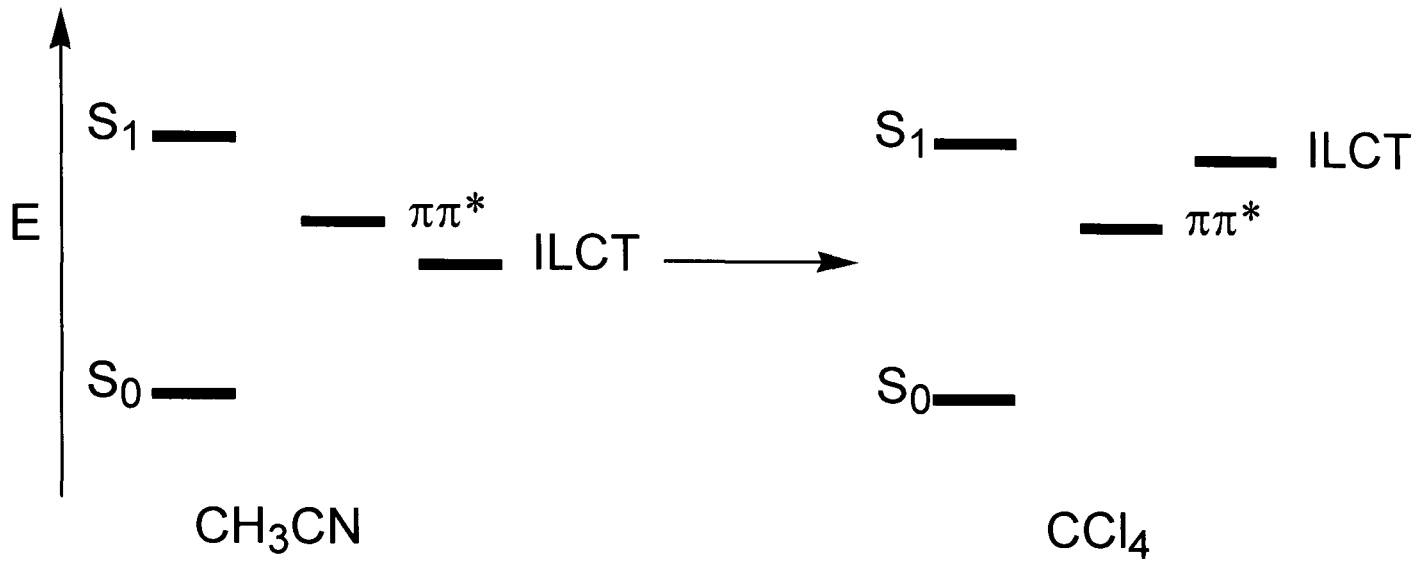

Scheme 15: Schematic representation of the solvent effect on the lowest-energy excited state of the dimethylaniline substituted complex. The large charge separation associated with the charge transfer transition, ILCT, makes it more stable in polar solvents such as CH_3CN. Meanwhile, the relatively unpolarised ligand-centred transition, π-π*, means this transition remains relatively unchanged by the solvent.

The ^{3}ILCT excited-state has also been credited with moderation of excimer/exciplex quenching in such compounds because the excited-state is less susceptible to adduct formation with ground-state molecule which plays the role of the Lewis base in the process of excimer formation. Hence the low k_q values observed for self-quenching in $L^{16\text{-}17}PtCl$, Table 2. However, since the excited-state switching is observed in $L^{16}PtCl$ upon changing of solvent systems, excimer emission is observed for the complex in lower polarity solvents, when sufficient solubility is available, as observed for the toluene spectrum in Figure 33.

Like the other complexes in this study, the ^{3}ILCT excited-states are susceptible to oxygen quenching, as previously discussed. The quenching by dioxygen is even more striking for the ^{3}ILCT states than the aforementioned ^{3}LC states, as has been previously documented for complexes with these types of excited-states.[241,242] Often this effect can lead to almost complete quenching of the charge-transfer emission at oxygen concentrations sufficient for ^{3}LC excited-states to still be significantly emissive, a feature that will become important in later discussions.

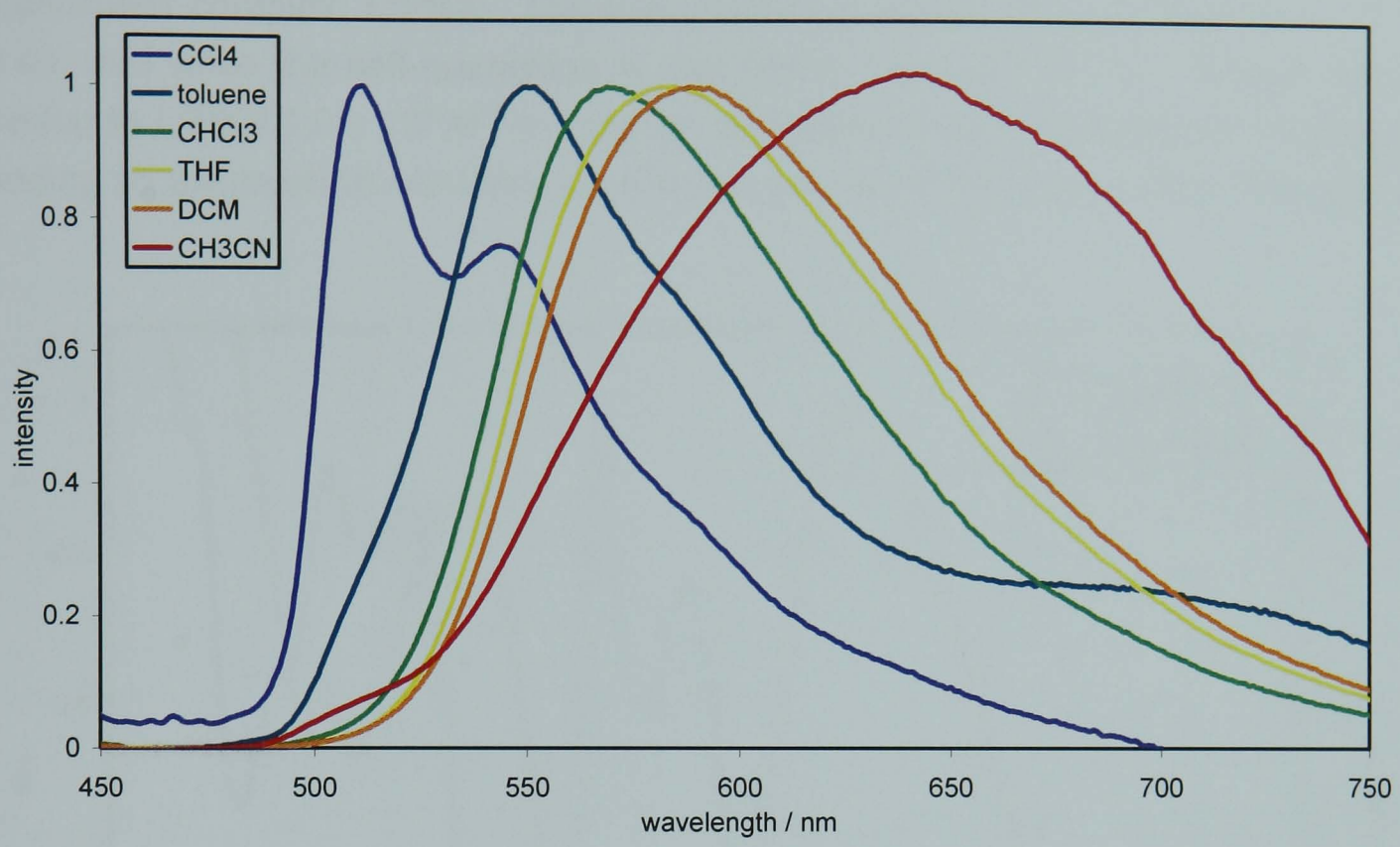

Figure 33: Emission spectra of $L^{16}PtCl$ at 295 K in several solvents of differing polarity, showing the strong positive solvatochromism. Note the change to a structured, high-energy emission spectrum in CCl_4, resembling the ^3LC emission from other N^C^N platinum complexes. Note also, the presence of excimer emission in toluene at the concentration employed (10^{-4} M).

2.3.2.4. Effect of protonation of the pendant amine of $L^{16}PtCl$

Protonation of $L^{16}PtCl$ in DCM by the addition of trifluoroacetic acid (TFA) results in a dramatic set of changes in the absorption and luminescence spectra, Figure 34 and Table 2. The emission maximum is blue-shifted by 3700 cm^{-1}, the profile becomes more structured, self-quenching and excimer emission at elevated concentrations become significant, and the monomeric luminescent lifetime is reduced by a factor of about two. These changes in the emission are accompanied by a blue-shift of the ^1MLCT absorption band. All of these effects are consistent with a process commonly known as excited-state switching, similar to that shown in Scheme 15, where the nature of the lowest-energy excited-state changes from ^3ILCT to the ^3LC state. However, in this case the process is driven directly by removing the influence of the electron-donating amine group through protonation of the lone-pair of electrons. The process of electron transfer determined by the oxidation potential of the donor and the reduction protential of the acceptor unit becomes thermodynamically much less favourable. The new photophysical data associated with $[L^{11}PtCl]H^+$ are similar to those of the mesityl

substituted complex, L^9PtCl. The luminescent quantum yield remains high, Φ = 0.40, and while the self-quenching is significant, 1.5 x 10^9 M^{-1} s^{-1}, the low value similar to L^9PtCl 1.0 x 10^9 M^{-1} s^{-1}, can be attributed to the net charge of the amine adding an electrostatic repulsive force to the process of excimeric dimer formation.

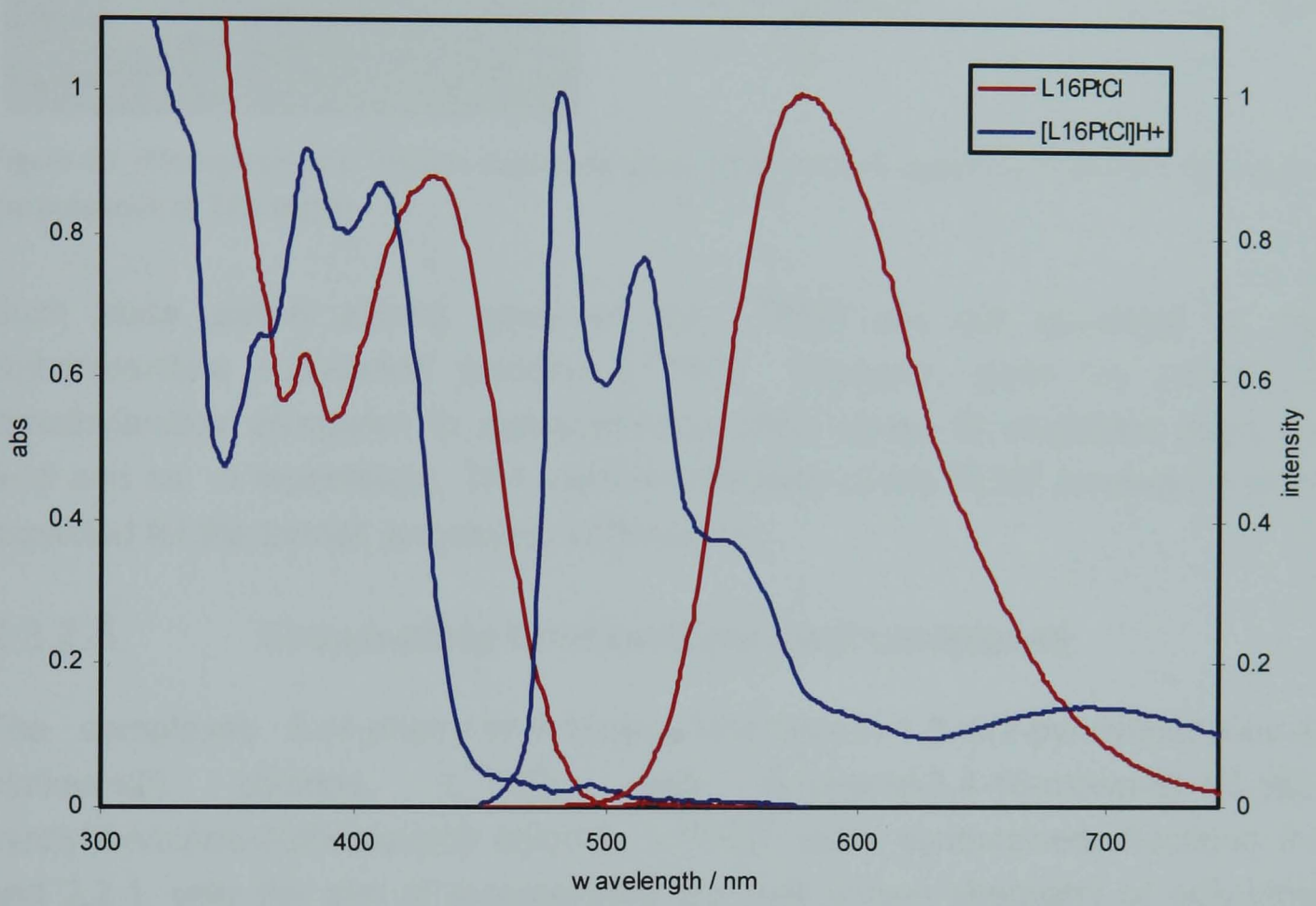

Figure 34: Emission and excitation spectra of $L^{16}PtCl$ in DCM, 6.0 x 10^{-5} M, 295 K, and the corresponding blue-shifted spectra, after the addition of trifluoroacetc acid (10^{-2} M). λ_{ex} = 408 nm in both cases (isosbestic point); λ_{em} = 588 nm and 488 nm, respectively; band-passes = 2 nm. Note the appearance of an excimer band for the protonated complex.

The effects of protonation are fully reversible upon neutralisation. The protonation-induced state-switching between two different types of excited-states with significantly different energies, both of which are highly emissive, is an unusual feature and visually quite dramatic, shown in Figure 35.

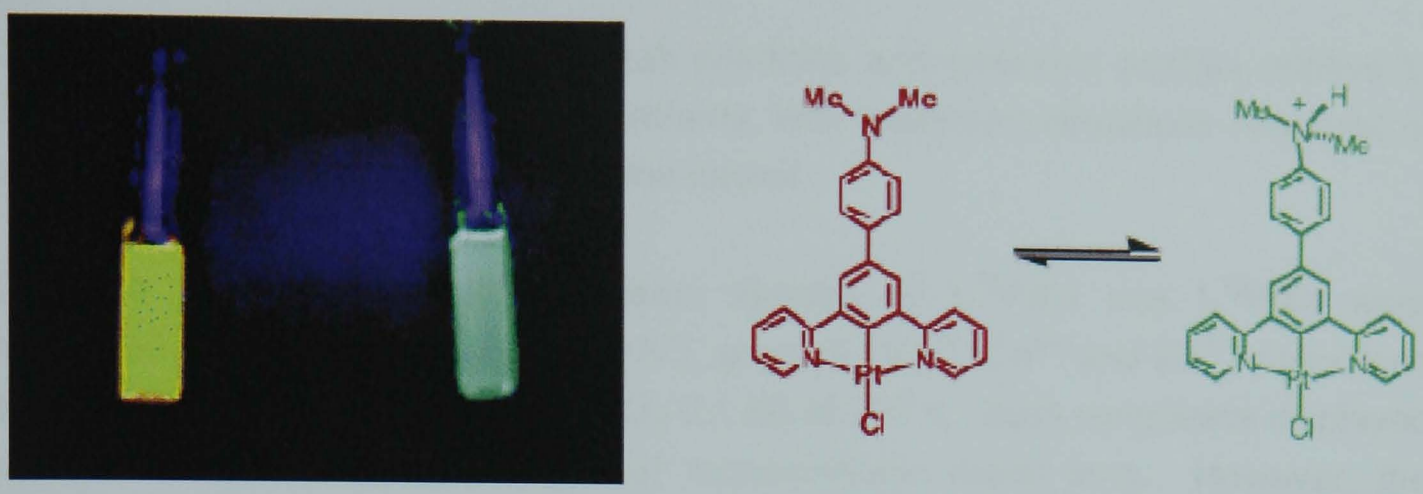

Figure 35: Photograph of $L^{16}PtCl$ in degassed dilute DCM solution under UV irradiation (left) and in the presence of TFA (right).

Such state switch effects observed for $L^{16}PtCl$ are not observed for the diphenylaniline substituted complex $L^{17}PtCl$. However, given the basicity of dimethylaniline compared to diphenylaniline (pKa values of conjugate acids are 5.15 and *ca.* -5 repectively), TFA induced inhibition of the ^{3}ILCT emission is to be expected for the former, but absent in the latter.

2.3.2.5. Crown-ether functional pendant complexes

The complexes 5-(4-phenyl-N-monoaza-15-crown-5)-1,3-di(2-pyridyl)benzene-2-platinum(II) chloride, $L^{18}PtCl$, and 5-(phenyl-3,4-18-crown-6)-1,3-di(2-pyrdiyl)benzene-2-platinum(II) chloride, $L^{19}PtCl$, were synthesised, Sections 2.1 and 2.2.1, with the aim of incorporating the well known chemistry of poly-ether crown systems for specific stochiometric metal-ion binding, coupled to the previously established luminescent properties of the N^C^N platinum complexes. Spectrochemical recognition of guest metal-ions is confirmed by the absence of spectral changes in the electronic spectra of the respective control complexes $L^{16}PtCl$ and $L^{13}PtCl$, respectively.

The absorption spectra for the crown ether complexes at RT in DCM are typical of N^C^N coordinated platinum complexes, with intense high energy transitions $\leq$ 300 nm ($\varepsilon \approx$ 36,000 L mol^{-1} cm^{-1} in DCM) associated with the conjugated ligand (π-π^*), followed by less intense lower energy bands (325–450 nm, 3,000–6,000 L mol^{-1} cm^{-1}) associated with ^{1}MLCT transitions. The presence of a band at 380 nm is consistent with the N^C^N coordinating motif. Again, the same negative solvatochromic behaviour is observed for the absorption spectra confirming the nature of the transitions as charge transfer, in both cases. Both crown-ether

pendant complexes have similar peak positions and emission profiles relative to their respective non-crown ether standards, with maximum deviations observed of *ca.* 2 nm, close to the uncertainty in the values.

Changes in absorption and emission spectra of $L^{18}PtCl$ and $L^{19}PtCl$ were monitored with group I (Li^+, Na^+ and K^+), group II (Mg^{2+}, Ca^{2+} and Ba^{2+}) metal ions and with Zn^{2+} in acetonitrile (Bu_4NClO_4 0.1 M) at 298 K. Both complexes displayed little or no change upon addition of mono-cationic metal ions. However, the complexes were more responsive to the dications, specifically, Ca^{2+} for $L^{18}PtCl$ and Zn^{2+} for $L^{19}PtCl$, shown in Figure 36 andFigure 37 respectively. Similar shifts were not observed in a control experiment using the crown-free complexes, indicating these shifts were due to the binding of the cations to the polyether cavity.

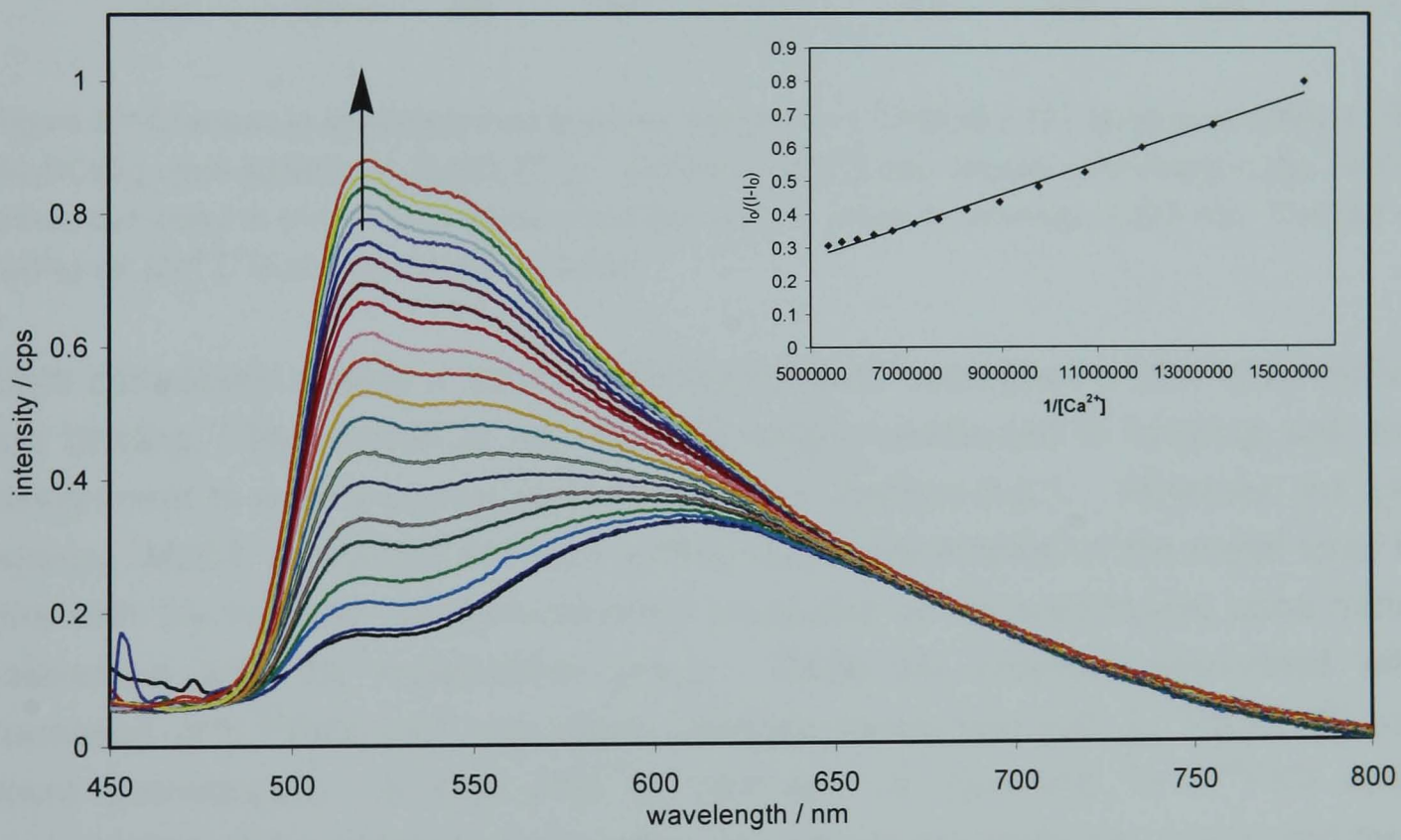

Figure 36: Luminescence spectra of $L^{18}PtCl$ (5×10^{-5} M) in acetonitrile (1.0 M Bu_4NClO_4), λ_{ex} = 369 nm, in the increasing presence of $Ca(SO_3CF_3)_2$. The insert shows the plot of $I_0/(I-I_0)$ vs $[Ca^{2+}]^{-1}$, the straight line suggest 1:1 binding.[99]

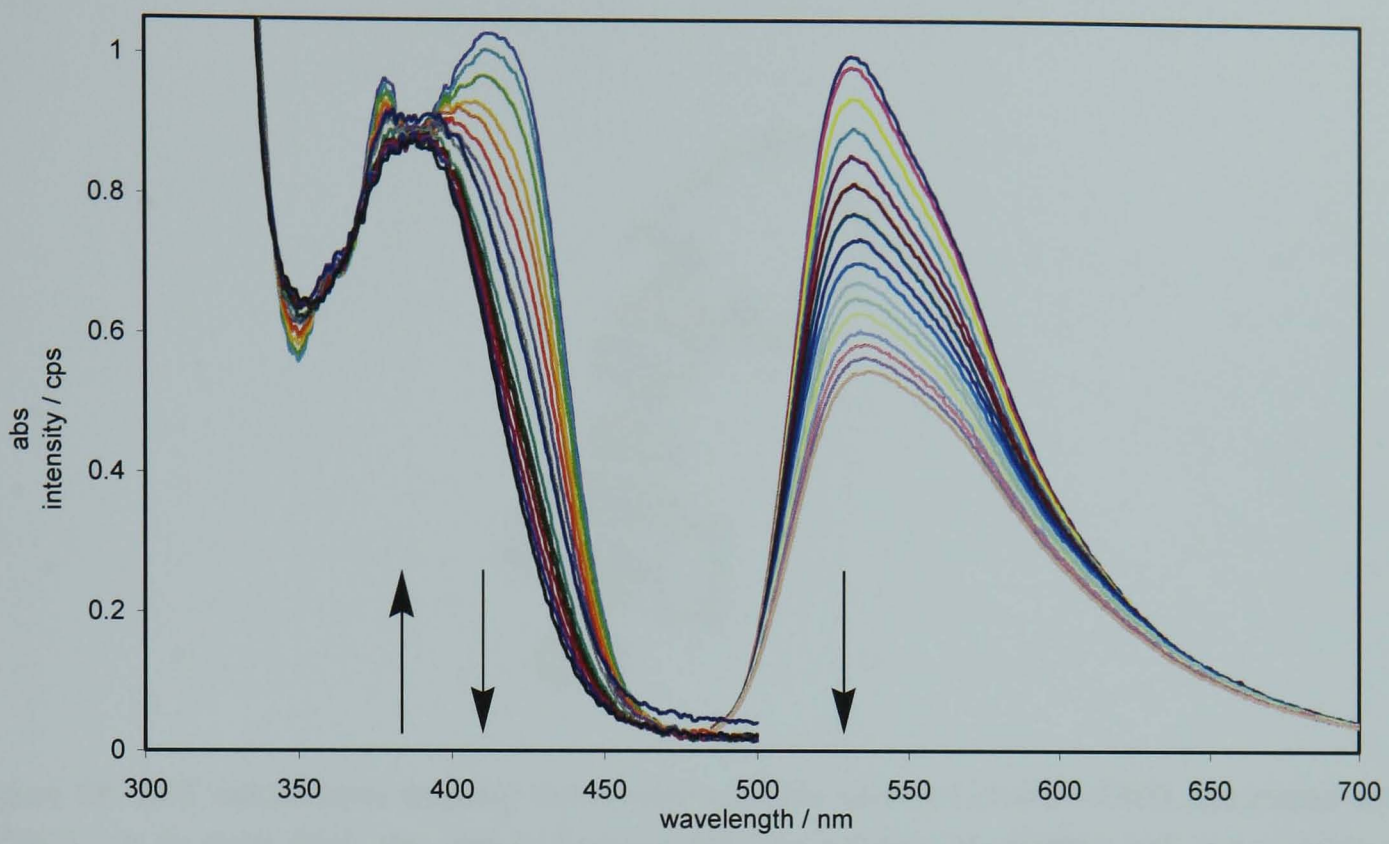

Figure 37: Changes in absorption and emission spectra for $L^{19}PtCl$ (3×10^{-5} M) in acetonitrile (1.0 M Bu_4NClO_4) upon addition of $Zn(SO_3CF_3)_2$. Addition of $[Zn^{2+}]$ ions causes a decrease in the ^{1}MLCT absorption band at 414 nm and concomitant decrease in emission intensity at 535 nm. The plot of $I_0/(I-I_0)$ vs $[Zn^{2+}]^{-1}$ is provided in the appendix.

Both complexes display a similar response in their absorption profile upon metal-ion binding. The bands at 380 nm are largely unaffected in keeping with the assignment to mainly pyridyl based transitions, Section 2.3.1. However, the low energy ^{1}MLCT transitions are blue shifted upon coordination of the metal ions, in line with the reduced electron-donating properties of the substitutent upon metal interaction with the crown-ether group. While the changes associated with formation of $[L^{18}PtCl.Ca]^{2+}$ are slight, changes associated with $[L^{19}PtCl.Zn]^{2+}$ are more pronounced. A blue shift of 1600 cm^{-1} is observed for $L^{19}PtCl$ upon coordination of the pendant crown-ether oxygens to the metal ion, confirming their electron-donating properties. Also the oxygens directly attached to the phenyl spacer groups are clearly demonstrated to play a significant role in the energy of the HOMO by computational DFT orbital calculations, Figure 38. Similar behaviour has been observed for (terpy)platinum(II)(S-benzo-15-crown-5) crown-ether system.[82]

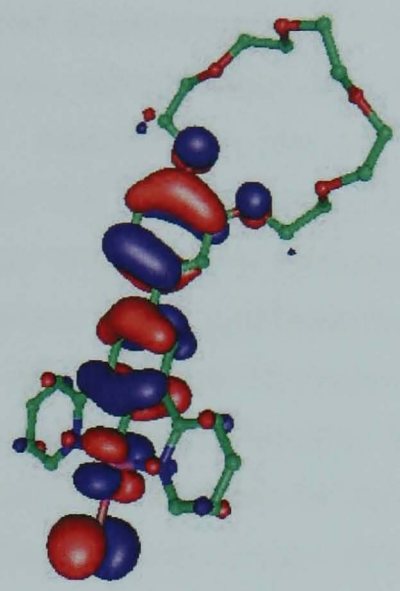

Figure 38: DFT calculations showing the electron-density contours of the HOMO associated with $L^{19}PtCl$. It is clear from the above diagram that the orbitals associated with the oxo-crown functionality are important in donating electron density toward the metal centre. As confirmed by the titration results complexation of Zn^{2+} removes the donicity of the phenyl bound oxygen atoms, an effect experienced by the metal centre, demonstrated by the blue shift of the ^{1}MLCT absorption band.

The luminescence spectra of $L^{19}PtCl$ upon the progressive addition of [Zn^{2+}] show no distinct change in profile or energy of the emission. This behaviour would suggest that the electron-donating ability of the pendant oxygen atoms is not important in governing the energy of the ^{3}LC transition. However, the emission intensity decreases monotonically throughout the additions, indicating an increase in the non-radiative decay processes induced by the binding of the metal ion. The emission intensity was significantly quenched by the addition of Zn^{2+} ions (20 equiv.) with a reduction of *ca.* 66% in the intensity.

Figure 36 presents the changes in the luminescence spectrum of complex $L^{18}PtCl$ upon addition of Ca^{2+}. The emission maximum at 521 nm grows-in with increasing Ca^{2+} concentration. No well defined isosbestic points can be identified from the titration data. However, the change evidently arises from the complexation of the cation with the azacrown ether receptor, which decreases the electron donating ability of the pendent. Upon complexation of Ca^{2+} the ^{3}ILCT transition from the aza-crown ether is raised in energy so that it no longer dominates the emission spectrum of the complex. The new band which appears at 521 nm is then

attributed to a ^{3}LC transition of the N^C^N coordination motif. The insert in Figure 36 shows a plot of $I_0/(I_0 - I)$ vs $[Ca^{2+}]^{-1}$, where I and I_0 refer to the emission intensity at 521 nm in the presence and absence of Ca^{2+}, respectively. A straight line in other platinum based aza-crown ether ionophores has been used to suggest 1:1 complexation of the cation.[99] Additionally, the Job's plot shown in the Appendix confirms a 1:1 binding mode for Ca^{2+}. The binding constant, log K_s = 1.15 (± 0.12), determined from computational calculations performed by Dr. J.-L. Fillaut, gave a much smaller value than observed for terpyridineplatinum(ii) aza-crown complexes, and also smaller than those of other aza-15-crown-5 ionophores reported in the literature. Because of the extremely weak binding of the calcium ion with the aza-crown system the emission spectrum appears to consist of an admixture of the ^{3}LC and ^{3}ILCT excited-states, similar to the emission observed for L^{17}PtCl.

The aza-crown-ether complex, L^{18}PtCl, was observed to decompose over time; the decomposition product is observed to emit at higher energy compared to L^{18}PtCl, yet consistent with the complex $[L^{18}PtCl.Ca]^{2+}$, observed as the shoulder at λ = 521 nm which increase in intensity with the addition of Ca^{2+}, in Figure 36. The shoulder persisted in the presence of base and EDTA, eliminating the influence of protonation and complexes cations. Photostability has been identified as a major issue with applicability of potential luminescent probes, and while cyclometallated homoleptic complex bis(phenylpyridine) platinum(II) decomposes to unknown products under irradiation with UV or daylight,[47] the cause of this compound's decomposition remains unknown.

2.4. Towards AlQ_3–Pt hybrid systems

8-Hydroxyquinoline and its halogenated derivatives have found extensive applications because of their ability to form complexes with many metal ions.[243,244] One of the more notable complexes is AlQ_3, Figure 39, which has displayed exciting luminescence and electron-transport properties when fabricated in OLEDs.[25,124,125,127] Unfortunately, however, aluminium is a relatively light metal-ion, particularly when compared with transition metals, and therefore is poor at promoting emission from triplet excited states. Due to the high level of triplet excited states generated through electroluminence, OLEDs can maximise performance by employing a conductive host material with a dispersed phosphorescent guest as the emissive material. To this end it is envisaged that by combining the properties of the good charge transport compound, AlQ_3, with one of

efficient phosphorescence, *e.g.* $L^{22}PtCl$, tris-(8-hydroxyquinoline-5,7-di(2-pyridyl)-6-platinum(II) chloride) aluminium, could be of potential interest.

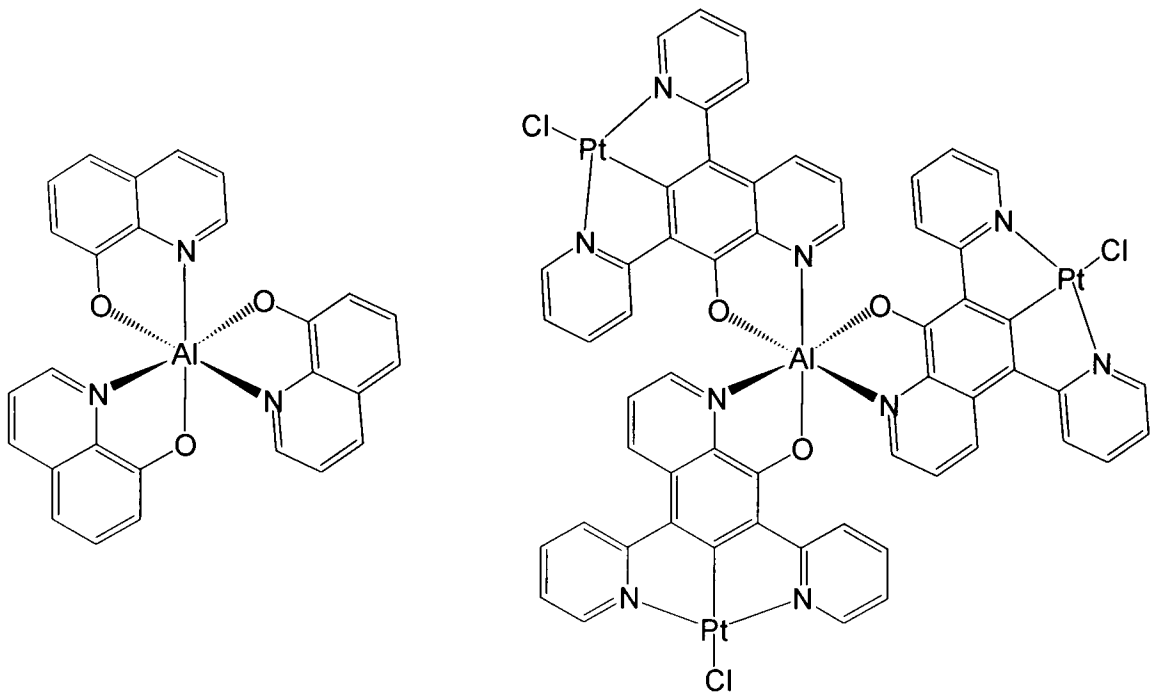

Figure 39: Common OLED electron-transport material, tris-(8-hydroxyquinoline)aluminium, AlQ_3, and target molecule, tris-(8-hydroxyquinoline-5,7-di(2-pyridyl)-6-platinum(II) chloride) aluminium.

2.4.1. Attempted synthesis of $Al(L^{22}PtCl)_3$ target complex

The commercially available starting material 5,7-dibromo-8-hydroxyquinoline was applied to the standard conditions outlined for the Stille cross-coupling reaction, Scheme 16: Route A, generated only crude quantities of the product 8-hydroxy-5,7-di(2-pyridyl)quinoline and in extremely poor yield, 2% (see Experimental, Section 8.1). The poor performance may be due to the free N^O site available to coordinate bidentately to the palladium catalyst. Palladium quinoline complexes are known to be very stable, so such complexation would deplete the reaction of the catalytic species.[243]

Protection of the alcohol functionality through various protecting groups was explored. Methyl protection of the alcohol, Scheme 16, Route B, led only to the deprotected ligand, HL^{22}, in 50% yield (a reasonable return for the Stille reaction). This was not as auspicious as it first appears, since protection of the alcohol is required to prevent platinum coordination with the N^O chelate system. Attempts to protect HL^{22} in the same fashion as the dibromo starting material gave a poor return of 4%.

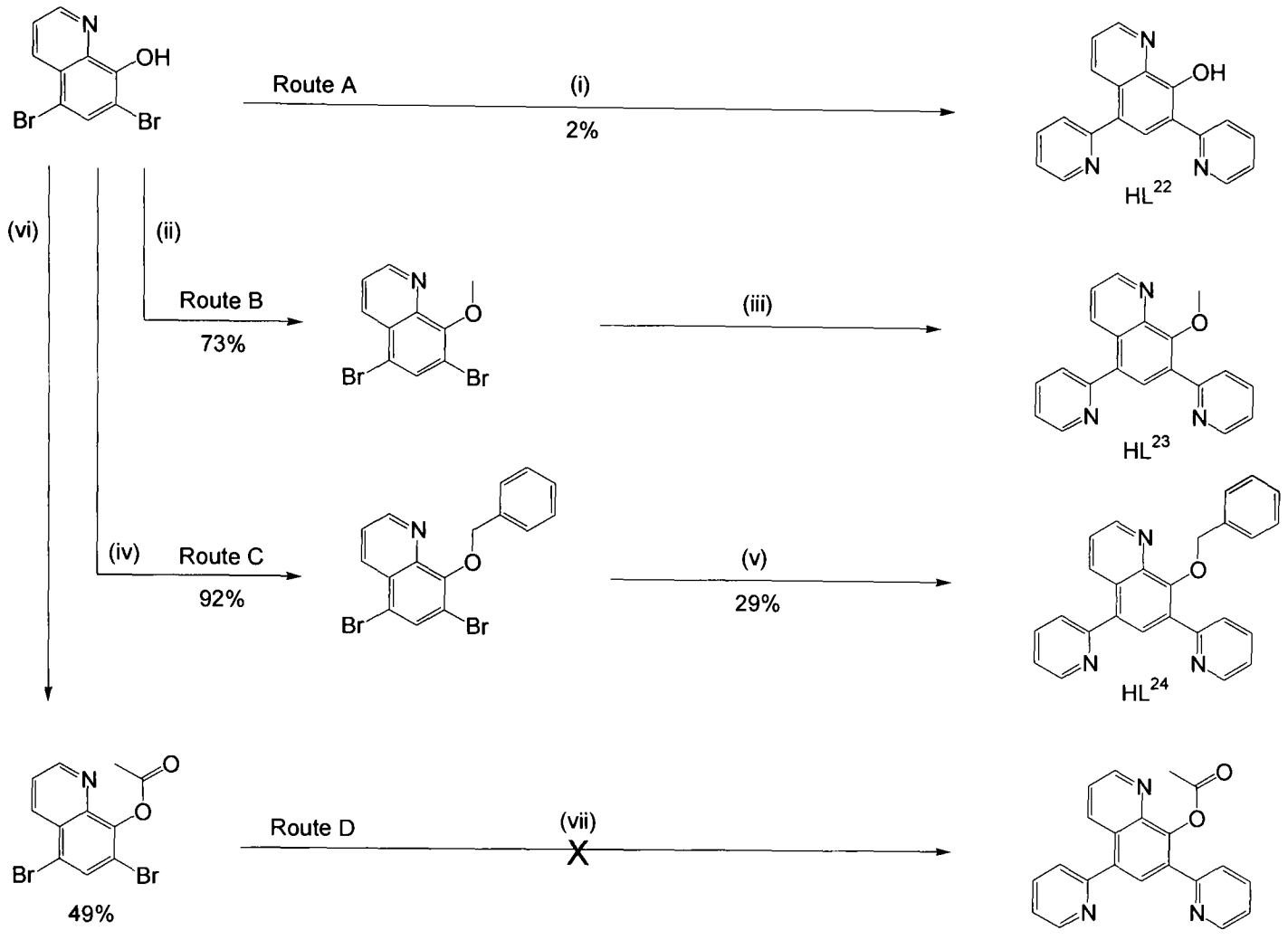

Scheme 16: Synthetic procedures investigated for the synthesis of novel ligand 5,6-di(2-pyridyl)-8-hydroxyquinoline. (i), (iii), (vii) 2-Tri-n-butylstannylpyridine, $Pd(PPh_3)Cl_2$, LiCl, toluene, 116°C. (ii) CH_3CN, CH_3I. (iv) Benzyl bromide, KOH, ethanol, 78°C. Acetyl bromide, DCM.

Initially, the benzyl-protected quinoline system, Scheme 16: Route C, was found to yield deprotected ligand HL^{22} in 25% yield, but did yield a small quantity, 2%, of the benzyl protected ligand, HL^{24}. A second reaction, monitoring product formation by GC, recovered a significant quantity of HL^{24}, 29%. The lack of any hydroxyl-functionalised compound identified by GC raised suspicions that deprotection may be occurring during work-up or purification. There is literature precedent of deprotection of methyl and benzyl protection groups in the presence of KF,[245,246] and therefore, it is thought of as no coincidence that the omission of the KF step in the work-up of this Stille reaction did yield the highest levels of product, with no evidence of the deprotected analogue recovered after the purification procedure.

Parallel synthetic attempts of utilising an acetate protecting group failed to yield any significant quantities of the desired compound, Scheme 16: Route D.

All attempts at direct cyclometalation of the protected quinoline ligands with K_2PtCl_4 were unsuccessful. It is believed that steric repulsion created by the overlapping of hydrogen atoms, H^4-qu and H^3-py^1, created through the fused ring coordination geometry of terdentate binding, is responsible. Considerable distortion has been observed in bis(2-phenylpyridine)platinum(II) and related compounds, where remarkable distortions are required for releasing the steric repulsions between H atoms in similar circumstances,[47,153,247] *e.g.* deviation of *ca.* 1.52 Å of one of the carbon atoms from the coordination plane was required to overcome this repulsion.[247] Therefore, it is believed that because of sterics enforced through metal centre binding, any possible complex formed cannot be planar. Disruption of a chelating ligand's π-conjugation system to accomodate steric restrictions is known,[33] however, in cases found thus far, the ligands are only bidentate and have a greater degree of freedom with respect to the other donor groups. The nature for the terdentate binding mode, aimed originally at restricting distortion, hinders such movement in the peripheral pyridine donors. In this case the quinoline based ligand system and the extended π-conjugation requires co-planarity with the coordination plane of the carbon requiring such distortion to overcome the induced steric repulsion, Scheme 17.

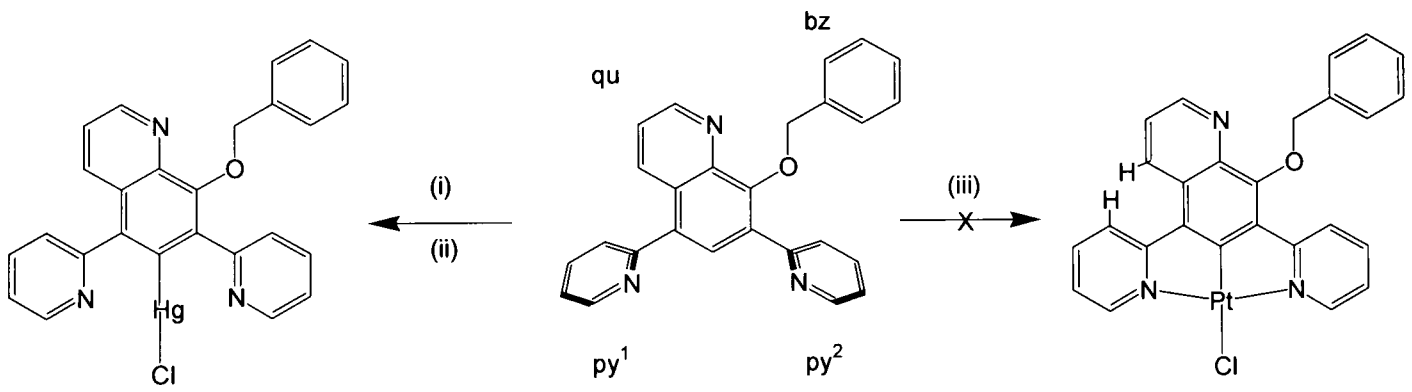

Scheme 17: Complexation of quinoline based ligand HL^{24} was successful for forming mercury(II) complexes, however, the known procedure was unsuccessful for platinum(II) complexes. Synthesis attempted via (i) $Hg(OAc)_2$, methanol; (ii) LiCl, methanol; (iii) K_2PtCl_4, glacial acetic acid.

Promisingly, however, the formation of metalated mercury(II) complex, $L^{24}HgCl$ was achieved under mild conditions. However, the pyridine nitrogens in this case are non-coordinating and therefore free to relieve the steric repulsion through rotational freedom around the benzene-pyridine bond.

2.4.2. 5-Substitution synthesis

Whilst attempts to synthesise complexes of 8-hydroxy-5,7-di(2-pyridiyl)quinoline were at their most fruitless, attentions were diverted to adapting the quinoline unit into a pendant group for the core N^C^N binding motif. 5,7-Dibromo-8-hydroxyquinoline was first converted to the corresponding methyl ether, Scheme 16: reaction (ii). Reaction with phenyllithium in diethyl ether, according to literature precedent,[248] afforded bromine-lithium exchange selectively at the 7-position. Quenching of the lithio derivative with $HCl_{(aq)}$ gave 5-bromo-8-methoxyquinoline. The good regioselectivity observed for the reaction is due to the stability of the 7-lithio derivative, originating from the *ortho*-stabilising effect of the methoxy group.[248] This product was successfully employed in the Suzuki reaction with the N^C^N boronate ester, HL-B_{neo}, to give the new 5-substituted ligand, 5-(1,3-di(2-pyridyl)-5-phenyl)-8-methoxyquinoline, HL^{21}, Scheme 18.

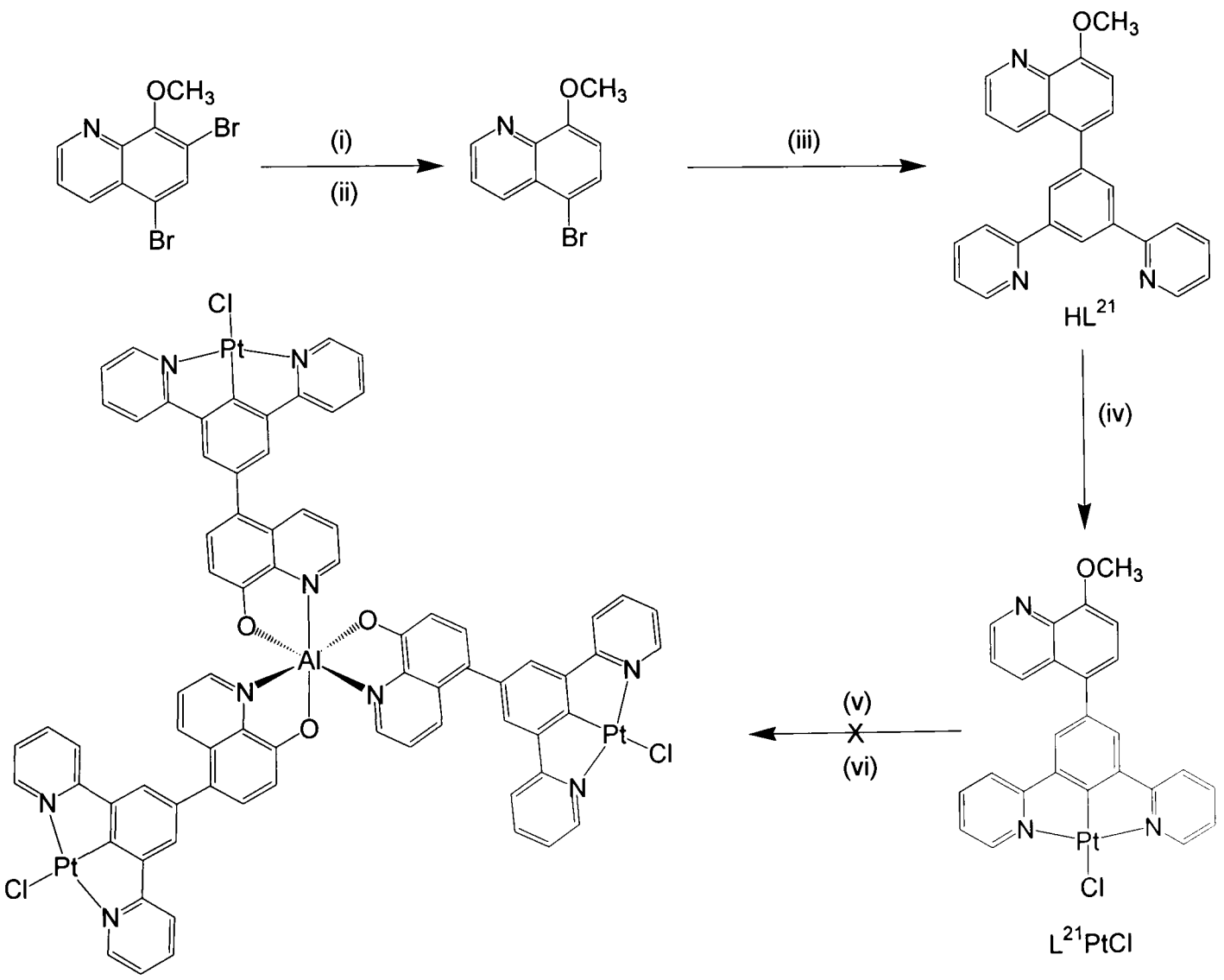

Scheme 18: (i) PhLi, diethyl ether, -75°C. (ii) $HCl_{(aq)}$. (iii) HL-B_{neo}, Na_2CO_3, $Pd(PPh_3)_4$, toluene:ethanol:water (6:6:1 mL respectively), 80°C. (iv) K_2PtCl_4, acetonitrile:water (5:2 mL respectively). (v) BBr_3, DCM.[249,250,251] (vi) Toluene, aluminium iso-propoxide.

$L^{21}PtCl$ was formed in 24% yield after direct complexation in acetonitrile/water mix. Demethylation of the quinoline unit and complexation of the hydroxyquinoline unit to aluminium is expected to lead to an insoluble, stable chelate compound. However, all attempts at this reaction were unsuccessful.

2.4.3. Photophysical properties

2.4.3.1. Absorbance

The absorption spectrum for the complex 1,3-di(2-pyridyl)-5-[5-8-methoxyquinoline]-benzene-2-platinum(II) chloride, $L^{21}PtCl$, is shown in Figure 40. Typical of 5-substituted N^C^N coordinated platinum(II) chloride complexes, it displays several intense transitions below 300 nm (ε = 23,000–47,000 L mol^{-1} cm^{-1}) which are assigned to ligand centred π-π^* transitions. Another band is prominent at 332 nm (ε = 12,680 L mol^{-1} cm^{-1}); this peak is not present in complexes such as L^1PtCl, therefore, the transition giving rise to this band is thought to be localised predominantly on the quinoline functionality. As observed for all of the previous complexes a band is observed at 380 nm (ε = 5,780 L mol^{-1} cm^{-1}) due to N^C^N-based transitions, while the band assigned to the ^{1}MLCT is found at 414 nm. The position of this band illustrates that there is significant interaction through π-conjugation between the N^C^N coordination plane and the quinoline substituent, despite the large steric repulsion induced by the presence of H^3-quinoline interacting with H^4-benzene. Frontier orbital diagrams generated by DFT and shown in Figure 41 confirm this hypothesis.

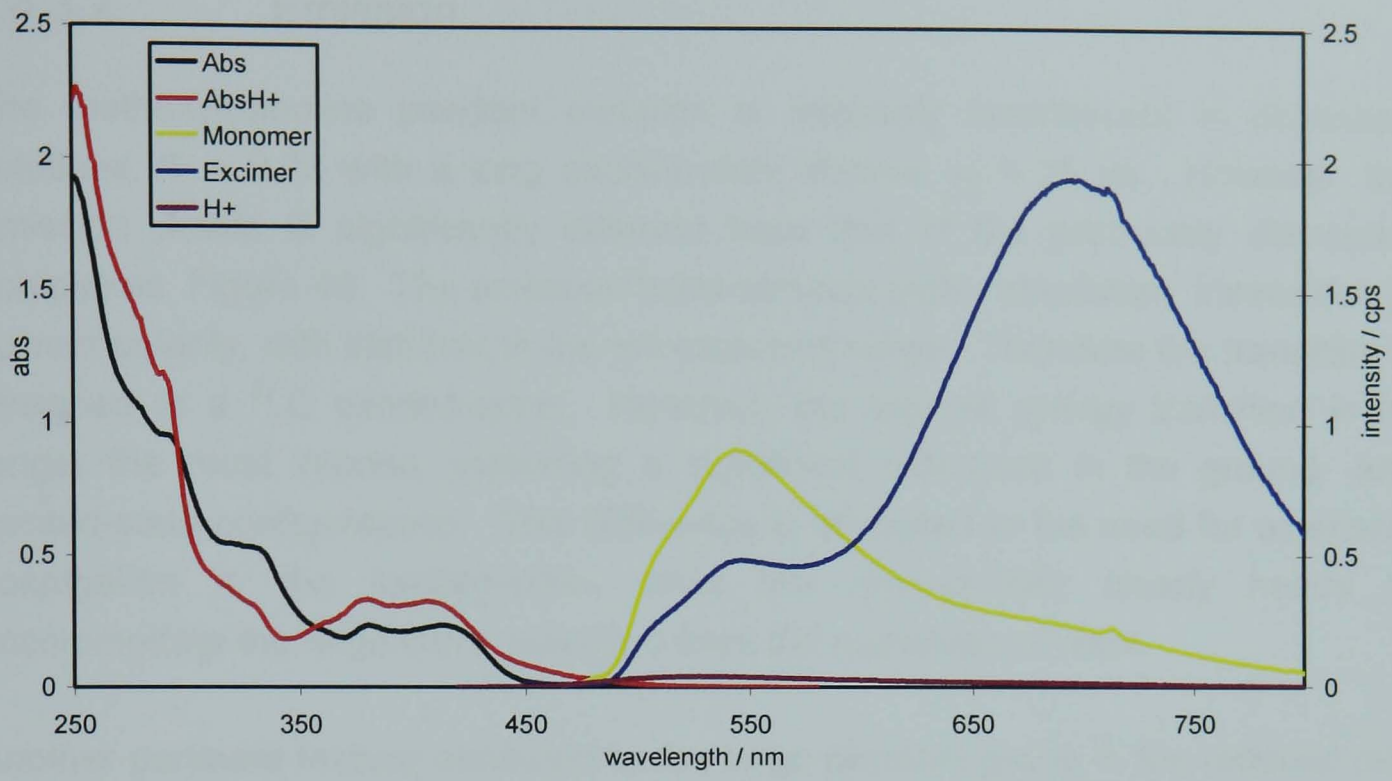

Figure 40: Electronic spectra of $L^{21}PtCl$ recorded in DCM at 25°C. Absorption spectra recorded in the absence (black) and presence (red) of TFA. Emission spectra recorded in the absence of TFA at low concentration (yellow), high concentration (blue), and in the presence of TFA (burgundy). Excitation of all emission spectra performed at the isosbestic point 357 nm.

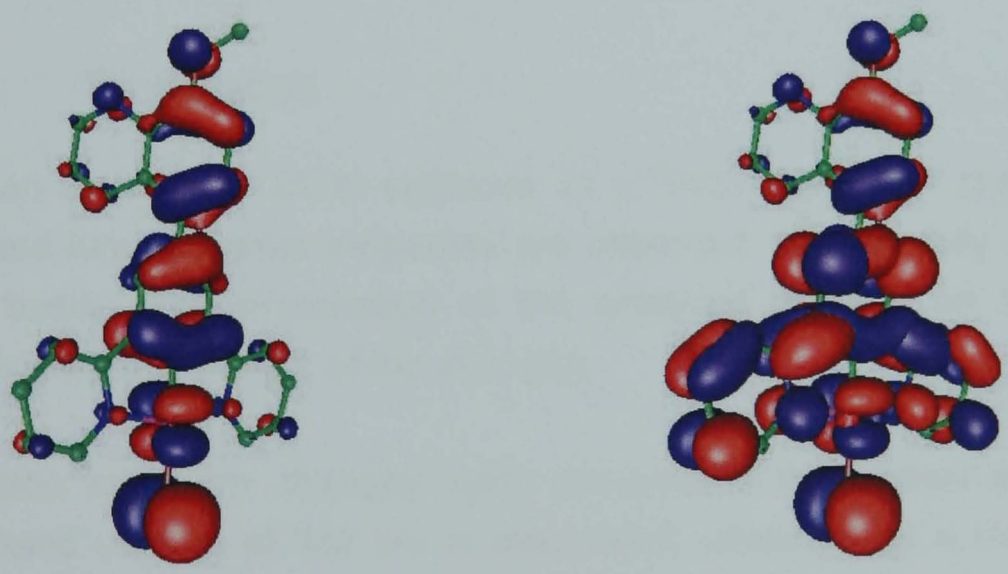

Figure 41: Frontier orbital diagrams generated by DFT calculations show the singlet HOMO (left) and LUMO (right) of the complex $L^{21}PtCl$. Importantly, both orbitals illustrate delocalisation across the N^C^N core and the 5-substituent.

2.4.3.2. Emission

The methoxyquinoline pendant complex is intensely luminescent in degassed solutions, Φ = 0.23 with a long excited-state lifetime, τ_0 = 25 µs. However, the emission profile is significantly different from that of the previously discussed complexes, Figure 40. The emission band remains highly structured, insensitive to solvent polarity, with lifetimes in the microsecond range. Therefore the transition is assigned to a ^{3}LC excited-state. However, the highest energy transition is no longer the most intense, indicating a significant difference in the ground- and excited-state configurations. This difference is attributed to the need for extensive conjugation in the excited-state, while the ground-state clearly needs to accommodate the large steric repulsion from the quinoline pendant.

Another pertinent feature attributed to the large pendant group is the reduced rate of self quenching observed, k_q = 5.1 x 10^{-8} M^{-1} s^{-1}, an order of magnitude less than the core structure, L^1PtCl, and half that of the sterically hindered mesityl complex, L^9PtCl. It is therefore hypothesised that while steric incumbrance plays an important part in disfavouring the bimolecular quenching process, the electronic interactions arising as a result of the electron rich quinoline unit must play an important role.

2.4.3.3. Protonation

Upon addition of TFA to DCM solutions of L^{21}PtCl significant changes in the absorption and luminescence properties are observed, that are fully reversible on addition of base. The protonation of the unbound nitrogen on the quinoline pendant is the expected origin of the changes.

The absorption spectrum changes upon protonation are shown in Figure 40. Firstly, the band centred at 332 nm is attenuated, observed as a reduction in its extinction coefficient by *ca.* 50%. There is almost no shift in the π-π* transition of the coordinated pyridines at 380 nm, while only a slight shift to higher energies of the ^{1}MLCT is observed, $\Delta\lambda_{max}$ = -7 nm. The electron-donating ability of the quinoline ligand is compromised upon protonation of the nitrogen, making the metal centre less electron-rich and formally more difficult to oxidise, while the region of the ligand making the most significant contribution to the LUMO, namely

the peripheral pyridines, remains largely unaffected by the protonation of the quinoline, Figure 41.

The effect of protonation on the luminescence is more striking. While there is no significant change in the spectral profile, the intensity of the emission is reduced to *ca.* 2% upon addition of acid. While the emissive band can still be assigned to ^{3}LC excited-states, with a slight blue-shift from the reduced donating character of the quinoline, there is a dramatic reduction in excited state lifetime from *ca.* 25 μs to 10 ns. Upon protonation of the compound the luminescence is effectively quenched by what may be considered an electron-transfer process to the protonated quinoline moiety. This provides an activated pathway for fast radiationless decay, so much so that non-radiative deactivation almost completely quenches the emission of the complex. No excimer emission or self-quenching is observed for $[L^{21}PtCl]H^+$, even in concentrated solutions. Evidently, the excited-state lifetime is too short for the requisite bimolecular process to occur.

CHAPTER 3

2,3':5',2''-TERPYRIDYL-4'-PLATINUM(II) CHLORIDE

3.2,3':5',2''-Terpyridyl-4'-platinum(II) chloride

3.1. Synthesis

The synthetic procedures explored during the synthesis of the target molecule 2,3':5',2''-terpyridyl-4'-platinum(II) chloride are shown in Scheme 20. The first step, the synthesis of HL[26], was readily achieved through the Stille cross-coupling reaction with commercially available 3,5-dibromopyridine. Attempts to form the desired product by direct metalation of this ligand were unsuccessful in this instance. The standard reaction for platinum complexation using K_2PtCl_4 in acetonitrile/water mixed solvent gave a complex mixture of compounds, from which the desired product could not be isolated. It can be easily envisaged that a large number of products are accessible from the many modes of coordination available to this particular ligand, Scheme 19. The target molecule requires the central pyridine to remain uncoordinated; however, its N atom is clearly the most accessible and likely to be the first to coordinate to labile metal ions. The central pyridine ring has three other possible sites for coordination. The desired location, C4, despite having two stabilising units flanking it is in competition with C2 and C6. The C2-positions, *ortho* to the central-pyridyl nitrogen, are more nucleophilic than the C4 site, and possess the stabilising influence of one pyridine nitrogen unit each, whilst also being a more kinetically favoured location for cyclometalation. Even though the reactions proceeded at reflux, the preferred position of cyclometalation on the basis of thermodynamics, C4, is not produced, or is indistinguishable amongst an assortment of platinum species formed by this reaction.

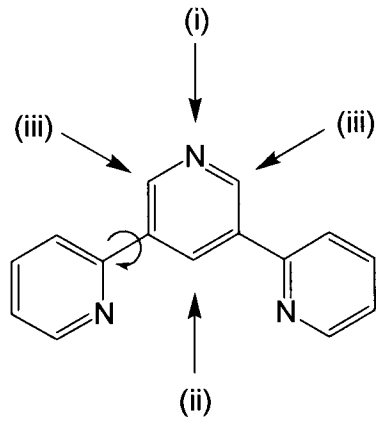

Scheme 19: The three distinct sites for metal-ion coordination available to the terpyridine ligand, HL[26], are shown above; (i) the central pyridine N-donor; (ii) C4-cyclometalation for N^C^N coordination; (iii) two identical sites of C2 or C6-cyclometalation for N^C coordination. Under standard platination conditions all sites will be competitive.

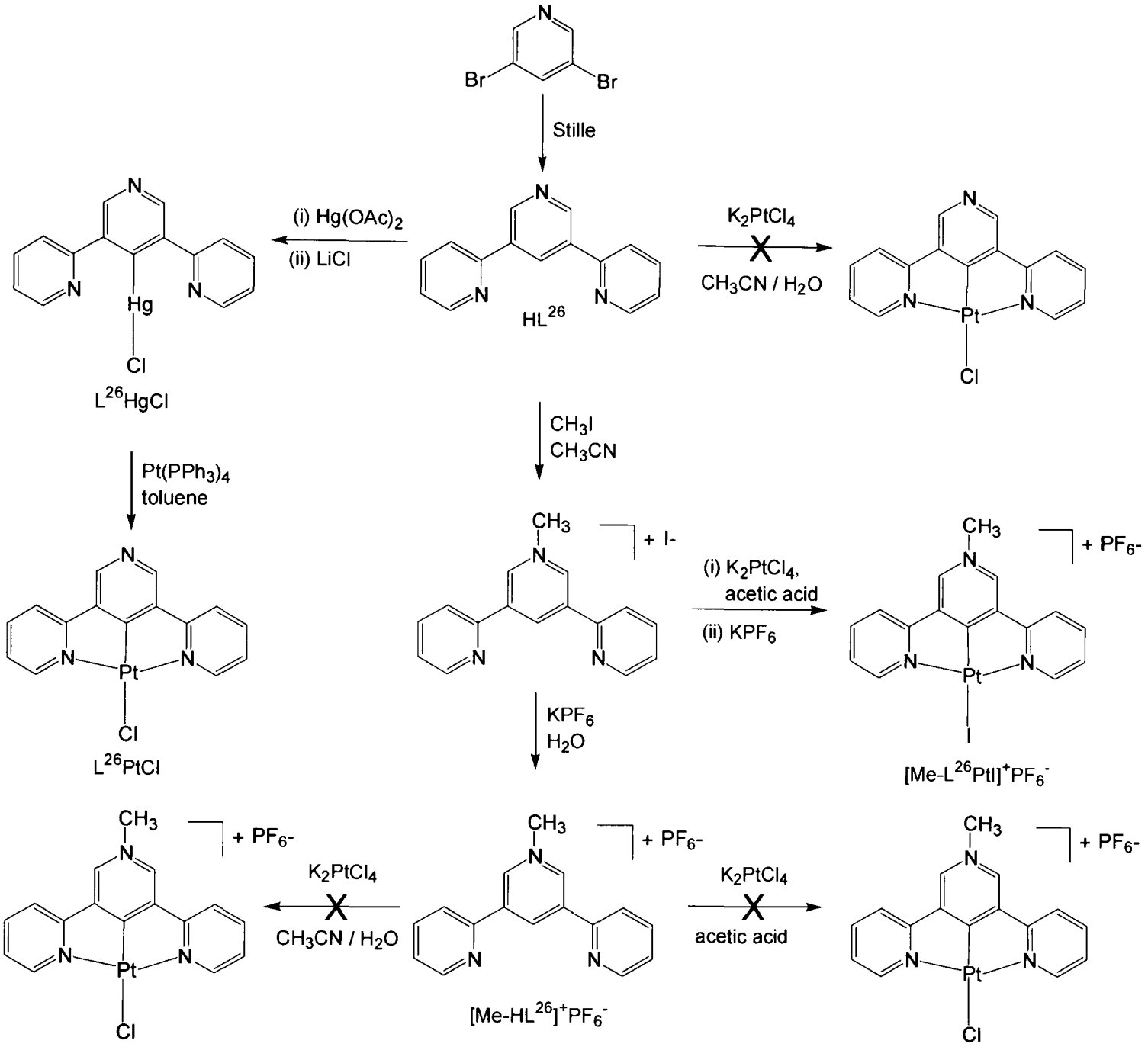

Scheme 20: Outline of the investigations undertaken towards the synthesis of target molecule $L^{26}PtCl$.

HL^{26} was reacted with iodomethane in DCM at room temperature yielding the N-methyl-4,6-(di2-pyridyl)pyridinium iodide salt. Methylation occurred only at the central pyridine ring with no competitive methylation of the peripheral pyridine-nitrogens. The ease with which the central pyridine is methylated adds some confirmation to the likelihood of kinetic metal-coordination at the central pyridine nitrogen in complexation reactions involving the unprotected ligand.

A single crystal of N-methyl-3,5-di(2-pyridyl)pyridinium iodide was obtained from slow evaporation of a saturated chloroform solution of the ligand. An ORTEP

diagram of the structure is displayed in Figure 42 with relevant bond lengths and angles listed. The structure confirms the selective methylation of the central pyridine ring while the other two pyridine units remain unreacted. The peripheral pyridines are again pointed away from one another to reduce electrostatic interactions between the lone pairs, but in this instance the pyridines are arranged pointing in the same direction, aligned in a head-to-head fashion.[225] The overall molecular structure is again not flat with angles between the planes of the central and peripheral pyridine rings displaying deviations from planarity, 17.8(3) and 14.5(3)°.

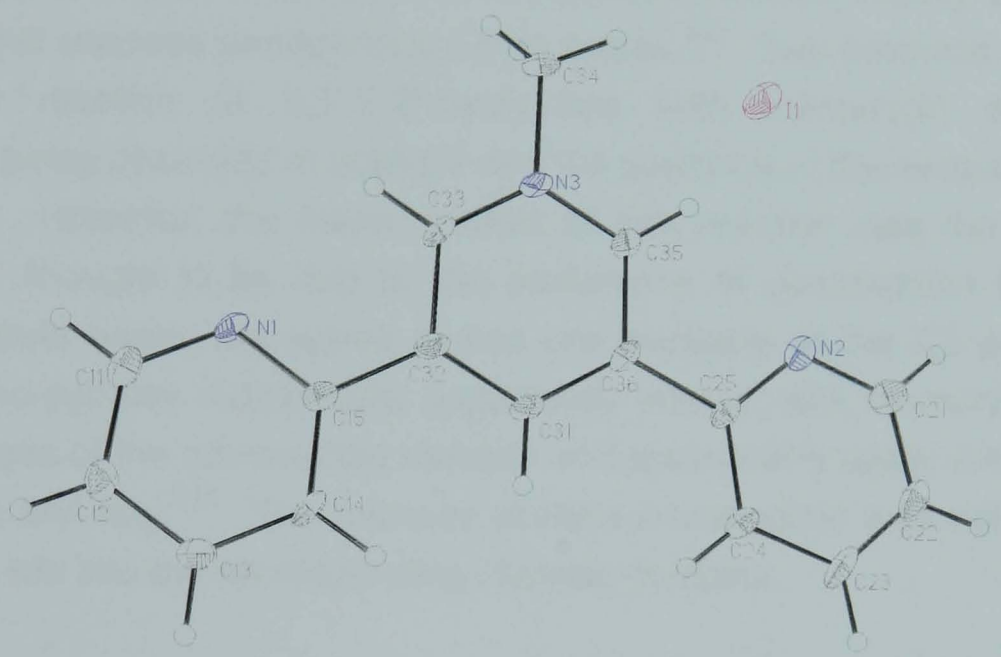

Figure 42: ORTEP diagram of N-methyl-3,5-di(2-pyridyl)pyridium iodide, N(3)–C(34) 1.475(8) Å; angles between the planes of the aromatic units connected by the following bonds C(32)–C(15) 17.8(3)° and C(36)–C(25) 14.5(3)°.

The newly formed N-methyl-3,5-di(2-pyridyl)pyridinium iodide salt was reacted with K_2PtCl_4 in glacial acetic acid to afford a poorly soluble solid after standard work-up procedures. The product was more readily workable after ion exchange *via* dissolution in a minimum amount of DMSO and recovery as an orange solid after slow addition to saturated aqueous KPF_6 solution. ^1H and ^{13}C NMR spectroscopy confirmed regioselective cyclometalation at the C4-position of the central pyridine, however, electrospray-ionisation mass spectrometric data revealed the sole product to be the metal complex containing iodine as the fourth coordinated ligand.

Ion exchange prior to complexation, I^- to PF_6^- salt, and subsequent complexation attempts were unfortunately problematic, Scheme 20. Multiple attempts using the standard complexation in acetonitrile/water neither yielded product nor recovered

starting material. Standard glacial acetic acid procedure gave a brown solid with clean NMR spectra and correct mass spectrometry data; however, this complex gave decidedly poor luminescent spectra, containing many unidentifiable impurities, even after many attempts at purification.

The synthesis of the complex $L^{26}PtCl$ was achieved by a transmetalation with $L^{26}HgCl$.[252,253] Transmetalation is a technique readily utilised for directing cyclometalation of platinum group metals, and is commonly used in the synthesis for many palladium compounds.[254] Mercury(II) acetate salts are known to easily attack aromatic compounds, and ortho-mercuration occurs readily with aromatic substrates that possess endogenous Lewis bases.[253] Two products are obtained through the reaction of 2,3':5',2''-terpyridine with mercury(II) acetate, with mercuration being observed at both C2 and C4 positions of the central pyridyl ring, Scheme 19. However, the major product of this reaction was the desired C4-coordination, thought to be due to the preference of coordination between two stabilising Lewis bases, compared to just one available at the C2 position. The mutually *ortho*-pyridine substituents supposedly interact with mercury diacetate in the early stages of the mercuration reaction and presumably assist the electrophilic attack of the aryl ring.[255] The mercury acetate intermediate was not isolated but converted *in situ* into the corresponding chloride complex.

The ^1H NMR spectrum of the mercury intermediate confirms the occurrence of C4 metalation and no proton resonance is observed for the H^4 from the central pyridine. The resonance for H^2 is flanked by ^{199}Hg ($I = ½$) satellites due to $^4J(^{199}Hg - ^1H)$ coupling, J = 84.0 Hz, proving a covalent C(4)–Hg bond. The relative abundance of ^{199}Hg is 16%, however, the satellites are broad and difficult to integrate due to the dynamic nature of the mercury(II) ion in d_6-DMSO.[256] The four resonances of the 2-pyridyl rings remain almost unchanged with respect to the free ligand, in particular the position of the H^3 and H^4 signals have remained in that respected order, consistent with non coordination of these pyridyl units. The mercury atom is therefore η^1-C monodentate coordinated to the central pyridine ring. Further support for this behaviour includes X-ray crystallographic studies of related compounds,[253,257] including 1,3-di(2-pyridyl)benzene-2-mercury(II) chloride,[252] in which the pyridine rings do not show pincer behaviour because the nitrogen lone pairs are not considered to be bonding. The nitrogens are then

thought only to be weakly interactive[255] and the 2-coordinate mercury ion to be linear, as is often the case for R-Hg-Cl compounds, such as (ppy)HgCl.[258]

The platinum(II) complex was synthesised *via* metal exchange with the labile mercury atom. Cyclometallated platinum(II) complexes have previously been prepared through transmetalation reactions with organo-mercury compounds using tetrakis(triphenylphosphine)platinum(0) in non-coordinating solvents.[252] Tetrakis-(triphenylphosphine)platinum(0) is a known source of many platinum(II) compounds which cannot be obtained easily by other routes,[259] and is readily prepared from tetrachloroplatinate and triphenylphosphine in basic alcohol.[260] Although known to decompose in air, $Pt(PPh_3)_4$ is sufficiently stable to be manipulated without inert atmosphere conditions and in many solvents. Following the reaction, extensive washing with diethyl ether was required to successfully remove all traces of liberated triphenylphosphine and the desired complex was isolated as an orange solid in 11% yield.

3.2. Photophysical properties

The absorption and emission spectra reported of $L^{26}PtCl$ were recorded in acetonitrile at RT, owing to low solubility in DCM, and shown in Figure 43 and Figure 44, respectively.

The absorption spectrum of $L^{26}PtCl$, Figure 43, bears a resemblance to those for the aryl-substituted complexes detailed above, Section 2.3.1, but with some substantial shifts to higher energy. Below 300 nm the bands are again assigned to ligand π-π^* transitions, however, the lowest energy envelope is significantly blue-shifted with respect to L^1PtCl, probably due to a lower electron density at the metal. Direct population of the ^3LC excited-state is clearly distinguishable at 464 nm strongly blue shifted by 900 cm^{-1} compared to L^1PtCl, and characteristically weak, $\varepsilon \leq 100\ M^{-1}\ cm^{-1}$.

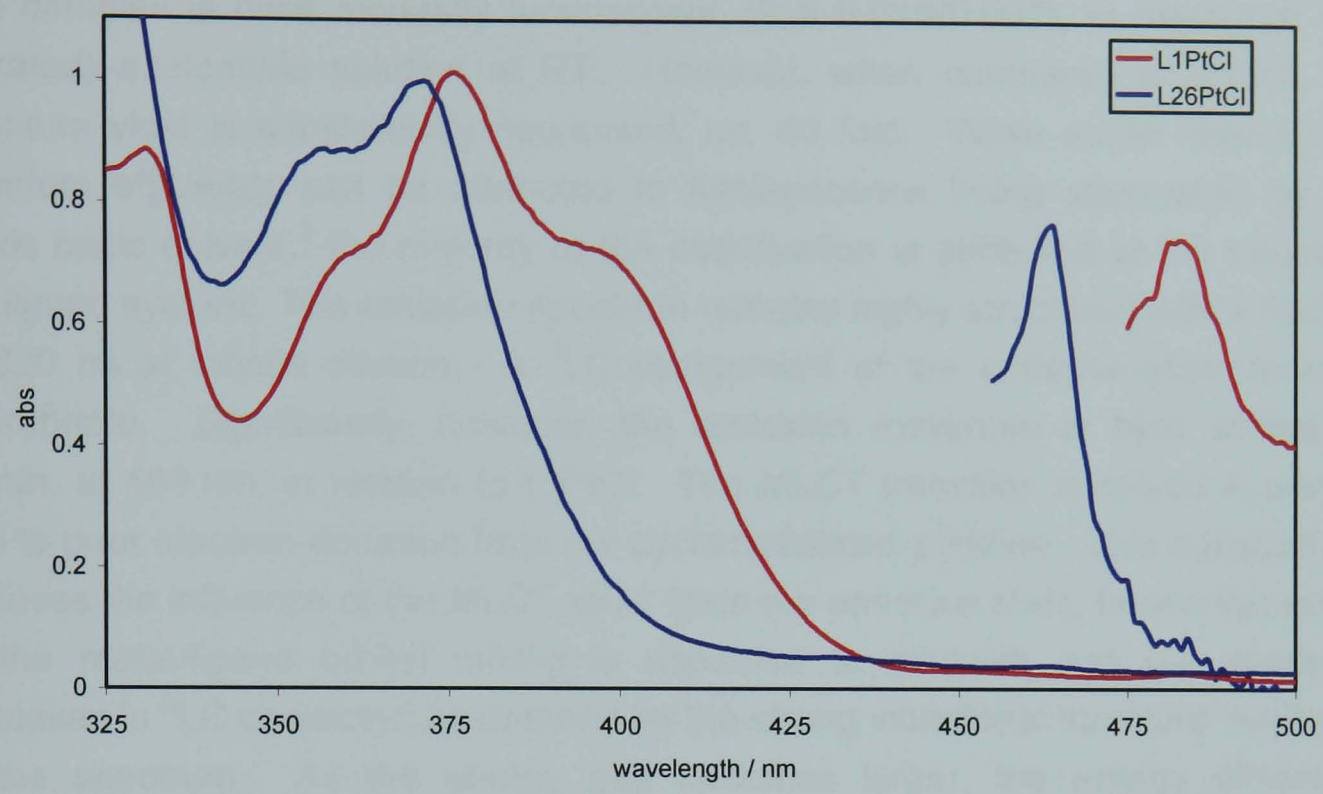

Figure 43: Normalised UV-Vis spectra of $L^{26}PtCl$ and $L^{1}PtCl$ recorded in acetonitrile at 298 K. Of note are the much higher energy transitions observed for the terpyridine complex, due to the diminished electron-donation to the metal centre.

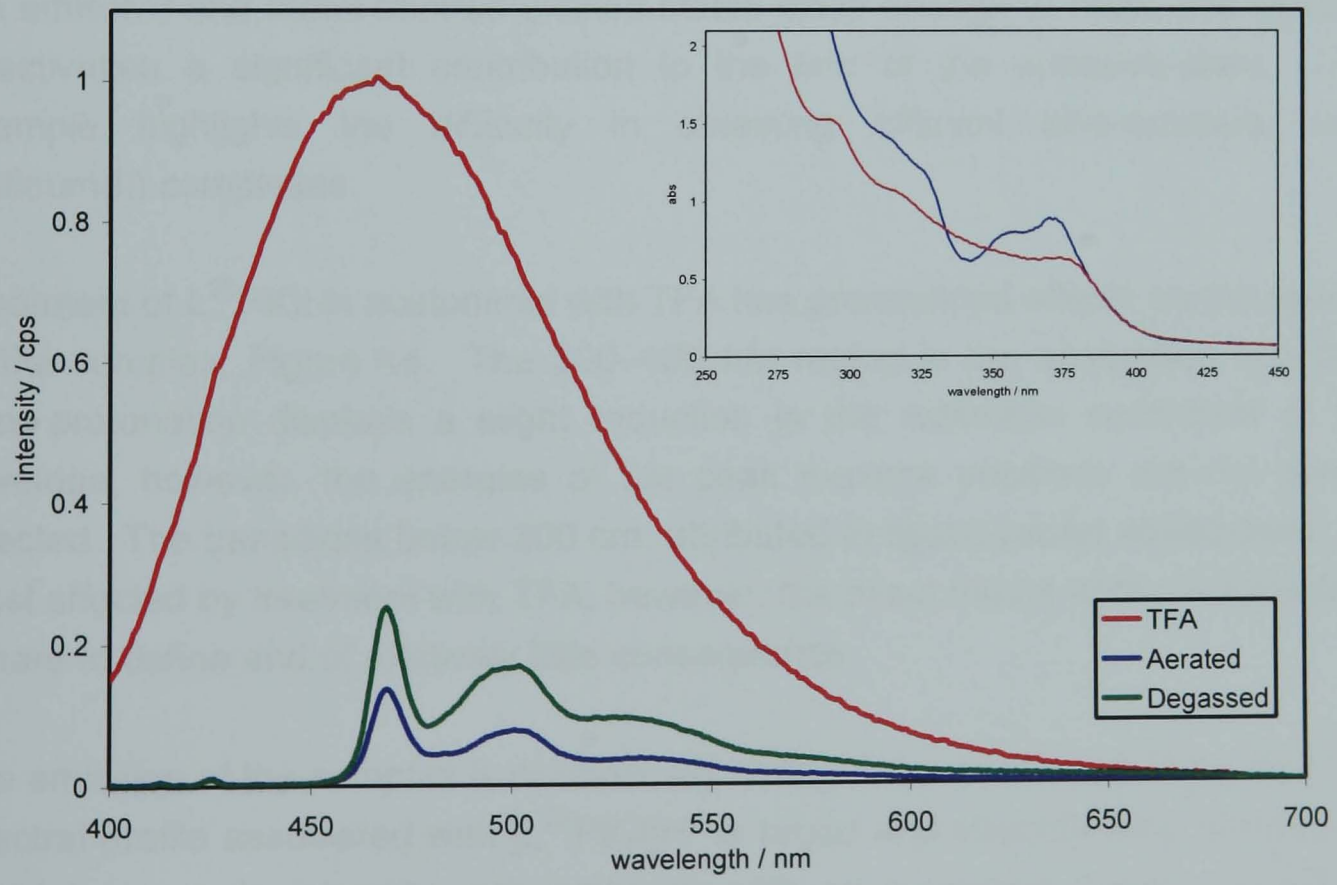

Figure 44: Emission spectra of $L^{26}PtCl$ in CH_3CN (2×10^{-4} M) at 295 K in the presence (blue) and absence (green) of air, as well as, after the addition of TFA (red) (10^{-2} M), λ_{ex} = 377 nm. The inset shows the absorption spectra of $L^{26}PtCl$ in the absence and presence of TFA.

The complex is itself modestly luminescent, Φ = 0.015(0.007), in degassed and (aerated) acetonitrile solution at RT. However, when compared to L^1PtCl, the quantum yield is substantially decreased, *ca.* 40 fold. While some reduction in quantum efficiency can be attributed to luminescence being attenuated by the Lewis basic solvent,[3] the majority of the deactivation is attributed to the nature of the ligand system. The emission spectrum remains highly structured with a lifetime of 320 ns at infinite dilution. A ^{3}LC assignment of the emissive-state remains appropriate. Significantly, however, the emission maximum is blue shifted by 22 nm, at 469 nm, in relation to L^1PtCl. The MLCT transition is raised in energy due to poor electron-donation from the cyclometallated pyridine. This substantially removes the influence of the MLCT state upon the emissive state, hence the extent of the metal-ligand orbital mixing is expected to diminish and the spectrum increases in ^{3}LC character, as denoted by the strong vibrational structure displayed in the spectrum. As the energy gap becomes larger, the energy difference between the deactivating d–d excited states is reduced. As discussed in the introduction, Section 1.1, electronic access to these states from the lowest energy excited-state is considered as the limiting factor for controlling the quantum yields of platinum complexes. The large blue-shift observed in this complex clearly brings the emissive and metal-centred excited states close enough to make this mode of deactivation a significant contribution to the fate of the emissive-state. This example highlights the difficulty in obtaining efficient blue-emitters using platinum(II) complexes.

Treatment of $L^{26}PtCl$ in acetonitrile with TFA has pronounced effects on the spectra of the complex, Figure 44. The 300–400 nm region in the absorption spectrum after protonation displays a slight reduction in the extinction coefficient of this envelope, however, the energies of the peak maxima positions are not greatly affected. The transitions below 300 nm, attributed to ligand based absorptions, are most affected by treatment with TFA, however, the exact nature of these transitions is hard to define and of relatively little consequence.

The emission of the complex is dramatically changed by addition of TFA. The new spectral profile associated with $[L^{26}PtCl]H^+$ is broad and structureless, showing an 8-fold increase in intensity, concomitantly with an increased oxygen sensitivity. The luminescent lifetime of the complex is greatly reduced to *ca.* 2 ns, raising the

possibility of fluorescent emission from dissociated ligand, HL^{26}, initiated by the strong acid.

CHAPTER 4

SOLID-STATE EMISSION OF THE BROMO-SUBSTITUTED COMPLEX, L^6PtCl

4. Solid-state emission of bromo-substituted complex, L^6PtCl

Initial attempts to synthesise the complex 1,3-di(2-pyridyl)-5-bromobenzene-2-platinum(II) chloride, through selective bromination of the platinum complex, L^1PtCl, using N-bromosuccinimide, were unsuccessful, Equation 7, despite previous reports highlighting the ability of a number of octahedral d^6-metal complexes to be selectively functionalised on the benzene ring at a position *para* to cyclometalation.[261] The reaction, in this case, appeared to produce a mixture of different species with little sign of the developing ^1H NMR singlet expected for the symmetrically identical remaining H atoms of the benzene ring.

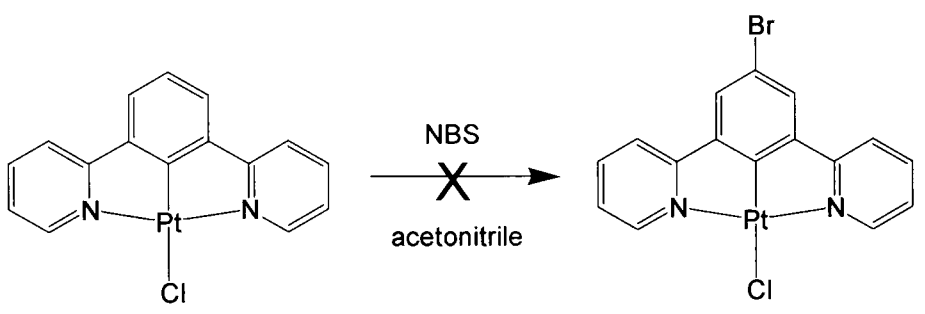

Equation 7: Reaction of L^1PtCl with NBS (N-bromosuccinimide) in acetonitrile failed to yield the desired product L^6PtCl.

However, complexation of HL^6 with K_2PtCl_4 in glacial acetic acid led to L^6PtCl as an orange solid in a reasonable yield of 52%. There was no evidence of oxidative addition of the aryl-halide bond, which has occasionally been used as a means to induce regioselective cyclometalation *via* metal insertion into such a bond.[71,262]

4.1. Crystal packing

There are many papers addressing the rich polymorphism of square-planar platinum(II) complexes,[2,33,36,38,39,41,55,86,263,264,265] some of which are found to display fascinating luminescent behaviour resulting from intermolecular electronic interactions in the solid state.[264,265,266] The complex L^6PtCl was found to crystallise in a number of different shapes and colours. Three of these, one yellow needle-like and two red-coloured cubic crystals have been structurally characterised by X-ray diffraction techniques, revealing at least three different crystal packing arrangements. A red crystal obtained from slow evaporation of a DCM/methanol solution, henceforth denoted as Br^1, gave poor quality crystallographic data

(R1 = 0.0833, wR2 = 0.1407). Recrystallisations from chloroform yielded two different coloured crystals from the same solution. A red cuboid crystal was formed at the bottom of the sample tube where there is no solvent evaporation. Therefore, this form probably crystallised slowly and is therefore thought to be the thermodynamically favoured product, denoted Br^2. During the evaporation process, a yellow needle-like crystal was observed to crystallise before the appearance of Br^2 around the uppermost part of an open necked crystallisation tube, and therefore thought to be a kinetic product, denoted Br^3. Multiple polymorphs from a single crystallisation are unusual but do occur in some cases.[2,33,39,41,263] Additionally, different crystal structures of square-planar complexes have also been observed to be dependent on the speed of crystallisation.[41,264]

In all three crystal structures of L^6PtCl, the structures possess the characteristic distorted square-planar geometry with similar bond lengths and angles to those previously described for this class of compounds, Section 2.2.3. Data for Br^2 and Br^3 are shown in Table 3. An ORTEP diagram representative of the monomeric structure of the complex is shown in Figure 45. The structure of Br^1 did not refine well enough to give reliable bond lengths and angles, although qualitative conclusions, particularly with regard to the packing, are appropriate to make.

The unit cell of Br^1 contains a pair of crystallographically inequivalent complexes. Each individual complex forms a head-to-head dimer with its opponent above its plane, Figure 46a), and this dimer is associated with an identical dimer below the plane in a head-to-tail orientation, Figure 46b), *i.e.* the arrangement is observed to follow an ABBAABBA... arrangement through the stacks. The stacking is arranged in a lateral drift pattern out towards the flanking pyridines with respect to each molecule, where the column of complexes continues unabated with each progressive addition to the stack, Figure 46c).

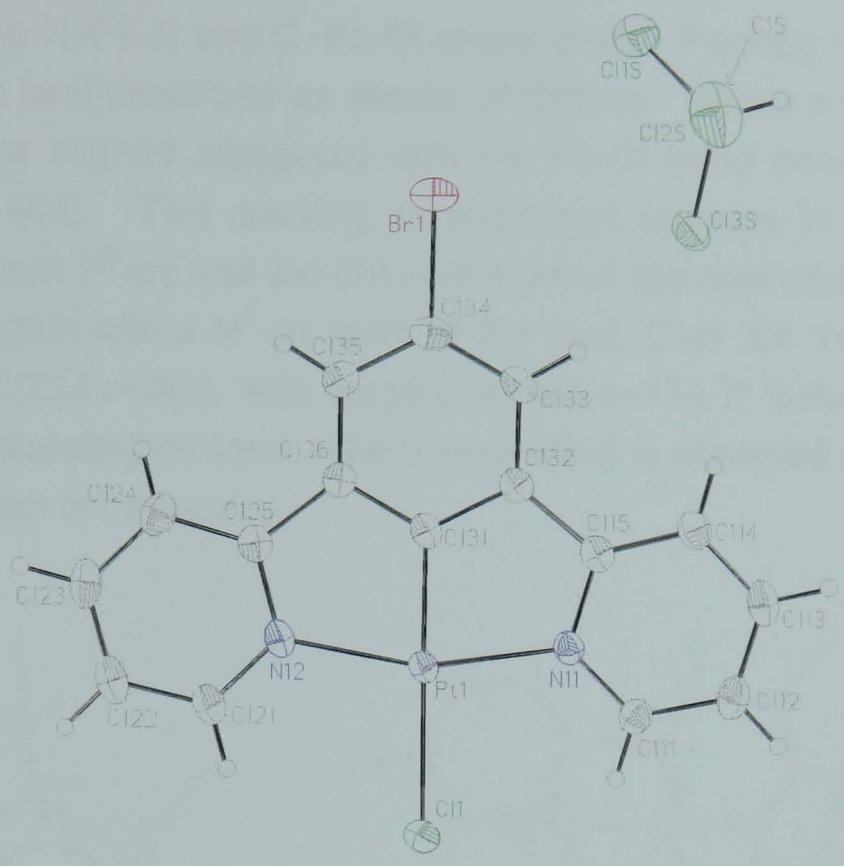

Figure 45: ORTEP diagram representing the monomeric structure of L^6PtCl taken from the crystallographic analysis labelled as Br^2 crystallised from saturated chloroform solution under slow evaporation.

L^6PtCl Bond	Br^2 (Å or °)	$Br^{2'}$ (Å or °)	Br^3 (Å or °)	$Br^{3'}$ (Å or °)
Pt(1)–C(131)	1.907(3)	1.902(4)	1.914(6)	1.894(3)
Pt(1)–N(11)	2.035(2)	2.030(2)	2.029(5)	2.033(3)
Pt(1)–N(12)	2.038(2)	2.030(2)	2.038(0)	2.036(3)
Pt(1)–Cl(1)	2.4214(8)	2.4147(10)	2.4108(16)	2.4132(7)
N(11)–Pt(1)–C(131)	81.00(11)	80.73(7)	8.6(7)	80.53(12)
N(12)–Pt(1)–C(131)	80.32(11)	80.73(7)	80.8(7)	80.80(11)
N(11)–Pt(1)–N(12)	161.30(10)	161.47(14)	161.5(2)	161.31(11)
C(131)–Pt(1)–Cl(1)	178.59(8)	180.0	178.88(18)	175.59(9)
C(131)-C(132)-C(115)	122.3(3)	112.2(3)	112.8(6)	111.6(3)

Table 3: L^6PtCl crystals structure data for the crystallographically inequivalent molecules each from the red cuboid and the yellow needle structure, Br^2 and Br^3, respectively. Bond angles are presented in degrees, while all lengths are quoted in Å.

If assigning the perpendicular direction through the stacks orthogonal to the plane of the monomeric complex as the *z*-axis, the *x* and *y* axes become the directions

through the bonds N–Pt–N and C–Pt–Cl respectively. Packing in these other two directions can be best described as sheets of ribbons. Within a particular "ribbon" the molecules are aligned staggered with the Pt–Cl bond pointing towards one another, Figure 46d). This packing arrangement appears to be stabilised by interactions between H^5-py and the chlorine atom of the next molecule, which is in turn interacting again with a H^5-py atom of the next, C–H···Cl'···H–C" *ca.* 3.6 Å for distances from C(222)–Cl(1), with angles of 164.4–174.7° between the chloride atoms and the interacting protons. The overall effect is observed as an interlocking zip-like ABA pattern of molecules.

a)

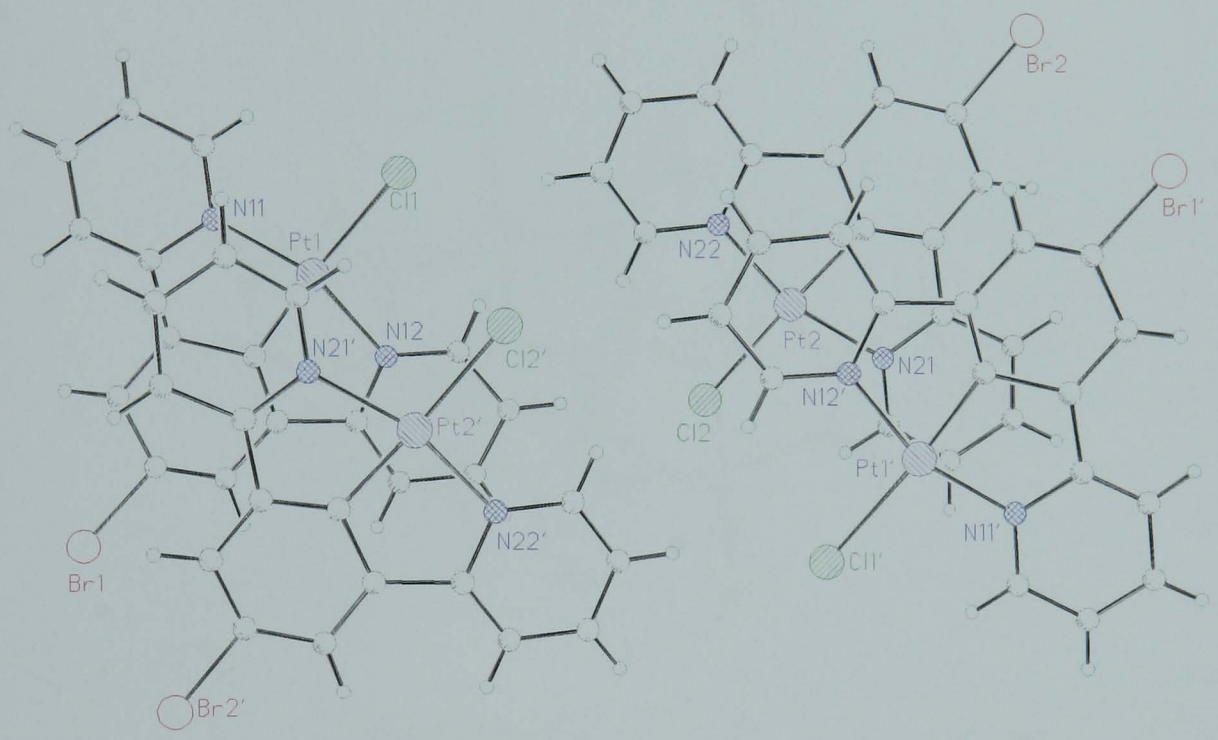

b)

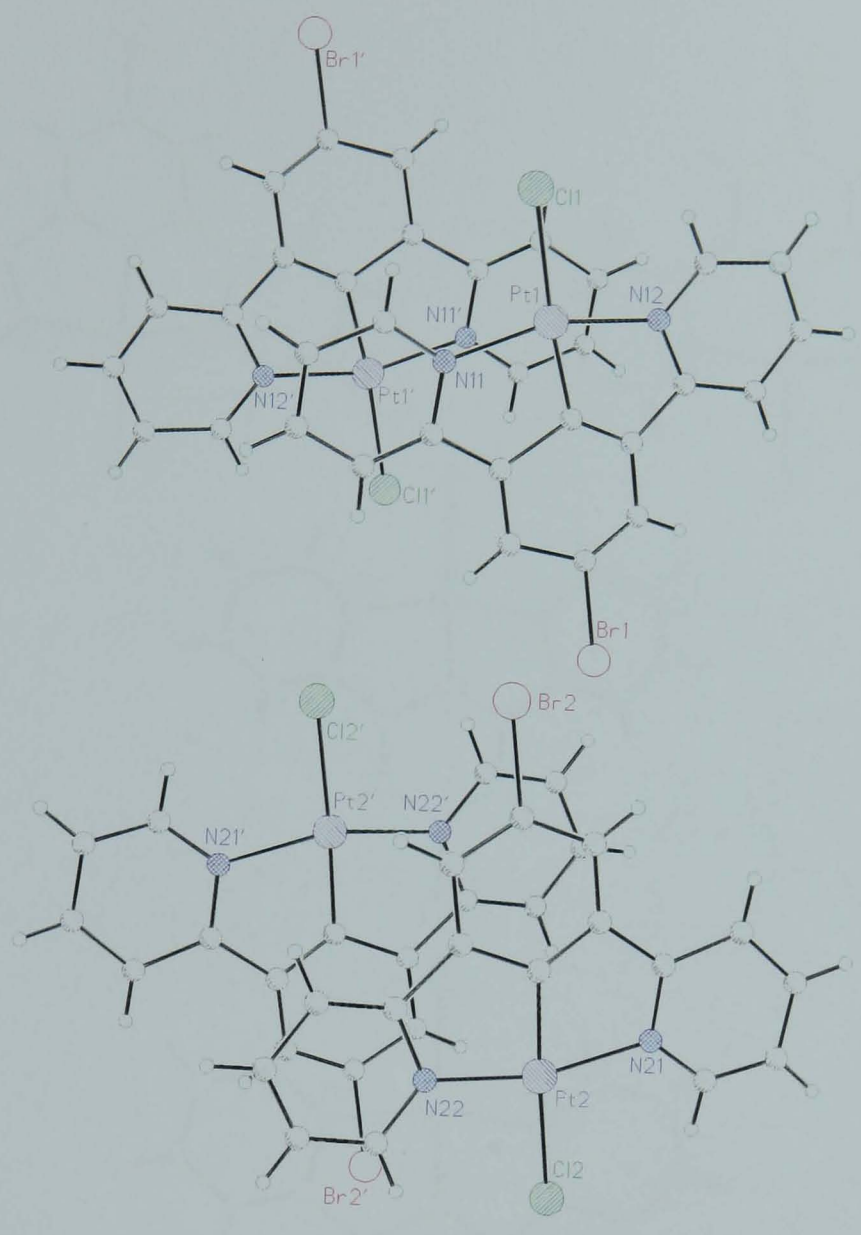
Br1'
Cl1
Pt1
N12
N11'
N11
N12'
Pt1'
Cl1'
Br1
Cl2'
Br2
Pt2'
N22'
N21'
N21
N22
Pt2
Cl2
Br2'

c)

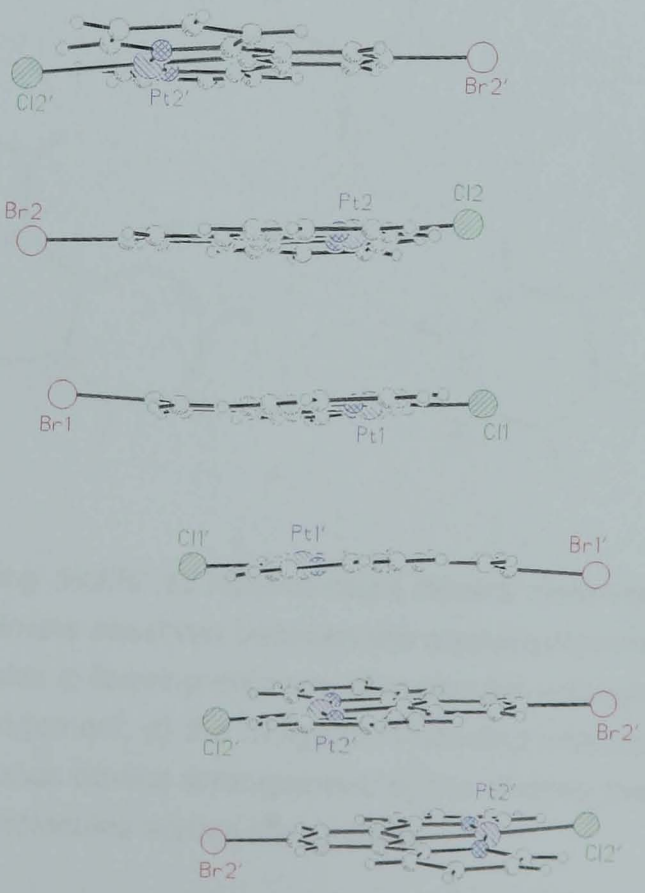
Cl2'
Pt2'
Br2'
Br2
Pt2
Cl2
Br1
Pt1
Cl1
Cl1'
Pt1'
Br1'
Cl2'
Pt2'
Br2'
Pt2'
Br2'
Cl2'

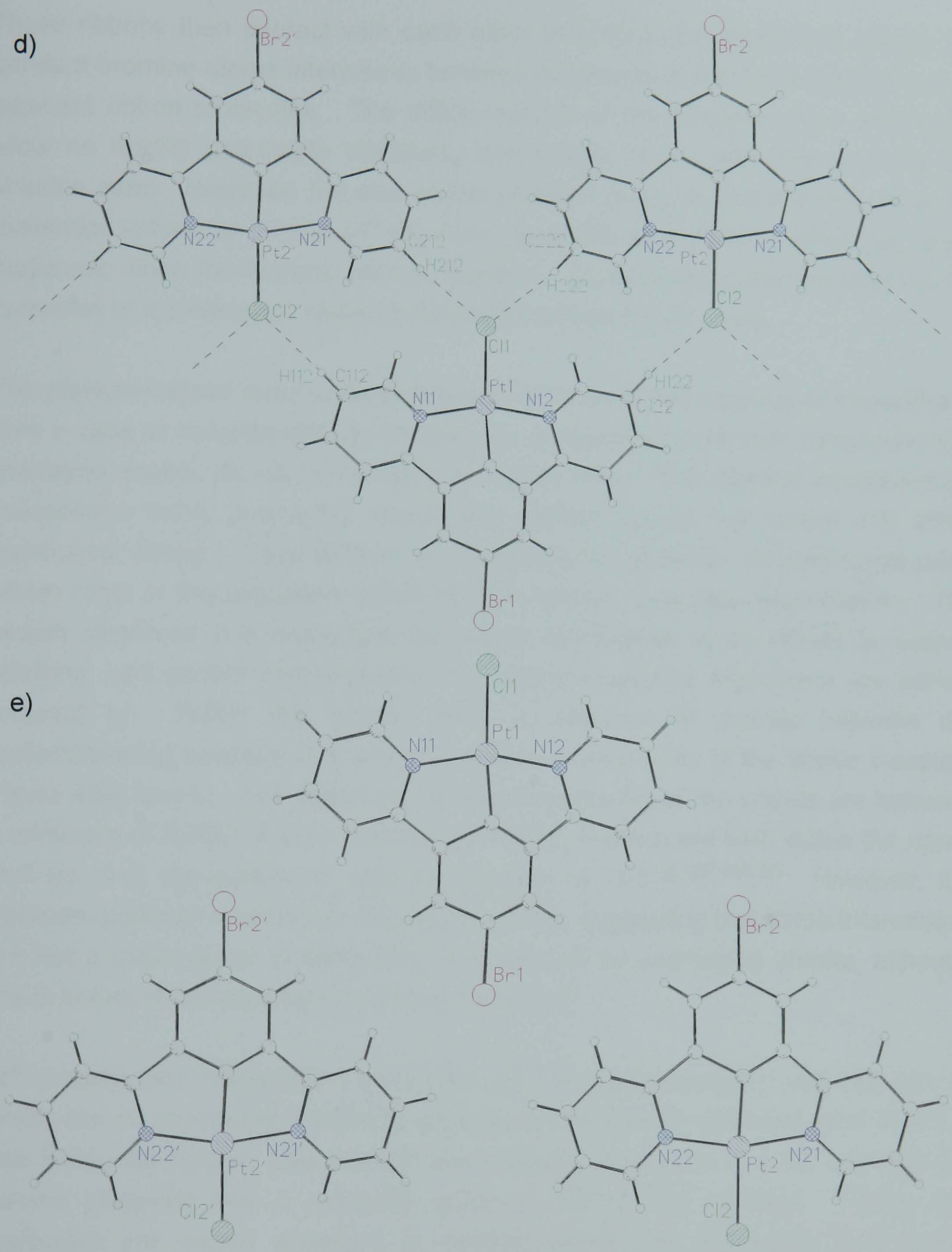

Figure 46: Br^1 crystal packing motifs: a) head-to-head dimers observed between the inequivalent complexes; b) head-to-tail dimers observed between the equivalent molecules; c) the square-planar structure of the complexes aids in forming columns of molecules arranged clearly in a head-to-head followed by head-to-tail arrangement; d) the Cl ligand H-bonding interactions between neighbouring complexes creates a continuous rib-like arrangement; e) the ribbons then interweave between one another creating a sheet of molecules across the *xy* plane.

These ribbons then interact with each other in a tail-to-tail interaction, where the pendant bromine atoms interweave between molecules in the spaces between two adjacent ribbon molecules. The diffuse nature of the bromine atom appears to allow no readily detectable stabilising interactions of the type observed for the chlorine atom. However, the size of this pendant group allows the snug fit of the molecules to form an overall 2-D structure: an interlocking effect is produced by the molecules when the ribbons interact together. Consequently, the net effect is the formation of a continuous sheet of molecules across the *xy* plane.

The aforementioned head-to-head followed by head-to-tail stacking of molecules is then a case of complementary, followed by antagonistic and then complementary overlayed sheets, as can been seen in Figure 46c). The specific intermolecular interactions within overlaying sheets are limited due to the lateral drift effect mentioned above. Face-to-face π-π interactions between stacked molecules, where most of the ring-plane areas directly overlap, is a rare phenomenon. The usually observed π-π interaction for planar compounds is an off-set or slipped stacking, and perfect phenyl-phenyl and pyridine-pyridine alignments are almost unheard of. Within this system there is evidence of overlap between the cyclometalating benzene ring and one of the pyridine units of the above complex, Figure 46a) and b). The distances between the planes of the sheets are between a minimum of 3.2901 Å and a maximum 3.5416 Å which are both within the upper limit for π–π interactions in organic species, *ca.* 3.8 Å.[267,268,269] However, the platinum–platinum vectors are not perpendicular, suggesting that these interactions are not a major factor in controlling formation of the overlaying sheets, although this is known to be important in related systems.[85]

Br^2 contains two independent molecules with its crystallographic unit cell, one of which sits on a two-fold symmetry axis; therefore these molecules exist in a 2:1 ratio within the crystal. The unit cell also contains chloroform in a 3:2 ratio and the solvent presence has a dramatic result on the crystal packing. Firstly, the molecules are clearly arranged in vertical stacks that intertwine their layers between one another, Figure 47a), so that the molecules now possess little relationship through the *x* and *y* axes assigned previously. The stacked molecules are aligned on top of one another, Figure 47b), with the centroid of the stack located on each molecule through the Pt–C cyclometalating bond, approximately three quarters along the bond towards the carbon atom. Due to one of the

molecules containing the 2-fold symmetry axis the molecules are arranged in an ABBABBA... formation. The stacks form a helical structure as the molecules are displaced in an anticlockwise motion down the stack. By taking the Pt–Cl bond as the starting position, it requires four molecules to complete a full rotation back to its original starting position. The homogeneous-stacked molecules are rotated 116.42°, while the heterogeneous stackings are rotated by 108.85° both above and below. The interplanar distances observed between the molecules are 3.3724 Å for the Pt(1)–Pt(1) homostacking and 3.4009 and 3.4485 Å for the Pt(1)–Pt(2) and Pt(2)–Pt(1) heterostacking, respectively. The intermolecular interactions created by short packing distances are clearly within the range for both π–π and Pt–Pt overlap between stacked molecules. Figure 48c) clearly shows good overlap between the N^C^N π-orbitals, however, because of the observed rotation, even though the centroid of the stacks is firmly placed on the Pt–C bond, the metal centres are significantly displaced from one another making metal-metal bonding interactions unlikely.[34]

a)

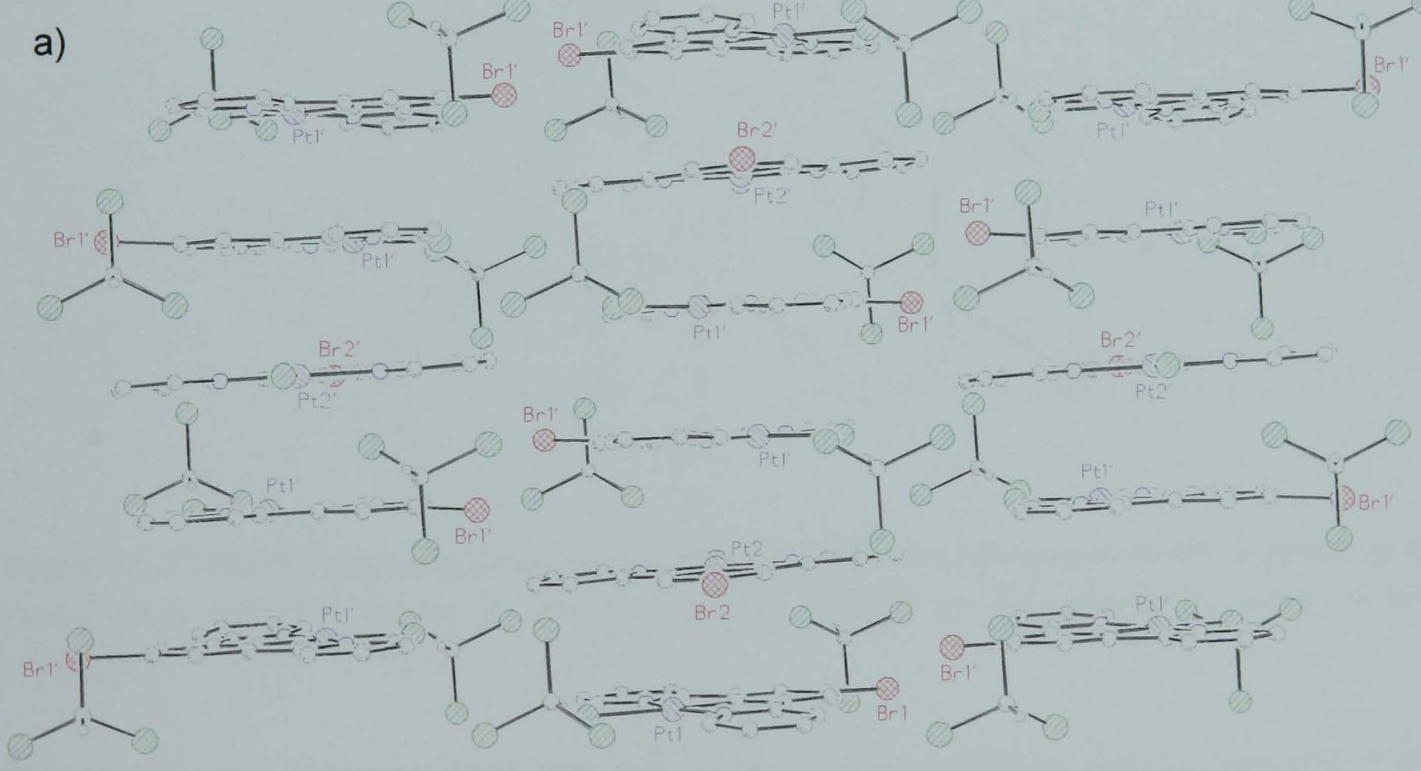

b)

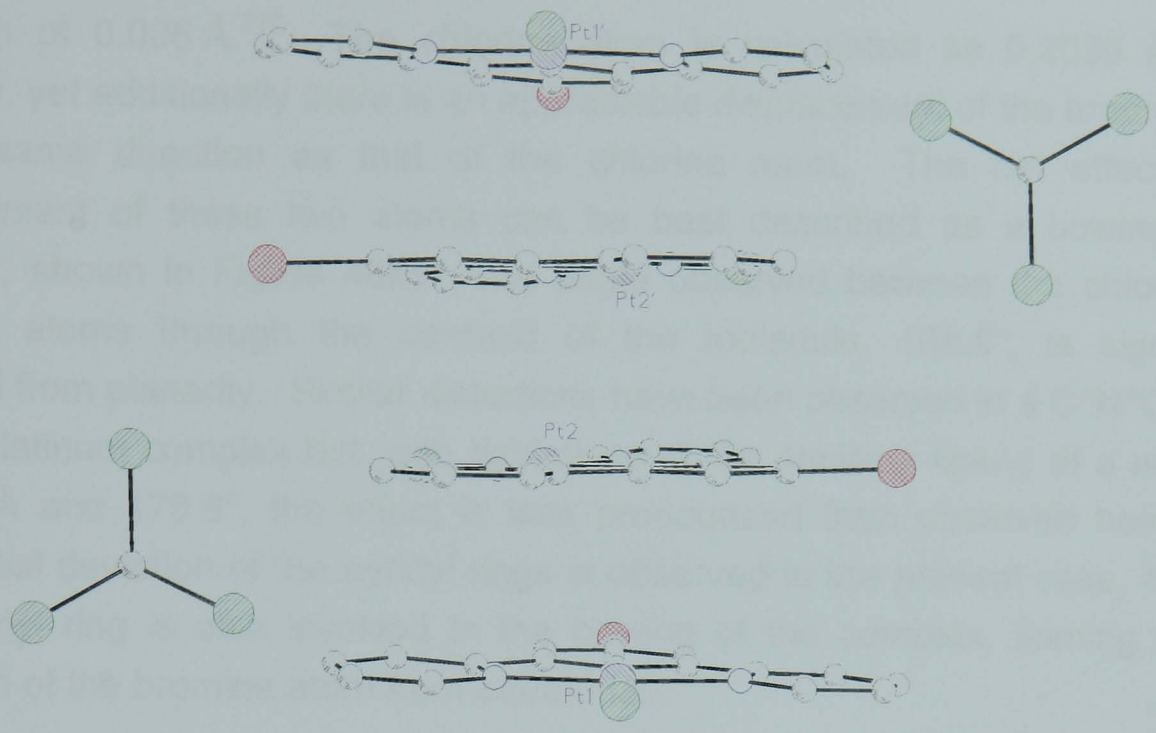

c)

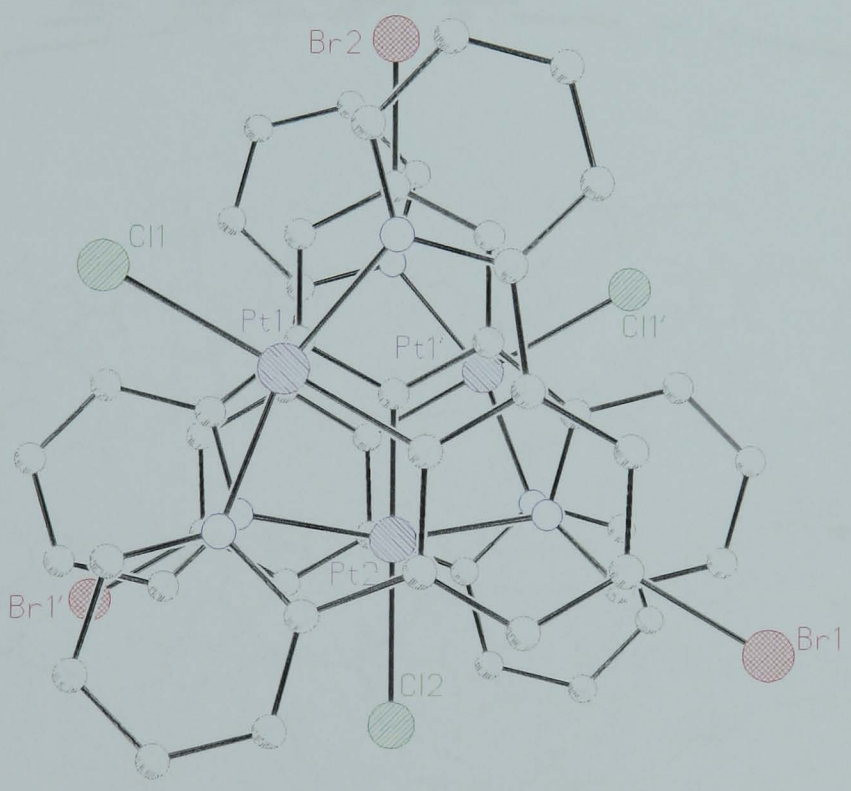

Figure 47: L^6PtCl, Br^2; (a) vertical stacks with little intermolecular interactions in the *xy* plane; (b) the stacks show helical rotations; (c) with the centroid through the cyclometalating bonds of each molecule.

Br^3 has some features that set the core of the complex apart from the other systems discussed thus far. The deviation from the mean best plane of the metal and coordinating atoms is far greater than observed in all the previous compounds, 0.0379 Å. By exclusion of the chlorine atom from the investigation into the plane between the platinum, cyclometalating carbon and the peripheral nitrogens, assigned as equatorial within the complex, the mean best plane shows a reduced

deviation of 0.006 Å.[270] The chlorine atom is calculated as 0.2039 Å out of planarity, yet additionally there is an appreciable displacement of the bromine atom in the same direction as that of the chlorine atom. The net effect of the displacement of these two atoms can be best described as a bowing of the complex, shown in Figure 48a). The angle observed between the chlorine and bromine atoms through the centroid of the molecule, 168.8°, is significantly deviated from planarity. Similar distortions have been observed in a C^N^C square planar platinum complex but, with deviations of the ancillary ligand at a maximum of 0.15 Å and 176.6°, the effect is less pronounced than observed here.[12] No substantial deviation of the pyridyl rings is observed in the present case, however, the phenyl ring is also involved in the bowing of the complex, leaning with the deviation of the bromine atom from equatorial.

a)

b)

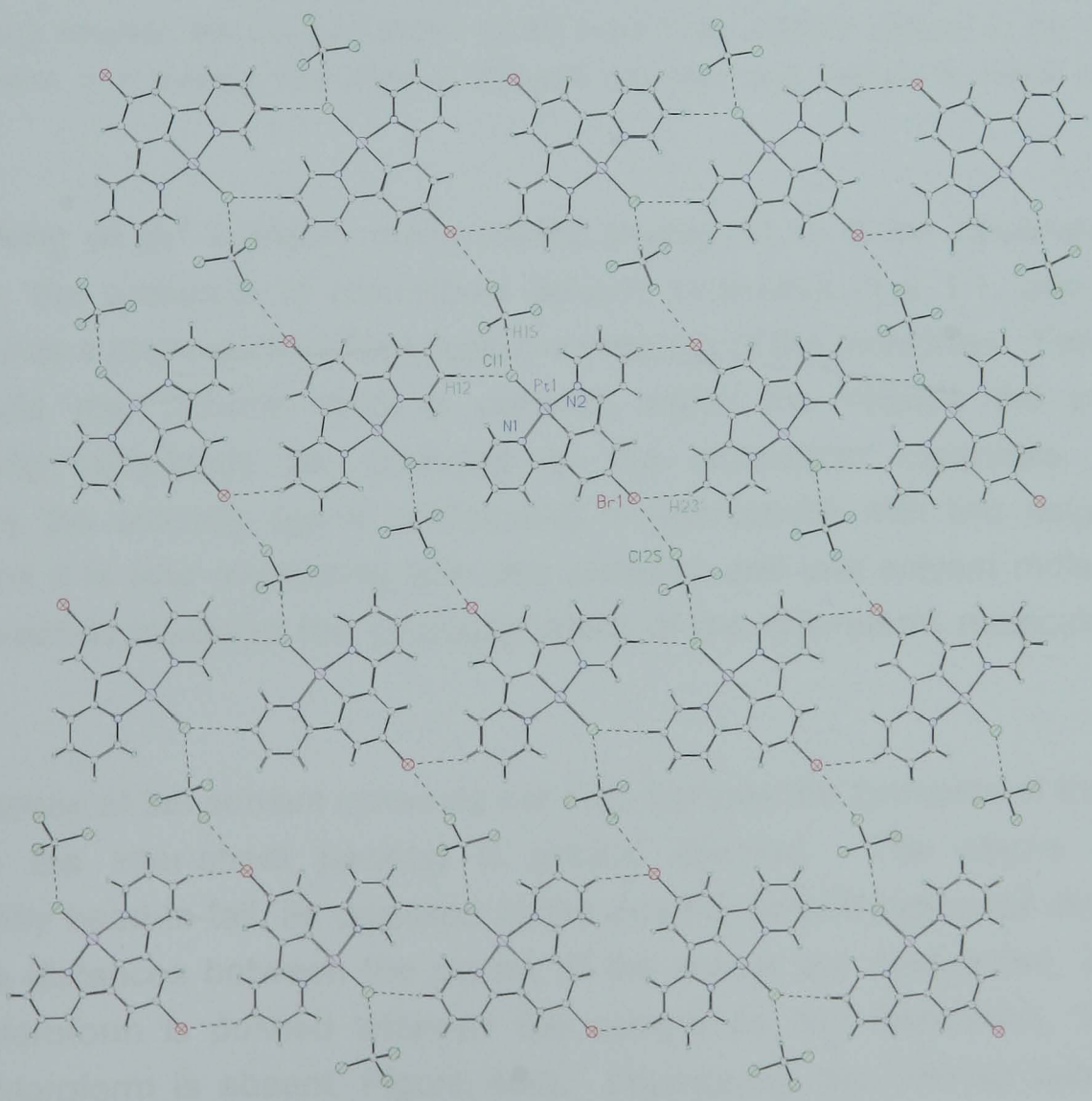

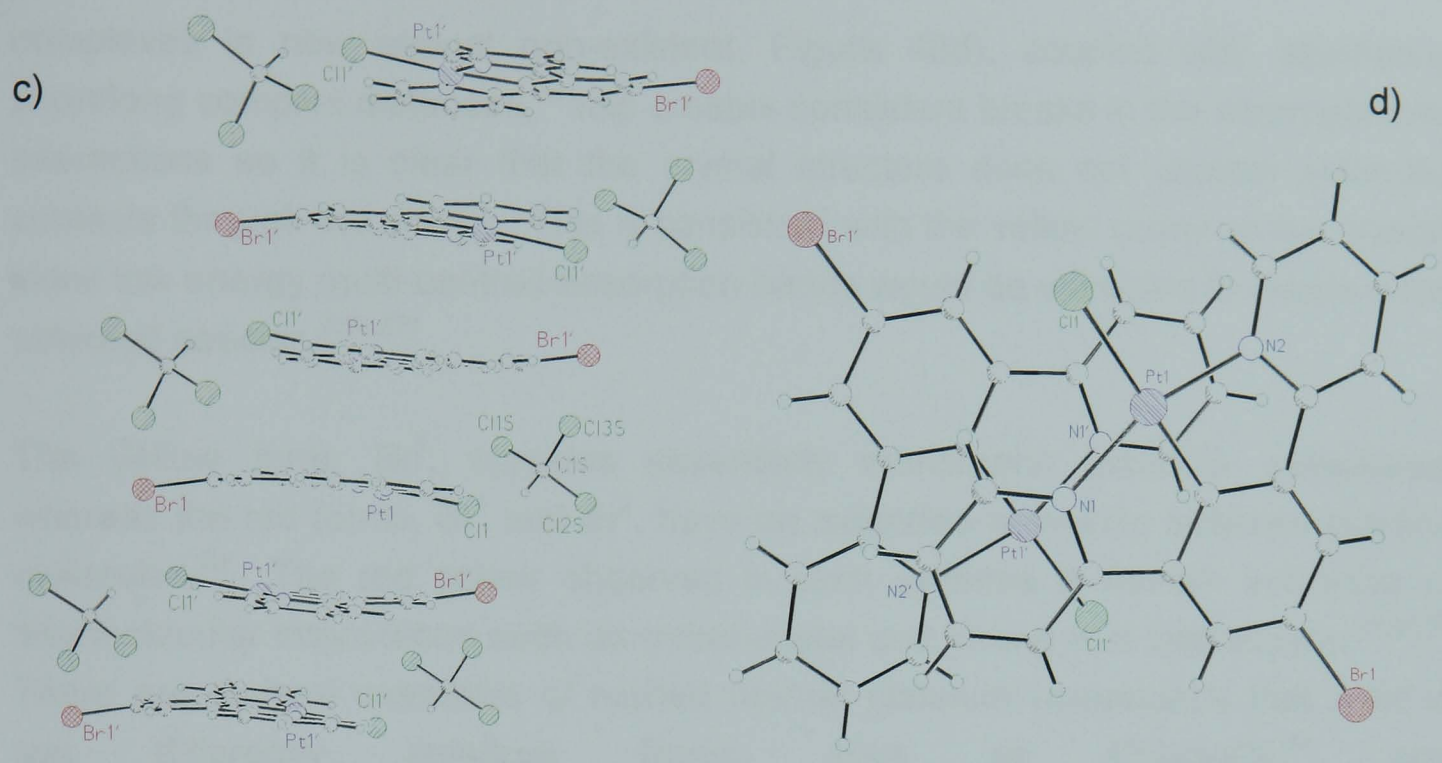

Figure 48: Br^3 a) a bowing effect due to the displacement from planarity of the chlorine and bromine atoms induced by the presence of chloroform; b) the ribbons described for Br1 are disrupted by the presence of $CHCl_3$; c) the chloroform interactions are clearly responsible for the bowing observed in Br2, wedging between the halogen atoms of the head-to-tail stacked dimers; d) the dimers are < 3.8 Å, within π-π overlap, the area of contacts are poor and unlikely to result in such an interaction.

The packing of Br^3 contains many motifs analogous to those observed in Br^1. However, the presence of chloroform solvent molecules in a 1:1 ratio with the complex has a pronounced effect upon the ordering of the molecules. Firstly, while the sheets and ribbons motif is present, within the ribbons the previously interlocking complexes are distorted by the chloroform molecules. Where previously the chloride ligand participated in interactions with two neighbouring complexes it is now interacting with one complex and one solvent molecule, the new interaction involving the hydrogen atom of the chloroform molecule, Figure 48b).

The presence of the solvent molecule not only disrupts the formation of the sheets, but also the inter-sheet packing is greatly affected. The stacks are now consistently head-to-tail, as opposed to the head-to-head/head-to-tail observed in Br^1. The distances between the planes of the sheets are elonganted, 3.6981 Å, when chloroform is pushed between the complexes, but depressed, 3.0316 Å, where chloroform is absent, Figure 48c). Importantly, the overlap between the

complexes is now almost non-existent, Figure 48d), coupled with alternating short/long complex distances,[39] this creates consistent breaks in the intermolecular interactions so it is clear that the crystal structure does not contain extended contacts through the stacks. This is consistent with the yellow colour of the crystal, since low energy multi-centred absorption bands would be expected to create a red coloured species.[2,53,271]

The yellow form, Br^3, contains essentially monomeric platinum complexes, whereas the red forms, Br^1 and Br^2, have an extended π-overlap between stacked molecules.[34] The red colour observed in such systems is usually indicative of intermolecular interactions such as metal–metal and strong π-π interactions.[51,55,86] There are several examples of related neutral platinum compounds that exist in two differently coloured forms, such as $Pt(bpy)Cl_2$[34] and $Pt(2,2'\text{-bipyrimidine})Cl_2$[85,272,273] and many examples of π-π interactions between related complexes have been reported,[51,53,56,75,274] even sterically hindered systems such as [Pt(^{t}Bu$_3$terpy){CH2C(O)Me}].[275] Although it is rational to rule out any metal–metal interactions in the structures observed here, where optimal alignment is not observed even when interatomic distances < 3.5 Å are met, the existence of ligand based π–π interactions within the 2D sheets in Br^1 and Br^2 are understandable from the intermolecular separation between the conjugated systems.[155]

Further single crystals of the complex were grown from a range of solvent systems, such as acetonitrile, DMSO, ethanol and acetone all with slow diffusion of diethyl ether. However, no further samples of sufficient quality for X-ray diffraction analysis could be obtained, even after several painstaking attempts.

4.2. Crystal emission

In order to facilitate a discussion of the crystal-packing effects on the excited states of L^6PtCl it is useful to consider first the solution-state electronic properties. The behaviours of several similar complexes are reported in Section 2.3 and there are several generalisations that apply to this class of compounds.

The absorption spectrum for L^6PtCl displays intense π–π* transitions < 300 nm, weaker transitions at 378 nm, and a negatively solvatochromic ^{1}MLCT transition at 418 nm, while the ^{3}LC transition is observed at 492 nm. The emission spectrum at

RT in DCM solvent is consistently of ^{3}LC character, 500 nm emission maximum for the 0-0 transition, with the appearance of excimeric emission at high concentrations, *ca.* 700nm. All appropriate spectra are shown in Figure 49.

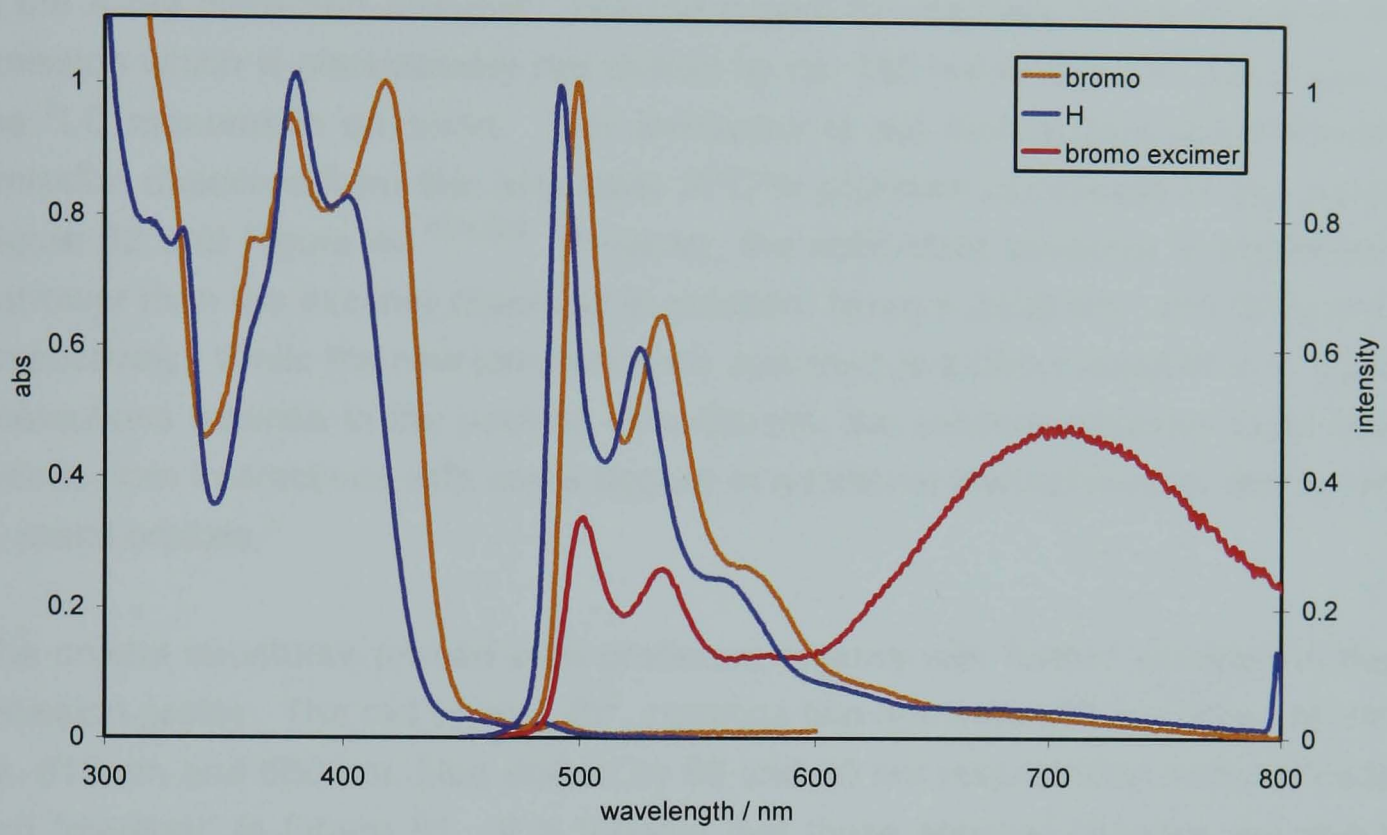

Figure 49: UV-Vis absorption and emission spectra of bromo and unsubstituted complexes, L^6PtCl and L^1PtCl respectively, in DCM solution at 298 K. Extinction coefficients and quantum yields are given in Table 2. L^6PtCl spectra recorded from dilute (10^{-5} M) and concentrated (10^{-4} M) solutions, λ_{ex} = 400 nm.

Unexpectedly, the relative energies of the absorption and emission transitions, save the excimeric emission, deviate somewhat from what might be expected. Both absorption and emission spectra are red-shifted with respect to L^1PtCl; the peak position of the ^{1}MLCT transition lies between that of the 2-pyridyl and 4-biphenyl complexes, while the ^{3}LC emission is in the order bromo < 2-pyridyl. Presumably the participation of the lone pair of electrons occupying the *p*-orbital in-plane with the conjugated π-bonding system of the aromatic ligand raises the energy of the HOMO, resulting in the red shift in the absorbance and emission spectra with respect to the unsubstituted complex L^1PtCl. This effect clearly outweighs the electron-withdrawing inductive effect associated with the halogen atom.

The luminescence spectra of Br^2 and Br^3 in the crystalline state are shown together in Figure 50. The yellow crystal Br^3 shows bright green, relatively high-energy, structured emission, characteristic of the monomeric ^{3}LC emission observed in dilute solutions. The emission fits nicely with the intermolecular packing observed in the X-ray diffraction analysis. The red crystal Br^2 displays broad, structureless emission which is considerably red shifted by *ca.* 180 nm to 681 nm, compared to the ^{3}LC monomeric emission. This behaviour is not inconsistent with excimeric emission observed from this and other N^C^N platinum complexes in this report, Figure 32 and Figure 49.[4,74,222] However, the solid-state emission is significantly narrower than the excimer observed in solution, fwhm = 2200 cm^{-1} and 3300 cm^{-1}, respectively. While the new luminescence spectrum is a direct result of π-π ligand interactions outlined in the packing descriptions, the excimer emission most likely results from interactions with some degree of additional involvement for the d_{z^2} and p_z metal orbitals.[1]

The crystal structures probed also produced regions with further variation in their emission profile. The red crystal, Br^2, contains two domains with emission maxima *ca.* 615 nm and 660 nm, blue shifted by 65 and 20 nm respectively, termed "weak" and "medium" in Figure 51. It is thought that these spectral changes are due to areas containing significant disruption to the extended intermolecular interaction. An increase in distances between the complexes in the crystal structure would produce weaker interactions between overlapping orbitals of neighbouring molecules, which can result in a greater HOMO to LUMO energy gap.[86] The shifts to higher energy are consistent with lengthening of the intermolecular distances, which affect the nature of the emitting state.

Additionally the previously monomeric emitting Br^3 was found to contain emissive domains displaying oligomeric behaviour. Unlike the emission observed in Br^2, the Br^3 domains still retain structure and the highest intensity band at *ca.* 550 nm is of sufficiently high energy to exclude assignment to the type of excited-states associated with Br^2. The opinion is held that the observed transitions are between weakly interacting dimers, and thus there is little perturbation of the emissive state compared with that assigened as monomeric in Br^3.

A fourth structure variant, Br^4, was found amongst the crystals from which Br^2 was obtained, the emission profile of which appears to show behaviour associated with

extensive and limited intermolecular interactions found in both red and yellow crystal forms, Figure 51. This crystal, however, was of insufficient quality to allow X-ray diffraction analysis to elucidate the possible origin of the contacts responsible. At present, the only conclusion from this fortuitous find is that there are additional structural profiles capable for this complex, making solid state luminescence from crystals or solids evaporated from different solvent systems a matter of possible interest for further investigation.

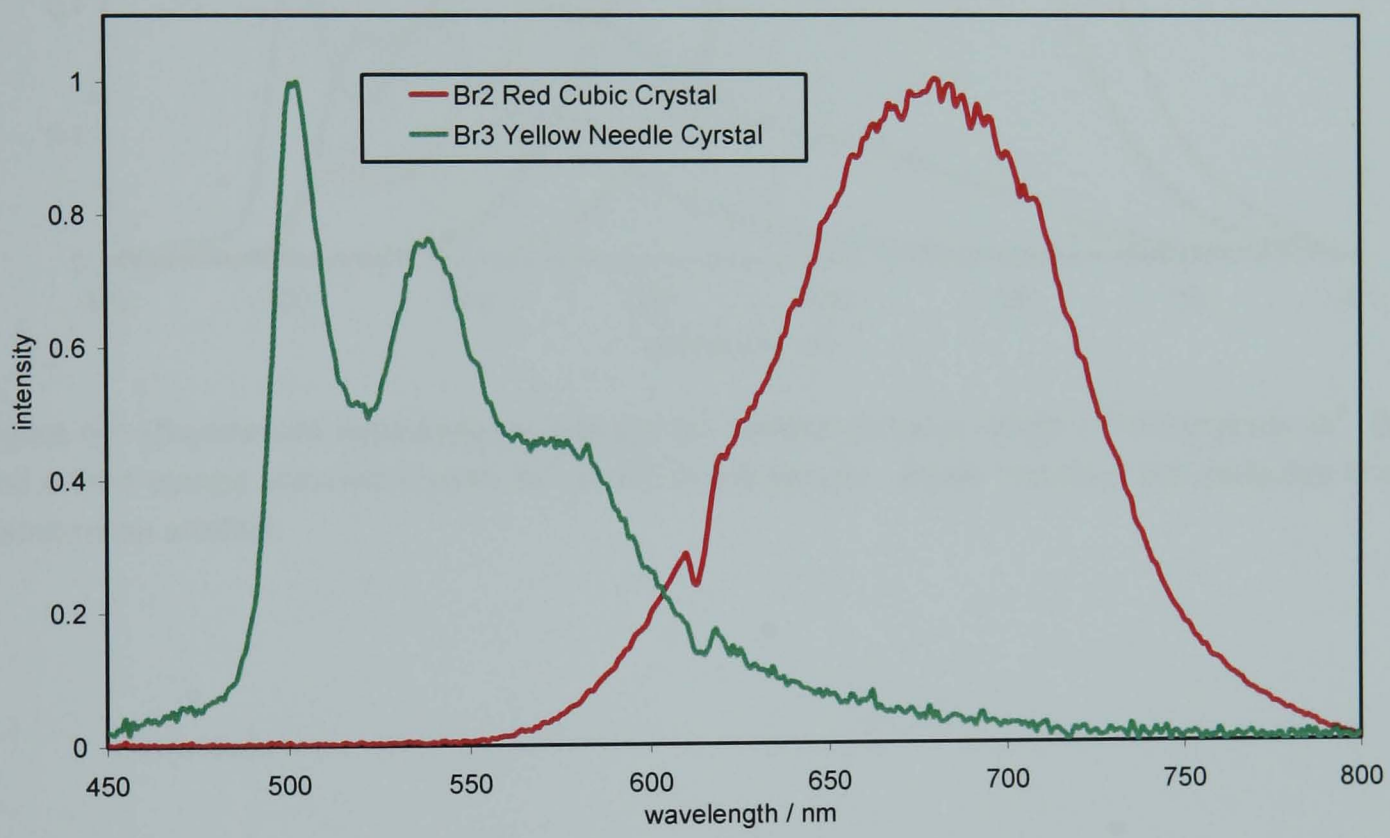

Figure 50: Uncorrected solid-state luminescence spectra of Br^2 and Br^3, two crystallographic polymorphs of L^6PtCl recorded on a fluorescence microscope using a CCD camera. The small "notch" at ca. 610 nm is an instrumental artefact.

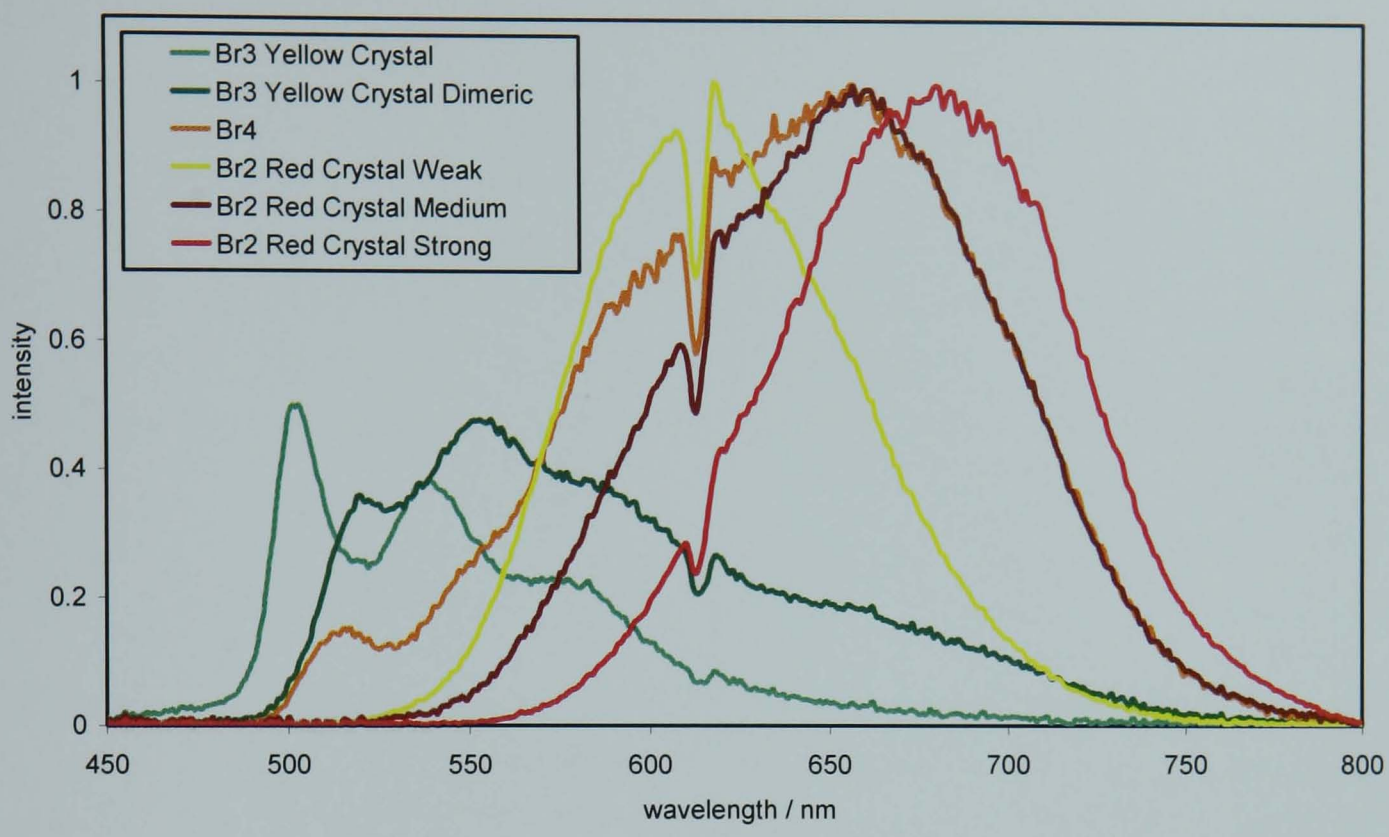

Figure 51: Uncorrected luminescence spectra for various domains within L^6PtCl crystals Br^2, Br^3 and a third orange coloured crystal, Br^4, found in the sample. Again "notches" are attributed to an instrumental artefact.

CHAPTER 5

APPLICATIONS IN PHOTO-OPTICAL DEVICES

5. Applications in photo-optical devices

Complexes displaying high quantum yields, tuneable emission energies and excimeric/ground-state interactions, have a wealth of possible applications as emissive centres for luminescent devices.[117,118,127,130] Examples of such systems are found utilising complexes with sensitivity to organic solvent vapours in vapochromism, aggregation effects signalling pressure and viscosity changes, oxygen concentration sensing, and probing of cryogenic temperatures, to highlight just a few.

5.1. Organic light emitting diodes

The newly synthesised cyclometallated platinum complexes fit many of the criteria for applications in OLEDs, including high spin-orbit coupling, formal charge neutrality, high quantum-yields of phosphorescence, and good thermal stability. Work incorporating a selection of these complexes into OLEDs has been performed by Dr. V. Fattori and her colleagues in the Istituto per la Sintesi Organica e la Fotoreattività, Bologna, Italy, and the devices examined displayed extremely high performances in terms of efficiency.[276]

OLED performance was tested in a multi-layer structure, similar to Figure 12, using the N^C^N platinum complexes as triplet-harvesting dopants in the emissive layer. An important feature of this work was the use of a mixed matrix of two materials hosting the luminescent platinum complexes, combining good hole transporting properties with good electron transporting properties, in a ratio of 47:47:6 hole:electron-transport:dopant material, respectively. In contrast to using hole-only or electron-only transporting hosts, the charge recombination is not restricted to a narrow zone close to the layer interface, but excitons produced from charge recombination are formed throughout the emitting layer. Thus, it is clear that shrewd cell design is a crucial factor in maximising external quantum efficiencies of devices.

Due to the high phosphorescence quantum yields of the 5-substituted complexes, Table 2, and to the efficient energy transfer observed from both singlet and triplet excited-states of the host to the emitting guest, external electroluminescence quantum efficiencies as high as 4–16% photons/carrier were achieved, values which are extremely high and comparable to the most efficient

electrophosphorescent devices reported thus far.[25,27,125,129,133] Furthermore, tuning of the electroluminescence spectra from the yellow to the blue-green region of the chromaticity diagram is obtained simply by changing the choice of 5-substituted cyclometalating complex, as clearly demonstrated in Figure 52, concurrent with the tuning of the monomeric emissive behaviour of the cyclometalating complexes in fluid solution.[222]

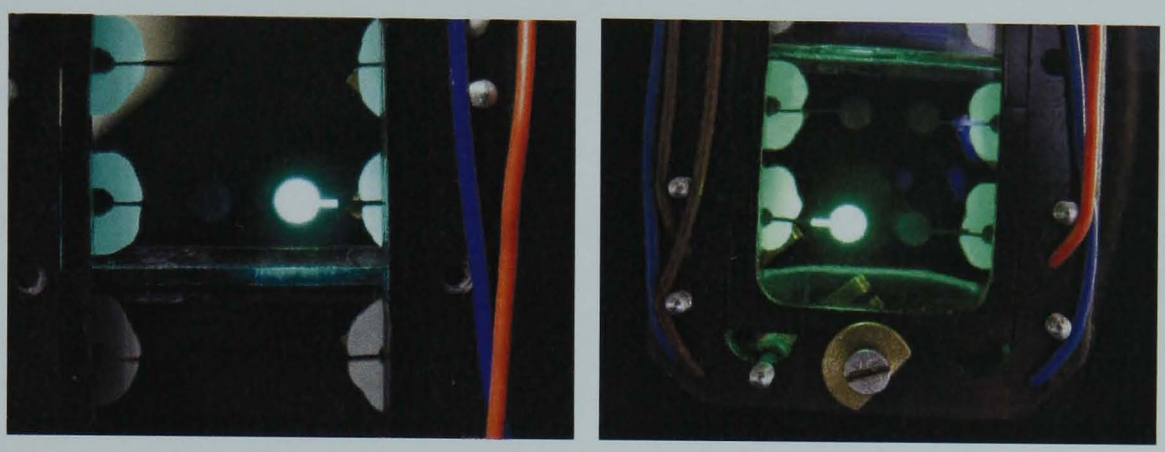

Figure 52: Left: Blue-green emission from OLED utilising 3,5-di(2-pyridyl)benzoate-2-platinum(II)-chloride. Right: Green emission from OLED utilising, L^2PtCl. Not shown: the Commission Internationale de L'Eclairage (CIE) coordinates for the devices incorporating pyridine-substituted complex, L^7PtCl, are close to the National Television Standards Committee recommended green for video display.

Controlling bimolecular interactions, such as excimers, is important for increasing device efficiency and/or tuning the emission achieved from the device.[26] Although the term excimer strictly applies to the excited dimers formed in solution from the combination of an excited- and ground-state monomer under diffusion control, the desired emission colour of many Pt(II) compounds can be attenuated by the facile formation of excimers.[277] When the complexes L^nPtCl were utilised as pure films the axial interactions of square-planar platinum complexes became important. However, low doping concentrations of the platinum complexes, typically *ca.* 6%, were found to sufficiently disperse the complexes that only monomeric emission was observed. The relatively short excited-state lifetimes of the N^C^N platinum(II) complexes are favourable to reduce roll-off (reduced device efficiency at high currents) due to electric field induced exciton quenching effects, exciton-exciton annihilation and charge carrier-exciton interactions, compared to complexes with longer lived excited-states.[131,278,279]

5.2. O_2 sensitive systems

Recent years have seen a growing interest in thin film oxygen sensors for sensing both gaseous and dissolved oxygen.[117,119] To date, most luminescent sensors have concentrated on a single lumophore with emphasis on the accurate measurement of oxygen concentration through Stern-Volmer analysis, which requires a degree of scientific expertise.[280],[281] In work performed by Evans and Douglas at the Department of Chemistry, University of Wales Swansea, U.K., the complex L^7PtCl was incorporated into a dual lumophore system for oxygen sensing. The two luminescent components, L^7PtCl and platinum octaethylporphyrin (PtOEP) display distinguishable luminescent colours whilst displaying large differences in oxygen sensitivities. The combined features of these two platinum complexes have been utilised to generate an oxygen sensor displaying a series of red to orange to green "traffic light" colour changes.

Platinum(II) porphyrin complexes are known to possess long-lived triplet excited-state lifetime (λ_{em} = 646 nm, Φ = 0.5, τ = 100 μs)[119] when compared to that of the platinum N^C^N complex which is relatively short (λ_{em} = 506 nm, Φ = 0.57, τ = 9.2 μs), therefore Pt(OEP) is more sensitive to oxygen quenching. As a general rule of thumb, when considering diffusion-controlled bimolecular-quenching processes, such as oxygen quenching, the longer a molecule exists in the excited-state, the greater the probability of encountering and being quenched by an oxygen molecule. The relatively short lifetime of L^7PtCl makes it relatively insensitive to oxygen allowing it to be used to monitor higher oxygen concentrations, for example, if the reader recalls from Section 2.3.2.2, L^7PtCl remains significantly luminescent in the presence of 1 atmosphere of air, Table 2. The porphyrin complex therefore is suitable for detecting very low oxygen concentrations.

Importantly, the luminescent energies of the two complexes are distinct. The porphyrin displays intense red luminescence, λ_{em} = 646 nm, while L^7PtCl is a bright green emitter, λ_{em} = 506 nm. L^7PtCl in concentrated solutions displays self-quenching accompanied by excimer emission which is also red emissive, λ_{em} = 690 nm. However, at concentrations employed in the above sensor there is no evidence of excimer emission, meaning all red emission detected from the device can be directly associated with Pt(OEP). By combining the two lumophores in the same device accurate detection over a wide range of oxygen concentrations is possible. In the absence of oxygen, emission is dominated by the porphyrin

layer of the device due its larger extinction coefficient at the excitation wavelength, and this response is seen as red emission from the device. As the oxygen concentration is increased the porphyrin layer is preferentially quenched due to a higher sensitivity of its longer-lived excited-states, therefore L^7PtCl will remain emissive beyond oxygen concentrations which completely quench Pt(OEP) emission. The overall result can be visualised in Figure 53, where a gradual yet dramatic colour change is observed upon increasing oxygen concentrations, starting from red emission at $[O_2] = 0$, to mixed emission seen as orange at low $[O_2]$, while at higher concentrations only green emission can be seen. The additional attractive feature of this device is that while rough concentrations can be analysed through colorimetric analysis, precise evaluation of oxygen concentration is also available through Stern-Volmer analysis of emission intensities. This red-orange-green response provides a simple and rapid method for both qualitative and semi-quantitative analysis of oxygen concentration. Additionally, the phenomenon of complex aggregation can lead to inhomogenous dye distribution in the polymer matrix resulting in the formation of aggregates which can lead to non-linear Stern-Volmer plots for oxygen responses,[119] and although no such effect was observed in this study, because there are two emissive species present, both complexes can be used as an internal check to confirm the measurements achieved through the other compound.

% O_2	Sensor Colour
0	
5-10	
30-100	

Figure 53: Traffic light response of the dual luminophore oxygen sensor, λ = 366 nm (UV lamp). At low oxygen concentrations red emission dominates from the porphyrin complex due to higher extinction coefficients compared to the N^C^N platinum complex. Upon increasing oxygen concentrations the device is observed to display dual, orange, followed by pure N^C^N green luminescence. Photographs were taken with a Nikon Coolpix 3700 digital camera.

CHAPTER 6

ANCILLARY LIGAND METATHESIS

6. Ligand metathesis

It has been shown that the nature of the ancillary ligands can have a strong effect on the lowest emitting excited-state of terdentate platinum complexes.[55,81] The modification of charge, electron-donating or -withdrawing character of the ligand, and solubility can serve to tune its properties. It was with this in mind that substitution of the fourth coordination site of the N^C^N terdentate platinum structure was investigated, with particular attention paid to developing acetylide substituted complexes.

6.1. Synthesis and structures of L^nPtL' (n = 1 and 2, L' ≠ Cl)

6.1.1. L' = Pyridines

Initial attempts to generate the cationic derivative 1,3-di(2-pyridyl)benzene-2-platinum(II)-N-pyridine, $[L^1Ptpy]^+$, according to procedures outlined for N^N^C coordinated complexes,[3,53,54] only recovered starting material, even when the reaction was performed in a large excess of neat pyridine. This is despite the fact that van Eldik *et al.* have found that the (N^C^N)Pt–Cl bond is ~ 10^5 times more labile than the corresponding (N^N^C)Pt–Cl bond. Presumably, even though the kinetics are more favourable for the N^C^N system, the thermodynamics strongly favoured the chloro starting material.

It was subsequently found that such cationic derivatives could be obtained by prior abstraction of the halide ion using silver salts in acetone, Scheme 21.[70,71,72] However, care was required when isolating the required product not to expose the complex to Lewis bases, including CH_3CN. The pyidyl complexes decomposed readily when left standing, even in acetone solution, over as little as a few hours. The series of complexes $[L^nPtpy]^+$ (n = 1, 2, 3, and 7 and new complex 3,5-di(2-pyridyl)benzoate-2-platinum(II)-N-pyridine) could be prepared as their trifluoromethanesulfonate salts and purified by washing in anhydrous acetone. Additionally, the complex $[L^1Pt$-N-(N',N'-dimethylaminopyridine)$]^+$ trifloromethanesulfonate could be obtained through identical procedures, and found to be somewhat less susceptible to degradation in solution.

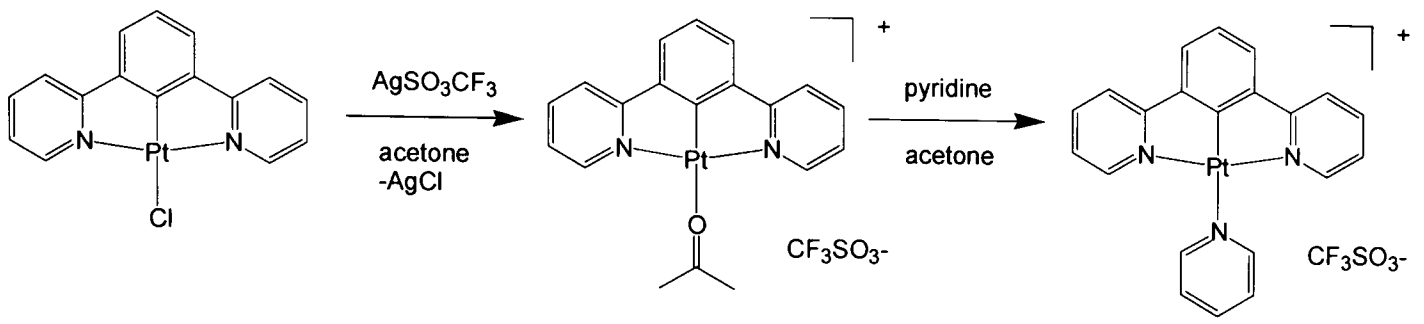

Scheme 21: Chloride ligand metathesis requires prior abstraction of the chloride ion using silver compounds, as shown above.[70]

^{1}H NMR spectra of the pyridyl substituted complexes are readily assigned and confirmed by COSY and NOESY. Upon changing the fourth substituent on the ligand from chlorine to pyridyl ligand, the donor rings *cis* show a marked upfield shift for the proton H^6-py. This is in accordance with the observed deshielding nature of halogen substituents,[282] accompanied by the proton being placed in the anisotropic shielding region of the ring current of the newly bonded pyridine unit, nearly perpendicular to the coordination plane.

Single crystals suitable for X-ray diffraction analysis of the complexes $[L^1Ptpy]SO_3CF_3$, $[L^2Ptpy]SO_3CF_3$, and $[L^1Pt(DMAP)]SO_3CF_3$ were obtained by slow evaporation of saturated acetone solutions of the appropriate complex.

ORTEP diagrams of the crystal structure determinations for the new pyridine based complexes are shown in Figure 54–Figure 56. All complexes have similar bond lengths and angles around the coordination of the N^C^N donor compared to those already discussed, Section 2.2.3.1. The main features of note for these compounds is the Pt–N(pyridine) bond distance for the new ligands, $[L^1Ptpy]^+$ = 2.140(3) Å, $[L^2Ptpy]^+$ = 2.114(6) Å, $[L^1Pt(DMAP)]^+$ = 2.134(4) Å, are considerably longer than such bonds in N^N^C systems, $[(N^N^C)Ptpy]^+$ = 2.029(6) Å and $[(N^N^C)Pt(DMAP)]^+$ = 2.032(8) Å,[54] and longer than *trans*-$[Pt(pyridine)Cl_2]$ = 1.98 Å.[283] In all three pyridine complexes the ancillary pyridine ligand is nearly perpendicular with respect to the plane of the cyclometallated N^C^N unit, 68.21(5), 58.29(12), and 59.21(6)° for L^1, L^2 and DMAP, respectively.[284] Almost certainly, this orientation of the ancillary ligands is adopted to relieve the steric repulsion between H^6-py of the terdentate ligand and the hydrogen atoms at the 2/6-postions of the ancillary. However, any deviation from orthogonality will increase overlap between $5d_{z^2}$ orbitals of the metal centre with the π-aromaticity of the pyridine units.[56] It is noted that for the complex containing the

dimethylaminopyridine ligand, the C–NMe_2 bond between the amine and the pyridine ring (1.343(7) Å) is shorter than a normal C–NH_2 single bond (*ca.* 1.44 Å), indicating that there is delocalisation of the lone pair of electrons of the amine nitrogen into the pyridine ring. This increased donor strength, although only having a marginal effect on the bond length formed between the metal centre and the pyridine unit in the crystalline phase, probably accounts for the noticeable increase in complex stability in the presence of competing Lewis bases in solution, mentioned above.

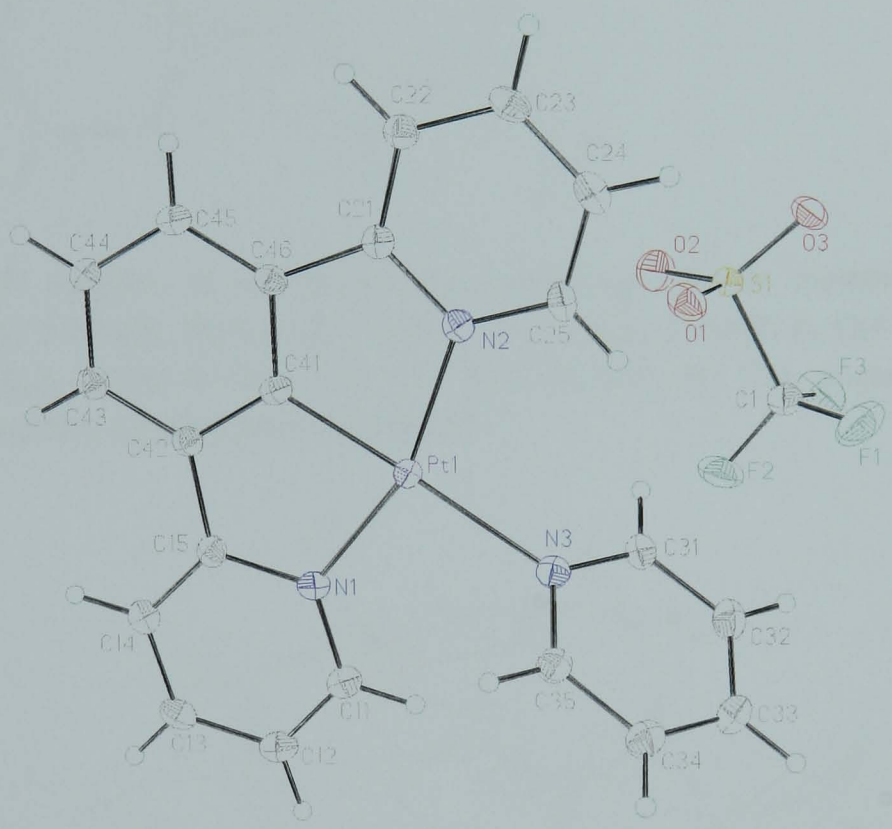

Figure 54: ORTEP diagram of $[L^1Ptpy]SO_3CF_3$ confirming chloride metathesis. Pt(1)–C(41) 1.908(3), Pt(1)–N(1) 2.039(3), Pt(1)–N(2) 2.039(3), Pt(1)–N(3) 2.140(3) Å, C(41)–Pt(1)–N(1) 80.81(12), C(41)–Pt(1)–N(2) 80.13(12), C(41)–Pt(1)–N(3) 178.07(11), N(1)–Pt(1)–N(2) 160.93(11), angle between platinum coordination and ancillary pyridine plane 68.21(5)°.

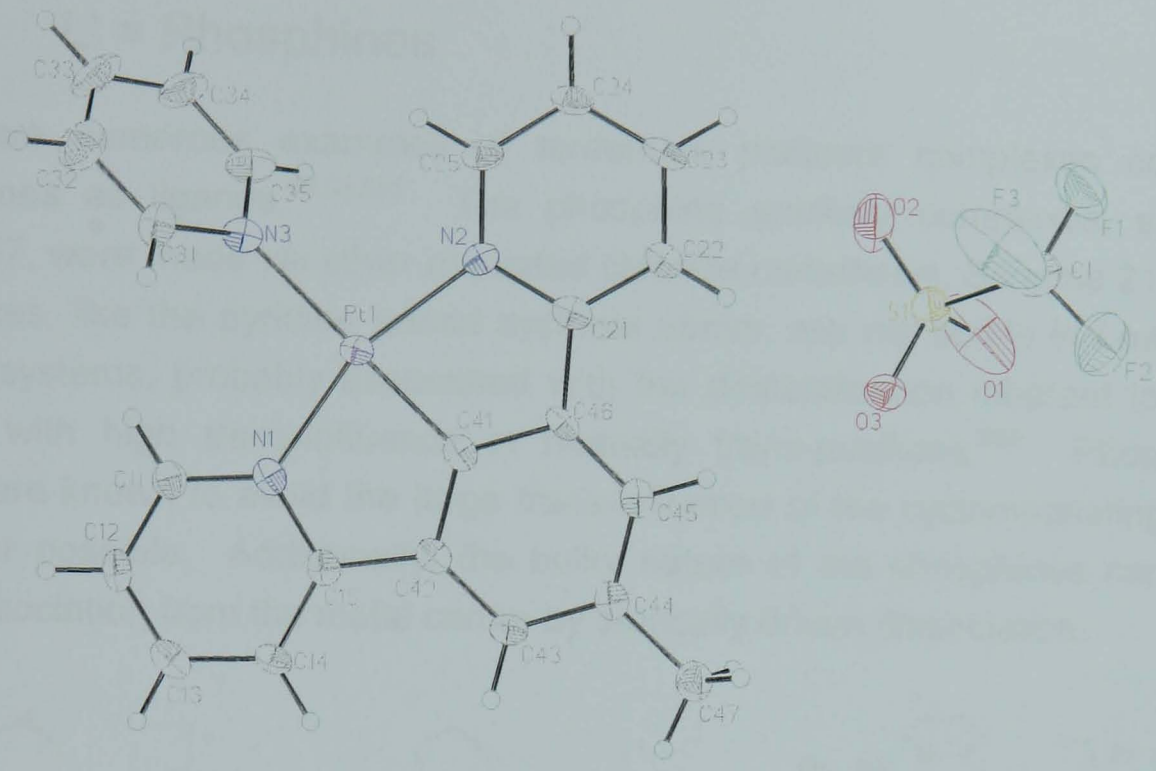

Figure 55: ORTEP diagram of $[L^2Ptpy]SO_3CF_3$ confirming chloride metathesis. Pt(1)–C(41) 1.898(7), Pt(1)–N(1) 2.029(5), Pt(1)–N(2) 2.028(5), Pt(1)–N(3) 2.114(6) Å, C(41)–Pt–N(1) 80.2(3), C(41)–Pt–N(2) 80.8(3), C(41)–Pt–N(3) 179.7(3), N(1)–Pt–N(2) 161.1(2), angle between platinum coordination and ancillary pyridine plane 58.29(12)°.

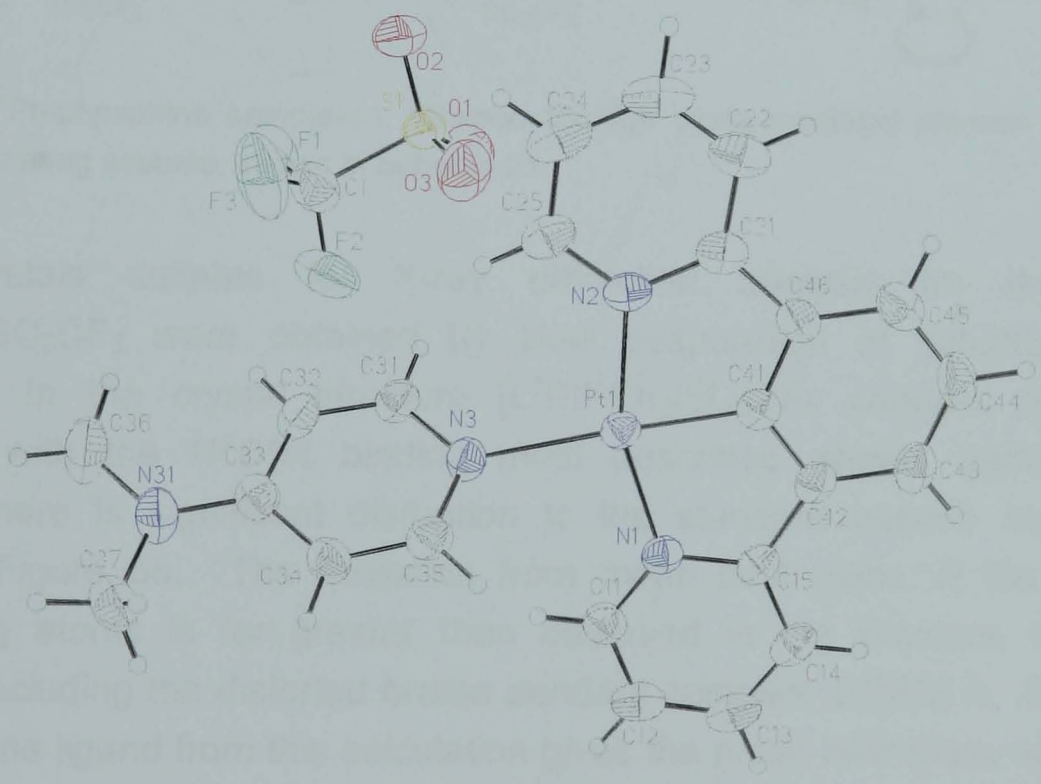

Figure 56: ORTEP diagram of $[L^1Pt(DMAP)]SO_3CF_3$ confirming chloride metathesis. Pt(1)–C(41) 1.916(5), Pt(1)–N(1) 2.037(4), Pt(1)–N(2) 2.035(4), Pt(1)–N(3) 2.134(4) Å, C(41)–Pt(1)–N(1) 80.27(18), C(41)–Pt(1)–N(2) 80.37(19), C(41)–Pt(1)–N(3) 176.49(17), N(1)–Pt(1)–N(2) 160.65(17), angle between platinum coordination and ancillary pyridine plane 59.21(6)°. This structure has a destructive phase transition between 210 and 100 K from monoclinic to triclinic.

6.1.2. L' = Phosphines

There are numerous examples of terdentate platinum complexes containing phosphines as ligands.[40,53,285] The phosphine ancillary complexes, shown in Figure 57, were made *via* silver mediated chloride metathesis, Scheme 21. These complexes, like the pyridine based systems above, are not stable in Lewis basic solvent systems, probably associated with the destabilisation inherent to placing ligands with high *trans*-influence in mutually *trans*-positions.[285] Phosphorous donors are known to avoid the large *trans*-influence of the cyclometalating carbon wherever possible. Additionally, the bulky nature of the phosphines can induce their dissociation from the metal centre by sterically driven dissociation.

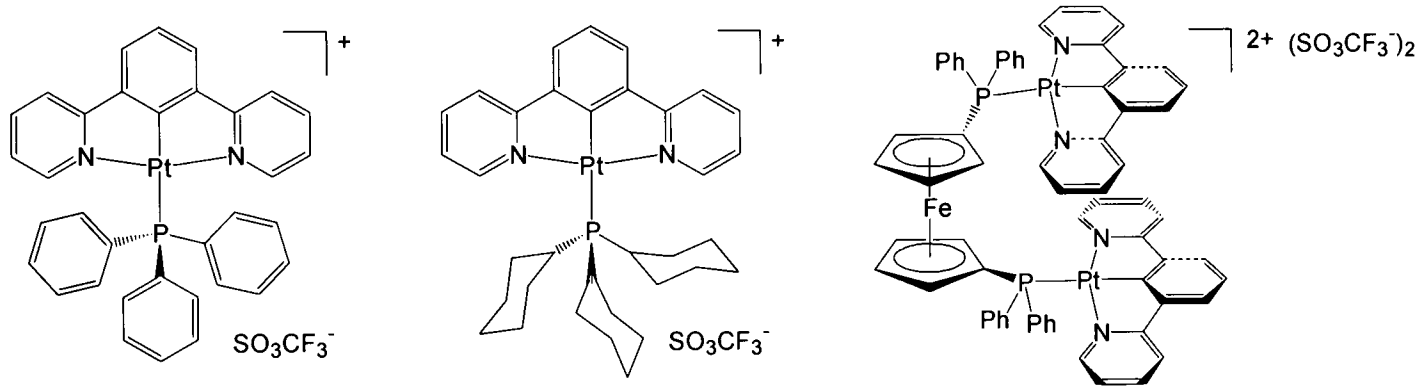

Figure 57: L^1Pt–phosphine complexes obtained through silver mediated chloride metathesis in weakly coordinating acetone, shown in Scheme 21.

Single crystals suitable for X-ray diffraction analysis for the complex $[L^1PtPPh_3]SO_3CF_3$ were obtained by slow evaporation of saturated acetone solutions. In the crystal structure $[L^1PtPPh_3]SO_3CF_3$ contains the features consistent with the N^C^N binding motif described above, Section 2.2.3.1, however, there is significant disruption to the standard pseudo square-planar geometry, Figure 58. The deviation from mean best plane of the metal and coordinating atoms is far greater than observed in the previous compounds, 0.1690 Å, including the distorted bromo pendant complex, 0.0379 Å. Exclusion of the phosphine ligand from this calculation gives the mean best plane with reduced deviation of 0.0593 Å, and the phosphorus atom is calculated as 0.8599 Å out of planarity. The Pt–P bond distance 2.3656(6) Å is considerably longer than in other terdentate binding systems; an increase in bond length of 0.15 Å compared to $Pt(C^N^C)PPh_3$ (2.2156(9) Å)[56] and over 0.12 Å to related complexes of $Pt(N^N^C)PPh_3$ (2.243(3) Å).[40] Increase in bond length is a direct response to an admixture of factors including the very strong *trans*-influence exerted by the short

carbanion bond and the large steric influence exerted on the bond by the three phenyl units attached to the phosphorus atom.

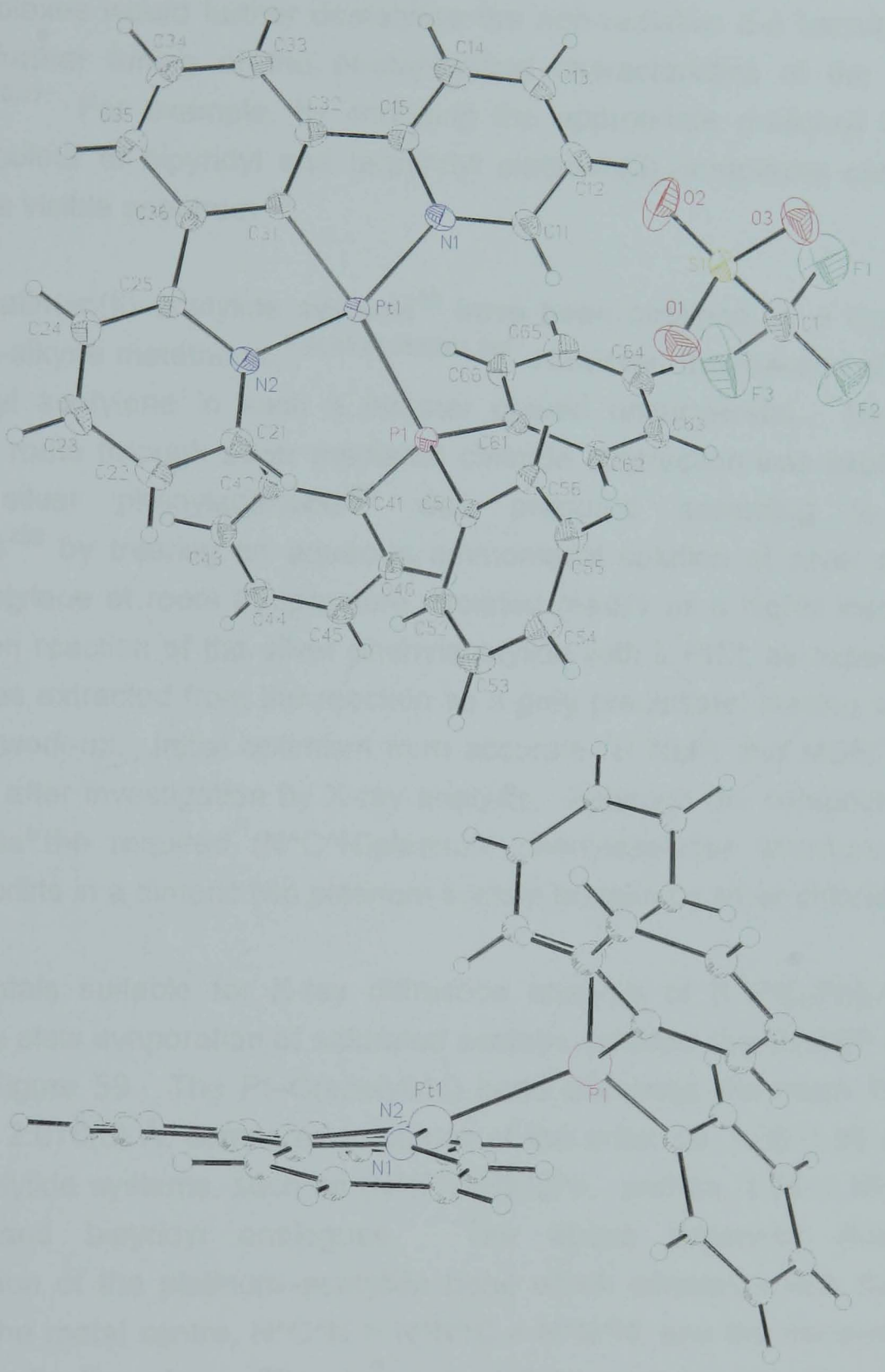

Figure 58: ORTEP diagram of $[L^1PtPPh_3]SO_3CF_3$, note the extreme deviation from the standard planar coordination geometry induced by the packing constraints of the sterically demanding ligand. Pt(1)–C(31) 1.954(2), Pt(1)–N(1) 2.0583(19), Pt(1)–N(2) 2.0553(19), Pt(1)–P(1) 2.3656(6) Å, C(31)–Pt(1)–N(1) 79.10(8), C(41)–Pt(1)–N(2) 79.72(8), C(41)–Pt(1)–P(1) 176.49(17), N(1)–Pt(1)–N(2) 160.65(17)°. The phosphorus is 0.8599 Å deviated from the ideal pseudo square planar geometry.

6.1.3. L' = Acetylides

It was envisaged that incorporation of anionic acetylide ligands into cyclometallated Pt(II) complexes would further destabilise the non-radiative d-d transitions, whilst enabling further tuning of the photophysical characteristics of the complexes formed.[45,76,77] For example, by choosing the appropriate σ-alkynyl ligands the emission colour of bipyridyl and terpyridyl platinum(II) complexes can be tuned through the visible spectrum.[55]

Related platinum(II) acetylide systems[55] have been obtained by a CuI-catalysed chloride-to-alkyne metathesis.[5,44,64,81,286,287,288] However, the reaction of the L^1PtCl with phenyl acetylene in such a manner proved unsuccessful. Therefore, an alternative route through silver mediated chloride abstraction was explored. The complex silver phenylacetylide[289] was prepared according to literature procedures[290] by treating an aqueous ammoniacal solution of silver nitrate with phenyl acetylene at room temperature, isolated readily as a highly insoluble grey solid. Upon reaction of the silver phenylacetylide with L^1PtCl, as expected, silver chloride was extracted from the reaction as a grey precipitate, leaving a bright red solid after work-up. Initial optimism from accurate ^1H NMR and $MSEI^+$ data was short lived after investigation by X-ray analysis. Although the compound isolated did possess the required (N^C^N)platinum phenylacetylide structure, the new molecule exists in a dimeric two platinum system bridged by silver chloride.

Single crystals suitable for X-ray diffraction analysis of $[L^1PtC_2Ph]_2AgCl$ were obtained by slow evaporation of saturated acetone solution; the ORTEP diagram is shown in Figure 59. The Pt–C(acetylide) bond distances are much longer than anticipated 2.070(3) Å, compared to values of the order *ca.* 1.96–1.98 Å[55] in the N^N^C acetylide systems, such as $(N^N^C)PtC_2Ph$, and *ca.* 1.94–1.96 Å[45,113] for terpyridyl and bipyridyl analogues. The above distances illustrate the destabilisation of the platinum–acetylide bond which correlates with the electron density at the metal centre, N^C^N > N^N^C > N^N^N, and the *trans*-influence of the opposite ligating atom. The phenyl ring of the acetylide ligand is orthogonal with respect to its own planar N^C^N ligand, 170.8°, yet co-facial π-stacking between the phenyl ring of the acetylide and one of the pyridine units from the opposite N^C^N ligand is observed, aided by a deviation from linearity observed in the linear carbon structure, shown in Figure 59.

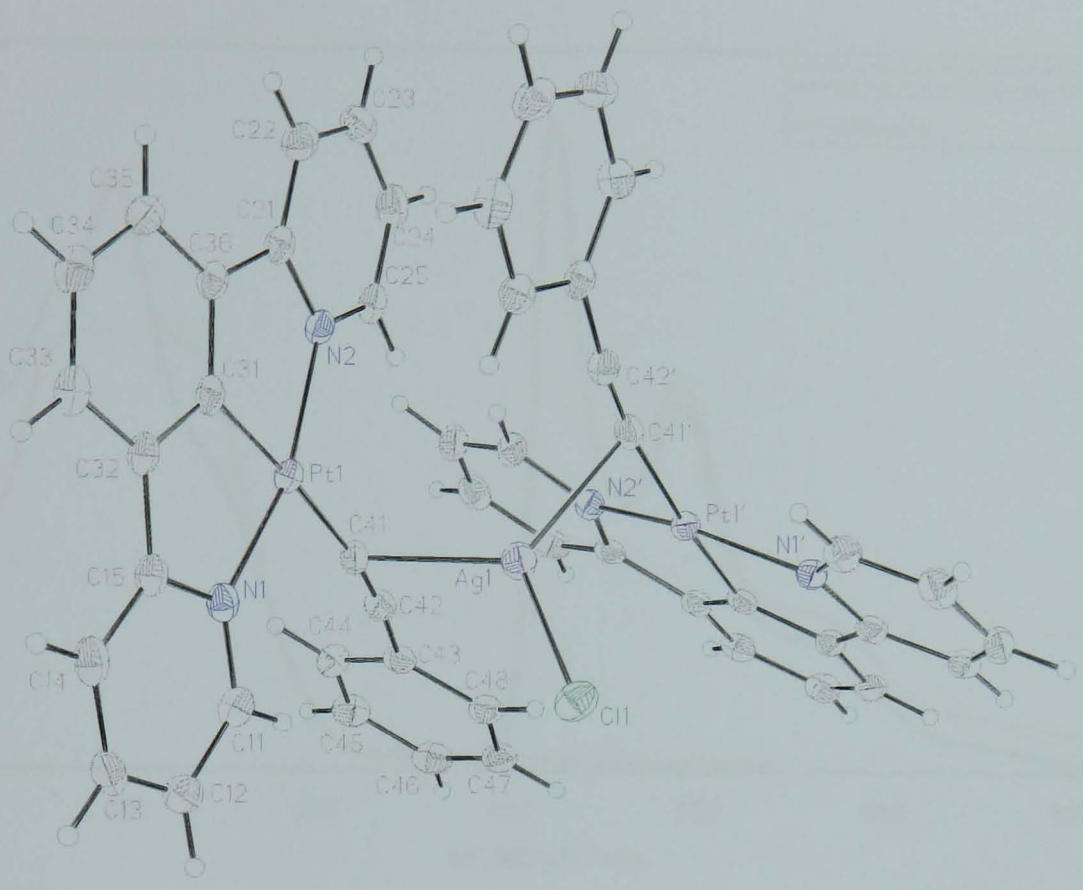

Figure 59: ORTEP diagram of $[L^1PtC_2Ph]_2AgCl$, noteworthy is the orthogonal orientation of the phenylacetylide ligand with respect to the (N^C^N)Pt coordination plane, however, the phenyl groups are then parallel with the (N^C^N)Pt coordination plane of the bridged opponent. Pt(1)–C(31) 1.940(2), Pt(1)–N(1) 2.038(2), Pt(1)–N(2) 2.035(2), Pt(1)–C(41) 2.070(3) Å, C(31)–Pt(1)–C(41) 175.64(10), C(31)–Pt(1)–N(1) 79.97(10), C(31)–Pt(1)–N(2) 79.77(10), N(1)–Pt(1)–N(2) 159.67(8), C(41)–C(42)–C(43) 174.9(3)°. The coordinations between the acetylene units and the silver atom are shown as coordinations between Ag1 and C41/C41', the exact nature of these interactions is an interaction with the carbon–carbon multiple bonds.

Finally, for all of the L' ≠ Cl complexes it is noteworthy that the cyclometalating platinum carbon bonds appear to increase in length in relation to the donating power of the ancillary ligand $[L^1Ptpy]^+$ and $[L^2Ptpy]^+$, 1.908(3) and 1.908(6) Å respectively, $[L^1Pt(DMAP)]^+$, 1.916(5) Å, and finally $[L^1PtPPh_3]^+$ 1.954(2) Å, confirming the influence each ligand has upon the stability of the cyclometalating bond. Additionally, due to the fact that the –C≡CPh group displays a higher *trans*-influence than the phosphorus or pyridine donors, the desired product is appreciably more unstable.

6.2. Photophysics

The photophysical properties of the phosphorus systems $[L^1PtPR_3]SO_3CF_3$ (R = Ph and Cy) were measured at RT in acetone to minimise decomposition of the complexes during measurements.

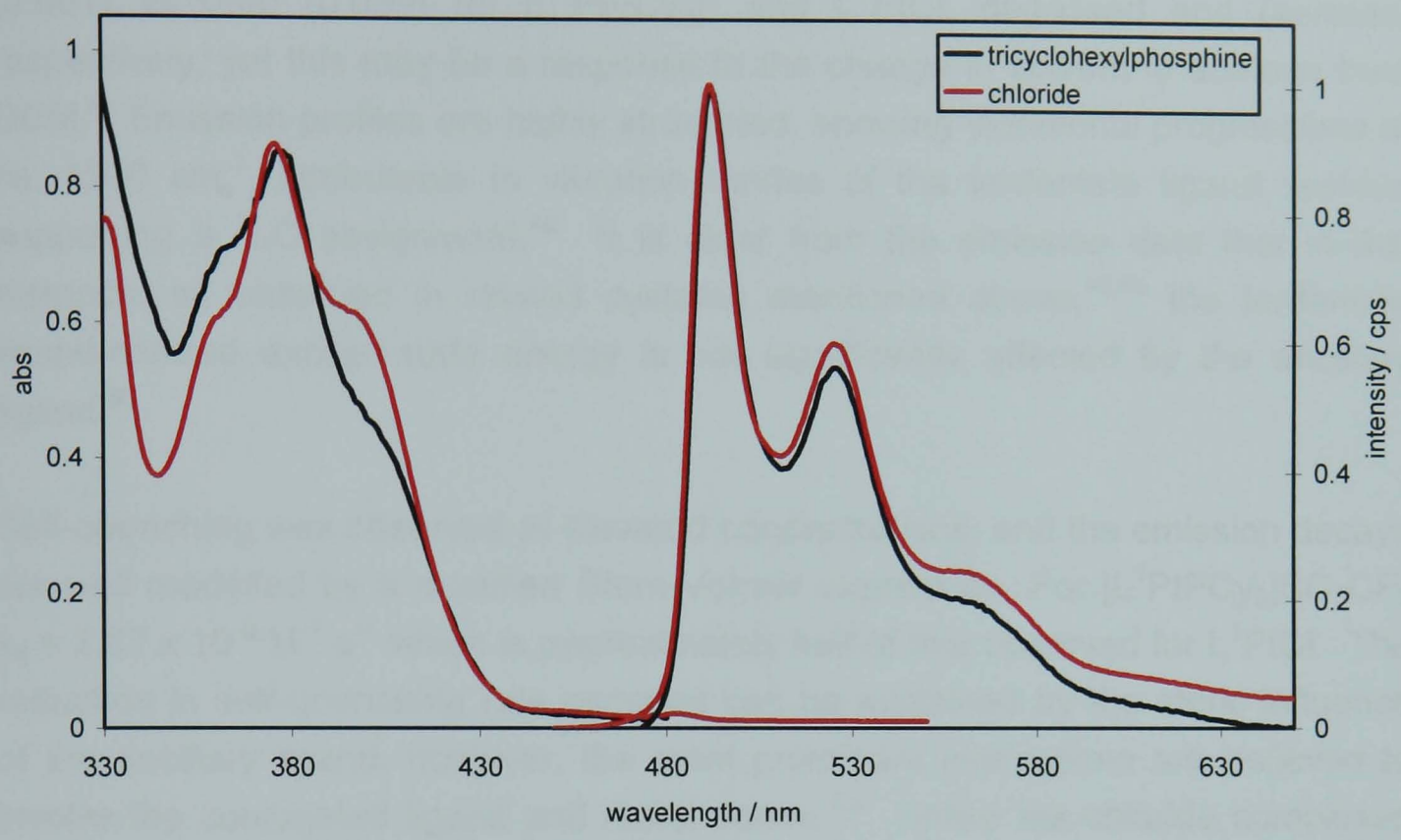

Figure 60: UV-Vis and emission spectra for the tricyclohexylphosphine substituted complex, $[L^1PtPCy_3]SO_3CF_3$ in acetone at room temperature, λ_{ex} = 400 nm. Substitution of ancillary ligand has almost no effect on the nature of the ^{3}LC transition, while a slight reduction in the extinction coefficient associated with the ^{1}MLCT band is observed, similarly observed in (N^N^C)PtL' (L' = Cl *vs* PPh_3).[40] UV-Vis: 328 (7860), 338 (7820), 361 (6670), 377 (6580), 399 nm (2030 L mol^{-1} cm^{-1}). Emission: 492, 527, 562 nm; Φ = 0.027(0.001); t0 = 4.8 us; kq self quenching = 2.87 x 10-9

6.2.1. Absorbance

Predictably, there is a slight blue shift associated with the ^{1}MLCT bands upon ligand metathesis. This feature can be explained through the formal positive charge now associated with the metal centre and the increase in energy that is required to promote an electron from the metal orbitals. Additionally, a blue shift in λ_{max} of this transition was observed on reducing the donating qualities of the ancillary ligand; similar observations have been seen for related terpyridine complexes, (N^N^C)PtL' (L' = Cl *vs* Py).[54]

6.2.2. Emission

Complexes are still emissive at room temperature in solution, which is favourable compared to related systems, *e.g.* [(phbpy)PtL'][ClO_4] (L' = pyridine, 4-aminopyridine, 2, 6-diaminopyridine, PPh_3).[40,54] However, the quantum efficiency of the systems is greatly reduced compared to the parent complex, Φ = 0.027

(0.001) *vs* 0.60 (0.039) for $[L^1PtPCy_3]^+$ and L^1PtCl, degassed and (aerated) respectively, yet this may be a response to the change in solvent to acetone from DCM.[4] Emission profiles are highly structured, showing vibrational progressions of *ca.* 1300 cm^{-1}, attributable to vibration modes of the terdentate ligand system, supporting a ^3LC assignment.[40] It is clear from the emission data that in this instance, as observed in related systems mentioned above,[40,54] the terdentate ligand-centred excited-state energy is not significantly affected by the ancillary ligand.[56]

Self-quenching was observed at elevated concentrations, and the emission decays are well modelled by a modified Stern-Volmer expression. For $[L^1PtPCy_3]SO_3CF_3$ $k_q = 2.87 \times 10^{-9}\ M^{-1}\ s^{-1}$ which is approximately half of that observed for L^1PtCl. The reduction in self-quenching rate constant can be explained by the steric influence of the ancillary ligand, however, the most prominent interactions are believed to involve the conjugated ligand and metal centre.[1,4] Unlike the chloride complexes the excited-state quenching was not accompanied by excimeric emission, the lack of which from these phosphine platinum complexes is consistent with previous related systems, *e.g.* (C^N^C)$PtPPh_3$.[56] The exact reason for this behaviour is unknown, but it is easy to envisage that the large steric effects of the phosphine substituents, coupled with the formal charge associated with the new complex, play an important role in this behaviour. However, for $Pt(dbbpy)(CN)_2$, excimer-emission is not observed in CH_3CN. The coordinating properties of the solvent may increase the non-radiative decay rate of the excimer.[4]

6.3. Conclusions on ancillary metathesis

It is believed that the strong destabilising nature of the cyclometalating bond generates a system disadvantageous to formation of new complexes with strongly donating ancillary ligands, although all blame cannot be attributed to the cyclometalating bond, since success incorporating *trans*-carbanions has been achieved in platinum(II) pincer complexes which contain softer donors than pyridine in the *cis*-positions.[64] Overall, the high electron-density located at the metal centre is the major influence and a product of the cumulative effects induced by the N^C^N binding motif, employed here. It is noteworthy, however, that compounds containing chelated cyclometallated bonds are thermally stable in organic solvents, wheras complexes containing monodentate σ-bonded carbanions have a tendancy to decompose. Additionally, it is noted in bis(C^N) complexes

that *cis*-formations are greatly prefered over *trans*-orientated cyclometalating bonds, and molecules will even undergo sufficient physical distortion or strain to avoid such a bonding configuration.[47]

CHAPTER 7

PALLADIUM(II) CHEMISTRY

7. Palladium chemistry

As with platinum, palladium(II) metal-ions are well known for their ability to undergo orthometalation by activating C–H bonds. Therefore, as part of this research, C2-cyclopalladated derivatives of HL^1 were targeted.

7.1. Direct cyclometalation

Cárdenas *et al.* have previously demonstrated that cyclopalladation does not occur when 1,3-di(2-pyridyl)benzene, HL^1, is reacted with Li_2PdCl_4 or with other Pd(II) chloride species item 2; Figure 14.[66] It is believed to be hard to induce C–H activation using $PdCl_4^{2-}$ as a metal source, however, bond activation does occur when the ligand is reacted with $Pd(OAc)_2$, yet contrary to the behaviour of platinum, the product is a C4/C6 double metalated species bridged by four acetate units, in which the ligand binds twice bidentately similar to phenylpyridine. Clearly, cyclometalation at the C4 position of the phenyl ring must be kinetically favoured over reaction at the more hindered C2 position. Versatile binding is a unique feature of N^C^N systems, since P^C^P and S^C^S pincer systems are not currently known to encounter such diversity.[66,67]

An initial synthetic strategy centred around blocking the kinetically favoured 4,6-biscyclopalladated product with the ligand, HL^3, was used. This approach has already proven successful for the complexation of iridium.[291] The only feasible product from the reaction of HL^3 with Li_2PdCl_4 was the terdentate mono-nuclear product, Equation 8. Additionally, the reaction takes place readily under conditions identical to those which failed to induce metalation for HL^1, as outlined by Cárdenas.[66]

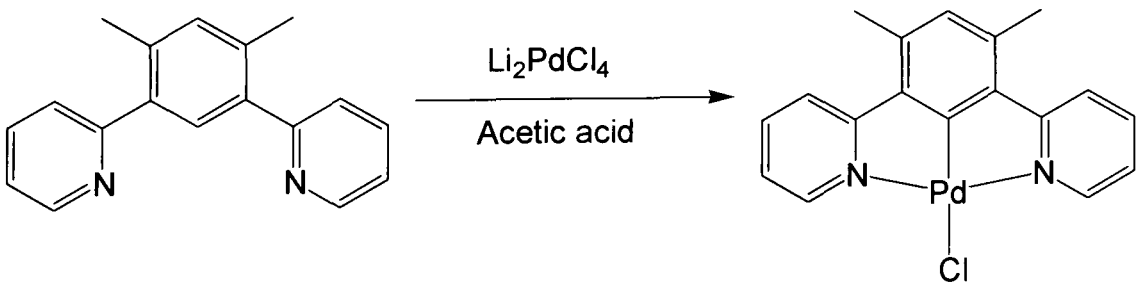

Equation 8: Direct metalation between HL^3 and Li_2PdCl_4 generates the thermodynamic product, L^3PdCl, due to methyl groups blocking the previously favoured kinetic sties.

The desired N^C^N binding coordination was confirmed by ^{1}H NMR with the disappearance of the high-frequency signal responsible for the proton situated between the two pyridine rings. Further spectroscopic details were similar in nature to the platinum(II) analogues, Section 2.2.2. Without the presence of satellites, the resonance which accompanies H^6-py moves to higher frequency $\Delta\delta$ 0.5 – 0.6 ppm, a slight shift to higher frequency is followed with H^3/H^4-py, but another distinguishing feature is the large shift upfield $\Delta\delta$ 0.5 ppm of the resonance for the H atom *para* to the cyclometalation point. Further evidence came from elemental analysis, but final proof came from single crystal X-ray diffraction.

The X-ray structure determination of L^3PdCl, from single crystals obtained by slow evaporation of a saturated chloroform solution, proves the mononuclear nature of these complexes and the terdentate binding mode with both nitrogens coordinated to a single metal centre. The structure closely resembles that of the related platinum derivatives discussed previously, Section 2.2.3,[74,222] and that of the original structure, L^1PtCl, studied by Cárdenas.[66] An ORTEP diagram of L^3PdCl is shown in Figure 61 with a list of the principal bond lengths and angles. The palladium atom displays an approximate square planar coordination. The Pd–C(31) bond distance 1.9173(15) Å, is again characteristically short due to the mode of coordination, *e.g.* (N^N^C)PdCl complexes 1.997(4)–2.067(3) Å,[41,52,151] (N^C^N)PdBr complexes 1.924(2) Å,[157] and the Pd–N bond distances, 2.0321(13) Å and 2.0328(14) Å, are shorter than those observed in related complexes containing N(sp^3)^C^N(sp^3) coordination.[15741] The bite angle of the chelating ligand, N(1)–Pd–N(2) 161.29(6)°, is systematic of terdentate binding motif and compares well to that of related systems, N^N^N,[202] N^N^C,[41,52,75,151] N^C^N,[74,157,222] or C^N^C[57] coordination modes.

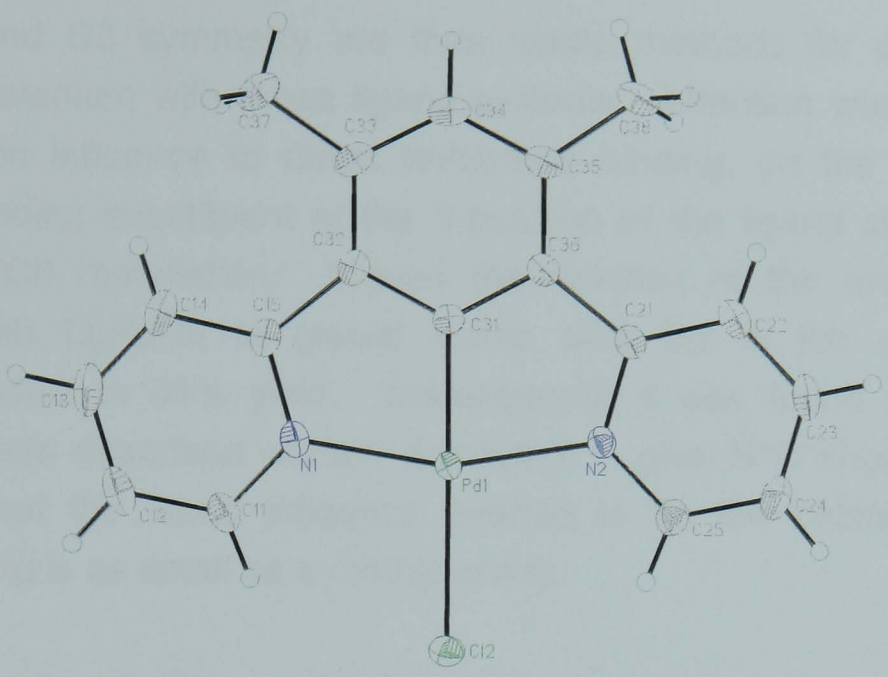

Figure 61: ORTEP diagram representative of the complex L^3PdCl, confirming the terdentate, N^C^N "pincer"-type binding mode of the ligand system with palladium. Pd(1)–C(31) 1.9173(15), Pd(1)–N(1) 2.0328(14), Pd(1)–N(2) 2.0321(13), Pd(1)–Cl(2) 2.4451(4) Å; C(31)–Pd–N(1) 80.52(6), C(31)–Pd-N(2) 80.78(6), N(1)–Pd–N(2) 161.29(6), C(31)–Pd–Cl(2) 178.27(5), C(31)–C(32)–C15 113.26(14)°.

HL^7 was also synthesised with a view to creating N^C^N coordinated palladium(II) complexes. The ligand has C_3 symmetry and displays three identical coordination sites, Scheme 22. By reacting Li_2PdCl_4 with HL^7 in a 1:1 ratio in acetic acid, the desired mono-nuclear palladium product was observed with similar changes in the ^1H NMR spectrum to that for L^3PdCl. Depotonation of the unbound nitrogen was required during the work-up, consistent with the behaviour observed for the platinum(II) derivative, Section 2.2.1.[222]

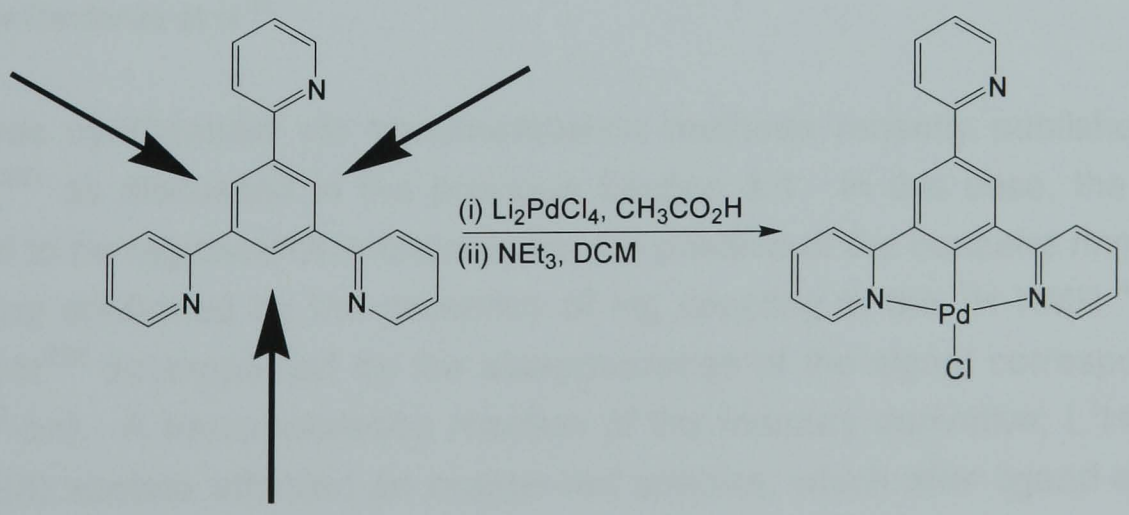

Scheme 22: C3 symmetry of the ligand HL^7 means that all ortho coordination sites are identical and should lead to N^C^N coordination. Direct cyclopalladation under standard conditions, followed by deprotonation, yielded the desired product.

Site blocking and C3 symmetry are thus viable methods for directing N^C^N metalation of palladium with these ligand systems. Attention was then turned to the use of steric influence to direct terdentate binding, on the grounds that a sterically demanding substituent at the 5-position of the ligand should inhibit the competitive C4/C6 metallation. Indeed the reaction of the mesityl-substituted ligand, HL^9, with Li_2PdCl_4 in glacial acetic acid led to the desired N^C^N-coordinated product in 31% yield. Subsequently it was found that all the C5-substituted ligands described earlier, Section 2.1, give N^C^N-palladation. The conclusion is that the steric influence needed to tip the balance in favour of terdentate binding is as small as a methyl group.

During the course of this research, direct cyclopalladation of the 1,3-di(2-pyridyl)benzene binding motif was published by a separate research group,[197] but it is not conclusive to whether their success is due to the nature of the palladium salt employed, as claimed, or a modification of the steric approach used here, Equation 9.

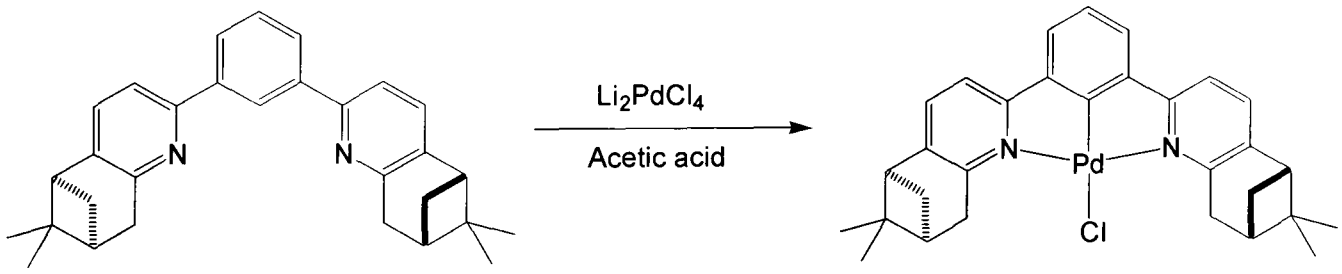

Equation 9: Direct N^C^N cyclopalladation of 1,3-di(2-pyridyl)benzene structure published by Stoccorro *et al.*[197] However, it is possible that steric incumberance of the chloride ligands, similar to that observed in this research, would disfavour formation of the bis-ortho complex previously observed by Cardenas et al.[66]

L^1PdCl was synthesised *via* transmetallation methods recently published in the literature,[252] as discussed in the previous Section 3.1. In this case, the reaction was found to be regioselective towards the C2 position of the benzene ring, binding again being confirmed by the presence of Hg coupling in the ^1H NMR $^4J(^{199}Hg–^1H) = 69$ Hz[252] accompanied by the disappearance of the signal corresponding to (1H, s, H^2-bn). A transmetalation reaction of the mercury derivative, L^1HgCl, with palladium(II) acetate afforded an orange-red species, which after ligand exchange induced by introduction of an excess of lithium chloride, gave the desired cyclometallated complex cleanly and in good yield, Equation 10.

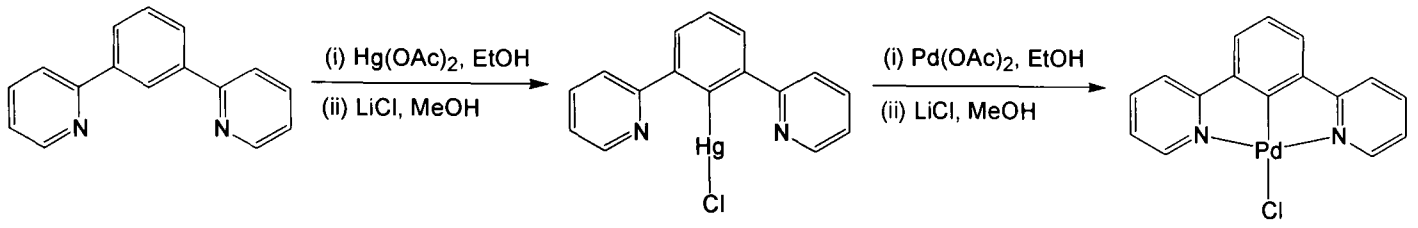

Equation 10: Regioselective cyclopalladation to form L^1PdCl, directed by transmetalation reaction of the Hg(II) intermediate, L^1HgCl.

Chloride ligand metathesis could easily be achieved *via* methods analogous to those developed for the platinum derivatives, Equation 11. Extraction of the chlorine atom with silver trifluoromethanesulfonate in acetone is then easily followed by replacement with the new ligand, *e.g.* N,N-dimethylamino-4-pyridine $[L^3Pd(DMAP)]OTf$. The change of ligand has a profound influence on the ^1H NMR spectrum of the N^C^N coordinating ligand. There is a dramatic shift to lower frequency in the resonance for H^6-py^1, $\Delta\delta$ 1.3 ppm, which can be rationalised in the same way as the platinum counterpart, by the deshielding nature of the halogen being replaced by the dimethylaminopyridine unit which gives the nearest H atoms shielding by being near the ring field of the heterocycle. Furthermore, deshielding of the remaining signals is indicative of the increased formal charge associated with the coordinated metal ion (H^3/H^4-py $\Delta\delta$ +0.3, H^5-py $\Delta\delta$ +0.2, H-bn $\Delta\delta$ +0.3 ppm). The coordination of the dimethylaminopyridine substituent, and which nitrogen is involved, is confirmed with through-space coupling in the ^1H–^1H NOESY NMR, between the *ortho*-protons from each pyridine, H^6-py^1 and H^2-py^2, respectively. There is no evidence of coordination through the dimethylamino fragment.

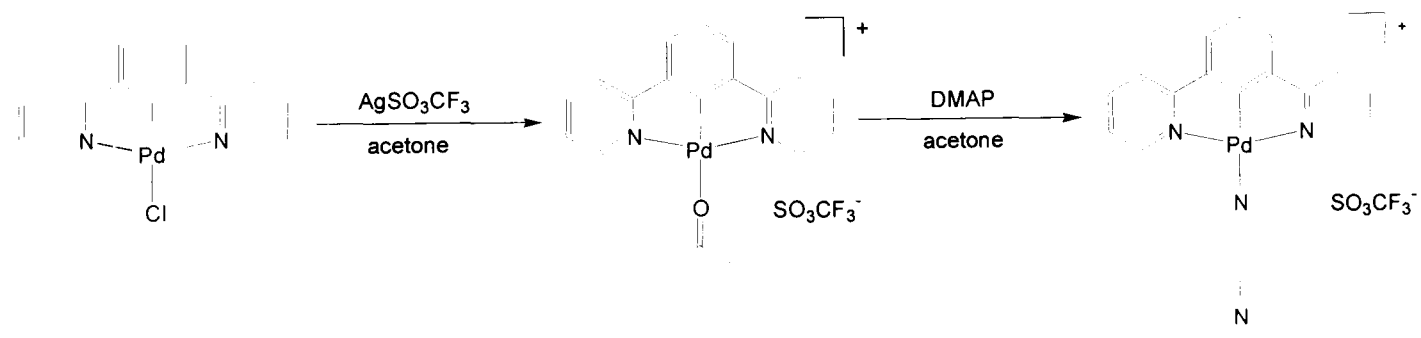

Equation 11: Chloride metathesis is readily achieved through simple silver mediated chloride abstraction followed by displacement of the weakly coordinating solvent with the desired new ligand, in this case 4-N,N-dimethylaminopyridine.

7.2. Photochemistry

The change from N^N^C to N^C^N coordination motif has already been shown, in the case of platinum(II) complexes, to be extremely successful in increasing the ligand field strength thus inducing a vast improvement in the effiency of phosphorescence.[74,222] Many examples of N^N^C coordinated palladium complexes have been investigated with attempts to induce luminescence in fluid, room temperature solutions,[52,75,155] all without significant success. The failure of such systems has been attributed to low-lying metal centred states, similar to those that plagued platinum(II) photochemistry. By reducing the cyclometalating bond length it was again envisaged that the energy of the metal centred excited-states could be raised so promoting luminescence over non-radiative decay. Previously, N^C^N coordinating ligands have been shown to induce solution state luminescence from palladium complexes, albeit extremely weak.[147]

Unfortunately, the series of palladium complexes, L^nPdCl (n = 1, 2, 3, 6 – 9, 16) were found to be non-emissive in fluid solutions at room temperature. Clearly, non-radiative deactivation is still too fast at RT, presumably because the d-d states remain too low in energy. No investigations have been made into solid state emissive properties at room temperature (the compounds appear non-emissive to the naked eye under irradiation from a UV-source, λ_{ex} = 365 nm). However, all complexes are emissive in a rigid glass (diethyl ether:isopentane:ethanol 2:2:1 v/v) at 77 K. Complete photophysical data of the palladium series of complexes are shown in Table 4.

Complex	Substituent	Absorbance λ_{max} / nm (ε / L mol^{-1} cm^{-1})	Emission λ_{max} / nm	τ_0 / µs
L^1PtCl	H	328 (5620), 353 (5950), 370 (7740)	466, 503, 531	175
L^2PtCl	Methyl	327 (5670), 363 (6460), 381 (8820)	474, 510, 540	177
L^3PtCl	Xylene[a]	337 (9220), 351 (8220), 369 (8160)	469, 504, 535	201
L^6PtCl	Bromo	323 (5930), 365 (7220), 383 (10610)	470, 507, 537	162
L^7PtCl	Pyridine	326 (6640), 365 (5620), 382 (7560)	478, 505, 540	153
L^8PtCl	Tolyl	325 (5880), 371 (6630), 385 (7030)	481, 516, 552	162
L^9PtCl	Mesityl	314 (6260), 327 (4530), 362 (4330), 379 (5860)	470, 506, 536	170
$L^{16}PtCl$	Dimethylaniline	315 (23310), 392 (5140)	527, 564, 616	264
$[L^{16}PtCl]H^+$	[Dimethylaniline]H^+	324 (6360), 360 (5390), 378 (6530)	476, 510, 543	-
$[L^3Pt(DMAP)]SO_3CF_3$	Xylene[a]-DMAP		469, 504, 533 556[b]	-

Table 4: UV-vis absorption data measured in DCM at 295 K, except where otherwise stated. Emission data recorded in EPA glass (diethyl ether:isopentane:ethanol [2:2:1 (v/v) respectively) at 77 K, lex = 370 nm. Lifetime data recorded in EPA glass at 77 K, lex = 374 nm. a Xylene abbreviation represents the ligand 4,6-di(2-pyridyl)-m-xylene. b Emission represents the maximum from the multicomponent emission recorded at high concentration.

7.2.1. Absorbance

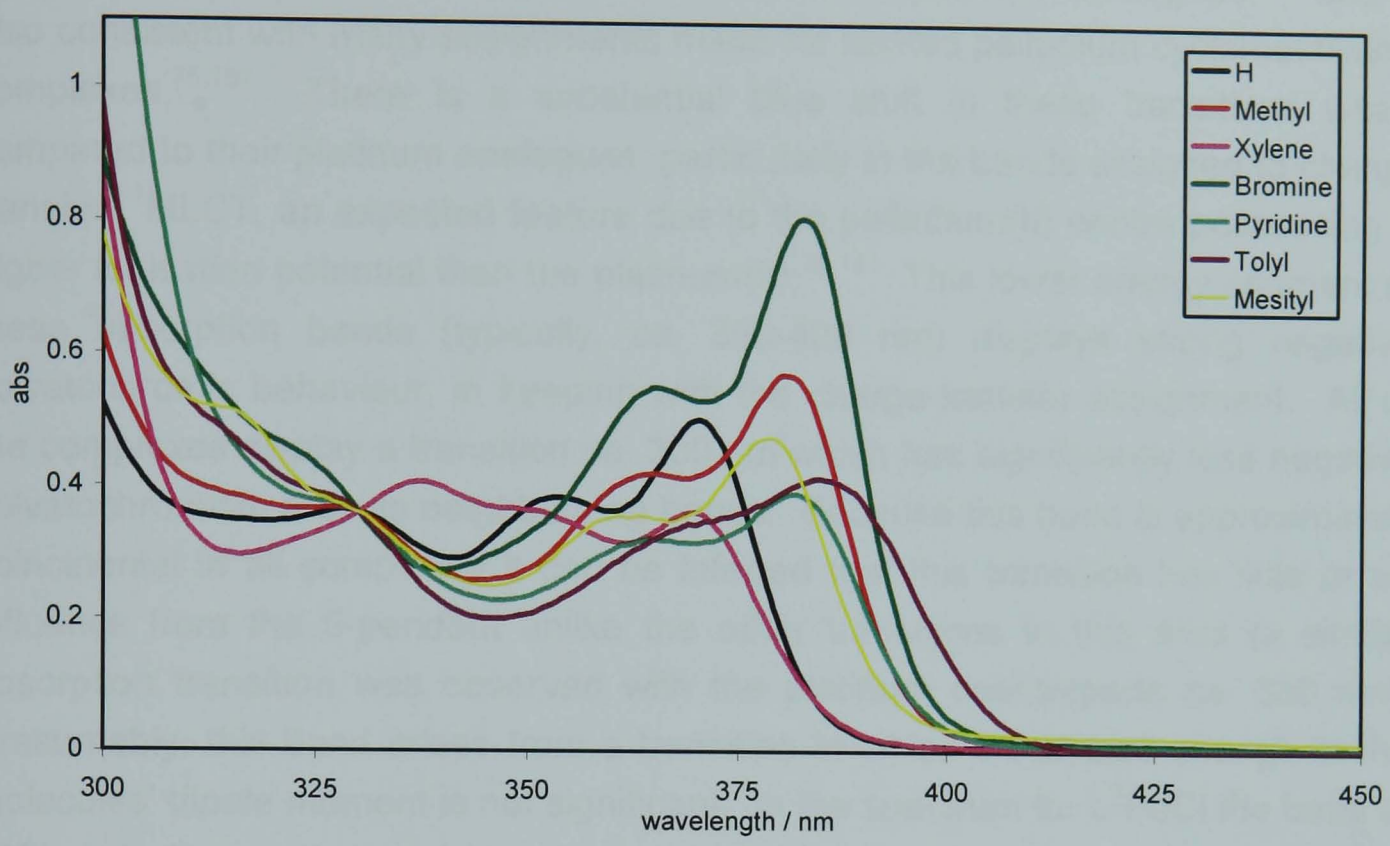

Figure 62: UV-Vis absorption profiles of L^nPdCl (n = 1, 2, 3, 6 – 9, 16) in DCM at room temperature. Spectra are normalised at 330 nm

All complexes show several high-energy intense absorptions below 300 nm (ε = 21,000–46,000 L mol^{-1} cm^{-1} in DCM) that are assigned to metal perturbed ligand-centered transitions (π–π^*) of the aromatic N^C^N coordinating ligand. The extinction coefficients (ε) of these bands increase concurrently with the conjugation associated with attaching a large aromatic substituent to the pendant position of the palladium complex. This feature is best exemplified by the difference between the non-conjugated R = H, L^1PdCl (283 nm, ε = 21,000 L mol^{-1} cm^{-1}), the strongly-conjugated R = *p*-tolyl L^8PdCl (283 nm, ε = 43,000 L mol^{-1} cm^{-1}) and the weakly conjugated R = mesityl L^9PdCl (283 nm, ε = 24,000 L mol^{-1} cm^{-1}).

The lower energy components of the absorption spectra for the complexes L^nPdCl (n = 1, 2, 3, 6–9) are shown in Figure 62, while the N,N-dimethylaniline substituted complex, $L^{16}PtCl$, exhibits an absorption spectrum that is significantly different from the rest of the series and will be presented and discussed later. The complexes exhibit less intense transitions than those below 300 nm at lower energy (300–400 nm ε = 5,000–9,000 L mol^{-1} cm^{-1} in DCM). Interpretation of this section is complicated by the fact that this region is clearly comprised of more than one

transitions of the most red shifted complexes effectively hide the presence of these spin forbidden transitions, as is the case for L^8PdCl and $L^{11}PdCl$.

7.2.2. Emission

All of the palladium complexes are luminescent in EPA glass at 77 K, but none of the compounds appear to be emissive above that temperature, with the exception of $[L^3Pd(DMAP)]OTf$. There is a clear transition observed upon the freezing of the EPA solvent, where luminescence is suddenly "switched on" during the phase transition, and there is essentially complete quenching of the emission when they are warmed back through the glass transition temperature. The lack of room-temperature luminescence of these palladium complexes is not surprising since mononuclear palladium complexes displaying this type of luminescence are very rare, usually attributed to the presence of low-lying MC states.[150,151,154,155] While the cyclometallated approach alone has not been sufficient for inducing luminescence from palladium compounds, further research into pincer induced cyclometalation of palladium complexes coupled with low-energy ILCT transitions, similar to that utilised by McMillan for platinum terpyridine systems, could be rewarding.[42]

The emission data for all the complexes are summarised in Table 4 and representative spectra are shown in Figure 63–Figure 67. Excitation spectra of all the complexes at 77 K are similar to the RT absorption profiles of the complexes with coincidental peak maxima, however, at 77 K where better resolution of band structure is frequently noted, the peaks are sharper and more defined. Total confirmation was achieved through absorption spectra recorded at 77 K for L^1PdCl, where a sudden sharpening in the spectral profile accompanies the movement through the glass transition of the solvent.[160] The emission results for the bromo, dimethylamino substituted complexes, and 4-N,N-dimethylaminopyridine ancillary complex, L^6PdCl, $L^{16}PdCl$, and $[L^3Pd(DMAP)]OTf$ respectively, are anomalous and will be discussed separately.

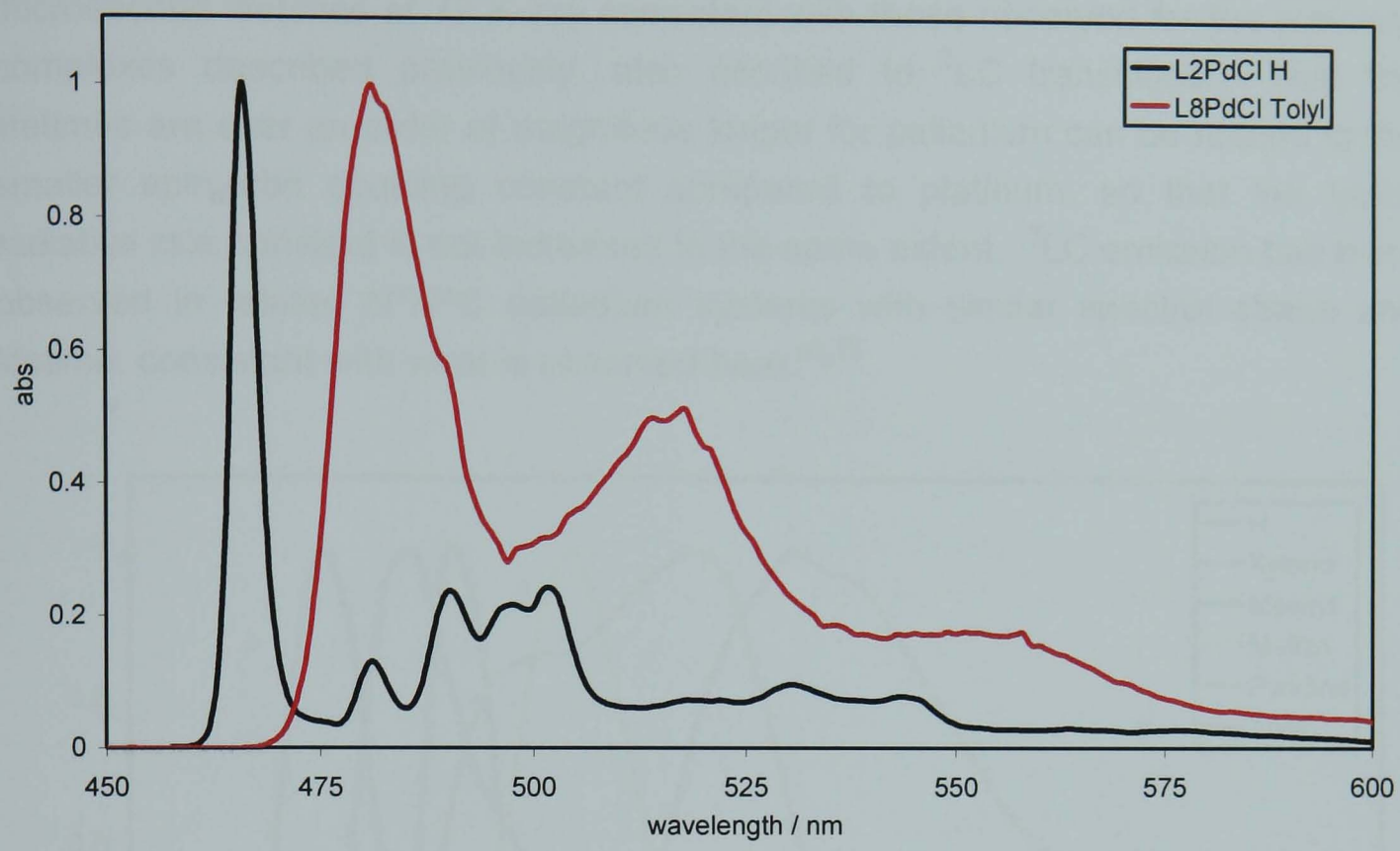

Figure 63: Emission data for L^1PdCl and L^8PdCl, both in EPA at 77 K, λ_{ex} = 380 nm. Bands become broader with less detail upon increasing aromaticity of the N^C^N ligand, where an increase in the number of possible energy conformations is available through rotation of the 5-substituent.

The emission spectra at 77 K in rigid matrix are highly structured, with vibronic progressions *ca.* 1400 cm^{-1} characteristic of breathing modes of the aromatic ligand framework, similar to other phenyl pyridine based complexes,[74,222] and typical of ^{3}LC emission observed in similar palladium complexes.[57,155] For all the palladium complexes, the lifetime decays of the high-energy band measured at each vibronic peak maximum are in the range of 100–200 μs indicative of triplet natured metal complex phosphorescence. The highest intensity transition is also the one of highest energy (0-0 transition), indicating limited geometrical change occurring between the excited- and ground-states. Upon ligand substitution from H to larger aromatic groups, the free-rotation about the 5-position creates an increased number of available energy transitions, highlighted by the difference between the spectra for L^1PdCl and L^8PdCl shown in Figure 63, where the emission profile changes from one containing predominantly sharp vibrational detail to a spectrum containing broad sweeping bands. This feature is further exemplified by the reduced degree of rotation available to the sterically hindered mesityl substituted complex, L^9PdCl, and thus, this spectrum contains structure more similar to that of the unsubstituted system. The structured luminescence and

microsecond lifetimes at 77 K are consistent with those observed for the platinum complexes described previously, also ascribed to ^{3}LC transitions. That the lifetimes are over an order of magnitude longer for palladium can be related to the smaller spin-orbit coupling constant compared to platinum, so that the triplet radiative rate constant is not increased to the same extent. ^{3}LC emission has been observed in related N^N^C palladium systems with similar spectral shape and lifetime, consistant with what is observed here.[52,75]

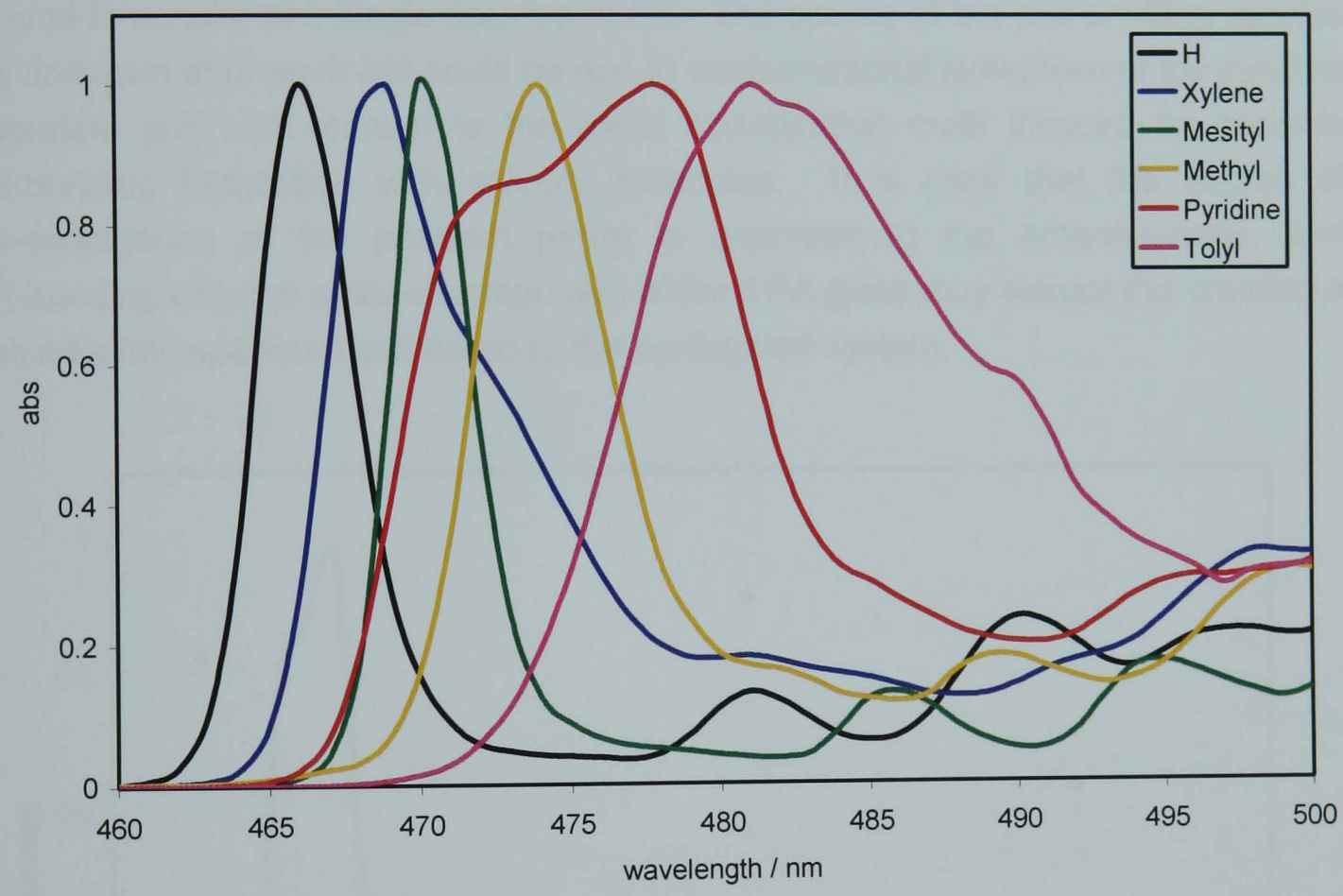

Figure 64: L^{n}PdCl (n = 1 – 3, 7 – 9) in EPA at 77 K. Observed red shift in emission observed by change in functionality of cyclometalating benzene ring.

The emission maxima for each complex are red shifted in the order of H < xylene < mesityl < methyl < pyridine < tolyl and can be rationalised with the same argument used to describe the tuning of luminescence of the platinum analogues, namely the electron-donating ability of the 5-pendant substituent. This lowers the energy of the ^{3}LC transition by predominantly raising the energy of the HOMO. This effect is the strongest with the electron-donating, highly conjugated *p*-tolyl substituent and much less so for the sterically hindered mesityl substituent, Figure 64.

Interestingly, at 77 K the luminescence spectrum of L^7PdCl displays two emission profiles with separate vibronic progressions separated by 400 cm^{-1}, Figure 65. A similar effect has been observed for (phpy)Pt(acac) complexes at 77 K.[46] While the spectra could be explained as being due to two vibronic progessions on a single electronic transition, different excitation spectra suggest that this is not the case. Therefore, the best explanation for the low-temperature spectrum of this complex is the appearance of two different emitting species in the low temperature glass; however, the complex was carefully examined by ^1H NMR spectroscopy and found to consist of a single species at RT. The source of the two emitting species is unknown at present but could be due to conformational isomerism of the pyridine pendant unit with respect to the metal coordination motif induced by possible H-bonding interaction with solvent molecules. It is clear that the degree of π-conjugation of the pendant group is important to the emissive-state, and H-bonding with the ethanol component of the EPA glass may disrupt this creating a blue shifted spectrum compared to the conjugated system.

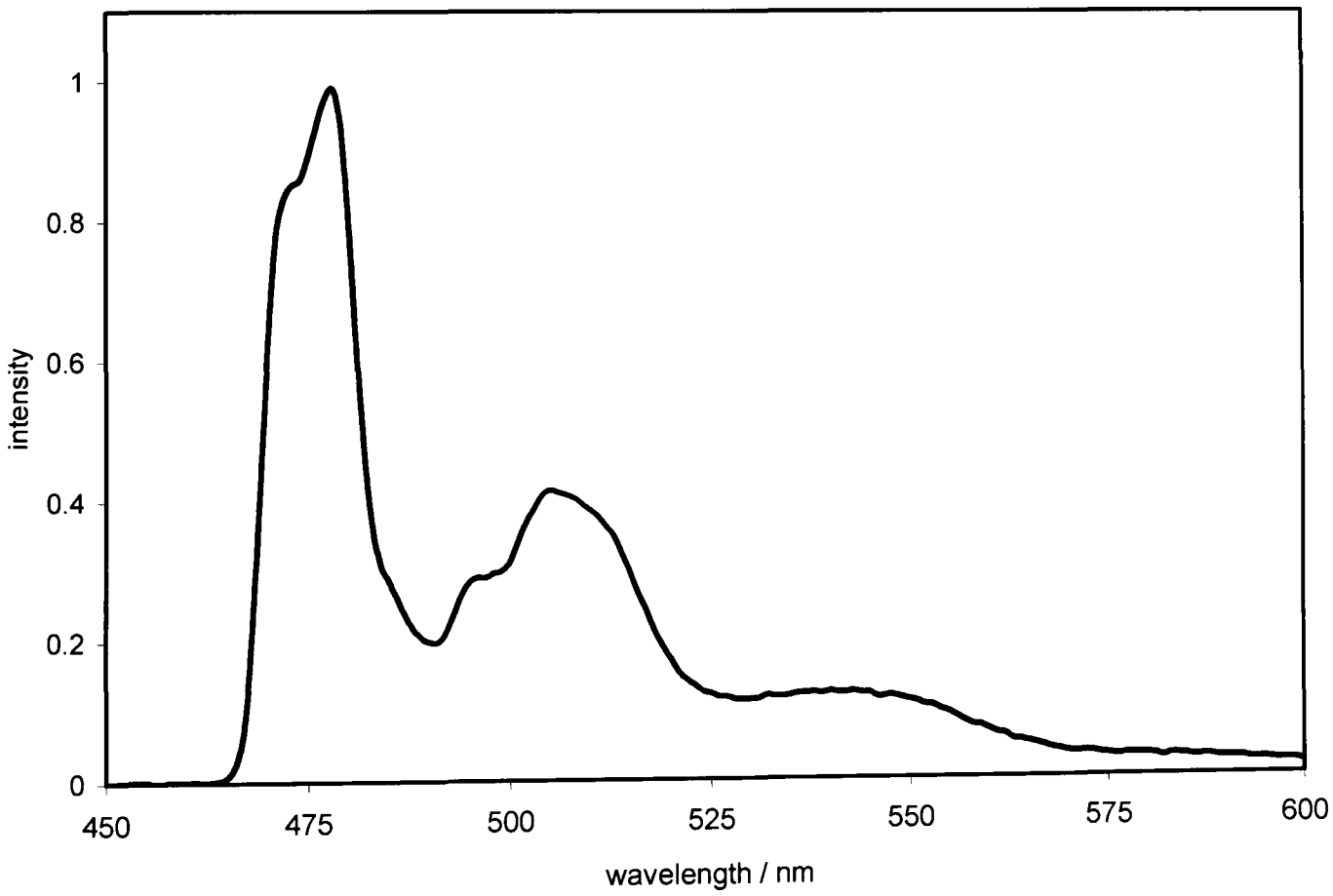

Figure 65: Emission spectrum of 5-(2-pyridyl)-substituted palladium complex, L^7PdCl, in EPA at 77 K, λ_{ex} = 380 nm. Clearly, the spectrum shows two separate vibrational progressions, which have been attributed to H-bonding of the uncoordinated pyridine pendant of L^7PdCl.

7.2.3. L^6PdCl, Bromo functionalised complex

The pendant bromine atom has a slightly stabilising effect on the ^{1}MLCT absorption transition, with an effect somewhere between the electron-donating properties of 5-position subsituents methyl and tolyl. The participation of a lone pair of electrons occupying the p-obrital in-plane with the conjugated π-bonding system of the aromatic ligand raises the energy of the HOMO indicated in the red shift in the absorbance spectra with respect to hydrogen, L^1PdCl. The bromine's p-orbital electrons are donated by resonance with the conjugated N^C^N system and this appears to outweigh its inductive electron-withdrawing character.

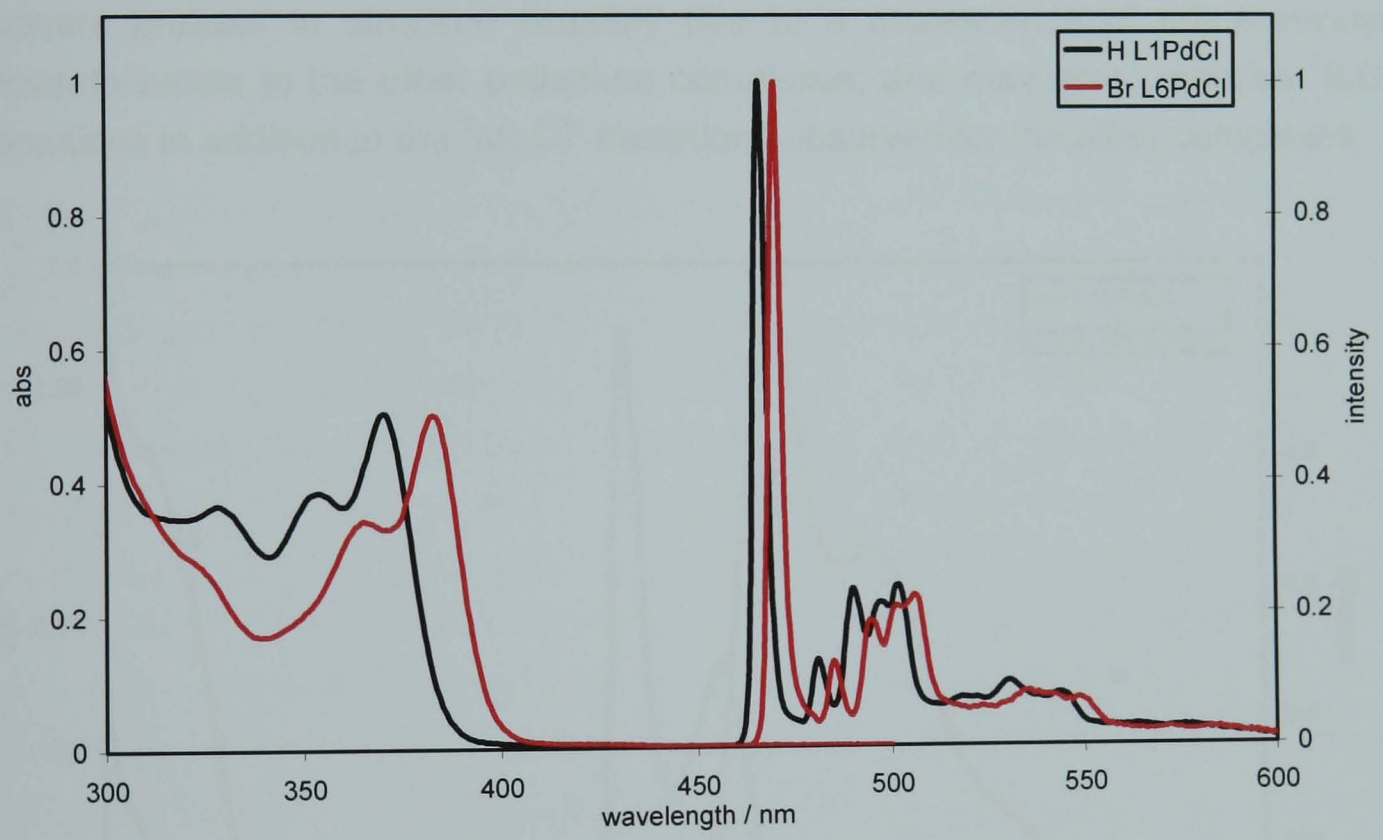

Figure 66: Uv-vis and emission profiles for complexes L^1PdCl and L^6PdCl in DCM and EPA (2:2:1 v/v diethyl ether: isopentane: ethanol) at room temperature and 77 K respectively.

The effect of the bromine atom in the emission spectrum is less pronounced than that observed in the absorption spectrum, $\Delta\lambda_{max}$ = 13 nm and 4 nm in absorption and emission respectively compared to L^1PdCl. This may be explained by the different effects the bromo has upon the relative transitions involved. While the bromine atom, positioned *para* with respect to the coordinated metal centre, is ideally positioned to influence the ^{1}MLCT transition, the position *meta* to the pyridyl units limits the resonance influence upon the ^{3}LC transition. Therefore, the balance of electron-withdrawing/-donating inductive/resonance effects is different

for the two transitions. In both transitions the bromine atom is considered to be electron-donating with respect to hydrogen, $L^{1}PdCl$, yet this effect is greater in the $^{1}MLCT$ transition, Figure 66.

7.2.4. $L^{16}PdCl$, N,N-dimethylaniline pendant complex

The absorption spectrum of the dimethylaniline-substituted complex, $L^{16}PdCl$, is shown in Figure 67. In the 300–330 nm region the complex displays intense absorption bands attributed to n-π* transitions involving the dimethylamine fragment. The low energy envelope, 350–400 nm, is significantly red shifted, as expected for the donating nature of the amine substituent; additionally, the band appears broader in structure possibly due to a coalescence of the previously separate bands in the other palladium complexes, and may also comprise $^{1}ILCT$ transitions in addition to the $^{1}MLCT$ transitions observed for the other complexes.

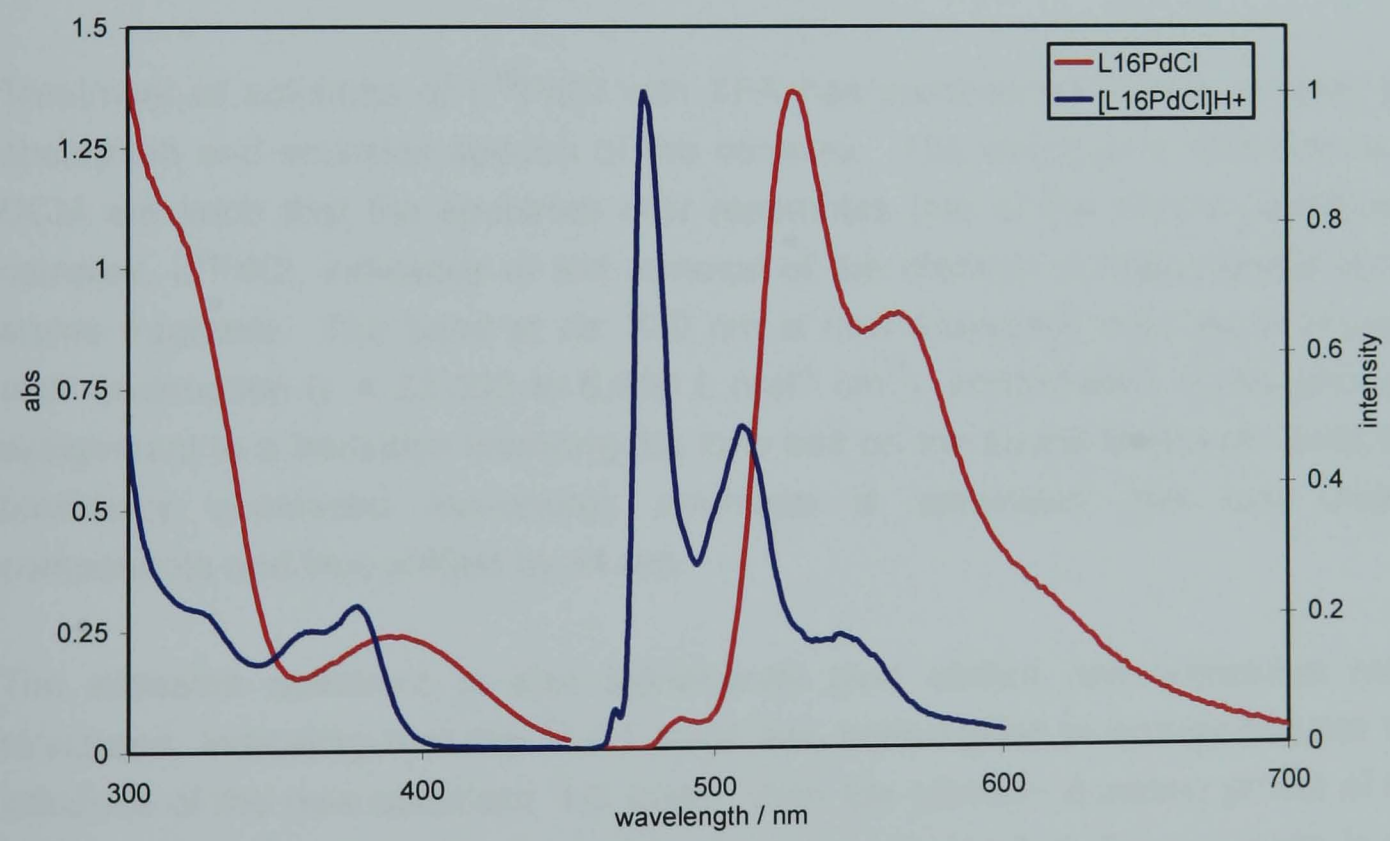

Figure 67: UV-Vis absorbance spectra in DCM at 295 K; and emission spectra recorded in frozen EPA glass (2:2:1 (v/v) diethyl ether:isopentane:ethanol) at 77 K, λ_{ex} = 400 and 370 nm respectively, before and after the addition of trifluoroacetic acid.

The emission spectrum remains structured, yet significantly red shifted, by almost 50 nm when compared to the tolyl-substituted complex, $L^{8}PdCl$, the previously most red-shifted complex in the series. The significant red shift, coupled with the

behaviour observed upon protonation, discussed below, leads to a tentative assignment of mixed excited-state origin of both ^{3}LC and ^{3}ILCT. This mixing of excited-states due to their relative closeness energetically has been observed in other cyclometallated palladium complexes[161] as well as similar behaviour for the analogous platinum(II) complex, Section 2.3.2.3. It is thought that the solvent employed plays a significant part in the energy associated with the charge transfer state; as shown in Figure 28, the ^{3}ILCT excited-state is stabilised in polar solvents and dominates the emission of the complex, while in non-polar solvent the charge transfer state is no longer lower in energy than the ^{3}LC state. The polarity of the EPA solvent is sufficient to lower the energy of the ^{3}ILCT state so that there is sufficient mixing between the two states so that while being strongly red shifted, broad, and relatively long lived (τ_0 = 264 μs), typically all features of charge transfer states, the emission is also highly structured, typically a feature of ligand centred emission. This mid-point behaviour is observed for the platinum analogue in similar mid-polarity solvents, Figure 33.

Treatment of solutions of L^{16}PdCl with TFA has pronounced effects on both the absorption and emission spectra of the complex. The changes in absorbance in DCM are such that the spectrum now resembles that of the mesityl substituted complex, L^{9}PdCl, indicative of the removal of the electron donating ability of the amine fragment. The band at *ca.* 330 nm is now drastically reduced in strength after protonation (ε = 23,000 to 6,000 L mol^{-1} cm^{-1}), confirmation of the previous assignment to a transition involving the lone pair on the amine fragment. Also, the previously coalesced low-energy envelope is separated into two distinct components and blue shifted by 14 nm.

The emission spectrum is also significantly blue shifted and somewhat more structured, indicating that the ^{3}ILCT state has been raised in energy beyond the influence of the now dominant ^{3}LC state. With the electron donating power of the amine completely removed, the most prominent influence on the spectrum is the extension of conjugation provided by the phenyl spacer unit, with the slight electron withdrawing effect of the protonated amine. The highest intensity component of the emissive band is consistent with this feature, λ_{em} = 476 nm now slightly blue shifted with respect to L^{7}PdCl.

7.2.5. [L^{3}Pd(DMAP)]OTf

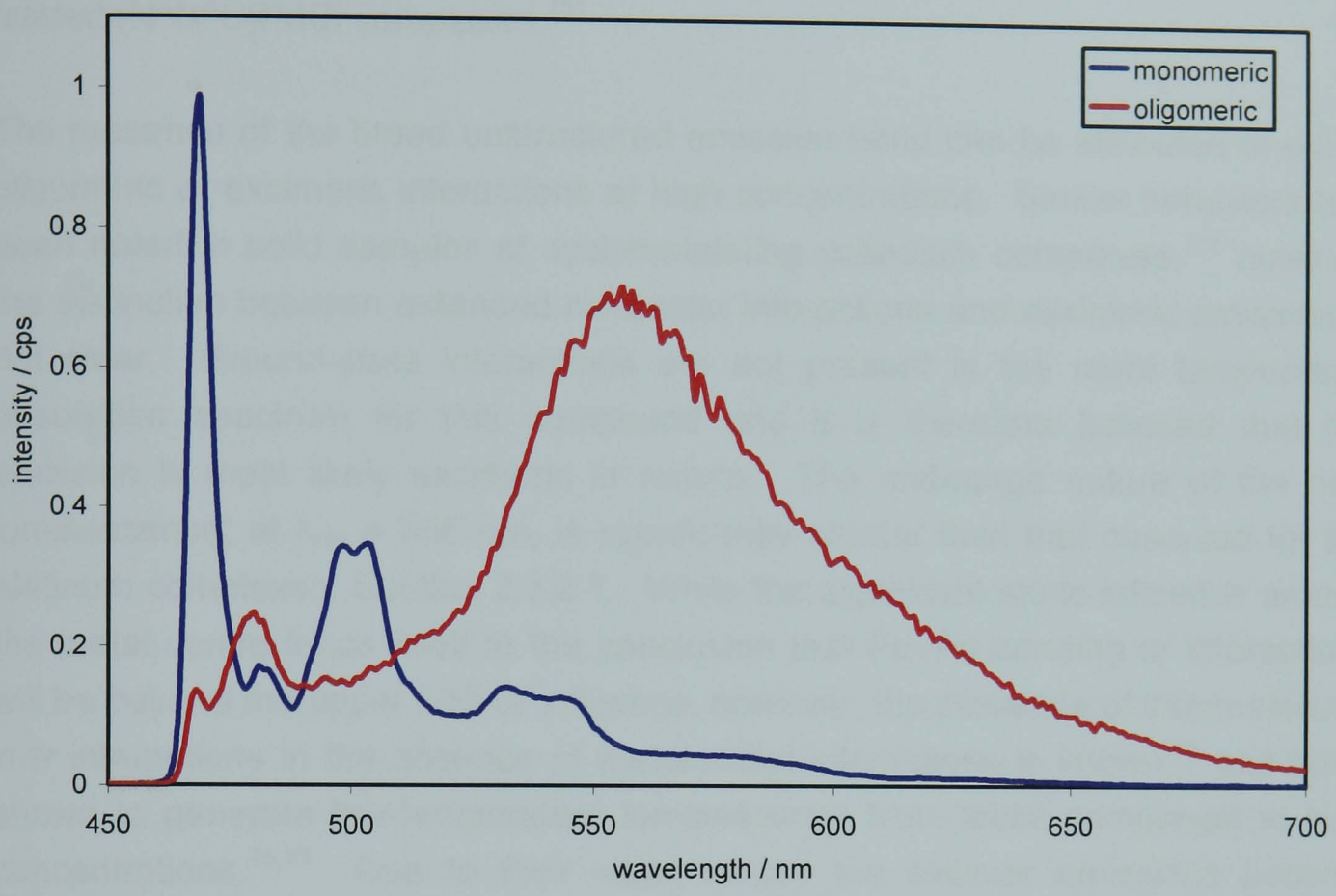

Figure 68: Luminescence spectra of [L^{3}Pd(DMAP)]SO_3CF_3 in dilute and saturated concentrations of EPA solutions measured at 77 K, λ_{ex} = 370 nm. The broad unstructured band displayed by the concentrated sample persisted at temperatures above the solvent's glass transition temperature.

In the absorption spectrum of [L^{3}Pd(DMAP)]SO_3CF_3 the energy of the ^{1}MLCT band is blue shifted in keeping with the increased difficulty in oxidising the metal centre now bearing a formal charge.

The emission spectrum in dilute conditions is consistent with that of its parent complex, L^{3}PdCl, with essentially identical peak maxima. Significantly, similar to the platinum complexes, the emissive nature of the complex shows little effect from ancillary ligand substitution, Section 6.2.2. However, at high concentrations, the emission profile displays significant changes clearly representing a different electronic transition, characteristic of multi-component luminescence. A concentrated solution gives a relatively broad unstructured peak (fwhm = 2050 cm^{-1}) at 556 nm, which develops at the expense of the high-energy vibronic emission at 469 nm. Additionally, as the sample is warmed through the glass-transition, the emission profile from the broad band persists, while the

monomeric type emission observed in dilute solutions is only activated after freezing of the EPA solvent. Similar red shifts in emission have been observed for related (N^N^C)PdCl complexes.[151]

The presence of the broad unstructured emission band can be attributed to either oligomeric or excimeric interactions at high concentrations. Similar behaviour has been noted in solid samples of cyclometalating palladium complexes,[151] however the distinction between extended molecular interactions and excimeric emission is not clear. Ground-state interactions are not present in the room temperature absorption spectrum for this compound and it is therefore believed that the emission is most likely excimeric in nature. The mid-range nature of the new luminescence, at λ_{em} = 556 nm, is significantly shorter than that observed for the platinum complexes, Section 2.3.2.1. While the significant steric influence around the metal centre lends itself to the conclusion that Pd–Pd bonding or interactions will be beyond the upper limit of influence, however, the presence of intermolecular π-π interactions in the absence of metal-metal interactions is known,[56] and been shown to generate low-temperature luminescence from metal complexes at high concentrations.[75,79] Due to their weak nature the excimer emissions become destabilised at increasing temperatures as these interactions become less favourable and so the complex is non-emissive at 298 K.

The fact that this type of emission is observed for $[L^3Pd(DMAP)]SO_3CF_3$ and not the chloride ancillary ligands is attributed to their relative insolubility in the EPA solvent.

7.3. Catalysis

The so called "pincer" ligands have attracted vast attention as catalytic species, Section 1.2.3, with fierce arguments to their mode of action as either active centres or precatalytic by-standers. Particular attention has been paid to the Heck cross-coupling reaction, Scheme 3, which provides an effective route for the coupling of a suitable aryl halide to an olefin through formation of a new C–C bond between the two sp^2 carbons. Due to its wide scope and enormous synthetic potential, this reaction is often examined as the benchmark for testing and comparing the relative activities of new catalytic systems.

Pincer-type systems containing mulitdentate N ligands have received significantly less attention compared to phosphorus and sulfur donor systems, and usually focused upon sp^3 donor nitrogens. However, among their many advantages are listed exceptional thermal stability and the potential to produce systems with high TONs (turnover numbers = moles of product produced per moles of catalyst). Specifically in the context of this work, the N^C^N coordinated palladium complex L^1PdCl has been identified as a high performance catalyst in the Heck coupling of iodobenzene and methyl acrylate. Under microwave heating turnover numbers as high as 280,000 h^{-1} have been observed for this complex.[252] In view of these promising results, it was deemed interesting to examine the catalytic activity of the palladium complexes developed in this body of work. Particularly, since it has been demonstrated that the ligand systems employed here offer the ability to electronically tune the coordinated metal-centre through modification of the ligand substituents on the cyclometallated benzene ring, Sections 2.2.4 and 7.2. It has been commented upon that if, as expected, oxidative addition of the aryl halide bond is the rate limiting step in the catalytic cycle, increasing nucleophilicity of the metal centre should yield catalytic species with increased activity, and also potentially unlock aryl-bromide and -chloride compounds as potential reagents in this key synthetic protocol.

All of the palladium complexes examined here L^nPdCl (n = 1–3, 6–9, 16) were efficient catalysts when used in the Heck coupling between iodobenzene and methyl acrylate. For comparative purposes, the experiments were run in parallel at 140 °C, at a substrate to Pd ratio of 0.025 mol%, and measured at specific timed intervals. The progress of each reaction was monitored by ^1H NMR through use of a known quantity of internal standard, di(ethylene glycol) dibutyl ether, the results of which are displayed in Figure 69. In all cases the reactions are completely diastereoselective and methyl *trans*-cinnamate is obtained as the exclusive reaction product; no *cis*-cinnamate is detected by ^1H NMR experiments on the reaction mixture. No apparent precipitation of palladium was noticed during the reaction, and the solutions at the end of each experiment were always clear and transparent. Surprisingly, but not uniquely, the catalysts remained active with the apparatus open to air;[61] lack of careful exclusion of air and water provided no loss in catalytic performance, selectivities or yields.[146] The catalyst remains highly active after the reaction is complete, and upon addition of more substrates catalysis is resumed, leading to the coupling product in essentially the same yield.

The fact that a reaction mixture retains activity throughout several cycles provides evidence for the stability of the system and shows its potential use for recycling experiments.

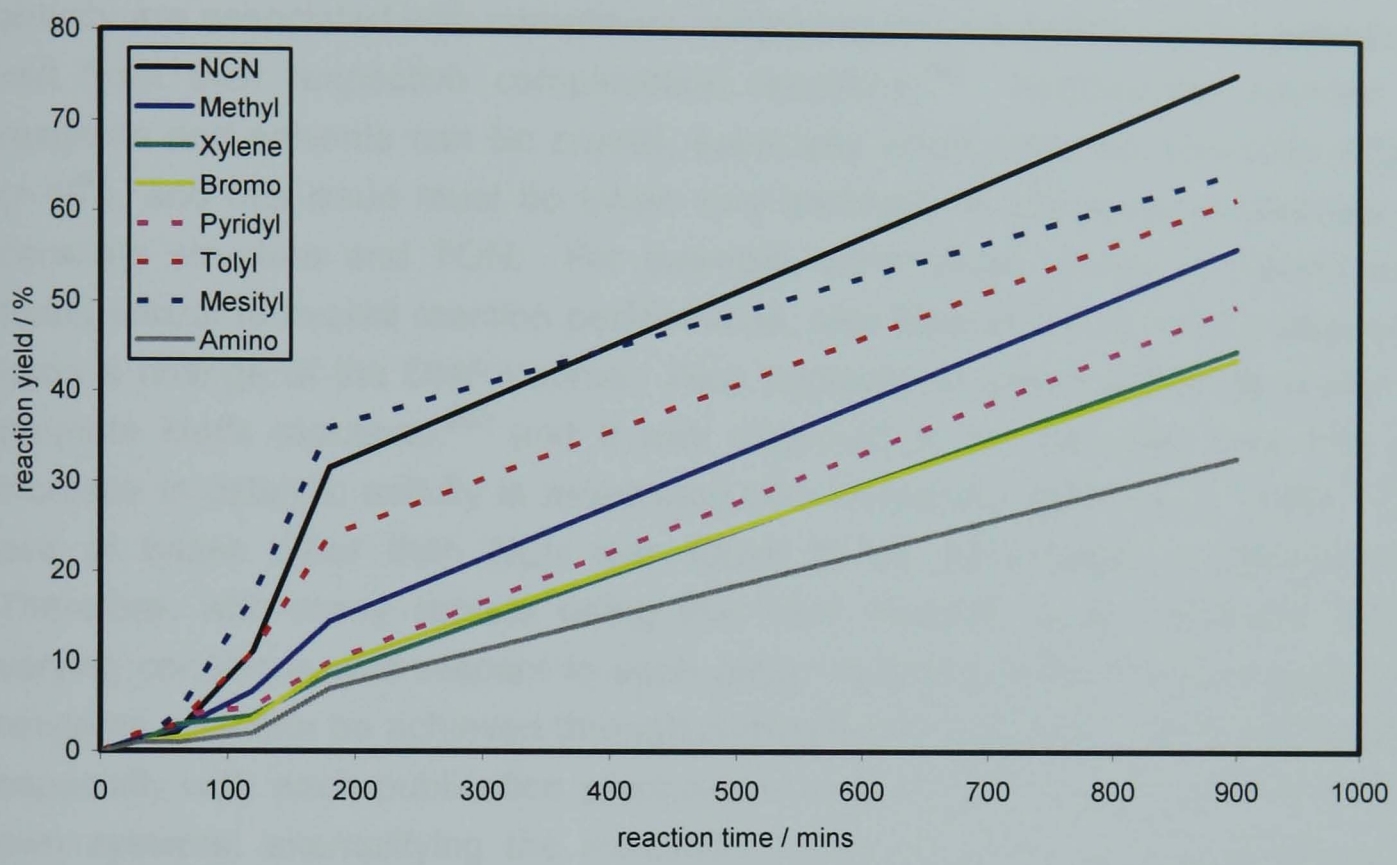

Figure 69: Catalytic activity of the palladium complexes, L^nPdCl (n = 1–3, 6–9, 16), in the Heck cross-coupling reaction between iodobenzene and methyl acrylate. Reaction conditions: triethylamine (2.2 mmol), iodobenzene (2.0 mmol), methyl acrylate (2.8 mmol), internal standard di(ethylene glycol) dibutyl ether (1.0 mmol), and palladium catalyst (5×10^{-4} mmol, 0.025 mol%) in DMF (5 mL) at 140 °C. Reactions monitored via removal of small aliquots from the reaction, reduced in vacuo, dissolved in $CDCl_3$ for ^1H NMR analysis. Relative peak intensities compared to those of known internal standard, di(ethylene glycol) dibutyl ether. Dotted lines indicate data obtained for complexes which did not posses the complement of precise elemental analysis data, and therefore data may not be taken as accurate.

Unfortunately, the high performance TONs associated with the parent complex, L^1PdCl,[252] could not be reproduced. Although, for a specific system, high TONs and TOFs can be achieved through selection of correct conditions, including reaction time and catalyst loadings (for example, a catalyst's TON can easily be increased by reducing loadings and elongating reaction times, while TOF is somewhat more difficult to optimise), variations made to the experimental parameters failed to yield similar values to those previously reported. Over the course of this work it has been noted that the catalytic activity of the complexes is

extremely sensitive to minor environmental factors. When catalysts are used at very low loadings, the issue of reproducibility must be addressed, as it is likely that even traces of impurities in the solvent or reagents will affect the maximum TON. This was particularly noted with the purity of the catalysts, where vast increases in activity are associated with complexes containing trace quantities of the palladium salt from their respective complexation reactions.[292] Additionally, sources of reagents and solvents can be crucial, especially when trying for ultra-high TONs ($> 10^6$), and this issue must be taken very seriously in any study in attempts to correlate structure and TON. For example, commercial source of solvent was found critical to overall reaction performance, with fluctuations in activity observed upon a change of the DMF source. Also, increase in water content is known to promote Heck reactions,[200] and it was observed to be the case here that an increase in catalytic activity is associated with increasing additions of water. The use of bases other than NEt_3 was found to be detrimental to performance. Therefore, with many reports using the Heck reaction often performed under varying conditions with respect to each other, including solvent, temperature and reagents, little can be achieved through comparison of systems in different reports, especially with each publication preoccupied with establishing the merits of their own systems, exemplifying the maximum turnovers of the specific compounds explored and only in some footnotes can one find hints where reproducibility has indeed been an issue.[190]

As a general trend, the complexes containing chloride as the ancillary ligand are quite close in activity, whilst experiments run using [L^3Pd(DMAP)]OTf appeared completely inactive under identical conditions. This result is in keeping with the idea that a nucleophilic metal-centre is required to increase oxidative addition, where prior dissociation to a cationic centre is detrimental to this process. However, contradictory reports have also been found in literature.[174]

The observed reactivity trend of the chloride complexes could be considered in terms of the electron density of the metal. If the rate determing step of the Heck reaction is the oxidative addition of the halide, as is thought likely by numerous authors,[175,197] one common aspect of all pincer metal complexes is the high electron density on the metal centre. The nucleophilic behaviour of these complexes results from the monoanionic coordination of the ligand and the strong electron donating carbanion of N^C^N systems. Although *para* substituents have

been observed to influence the catalytically active centre,[262,293] with oxidative addition of the aryl-I bond to the metal expected to be facilitated by increased electron density at the metal centre, the data observed are the opposite to what is expected to fit this as the rate-determining step. Either a subsequent rate determining step with different electronic requirements, such as olefin insertion proposed by Shaw, may account for this observation; or the increasing *trans*-influence on the ancillary ligand from the more donating complexes may increase competitive ancillary ligand dissociation. This dissociation is precisely what is believed detrimental to the activity of [L^3Pd(DMAP)]OTf.

However, in light of the results obtained here and following perusal of the literature, it is believed that the activity of the catalytic species in the Heck reaction is a complex mixture of many factors. The Heck reaction is a flexible methodology, and it is thought to be able to adopt different reaction mechanisms according to conditions.[174] Increasing electron density at the metal may be important in controlling the formation of a Pd(IV) octahedral intermediate through aryl-halide insertion. However, when this pathway is in competition with (in this case) chloride dissociation to a species of reduced activity, increased donating ability of pendant groups can become detrimental to the desired goal, Scheme 23. Additionally, an increase in activity associated with the electron density may be offset by steric impediments, similarly observed through functionalisation through the pyridine donors.[197,293] While the possibility of pyridine donor dissociation could aid the stabilisation of catalytic intermediates,[201,202] such as forming an octahedral palladium complex, the sterics associated with the pyridyl rings in this instance are somewhat dismissive of this process being advantageous to a catalytic process.

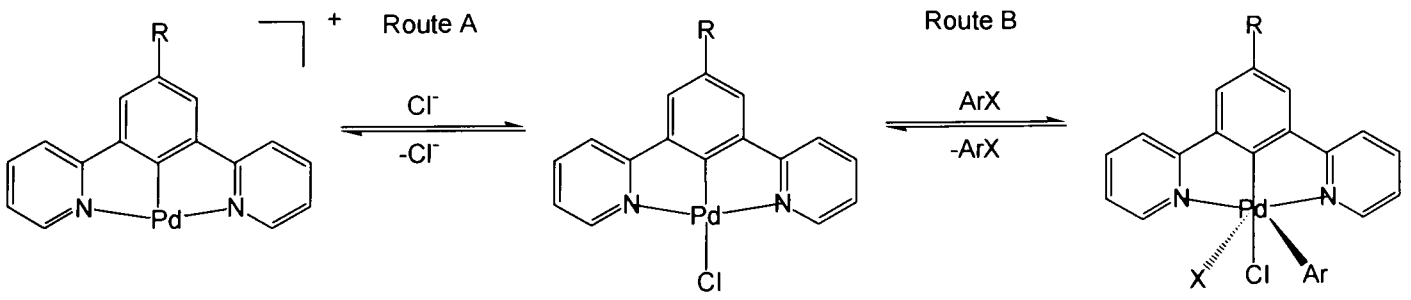

Scheme 23: Competitive modes of action for the N^C^N palladium complexes. Assuming the complex is itself the active species, Route B being the catalytic cycle, Route A is thought to be generating a non- or reduced activity species detrimental to the reaction efficiency.

Contrary to the discussion above there is no conclusive evidence for the activity of the metal complexes as discrete units. The clear presence of an induction period detected in the reaction slopes of all the complexes insinuates their activity as simple reservoirs of colloidal palladium, leaching active metal into the solution at varying rates, similar observations having been made with palladacycles.[105] The need for high temperatures for palladacycles to become active may be due to the need to either form Pd(IV) intermediate or required for decomposition of the highly stable systems, therefore a correlation between the thermal stability and the observed catalytic activity of the complexes may be prudent.

Although apparently the scope of the activity of these complexes is limited to aryl iodides, the catalytic activities are comparable to that of the parent complex, and indicate a great potential for complexes of similar design. The *para*-position of the benzene ring is an important site for possible anchoring, an important feature for potential as heterogeneous industrial applications. Overall, however, the new catalysts and the results disclosed here remain of interest from a mechanistic point of view in the debate around the Heck cross-coupling reaction.

CHAPTER 8

EXPERIMENTAL

8. Experimental

All solvents were Analar® quality with the exception of acetonitrile, which was HPLC grade, and were used as supplied unless otherwise stated. Diethyl ether, THF and toluene were distilled under a nitrogen atmosphere from sodium wire. Where stated as dry, DMSO was distilled from calcium hydride under reduced pressure, and stored over 4 Å molecular sieves. Water was purified using the "Purite$_{STILL}$ plus" system and had a conductivity of 0.04 μS cm^{-1} or lower. Reagents were used as supplied.

Thin layer chromatography was carried out using neutral aluminium oxide plates (Merck Art 5550) or silica plates (Merck Art 5554), both types being fluorescent on irradiation at 254 nm. Column chromatography was carried out using neutral alumina (Aldrich Oxide 90, activity I, 70–230 mesh), or using silica (Merck Silica Gel 60, 230–400 mesh).

NMR spectra were recorded on a Varian Mercury-200 (200 MHz for ^{1}H), a Varian Unity-300 (300 MHz for ^{1}H), a Varian Mercury-400 (400 MHz for ^{1}H, 101 MHz for ^{13}C), a Bruker Avance-400 (400 MHz for ^{1}H, 101 MHz for ^{13}C) or a Varian Inova-500 (500 MHz for ^{1}H, 126 MHz for ^{13}C) spectrometer, and were referenced to residual protiosolvent resonances. All chemical shifts (δ) are quoted in ppm and coupling constants (J) in Hz, reported as follows; chemical shift (δ) (ppm) (number of protons, multiplicity, coupling constant J (Hz), assignment. ^{1}H-NMR spectra were assigned with assistance from ^{1}H–^{1}H COSY (correlation spectroscopy, through bond interactions) and ^{1}H–^{1}H NOESY (nuclear Overhauser effect spectroscopy, through space interactions) spectra. ^{13}C-NMR spectra were recorded with proton decoupling, and were assigned with assistance from ^{1}H–^{13}C HSQC (heteronuclear single quantum correlation) and ^{13}C DEPT (distortionless enhancement by polarization transfer) spectra.

Electron-ionisation mass spectra were recorded with a Micromass AutoSpec spectrometer, with GC-MS on a Thermo Finnigan TRACE GCMS. Electrospray ionisation mass spectra were recorded with a Micromass LCT spectrometer with methanol or acetonitrile as the carrier solvent. MALDI mass spectra were recorded by the EPSRC National Mass Spectrometry Service at the University of Wales, Swansea. Accurate mass spectra were recorded with a Micromass LCT

spectrometer at 5000 resolution using sodium iodide as the reference. Accurate mass spectra were also recorded by the EPSRC National Mass Spectrometry Service.

Infra-red spectra were recorded with a Perkin-Elmer 1720X FTIR spectrometer operated using GRAMS software. Samples were examined as KBr discs (solids), thin films pressed between KBr plates (liquids or dissolved in $CDCl_3$ followed by reference spectral subtraction).

Elemental analysis was performed using an Exeter Analytical E-440 elemental analyser.

Single crystal X-ray diffraction experiments were carried out on a SMART 3-circle diffractometer with a CCD area detector, using graphite-monochromated Mo K_α radiation (λ = 0.71073 Å). The structures were solved by direct methods and refined by full-matrix least squares against F^2 of all data, using SHELXTL software.

UV-visible absorption spectra were recorded using a Biotech Instruments XS spectrometer operating with LabPower software. All samples were studied in quartz cuvettes of 1 cm pathlength, against a reference of pure solvent contained within a matched cuvette. Extinction coefficients were determined by a dilution technique and graphical application of the Beer-Lambert law, Equation 12.

$$A(\lambda) = \varepsilon(\lambda)\, c\, l$$

Equation 12: Beer-Lambet law, where $A(\lambda)$ is the absorbance at a specified wavelength, $\varepsilon(\lambda)$ is the related extinction coefficient ($dm^3\ mol^{-1}\ cm^{-1}$), c is the concentration of the absorbing species and l is the path length (cm).

Steady-state luminescence spectra were recorded using an Instruments S.A. Fluoromax-2 spectrometer, equipped with a Hamamatsu R928 photomultiplier tube. All samples were studied in quartz fluorescence cuvettes of 1 cm pathlength. Solutions were prepared so that the absorbance was ~0.1 to minimise inner filter effects. Emission was detected at right angles to the excitation source, with appropriate filters used where required to remove second order peaks. All emission spectra were corrected after data acquisition for dark count and for the spectral response of the detector. Excitation spectra were automatically corrected

for lamp output, through use of a beam splitter, which directs 8% of the excitation light to a reference photodiode.

Aerated luminescence quantum yields were recorded using a dilution technique with respect to a standard of 1,3-di(2-pyridyl)benzene-2-platinum(II) chloride in DCM solution (Φ = 0.60).[74] The quantum yield to be determined may be calculated with respect to the standard by application of Equation 13 where Φ is the luminescence quantum yield, (dI/dA) is the gradient from the plot of integrated emission intensity *vs.* absorbance, η is the refractive index of the solvent, and Φ_{ST}, $(dI/dA)_{ST}$ and η_{ST} are the respective values for the standard. Only the gradient of the linear portion of the plot was determined. Degassed quantum yields were obtained from the ratio of integrated emission intensities from degassed and aerated solutions of the same sample.

$$\Phi = \Phi_{ST}\left(\frac{\left(\frac{dI}{dA}\right)}{\left(\frac{dI}{dA}\right)_{ST}}\right)\left(\frac{\eta^2}{\eta_{ST}^{\ 2}}\right)$$

Equation 13: Equation for the determination of quantum yields in solution, where Φ is the luminescence quantum yield, (dI/dA) is the gradient from the plot of integrated emission intensity *vs.* absorbance, n is the refractive index of the solvent, and Φst, (dI/dA)st and nst are the respective values for the standard.

Low temperature (77 K) experiments were performed using a glass vacuum cold finger apparatus built in house. Measurements where performed in quartz NMR tubes frozen in liquid nitrogen contained in the apparatus resevoir.

The luminescence lifetimes of the complexes upto *ca.* 10 μs were measured by time-correlated single-photon counting, excited at 374.0 nm with an EPL-375 pulsed-diode laser (pulse length of 60 ps) at an appropriate repetition rate, typically at least 5-10 times longer pulse period than the lifetime, and the emitted light was detected at 90° after passage through a monochromator using a Peltier-cooled R928. Luminescence lifetimes in excess of around 10 μs (e.g Pd complexes at 77K) were measured by multichannel scaling, with data being collected typically

over 800 μs using 512 channels, following excitation with a xenon flashlamp operating at 100 Hz (pulse length of 2 μs). Light from the flashlamp was first passed through an excitation monochromator.

Density Functional Calculations B3LYP density functional theory calculations were performed using the Gaussian98 software package. "Double-ζ" quality basis sets were employed for the ligands (6-31G) and the Ir (LANL2DZ). The inner core electrons of Ir were replaced with a relativistic effective core potential (ECP), leaving the outer core $[(5s)^2(5p)^6]$ electrons and the $(5d)^6$ valence electrons of Ir(III). The geometries were fully optimised without symmetry constraints. Time-dependent DFT (TD-DFT) calculations were performed at the optimised ground-state geometries using the B3LYP functional.

8.1. General procedures

8.1.1. Stille cross-coupling reaction

The methodology used was based on the procedure outlined by Cardenas *et al.*[66] Toluene was added to a mixture of aryl-bromide (1 equiv.), 2-tri-n-butylstannylpyridine (1.25 equiv.), lithium chloride (8 equiv.) and bis(triphenylphosphine)palladium(II) dichloride (0.07 equiv.) contained in an oven dried Schlenk tube. The mixture was degassed *via* four freeze-pump-thaw cycles and placed under an atmosphere of dinitrogen. The reaction was stirred at reflux temperature (116°C), typically for 18–24 h. A saturated aqueous solution of KF (5 mL) was added to the reaction after cooling to ambient temperature, and the mixture stirred for 30 min. An insoluble residue was removed by filtration and washed with toluene. The combined toluene filtrate and washings were reduced *in vacuo* giving a crude brown residue, which was extracted into DCM (150 mL), and washed with aqueous $NaHCO_3$ (5% by mass, 2 x 100 mL). The organic phase was dried over anhydrous K_2CO_3, filtered and evaporated to dryness. Further purification was compound specific: details for individual compounds are given later in this chapter.

8.1.2. Miyaura cross-coupling reaction

The methodology used was based on the procedure outlined in the literature.[215] Aryl bromide (1 equiv.), potassium acetate (3 equiv.), and either bis(neopentyl

glycolato)diboron or bis(pinacol ester)diboron (1.2 equiv.) were dissolved in anhydrous DMSO. The mixture was degassed thoroughly using the freeze-pump-thaw technique and placed under an atmosphere of dinitrogen. A catalytic amount of 1,1'-[bis(diphenylphosphino)-ferrocene]palladium(II) dichloride was added to the mixture under a positive flow of dinitrogen. The reaction mixture was heated at 80°C until no trace of the aryl bromide starting material was detectable by thin-layer chromatography, typically 6 h. The reaction was then allowed to cool to ambient temperature, whereupon toluene was added (typically *ca.* 3 x the volume of DMSO), and the solution washed with successive quantities of water. The organic layer was retained, dried over potassium carbonate, filtered and the solvent removed *in vacuo*. The product was typically isolated as a pale brown solid and could generally be used in a subsequent Suzuki coupling reaction without further purification.

8.1.3. Suzuki cross-coupling reaction

Aryl bromide (~ 1 equiv.), aryl boronic acid (~ 1 equiv.) (a slight excess of one reagent was governed by which was deemed more precious or with respect to considerations with regard to ease of final purification) and Na_2CO_3 (1.2 equiv.) were mixed, and the selected solvent (reaction specific) was added. The mixture was degassed *via* the freeze-pump-thaw technique, and placed under an atmosphere of dinitrogen. Under a positive flow of dinitrogen, the catalyst, tetrakis(triphenylphosphine)palladium(0) (0.08 equiv.) was added. The reaction was then stirred at room temperature for 1 h, before being heated to 80°C, typically for 24–72 h. The mixture was allowed to cool to ambient temperature, and the solvent evaporated *in vacuo*, before being taken into DCM (50 mL) and washed with water (4 x 50 mL). The organic phase was retained, dried, filtered and the solvent evaporated *in vacuo*, yielding the crude product, typically as a dark solid. Further purification was compound specific; details for individual compounds are given later in this chapter.

8.1.4. Platinum(II) complexation reaction

8.1.4.1. Method A: glacial acetic acid

The methodology used was based on the procedure outlined by Cardenas *et al.*[66] Glacial acetic acid was added to a mixture of potassium tetrachloroplatinate

(1 equiv.) and ligand (1.1 equiv.) and the mixture degassed *via* the freeze-pump-thaw technique. The reaction was heated at reflux (116°C) under an inert atmosphere of dinitrogen. The reaction was then allowed to cool to ambient temperature before work-up and the volume reduced *in vacuo*, to aid precipitation of the product. The solid was isolated and washed successively by centrifuge, with water, ethanol and diethyl ether (typically 4 x 5 mL of each), before extracting the product into DCM. The organic solvent was removed *in vacuo* typically yielding the product as a bright yellow solid.

8.1.4.2. Method B: acetonitrile/water

Potassium tetrachloroplatinate (1 equiv.) was dissolved in water and degassed *via* the freeze-pump-thaw technique. Meanwhile, the ligand (1.1 equiv.) was dissolved, or suspended, depending on solubility, in acetonitrile and degassed *via* the freeze-pump-thaw technique. Under an atmosphere of dinitrogen, the aqueous solution of K_2PtCl_4 was transferred, *via* canular, into the reaction vessel containing the ligand in acetonitrile. The mixture was then stirred at reflux temperature, typically for 72 h. The volume was then reduced *in vacuo*, to aid precipitation of the product. The solid was isolated and washed successively by centrifuge, with water, ethanol (or methanol) and diethyl ether (typically 4 x 5 mL of each), before extracting the product into DCM or acetonitrile. The organic solvent was removed *in vacuo*, giving the product, typically a bright yellow solid.

8.1.5. Palladium(II) complexation reaction

The methodology used was based on the procedure outlined by Cardenas *et al.*[66] Methanol (10 mL) was added to a mixture of palladium(II) dichloride (1 equiv.) and lithium chloride (3 equiv.). The mixture was degassed *via* the freeze-pump-thaw technique, and stirred at reflux (65°C) for 2 h. The solvent was then removed *in vacuo* to give a brown residue of Li_2PdCl_4. The Li_2PdCl_4 residue and ligand (1.1 equiv.) were then mixed in glacial acetic acid (10 mL) and degassed *via* the freeze-pump-thaw technique. The mixture was stirred at reflux temperature (116°C) under an atmosphere of dinitrogen, typically for 18 h, after which the reaction solvent was evaporated *in vacuo* to aid precipitation of the product. The solid was isolated and washed successively *via* centrifugation, with glacial acetic acid, methanol and diethyl ether (typically 4 x 5 mL of each). The product was then extracted with DCM and reduced to a beige solid *in vacuo*.

8.1.6. Chloride metathesis reaction

N^C^N coordinated metal chloride complex (1 equiv.) was suspended in acetone, treated with silver trifluoromethanesulfonate (1.1 equiv.), and stirred at room temperature for at least 1 h. Complete dissolution of the suspension occurred upon treatment with the silver salt and a distinct colour change was observed in all cases. A grey precipitate of AgCl was removed by centrifugation, while the filtrate was retained and treated with the new ligand (≥ 2 equiv.). The mixture was then stirred at room temperature for at least 1 h. The product generally precipitated from the reaction solvent, which could be aided by reducing the volume of solvent prior to work-up. The product was purified by several washings with small portions of cold acetone in the centrifuge, and the isolated solid dried under reduced pressure.

8.1.7. Catalytic screening: Heck cross-coupling reaction

The methodology used was based on similar procedures employed in literature to study catalytic activity.[61,146,252] Catalyst (5.0×10^{-4} mmol), NEt_3 (307 µL, 2.2 mmol), iodobenzene (224 µL, 2.0 mmol), methyl acrylate (252 µL, 2.8 mmol), DMF (5 mL), and bis(ethylene glycol) dibutyl ether (248 µL, 1.0 mmol, ^{1}H NMR standard) were added to the reaction vessel attached to a reflux condenser, placed into an oil bath preheated to 140°C and stirred for 90 h. A small aliquot (0.5 mL) was removed from the reaction mixture over regular timed intervals and diluted in DCM (10 mL). Each abstraction was worked up under identical conditions: the organic layer was extracted three times over water, dried over magnesium sulfate, filtered and the solvent evaporated *in vacuo*. The product was analysed by ^{1}H NMR, and the yield determined from relative peak integrals for the corresponding product and internal standard signals.

8.1.8. Catalytic screening: Suzuki cross-coupling reaction

The methodology used was based on similar procedures employed in literature to study catalytic activity.[146] Catalyst (3.4×10^{-6} mmol), K_2CO_3 (355 mg, 2.6 mmol), 4-bromoacetophenone (338 mg, 1.7 mmol), phenylboronic acid (247 mg, 2.0 mmol), DMA (5 mL), and bis(ethylene glycol) dibutyl ether (211 µL, 0.85 mmol, ^{1}H NMR standard) were added to the reaction vessel attached to a reflux condenser, placed into an oil bath preheated to 110°C and stirred for 24 h. The

mixture was allowed to cool to ambient temperature and an aliquot (1 mL) was then removed and diluted in DCM (10 mL). The organic layer was extracted three times over water, dried over magnesium sulfate, filtered and the solvent evaporated *in vacuo*. The product was analysed by ^{1}H NMR, and the reaction yield determined from ratios of peak integrals from the corresponding product and internal standard signals.

8.2. Synthesis details and characterisation for specific compounds.

8.2.1. N^C^N ligands and their precursors.

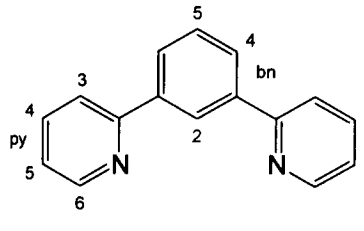

HL^1: 1,3-Di(2-pyridyl)benzene

The compound, previously synthesised by Cardenas *et al*,[66] was prepared *via* the Stille cross-coupling reaction using 1,3-dibromobenzene (1.07 g, 4.55 mmol), 2-tri-*n*-butylstannylpyridine (4.28 g of 92% purity, equivalent to 10.9 mmol), lithium chloride (1.55 g, 36.6 mmol), and bis(triphenylphosphine)palladium(II) chloride (202 mg, 0.29 mmol) all suspended in toluene (15 mL). The mixture was stirred at reflux for 24 h before work-up. Purification was performed by chromatography on silica gel, gradient elution from hexane to 35:65 hexane:diethyl ether (R_f = 0.6 in diethyl ether), leading to a brown oil (649 mg, 61%). Data were consistent with those previously reported.[66,74] In the case of an incomplete reaction the side product 1-bromo-3-(2-pyridyl)benzene was isolated. ^{1}H NMR (500 MHz, $CDCl_3$): δ 8.73 (2H, ddd, ^{3}J 4.8, ^{4}J 1.8, ^{5}J 0.9, H^6-py), 8.64 (1H, t, ^{3}J 1.7, H^2-bn), 8.07 (2H, dd, ^{3}J 7.6, ^{4}J 1.8, H^4-bn), 7.85 (2H, dt, ^{3}J 7.9, ^{4}J 1.1, H^3-py), 7.78 (2H, td, ^{3}J 7.7, ^{4}J 1.9, H^4-py), 7.60 (1H, t, ^{3}J 7.7, H^5-bn), 7.26 (2H, ddd, ^{3}J 7.2, ^{3}J 4.6, ^{4}J 1.0, H^5-py). ^{13}C NMR (126 MHz, $CDCl_3$): δ 157.4 (quat), 149.8 (H^6-py), 140.0 (quat), 136.9 (C^4-py), 129.4 (C^5-bn), 127.6 (C^4-bn), 125.7 (C^2-bn), 122.4 (C^5-py), 120.9 (C^3-py). MS (EI^+): *m/z* 232 $[M]^+$, 154 $[M - py]^+$.

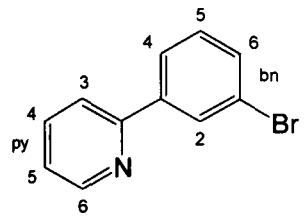

1-Bromo-3-(2-pyridyl)benzene

^{1}H NMR (400 MHz, $CDCl_3$): δ 8.70 (1H, ddd, ^{3}J 4.9, ^{4}J 1.7, ^{5}J 0.8, H^6-py), 8.18 (1H, t, ^{3}J 1.8, H^2-bn), 7.91 (1H, dd, ^{3}J 7.9, ^{4}J 1.7, H^6-bn), 7.77 (1H, td, ^{3}J 7.9, ^{4}J 1.9, H^4-py), 7.70 (1H, dt, ^{3}J 7.9, ^{4}J 1.2, H^3-py), 7.55 (1H, dd, ^{3}J 8.0, ^{4}J 2.1, H^4-bn), 7.35 (1H, t, ^{3}J 8.1, H^5-bn), 7.26 (1H, ddd, ^{3}J 7.3, ^{3}J 4.7, ^{4}J 1.2, H^5-py). ^{13}C NMR (101 MHz, $CDCl_3$): δ 155.9 (quat), 149.9 (C^6-py), 141.5 (quat), 137.0 (C^4-py), 132.0 (C^4-bn), 130.4 (C^5-bn), 130.1 (C^2-bn), 125.5 (C^6-bn), 123.2 (quat), 122.8 (C^5-py), 120.2 (C^3-py). MS (ES^+): *m/z* 234 $[M + H]^+$.

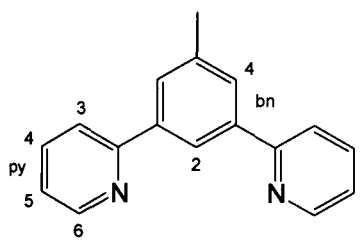

HL^2: 1,3-Di(2-pyridyl)-5-methylbenzene

This compound was prepared *via* the Stille cross-coupling reaction and as used previously,[74] using 3,5-dibromotoluene (1.49 g, 5.95 mmol), 2-tri-*n*-butylstannylpyridine (6.25 g of 88% purity, equivalent to 14.9 mmol), lithium chloride (1.80 g, 42.4 mmol), and bis(triphenylphosphine)palladium(II) chloride (225 mg, 0.32 mmol) all suspended in toluene (15 mL). The mixture was stirred at reflux for 72 h before work-up. Purification was performed by chromatography on silica gel, gradient elution from hexane to 20:80 hexane:diethyl ether mix (R_f = 0.8 in diethyl ether), leading to a brown oil (538 mg, 37%). Data were consistent with those previously reported.[74] ^{1}H NMR (300 MHz, $CDCl_3$): δ 8.70 (2H, d, ^{3}J 4.5, H^6-py), 8.35 (1H, s, H^2-bn), 7.89 (2H, s, H^4-bn), 7.82 (2H, d, ^{3}J 7.8, H^3-py), 7.75 (2H, td, ^{3}J 7.2, ^{4}J 1.8, H^4-py), 7.23 (2H, ddd, ^{3}J 7.2, ^{3}J 4.8, ^{4}J 1.2, H^5-py), 2.53 (3H, s, CH_3). ^{13}C NMR (75 MHz, $CDCl_3$): δ 157.1 (quat), 149.4 (C^6-py), 139.7 (quat), 138.9 (quat), 136.7 (C^4-py), 128.2 (C^4-bn), 122.6 (C^2-bn), 122.1 (C^5-py), 120.6 (C^3-py), 21.4 (CH_3). MS (EI^+): *m/z* 246 $[M]^+$.

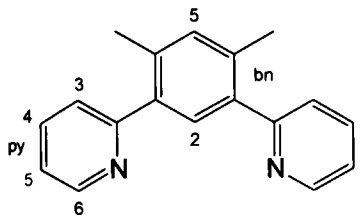

HL[3]: 1,3-Di(2-pyridyl)-4,6-dimethylbenzene

The compound was prepared *via* the Stille cross-coupling reaction and as used previously,[291] using 1,3-dibromo-4,6--dimethylbenzene (1.25 g, 4.74 mmol), 2-tri-*n*-butylstannyl-pyridine (4.74 g of 91% purity, equivalent to 11.8 mmol), lithium chloride (1.61 g, 37.9 mmol) and bis(triphenylphosphine)palladium(II) dichloride (202 mg, 0.28 mmol) all suspended in toluene (15 mL). The reaction was stirred at reflux for 3 d before work-up. Purification was performed by chromatography on silica gel, gradient elution from hexane to 60:40 hexane:diethyl ether mix (R_f = 0.5 in diethyl ether). The product was isolated as a colourless solid (834 mg, 68%). ^{1}H NMR (400 MHz, $CDCl_3$): δ 8.69 (2H, d, ^3J 4.9, H^6-py), 7.74 (2H, td, ^3J 7.8, ^4J 1.7, H^4-py), 7.48 (1H, s, H^5-bn), 7.46 (2H, dd, ^3J 7.8, ^4J 1.0, H^3-py), 7.24 (2H, m, H^5-py), 7.22 (1H, s, H^5-bn), 2.40 (6H, s, CH_3). ^{13}C NMR (101 MHz, $CDCl_3$): δ 159.6 (C^1-py), 149.1 (C^6-py), 138.2 (C^1-bn), 136.5 (C^4-py), 136.0 (C^2-bn), 133.5 (C^5-bn), 131.3 (C^3-py), 124.5 (C^5-py), 121.8 (C^4-bn), 20.2 (CH_3). MS (ES$^+$): *m/z* 261 [M + H]$^+$, 283 [M + Na]$^+$. Anal. Calcd. for $C_{18}H_{16}N_2$: C, 83.04; H, 6.19: N, 10.76. Found: C, 82.54; H 6.23; N, 10.57%.

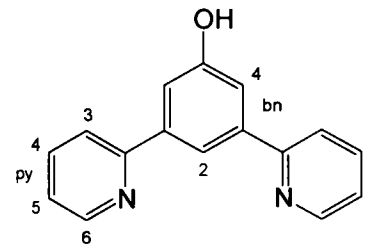

HL[4]: 5-hydroxymethyl-1,3,-Di(2-pyridyl)benzene

This compound was prepared *via* the Stille cross-coupling reaction using 3,5-dibromophenol (325 mg, 1.29 mmol), 2-tri-*n*-butylstannylpyridine (1.30 g of 89% purity, equivalent to 3.13 mmol), lithium chloride (440 mg, 10.4 mmol) and bis(triphenylphosphine)palladium(II) chloride (187 mg, 0.27 mmol) all suspended in toluene (8 mL). The mixture was heated at reflux for 3 d before work-up. Purification was performed by chromatography on silica gel, gradient elution from hexane to diethyl ether (R_f = 0.4 in diethyl ether). Product was isolated as a pale solid (105 mg, 33%). ^{1}H NMR (500 MHz, $CDCl_3$) δ 8.76 (2H, dd, ^3J 4.8, ^4J 1.3, H^6-

py), 8.04 (1H, t, ^4J 1.5, H^2-bn), 7.74 (4H, m, H^3-py, H^4-py), 7.57 (2H, d, ^4J 1.5, H^4-bn), 7.24 (2H, m, H^5-py). ^{13}C NMR (126 MHz, $CDCl_3$): δ 157.8 (quat), 157.2 (quat), 149.3 (C^6-py), 141.1 (quat), 137.4 (C^4-py), 122.6 (C^5-py), 121.5 (C^3-py), 117.9 (C^2-bn), 115.5 (C^4-bn). HRMS (ES^+): *m/z* 271.08407 $[M + Na]^+$, $[C_{16}H_{12}N_2O^{23}Na]$ requires 271.08418; *m/z* 249.10218 $[M + H]^+$; $[C_{16}H_{13}N_2O]$ requires 249.10224.

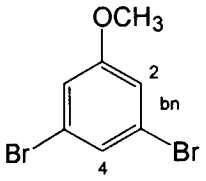

3,5-Dibromo-anisole

3,5-Dibromophenol (182 mg, 0.72 mmol) was dissolved in acetonitrile (20 mL) and treated with sodium hydroxide (29 mg, 0.73 mmol). The mixture was stirred for 2½ h at RT. Iodomethane (0.1 mL, 1.61 mmol) was added to the reaction and stirred for a further 8 h at RT. The reaction was diluted with DCM (50 mL) and washed with water (3 x 25 mL), dried over potassium carbonate, filtered and reduced *in vacuo* to an colourless solid (167 mg, 87%). ^1H NMR (400 MHz, $CDCl_3$): δ 7.25 (1H, t, ^4J 1.5, H^4-bn), 6.99 (2H, d, ^4J 1.5, H^2-bn), 3.78 (3H, s, CH_3).

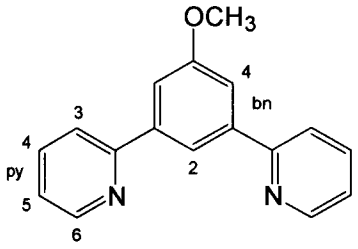

HL^5: 1,3-Di-(2-pyridyl)-5-methoxybenzene

This compound was prepared *via* the Stille cross-coupling reaction using 1,3-dibromo-5-methoxybenzene (123 mg, 0.46 mmol), 2-tri-*n*-butylstannylpyridine (440 mg of 95% purity equivalent to 1.14 mmol), lithium chloride (157 mg, 3.70 mol) and bis(triphenylphosphine)palladium(II) chloride (28 mg, 0.039 mmol) all suspended in toluene (6 mL). The mixture was heated at reflux for 43 h before work-up. Purification was performed by chromatography on silica gel, gradient elution from hexane to 35:65 hexane:diethyl ether (R_f = 0.6 in diethyl ether) to give the product as a colourless solid (100 mg, 82%). ^1H NMR (500 MHz, $CDCl_3$): δ 8.72 (2H, d, ^3J 4.6, H^6-py), 8.20 (1H, t, ^4J 1.2, H^2-bn), 7.84 (2H, d, ^3J 8.0, H^3-py), 7.77 (2H, td, ^3J 7.8, ^4J 1.6, H^4-py), 7.66 (2H, d, ^4J 1.2, H^4-bn), 7.26 (2H, dd, ^3J 7.1, ^3J 4.9, H^5-py), 3.98 (3H, s, CH_3). ^{13}C NMR (126 MHz, $CDCl_3$): δ 160.7 (C^5-bn),

157.2 (C^2-py), 149.7 (C^6-py), 141.3 (C^1-bn), 136.9 (C^4-py), 122.5 (C^5-py), 121.0 (C^3-py), 118.2 (C^2-bn), 113.3 (C^4-bn), 55.8 (CH_3). MS (ES^+): *m/z* 263 $[M + H]^+$. HRMS (ES^+): *m/z* 263.11815 $[M + H^+]$, $[C_{17}H_{15}N_2O]$ requires 263.11789.

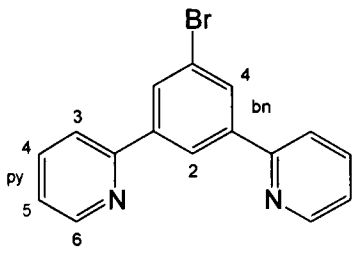

HL^6: 1,3-Di(2-pyridyl)-5-bromobenzene

This compound was prepared *via* the Stille cross-coupling reaction using 1,3,5-tribromobenzene (1.44 g, 4.55 mmol), 2-tri-*n*-butylstannylpyridine (4.24 g of 87% purity, equivalent to 10.0 mmol), lithium chloride (1.56 g, 36.7 mmol) and bis(triphenylphosphine)palladium(II) chloride (197 mg, 0.28 mmol) all suspended in toluene (15 mL). The mixture was stirred for 20 h at a temperature slightly lower than reflux (95–100 °C). After work-up, separation was performed by two consecutive chromatographic columns on silica gel, elution hexane to 50:50 hexane:diethyl ether (R_f = 0.8 in diethyl ether) yielding a colourless solid (785 mg, 56%). ^{1}H NMR (400 MHz, $CDCl_3$): δ 8.72 (2H, dd, ^3J 4.8, ^4J 1.7, H^6-py), 8.55 (1H, t, ^4J 1.6, H^2-bn), 8.22 (2H, d, ^4J 1.7, H^4-bn), 7.80 (4H, m, H^3-py, H^4-py), 7.28 (2H, ddd, ^3J 6.5, ^3J 5.1, ^4J 1.7, H^5-py). ^{13}C NMR (101 MHz, $CDCl_3$): δ 155.8 (quat), 149.9 (quat), 141.7 (quat), 137.1 (C^4-py), 130.5 (C^4-bn), 124.2 (C^6-py), 123.7 (C^2-bn), 123.0 (C^5-py) 120.9 (C^3-py). HRMS (ES^+): *m/z* 311.0205 $[M+H]^+$; $[C_{16}H_{12}N_2Br]$ requires 311.0184.

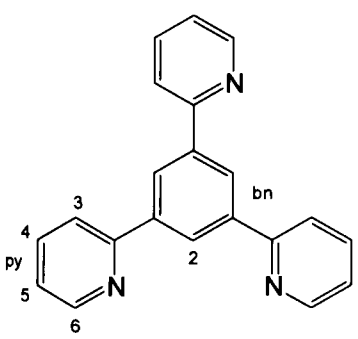

HL^7: 1,3,5-Tri(2-pyridyl)benzene

This compound was prepared *via* the Stille cross-coupling reaction using 1,3,5-tribromobenzene (822 mg, 2.61 mmol), 2-tri-*n*-butylstannylpyridine (4.34 g of 81% purity, equivalent to 9.50 mmol), lithium chloride (1.212 g, 28.6 mmol), and

bis(triphenylphosphine)palladium(II) chloride (154 mg, 0.22 mmol) all suspended in toluene (8 mL). The mixture was stirred at reflux 2 d before work-up. Purification was performed by chromatography on silica gel, gradient elution from hexane to 100% diethyl ether (R_f = 0.4 in diethyl ether). The product was isolated as a pale brown solid (296 mg, 38%). ^{1}H NMR (500 MHz, $CDCl_3$): δ 8.75 (3H, d, ^3J 4.8, H^6-py), 8.74 (3H, s, H-bn), 7.99 (3H, d, ^3J 8.0, H^3-py), 7.81 (3H, td, ^3J 7.7, ^4J 1.8, H^4-py), 7.29 (3H, ddd, ^3J 7.4, ^3J 4.9, ^4J 1.0, H^5-py). ^{13}C NMR (126 MHz, $CDCl_3$): δ 157.1, 149.7 (C^2-bn), 140.5 (C^2-py), 137.2 (C^4-py), 126.3 (C^6-py), 122.6 (C^5-py), 121.2 (C^3-py). HRMS (ES^+): *m/z* 310.13385 $[M + H]^+$; $[C_{21}H_{16}N_3]$ requires 310.13387. Anal. Calcd. for $C_{21}H_{15}N_3.½CH_2Cl_2$: C, 73.19; H, 4.86: N, 11.89. Found: C, 73.49; H 4.59; N, 11.89%. NMR data are consistent with values previously reported in CD_2Cl_2 for this compound, obtained as a side product from the reaction of 2-ethynylpyridine with $CpCo(PPh_3)_2$.[294]

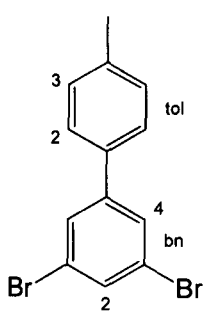

1,3-Dibromo-5-*p*-tolylbenzene

This compound was prepared via the Suzuki cross-coupling reaction using p-tolylboronic acid (47 mg, 0.35 mmol), 1,3,5-tribromobenzene (122 mg, 0.39 mmol), sodium carbonate (47 mg, 0.43 mmol) and tetrakis(triphenylphosphine)-palladium(0) (27 mg, 0.023 mmol) all suspended in toluene:ethanol:water (3:3:1 mL respectively). The mixture was stirred at 80°C for 40 h before work-up. Work-up varied slightly from the general procedure. The mixture was allowed to cool to ambient temperature before being taken into benzene (50 mL), washed with brine (2 x 25 mL) and water (2 x 25 mL). The organic phase was dried over magnesium sulfate, filtered and evaporated *in vacuo* to a brown oil. Purification was performed by chromatography on silica gel, elution hexane (R_f = 0.8 in 95:5 hexane:diethyl ether) yielding a colourless solid (70 mg, 62%). ^{1}H NMR (400 MHz, $CDCl_3$): δ 7.64 (2H, d, ^4J 1.8, H^4-bn), 7.61 (1H, t, ^4J 1.8, H^2-bn), 7.42 (2H, dt, ^3J 8.2, ^4J 1.8, H^2-tol), 7.26 (2H, coupling obscured by $CHCl_3$ signal, H^3-tol), 2.40 (3H, s, CH_3).

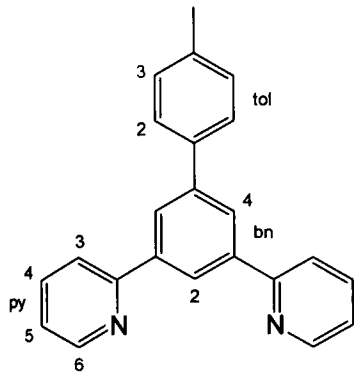

HL[8]: 1,3-Di(2-pyridyl)-5-(*p*-tolyl)benzene

Method A: This compound was prepared *via* the Suzuki cross-coupling reaction of *p*-tolylboronic acid (108 mg, 0.79 mmol) with 1,3-di(2-pyridyl)-5-bromobenzene (220 mg, 0.71 mmol), in the presence of sodium carbonate (99 mg, 0.93 mmol) and catalysed by tetrakis(triphenylphosphine)palladium(0) (28 mg, 0.024 mmol) suspended in a toluene:ethanol:water solvent mixture (3:3:0.5 mL respectively). The mixture was stirred at 80°C for 66 h before work-up. Purification was performed by chromatography on silica gel, gradient elution from hexane to hexane:diethyl ether (50:50) (R_f = 0.6 in diethyl ether). The product was a colourless solid (203 mg, 89%).

Method B: The compound was also prepared *via* the Stille cross-coupling reaction using 1,3-dibromo-5-(*p*-tolyl)benzene (70 mg, 0.22 mmol), 2-tri-*n*-butylstannyl-pyridine (270 mg of 85% purity equivalent to 0.62 mmol), lithium chloride (73 mg, 1.72 mmol) and bis(triphenylphosphine)palladium(II) dichloride (39 mg, 0.056 mmol) in toluene (6 mL). The mixture was stirred at reflux for 42 h before work-up. Purification was performed by chromatography on silica gel, gradient elution from hexane to hexane:diethyl ether (50:50) yielding a colourless solid (34 mg, 49%). Mp: 187°C. ^{1}H NMR (400 MHz, $CDCl_3$): δ 8.76 (2H, dd, ^3J 4.8, ^4J 1.8, H^6-py), 8.59 (1H, t, ^4J 1.6, H^2-bn), 8.31 (2H, d, ^4J 1.6, H^4-bn), 7.91 (2H, d, ^3J 7.9, H^3-py), 7.80 (2H, td, ^3J 7.8, ^4J 1.8, H^4-py), 7.69 (2H, d, ^3J 8.1, H_{meta}-tol), 7.28 (4H, m, H_{ortho}-tol, H^5-py), 2.43 (3H, s, CH_3). ^{13}C NMR (101 MHz, $CDCl_3$): δ 157.3, 149.7, 142.4, 140.4, 138.0, 137.5, 137.0, 129.6, 127.3, 126.3 (C^4-py), 124.4 (C^5-py), 122.5 (C_m-tol), 121.0 (C^3-py), 21.3 (CH_3). HRMS (ES^+): *m/z* 323.15413 $[M + H]^+$; $[C_{23}H_{19}N_2]$ requires 323.15428. Anal. Calcd. for $C_{23}H_{18}N_2.½CH_2Cl_2$: C, 79.91; H, 5.36: N, 7.99. Found: C, 79.65; H 5.89; N, 8.05%.

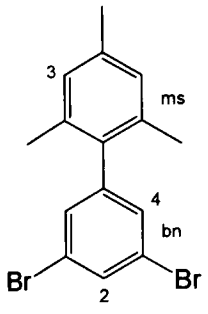

1,3-dibromo-5-mesitylbenzene

This compound was prepared *via* the Suzuki cross-coupling reaction using slightly modified conditions, based on those described in the literature,[213] in which a stronger base, barium hydroxide, is employed to facilitate coupling of the more hindered boronic acid. A Schlenk tube was charged with mesitylboronic acid (502 mg, 3.06 mmol), barium hydroxide (1.45g, 4.59 mmol), tetrakis(triphenyl-phosphine)palladium(0) (97 mg, 0.08 mmol) and 1,3,5-tribromobenzene (967 mg, 3.06 mmol). The flask was flushed with dinitrogen, and charged with degassed DME (6 mL) and water (1 mL), *via* cannular under positive pressure of dinitrogen. The mixture was stirred at 80°C for 20 h. After allowing the mixture to cool to room temperature, the product was extracted with benzene (50 mL), washed with brine (2 x 25 mL) and water (2 x 25 mL). The organic phase was dried over magnesium sulfate, filtered and evaporated *in vacuo*. Purification was performed by chromatography on silica gel, gradient elution from hexane to 94:6 hexane:DCM yielding a colourless solid (585 mg, 54%). ^{1}H NMR (400 MHz, $CDCl_3$): δ 7.66 (1H, t, ^{4}J 1.8, H^2-bn), 7.26 (2H, d, ^{4}J 1.8, H^4-bn), 6.94 (2H, s, H^3-ms), 2.33 (3H, s, *p*-CH_3), 2.02 (6H, s, *o*-CH_3). ^{13}C NMR (101 MHz, $CDCl_3$): δ 145.0, 137.7, 136.3, 135.7, 132.4 (C^2-bn), 131.3 (C^4-bn), 128.4 (C^3-ph), 123.1, 21.2 (*p*-CH_3), 20.8 (*o*-CH_3). A by-product of the reaction was 3,5-bis(mesityl)-bromobenzene (96 mg, 16%), a colourless solid. ^{1}H NMR: δ 7.30 (2H, H^2-bn), 6.95 (4H, H^3-ms), 6.89 (1H, H^4-bn), 2.34 (6H, *p*-CH_3), 2.08 (12H, *o*-CH_3).

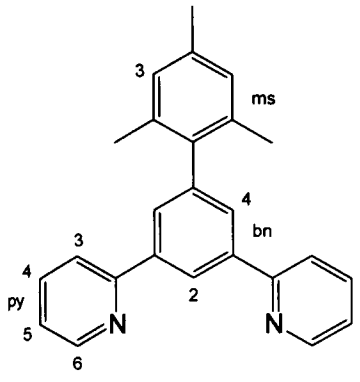

HL[9]: 1,3-Di(2-pyridyl)-5-mesitylbenzene

This compound was prepared *via* the Stille cross-coupling reaction using 1,3-dibromo-5-(mesityl)benzene (585 mg, 1.65 mmol), 2-tri-*n*-butylstannylpyridine (2.17 g of 70% purity, equivalent to 4.13 mmol), lithium chloride (559 mg, 13.18 mmol) and bis(triphenylphosphine)palladium(II) dichloride (69 mg, 0.098 mmol) all suspended in toluene (15 mL). The mixture was stirred at reflux for 40 h before work-up. Purification was performed by chromatography on silica, elution gradient hexane to 45:55 hexane:diethyl ether (R_f = 0.7 in diethyl ether). The product was isolated as a colourless solid (380 mg, 66%). ^{1}H NMR (500 MHz, $CDCl_3$): δ 8.73 (2H, d, ^3J 4.9, H^6-py), 8.72 (1H, s, H^2-bn), 7.90 (2H, d, ^3J 7.7, H^3-py), 7.88 (2H, d, ^4J 1.6, H^4-bn), 7.81 (2H, t, ^3J 7.4, H^4-py), 7.29 (2H, t, ^3J 6.2, H^5-py), 6.97 (2H, s, H^3-ms), 2.35 (3H, s, *p*-CH_3), 2.09 (6H, s, *o*-CH_3). ^{13}C NMR (126 MHz, $CDCl_3$): δ 157.4, 149.9, 142.4, 140.3, 138.8, 137.0 (C^4-py), 136.9, 136.2, 128.7 (C^3-ms), 128.3 (C^4-bn), 124.2 (C^2-bn), 122.7 (C^5-py), 121.0 (C^3-py), 21.2 (*p*-CH_3), 21.1 (*o*-CH_3). MS (ES^+): *m/z* 351.1852 $[M + H]^+$; $[C_{25}H_{23}N_2]$ requires 351.1856. Anal. Calcd. for $C_{25}H_{22}N_2$: C, 85.68; H, 6.33; N, 7.99. Found: C, 85.58; H, 6.30; N, 7.90%.

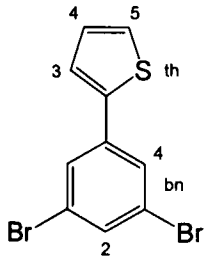

1,3-Dibromo-5-(2-thienyl)benzene

This compound was prepared *via* the Suzuki cross-coupling reaction using thiophene-2-boronic acid (49 mg, 0.38 mmol), 1,3,5-tribromobenzene (151 mg, 0.48 mmol), sodium carbonate (54 mg, 0.51 mmol) and tetrakis(triphenyl-phosphine)palladium(0) (37 mg, 0.032 mmol) suspended in a mixture of

toluene:ethanol:water (3:3:1 mL respectively). The mixture was stirred at 80°C for 40 h before work-up. Using a slightly different procedure, the mixture was diluted with benzene (50 mL), washed with brine (25 mL), followed by water (2 x 25 mL). The organic phase was dried over magnesium sulfate, filtered and reduced *in vacuo* to a brown oil. Purification was performed by chromatography on silica gel, elution hexane (R_f = 0.8 in 95:5 hexane:diethyl ether) yielding a white solid (60 mg, 49%). ^{1}H NMR (400 MHz, $CDCl_3$): δ 7.67 (2H, d, ^4J 1.8, H^4-bn), 7.56 (1H, t, ^4J 1.8, H^2-bn), 7.34 (1H, dd, ^3J 5.0, ^4J 1.2, H^5-th), 7.31 (1H, dd, ^3J 3.6, ^4J 1.2, H^3-th), 7.09 (1H, dd, ^3J 5.0, ^3J 3.6, H^4-th).

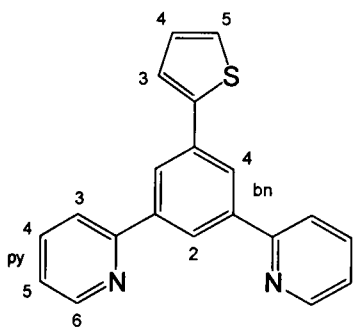

HL[10]: 1,3-Di(2-pyridyl)-5-(2-thienyl)benzene

This compound was prepared *via* the Stille cross-coupling reaction using 1,3-dibromo-5-(2-thienyl)benzene (60 mg, 0.19 mmol), 2-tri-*n*-butylstannylpyridine (255 mg of 90% purity, equivalent to 0.62 mmol), lithium chloride (66 mg, 1.56 mmol) and bis(triphenylphosphine)palladium(II) dichloride (36 mg, 0.051 mmol) all suspended in toluene (6 mL). The mixture was stirred at reflux for 60 h before work up. Purification was performed by chromatography on silica gel, gradient elution hexane to 60:40 hexane:diethyl ether (R_f = 0.8 in diethyl ether). The product was isolated as a colourless solid (51 mg, 86%). ^{1}H NMR (500 MHz, $CDCl_3$): δ 8.76 (2H, dd, ^3J 5.0, ^4J 1.6, H^6-py), 8.55 (1H, t, ^4J 1.6, H^2-bn), 8.34 (2H, d, ^4J 1.6, H^4-bn), 7.94 (2H, d, ^3J 7.9, H^3-py), 7.85 (2H, td, ^3J 7.9, H^4-py), 7.55 (1H, dd, ^3J 3.5, ^4J 1.1, H^3-th), 7.33 (3H, m, H^5-py, H^5-th), 7.13 (1H, dd, ^3J 5.0, ^3J 3.5, H^4-th). ^{13}C NMR (126 MHz, $CDCl_3$): δ 156.8 (quat), 149.6 (C^6-py), 144.0 (quat), 140.5 (quat), 136.8 (C^4-py), 135.4 (quat), 128.0 (C^4-th), 125.0 (quat), 124.9 (C^3-th, C^4-bn), 124.5 (C^2-bn), 123.8 (C^5-th), 122.4 (C^5-py), 120.8 (C^3-py). HRMS (ES$^+$): *m/z* 315.09498 [M + H]$^+$, $C_{20}H_{15}N_2{}^{32}S$ requires 315.09505; *m/z* 337.07694 [M + Na]$^+$; $C_{20}H_{14}N_2{}^{32}S^{23}Na$ requires 337.07699.

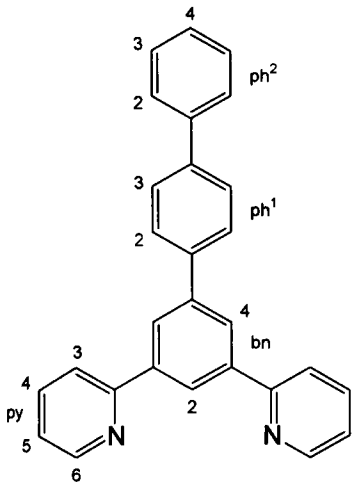

HL[11]: 5-(4-Biphenyl)-1,3-di(2-pyridyl)benzene

This compound was prepared *via* the Suzuki cross-coupling reaction using 1-bromo-3,5-di(2-pyridyl)benzene (134 mg, 0.43 mmol), 4-biphenylboronic acid (96 mg, 0.49 mmol), sodium carbonate (137 mg, 1.29 mmol) and tetrakis-(triphenylphosphine)palladium(0) (30 mg, 0.026 mmol) all suspended in DME (3 mL) and water (0.5 mL). The mixture was heated at 80°C for 67 h before work-up. Purification was performed by chromatography on silica gel, gradient elution from hexane to 50:50 hexane:diethyl ether (R_f = 0.8 in diethyl ether), followed by recrystallisation from hexane, yielding a colourless solid (80 mg, 48%). ^{1}H NMR (500 MHz, $CDCl_3$): δ 8.78 (2H, dd, ^3J 4.8, ^4J 0.8, H^6-py), 8.65 (1H, t, ^4J 1.5, H^2-bn), 8.40 (2H, d, ^4J 1.5, H^4-bn), 8.01 (2H, d, ^3J 7.9, H^3-py), 7.89 (4H, m, H^4-py, H^2-ph^1), 7.73 (2H, d, ^3J 8.4, H^3-ph^1), 7.67 (2H, dd, ^3J 8.4, ^4J 1.3, H^2-ph^2), 7.48 (2H, t, ^3J 7.9, H^3-ph^2), 7.36 (3H, m, H^4-ph^2, H^5-py). ^{13}C NMR (126 MHz, $CDCl_3$): δ 156.7, 142.3, 140.8, 140.7, 139.6, 138.0, 129.0 (C^3-ph^2), 128.0 (C^3-ph^1), 127.7 (C^2-ph^1), 127.6 (C^4-ph^2), 127.2 (C^3-ph^2), 126.9 (C^4-bn), 125.0, 122.9 (C^5-py), 121.6 (C^3-py). MS (ES^+): *m/z* 385 $[M + H]^+$; 385.1694 $[M + H]^+$, $[C_{28}H_{21}N_2]$ requires 385.1699; *m/z* 407.1514 $[M + Na^+]$, $[C_{28}H_{20}N_2{}^{23}Na]$ requires 407.1514. Anal. Calcd for $C_{28}H_{20}N_2$: C, 87.47; H, 5.24: N, 7.28. Found: C, 86.77; H 5.22; N, 7.14%.

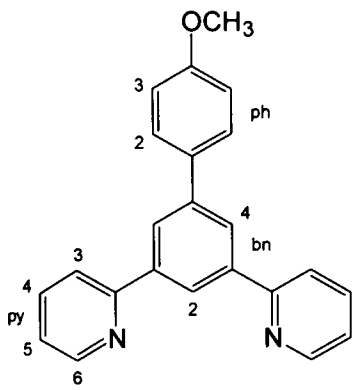

HL[12]: 1,3-Di(2-pyridyl)-5-(4-methoxyphenyl)benzene

This compound was prepared *via* the Suzuki cross-coupling reaction using 4-methoxyphenylboronic acid (58 mg, 0.38 mmol), 1-bromo-3,5-di(2-pyridyl)-benzene (106 mg, 0.34 mmol), sodium carbonate (149 mg, 1.41 mmol) and tetrakis(triphenylphosphine)palladium(0) (40 mg, 0.035 mmol) all suspended in a mixture of toluene:ethanol:water (4:4:1 mL respectively). The mixture was heated at 80°C for 2½ d before work-up. Purification was performed by chromatography on silica gel, elution 50:50 hexane: diethyl ether (R_f = 0.7 in diethyl ether) followed by recrystalisation from hexane (121 mg, 94%). ^{1}H NMR (500 MHz, $CDCl_3$): δ 8.74 (2H, ddd, ^3J 4.8, ^4J 1.7, ^5J 0.9, H^6-py), 8.54 (1H, t, ^4J 1.6, H^2-bn), 8.26 (2H, d, ^4J 1.6, H^4-bn), 7.89 (2H, d, ^3J 7.8, H^3-py), 7.79 (2H, td, ^3J 7.8, ^4J 1.8, H^4-py), 7.71 (2H, d, ^3J 8.8, H^2-ph), 7.27 (2H, ddd, ^3J 5.8, ^3J 4.8, ^4J 1.0, H^5-py), 7.01 (2H, d, ^3J 8.8, H^3-ph), 3.87 (3H, s, CH_3). ^{13}C NMR (126 MHz, $CDCl_3$): δ 159.5, 157.4, 149.8 (C^6-py), 142.0, 140.5, 136.9 (C^4-py), 133.5, 128.6 (C^2-ph), 126.1 (C^4-bn), 124.1 (C^2-bn), 122.5 (C^5-py), 121.0 (C^3-py), 114.3 (C^3-ph), 55.5 (CH_3). HRMS (ES^+): *m/z* 339.14903 $[M + H]^+$, $[C_{23}H_{19}N_2O]$ requires 339.14919.

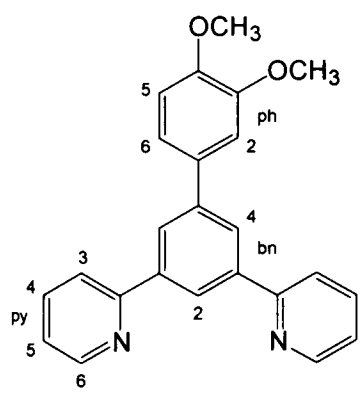

HL[13]: 1,3-Di(2-pyridyl)-5-(3,4-dimethoxyphenyl)benzene

This compound was prepared *via* the Suzuki cross-coupling reaction using 3,4-dimethoxyphenylboronic acid (103 mg, 0.57 mmol), 1-bromo-3,5-di(2-pyridyl)-benzene (169 mg, 0.55 mmol), sodium carbonate (80 mg, 0.76 mmol) and tetrakis-

(triphenylphosphine)palladium(0) (31 mg, 0.027 mmol) all suspended in a mixture of toluene:ethanol:water (3:3:0.5 mL respectively). The mixture was heated at 80°C for 2 d before work up. Purification was performed by chromatography on silica gel, elution gradient from hexane to diethyl ether (R_f = 0.5 in diethyl ether) yielding a colourless solid, which was then recrystallised from diethyl ether (64 mg, 31%). ^{1}H NMR (500 MHz, $CDCl_3$): δ 8.75 (2H, d, ^3J 4.6, H^6-py), 8.55 (1H, t, ^4J 1.5, H^4-bn), 8.27 (2H, d, ^4J 1.5, H^4-bn), 7.92 (2H, d, ^3J 8.0, H^3-py), 7.82 (2H, td, ^3J 7.8, ^4J 1.7, H^4-py), 7.31 (4H, m, H^5-py, H^2-ph, H^6-ph), 6.98 (1H, d, ^3J 8.3, H^5-ph), 4.00 (3H, s, *m*-CH_3), 3.94 (3H, s, *p*-CH_3). ^{13}C NMR (126 MHz, $CDCl_3$): δ 157.3, 149.7 (C^6-py), 149.2, 148.9, 142.3, 140.4, 137.0, 134.0, 126.2 (C^4-bn), 124.2 (C^2-bn), 122.5 (C^5-py), 121.0 (C^3-py), 119.9, 111.5 (C^5-ph), 110.7, 56.2 (*m*-CH_3), 56.1 (*p*-CH_3). MS (ES^+): *m/z* 369.3 $[M + H]^+$.

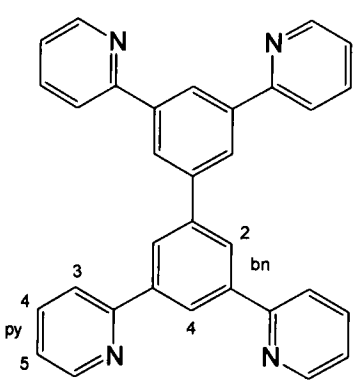

HL[14]: 1,1'-Bis-[3,5-di(2-pyridyl)benzene]

The product was prepared *via* the Suzuki cross-coupling reaction using 1-bromo-3,5-di(2-pyridyl)benzene (82 mg, 0.27 mmol), 1,3-di(2-pyridyl)-5-phenylboronic acid, neopentyl ester (87 mg, 0.25 mmol), sodium carbonate (80 mg, 0.76 mmol) and tetrakis(triphenyl-phosphine)palladium(0) (16 mg, 0.014 mmol). The mixture was heated at 80°C for 2 d before work up. Purification was performed by chromatograghy on silica gel, gradient elution from hexane to diethyl ether (R_f = 0.4 in diethyl ether). Product isolated as a colourless solid (12 mg, 10%). ^{1}H NMR (500 MHz, $CDCl_3$): δ 8.75 (4H, d, ^3J 4.8, H^6-py), 8.66 (2H, t, ^4J 1.5, H^4-bn), 8.43 (4H, d, ^4J 1.5, H^2-bn), 7.95 (4H, d, ^3J 8.0, H^3-py), 7.81 (4H, td, ^3J 7.7, ^4J 1.7, H^4-py), 7.29 (4H, ddd, ^3J 7.4, ^3J 4.8, ^4J 0.9, H^5-py). ^{13}C NMR (126 MHz, $CDCl_3$): δ 157.3 (C^2-py), 149.8 (C^6-py), 142.4 (C^3-bn), 140.7 (C^1-bn), 137.0 (C^4-py), 126.8 (C^2-bn), 125.0 (C^4-bn), 122.6 (C^5-py), 121.2 (C^3-py). MS (ES^+): *m/z* 463 $[M + H]^+$.

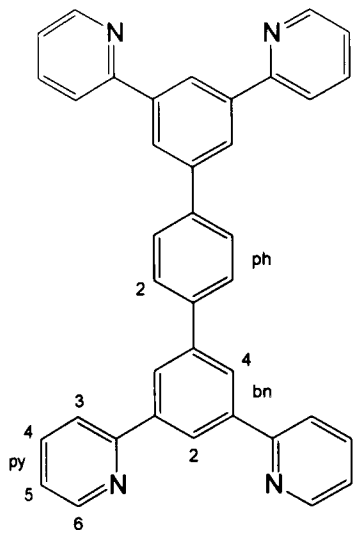

HL[15]: 1,4-Bis[1,3-di(2-pyridyl)-5-phenyl]benzene

This compound was prepared using a method similar to that of the Suzuki cross-coupling reaction outlined above, but requiring two couplings to a diboronic acid starting material. 1,3-Di(2-pyridyl)-5-bromobenzene (231 mg, 0.75 mmol), 1,4-benzene diboronic acid (61 mg, 0.37 mmol) and sodium carbonate (92 mg, 0.87 mmol) were suspended in a mixture of toluene:ethanol:water mix (6:6:1 mL respectively) and degassed *via* the freeze-pump-thaw technique. The mixture was placed under an inert atmosphere of dinitrogen and, under a steady gas flow tetrakis(triphenylphosphine)palladium(0) (24 mg, 0.021 mmol) was added. The mixture was stirred at 110°C for 24 h before the solvent was removed *in vacuo*. The solid was purified by chromatography on silica gel, elution diethyl ether (R_f = 0.2 in diethyl ether) to give a pale solid. This solid was then washed with acetone (3 x 2 mL) *via* centrifugation yielding a colourless solid when dried under reduced pressure (138 mg, 70%). ^{1}H NMR (400 MHz, $CDCl_3$): δ 8.75 (4H, d, ^3J 4.7, H^6-py), 8.60 (2H, t, ^4J 1.6, H^2-ph), 8.36 (4H, d, ^4J 1.6, H^4-ph), 7.93 (4H, d, ^3J 8.0, H^3-py), 7.89 (4H, s, H^2-bn), 7.81 (4H, td, ^3J 7.8, ^4J 1.8, H^4-py), 7.29 (4H, ddd, ^3J 7.4, ^3J 4.8, ^4J 0.6, H^5-py). ^{13}C NMR (101 MHz, $CDCl_3$): δ 157.2 (quat), 149.8 (C^6-py), 142.0 (quat), 140.6 (quat), 140.2 (quat), 137.1 (C^4-py), 127.9 (C^2-bn), 126.5 (C^4-ph), 124.8 (C^2-ph), 122.6 (C^5-py), 121.1 (C^3-py). MS (EI$^+$): 538 [M]$^+$, 460 [M – Py]$^+$.

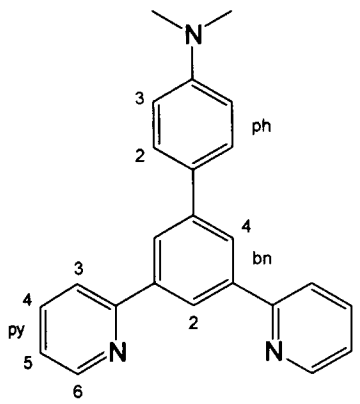

HL[16]: 5-[4-N,N-dimethylaniline]-1,3-di(2-pyridyl)benzene

This compound was prepared *via* the Suzuki cross-coupling reaction using 1,3-di(2-pyridyl)-5-benzene (381 mg, 1.23 mmol), 4-(N,N-dimethylamino)phenyl boronic acid (203 mg, 1.23 mmol), sodium carbonate (420 mg, 3.96 mmol) and tetrakis(triphenylphosphine)palladium(0) (58 mg, 0.050 mmol) suspended in a mixture of toluene:ethanol:water (3:3:1 mL respectively). The mixture was stirred at 80°C for 24 h before work-up. Purification was performed by chromatography on silica gel, gradient elution from hexane to 50:50 hexane:diethyl ether (R_f = 0.6 in diethyl ether) to give a colourless solid (55 mg, 13%). ^{1}H NMR (400 MHz, $CDCl_3$): δ 8.76 (2H, d, ^3J 5.0, H^6-py), 8.52 (1H, t, ^4J 1.5, H^2-bn), 8.28 (2H, d, ^4J 1.5, H^4-bn), 7.93 (2H, d, ^3J 8.0, H^3-py), 7.82 (2H, td, ^3J 8.0, ^4J 2.0, H^4-py), 7.71 (2H, d, ^3J 8.5, H^2-ph), 7.30 (2H, ddd, ^3J 7.5, ^3J 5.0, ^4J 1.5, H^5-py), 6.88 (2H, d, ^3J 8.5, H^3-ph), 3.03 (6H, s, CH_3). ^{13}C NMR (101 MHz, $CDCl_3$): δ 157.4 (quat), 150.0 (quat), 149.4 (C^6-py), 142.3 (quat), 140.1 (quat), 136.9 (C^4-py), 128.0 (C^2-ph), 125.6 (C^4-bn), 123.4 (C^2-bn), 122.3 (C^5-py), 121.0 (C^3-py), 112.9 (C^3-ph), 40.7 (CH_3). MS(EI^+): *m/z* 351 $[M]^+$. HRMS (ES^+): *m/z* 352.1809 $[M + H]^+$, $[C_{24}H_{22}N_3]$ requires 352.1808. Anal. Calcd. for $C_{24}H_{21}N_3$: C, 82.02; H, 6.02; N, 11.96. Found: C, 81.77; H, 5.99; N, 11.95%.

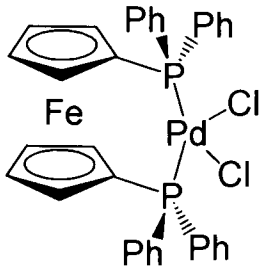

1,1'-[Bis(diphenylphosphino)]ferrocene palladium(II) dichloride

1,1'-Bis(diphenylphosphino)ferrocene (252 mg, 0.46 mmol) in a Schlenk tube under inert atmosphere was dissolved in dry, degassed toluene (10 mL). This solution

was then transferred, *via* cannular under positive pressure of dinitrogen, to the reaction vessel containing bis(acetonitrile)dichloropalladium(II) (121 mg, 0.46 mmol), under inert atmosphere. The mixture was stirred at room temperature for 24 h forming a bright orange precipitate in solution. The mixture was allowed to stand so the precipitate could settle to the bottom of the reaction vessel. The solvent was then removed using a filter cannular under positive pressure of dinitrogen, and the remaining solid was washed, in this manner, with a further quantity of dry degassed toluene (10 mL). The product, an orange solid, was dried *in vacuo* and stored in the reaction vessel under inert atmosphere. No spectral analysis of this compound was deemed necessary.

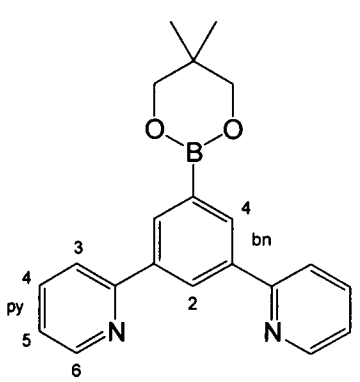

HL-B_{neo}: 1,3-Di(2-pyridyl)-5-phenylboronic acid, neopentyl ester

This compound was prepared *via* the Miyaura cross-coupling reaction outlined at the beginning of this chapter, using 1,3-di(2-pyridyl)-5-bromobenzene (110 mg 0.34 mmol), potassium acetate (118 mg, 1.20 mmol), bis(neopentyl glycolato)diboron (87 mg, 0.39 mmol) and 1,1'-[bis(diphenylphosphino)]ferrocene palladium(II) dichloride (20 mg, 0.027 mmol) in anhydrous DMSO (5 mL). The mixture was heated at 80°C for 6 h, by which time tlc showed no trace of bromo starting material. The product was obtained as a crude pale brown solid (114 mg, ~90%). ^{1}H NMR (500 MHz, $CDCl_3$): δ 8.74 (1H, t, ^{4}J 1.8, H^{2}-bn), 8.72 (2H, ddd, ^{3}J 4.9, ^{4}J 1.7, ^{5}J 0.9, H^{6}-py), 8.48 (2H, d, ^{4}J 1.8, H^{4}-bn), 7.89 (2H, dt, ^{3}J 8.0, ^{4}J 0.9, H^{3}-py), 7.76 (2H, td, ^{3}J 7.8, ^{4}J 1.9, H^{4}-py), 7.23 (2H, ddd, ^{3}J 7.4, ^{3}J 4.8, ^{4}J 1.1, H^{5}-py), 3.82 (4H, s, $-CH_2-$), 1.05 (6H, s, CH_3). ^{13}C NMR (126 MHz, $CDCl_3$): δ 157.7, 149.8 (C^{6}-py), 139.3, 136.8 (C^{4}-py), 133.1 (C^{2}-bn), 128.1 (C^{4}-bn), 122.2 (C^{5}-py), 121.0 (C^{3}-py), 72.49 (CH_2), 32.1 (C-alkyl quaternary), 22.1 (CH_3). MS (ES^+): *m/z* 345.17702 $[M + H]^+$; $[C_{21}H_{22}N_2O_2{}^{11}B]$ requires 345.17689.

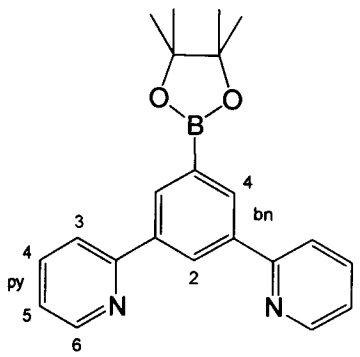

HL-B_{pin}: 1,3-Di(2-pyridyl)-5-phenylboronic acid, pinacol ester

This compound was prepared *via* the Miyaura cross-coupling reaction using 1,3-di(2-pyridyl)-5-bromobenzene (220 mg of 85% purity equivalent to 0.60 mmol), bis(pinacolato)diboron (170 mg, 0.67 mmol), potassium acetate (223 mg, 2.38 mmol) and 1,1'-bis(diphenylphosphino)ferrocene palladium(II) dichloride (50 mg, 0.06 mmol). The mixture was heated at 80°C for 24 h before work-up. Work-up was consistent with above methodology, HL-B_{neo}, yielding a brown solid (170 mg), which was used directly in the subsequent synthetic steps.

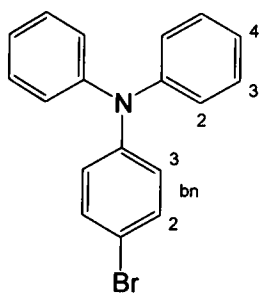

4-Bromo-N,N-diphenylaniline

This compound was prepared using the Goldberg reaction, a variation of the Ullmann coupling reaction, outlined in the literature. The following reagents were added to a degassed mixture of *m*-xylene (10 mL) and toluene (5 mL), in a two neck rbf, in the following order; diphenylamine (1.88 g, 11.1 mmol), 1-bromo-4-iodobenzene (4.73 g 16.7 mmol), 1,10-phenanthroline (72 mg, 0.40 mmol), cuprous chloride (40 mg, 0.40 mmol) and potassium hydroxide pellets (4.83 g, 86.1 mmol). The reaction was heated to reflux rapidly and stirred for a further 60 h. The reaction was allowed to cool to 75°C and partitioned between toluene (50 mL) and water (50 mL). After washing with an additional quantity of water (100 mL), the organic layer was decolourised by refluxing in the presence of aluminium oxide. The absorbents were removed by hot filtration, and the solvent removed *in vacuo*. Purification was performed by chromatography on silica gel, elution gradient hexane to 60:40 hexane:toluene (R_f = 0.8 in 60:40 hexane:toluene), yielding a

colourless solid (3.28 g, 91%).[92,295] ^{1}H NMR (400 MHz, $CDCl_3$): δ 7.34 (2H, dt, ^3J 9.1, ^4J 2.3, H^3-bn), 7.27 (4H, dd, ^3J 8.4, ^3J 7.4, H^3-ph), 7.09 (4H, dd, ^3J 8.4, ^4J 1.3, H^2-ph), 7.05 (2H, tt, ^3J 7.4, ^4J 1.3, H^4-ph), 6.96 (2H, dt, ^3J 9.1, ^4J 2.3, H^2-bn). GCMS (EI^+): 26.270 min; *m/z* 322.9 $[M]^+$, 243.0 $[M - Br]^+$.

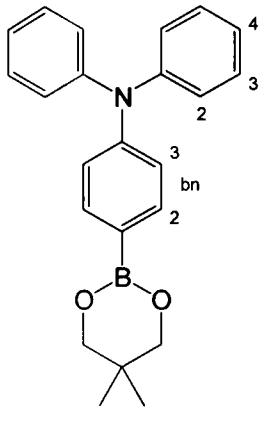

4-(N,N-Diphenylaniline)-benzeneboronic acid, neopentyl ester

This compound was prepared *via* the Miyaura cross-coupling reaction using 4-bromo-N,N-diphenylaniline (704 mg, 2.17 mmol), bis(neopenyl glycolato) diboron (549 mg, 2.43 mmol), potassium acetate (748 mg, 7.63 mmol) palladium(II)(dppf)Cl_2 (46 mg, 0.063 mmol) dissolved in DMSO (10 mL). The reaction was stirred at 80°C for 6 h before work up. The organic phase was dried over magnesium sulfate before being filtered, and the solvent removed *in vacuo*, yielding the crude product as a light brown solid (627 mg, 81 %), which was used in subsequent steps without further purification.[92] ^{1}H NMR (300 MHz, $CDCl_3$): δ 7.69 (2H, d, ^3J 6.6, H^3-bn), 7.27 (4H, t, ^3J 7.5, H^3-ph), 7.13 (4H, d, ^3J 7.5, H^2-ph), 7.06 (2H, d, ^3J 6.6, H^2-bn), 7.04 (2H, t, ^3J 5.1, H^4-ph), 3.77 (4H, s, CH_2), 1.04 (6H, s, CH_3). MS (ES^+): *m/z* 358 $[M + H]^+$.

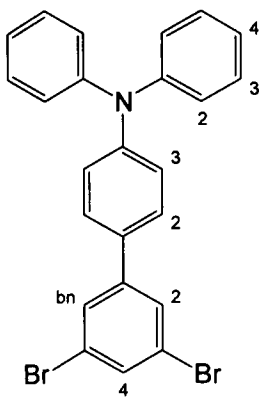

4-(3,5-dibromophenyl)-N,N-diphenylaniline

This compound was prepared *via* the Suzuki cross-coupling reaction using, 1,3,5-tribromobenzene (527 mg, 1.67 mmol), 4-(N,N-Diphenylaniline)benzene-boronic acid, neopentyl ester (627 mg, 1.75 mmol), sodium carbonate (467 mg, 4.41 mmol) and tetrakis(triphenylphosphine)palladium(0) (45 mg, 0.039 mmol) dissolved in ethylene glycol dimethyl ether (10 mL). The mixture was stirred at room temperature for 30 mins, before being stirred at 80°C for 2 d. The mixture was then allowed to cool to room temperature before being taken into DCM (100 mL) and washed with water (4 x 100 mL). The organic phase was reduced *in vacuo* and purification was performed by chromatography on silica gel, elution gradient hexane to hexane:diethyl ether (97:3 hexane:diethyl ether) yielding a pale off-white solid (342 mg, 42%). ^{1}H NMR (300 MHz, $CDCl_3$): δ 7.66 (2H, d, ^{4}J 1.8, H^4-bn), 7.62 (1H, s, H^2-bn), remaining peaks within multiplet range 7.55 – 7.45 ppm. MS (EI^+): *m/z* 479 $[M]^+$, 319 $[M - 2Br]^+$.

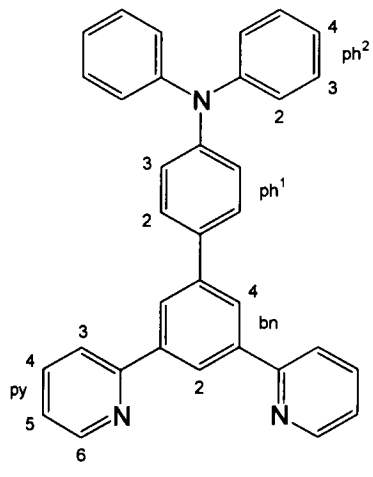

HL[17]: N, N-Diphenylamino-(N-phenyl-4')-1,3-di(2-pyridyl)benzene

Method A: Prepared using the basic methodology for the Stille cross-coupling reaction outlined in Section 8.1.1; using: 4'-(3,5-dibromobenzo)phenyl-N,N-diphenylamine (342 mg, 0.71 mmol), 2-tri-*n*-butylstannylpyridine (783 mg of 83%

purity equivalent to 1.76 mmol), lithium chloride (344 mg, 8.1 mmol), and bis(triphenylphosphine)-palladium(II) chloride (51 mg, 0.073 mmol) dissolved in toluene (10 mL). The mixture was heated at reflux for 4 d before work up. Purification was performed by chromatography on silica gel, gradient elution from hexane to 75:25 hexane:diethyl ether, leading to a colourless solid (27 mg, 8%).

Method B: Prepared *via* the Suzuki cross-coupling reaction using 1,3-di(2-pyridyl)-5-phenylboronic acid, neopentyl ester (178 mg, 0.52 mmol), 4-bromo-N,N-diphenylaniline (169 mg, 0.52 mmol), sodium carbonate (66 mg, 0.62 mmol) and tetrakis(triphenylphosphine)palladium(0) (48 mg, 0.042 mmol). The mixure was heated at 80°C for 2½ d before work-up. Purification was performed by chromatography on silica gel, gradient elution from hexane to 80:20 hexane:diethyl ether (R_f = 0.4 in 75:25 hexane:diethyl ether), followed by recrystallisation from hexane:diethyl ether yielding a colourless solid (76 mg, 31%). ^{1}H NMR (400 MHz, $CDCl_3$): δ 8.75 (2H, ddd, ^3J 4.8, ^4J 1.8, ^5J 1.0, H^6-py), 8.57 (1H, t, ^4J 1.7, H^2-bn), 8.29 (2H, ^4J 1.7, H^4-bn), 7.93 (2H, d, ^3J 8.0, H^3-py), 7.82 (2H, td, ^3J 7.8, ^4J 1.8, H^4-py), 7.66 (2H, d, ^3J 8.7, H^3-ph^2), 7.29 (6H, m, H^2-ph, H^5-py), 7.18 (2H, d, ^3J 8.7, H^2-ph^2), 7.15 (4H, m, H^3-ph), 7.04 (2H, tt, ^3J 7.3, ^4J 1.3, H^4-ph). MS (ES$^+$): *m/z* 476 [M + H]$^+$.

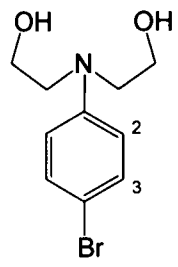

4-Bromo-N,N-bis(2-hydroxyethyl)aniline

4-Bromoaniline (4.16 g, 0.024 mol), sodium carbonate (3.06 g, 0.029 mol) and 2-chloroethanol (10 ml, 0.149 mol) were stirred at reflux (129 °C) for 4½ h. The mixture was allowed to cool to ambient temperature and separated between DCM (150 mL) and water (100 mL). The organic layer was extracted and reduced *in vacuo* yielding a dark brown solid. Separation was performed by chromatography on silica gel, elution with DCM, followed by a second column on silica gel, elution gradient 100% hexane to 100% diethyl ether. The product was isolated as a colourless solid (2.29 g, 37%). ^{1}H NMR (200 MHz, $CDCl_3$): δ 7.28 (2H, dt, ^3J 9.4, ^5J 2.3, H^3-bn), 6.55 (2H, dt, ^3J 9.2, ^5J 2.3, H^2-bn), 3.81 (4H, t, ^3J 5.0, -CH_2O-), 3.53 (6H, m, -NCH_2-, -OH). MS (ES$^+$): *m/z* 282 [M + Na$^+$]. Anal. Calcd. for

$C_{10}H_{14}BrNO_2$: C, 46.17; H, 5.42; N, 5.38. Found: C, 46.15; H, 5.41; N, 5.25%. IR (cm^{-1}): 3608 OH, 2941, 2879 $-CH_2-$, 1585, 1437, 1255.

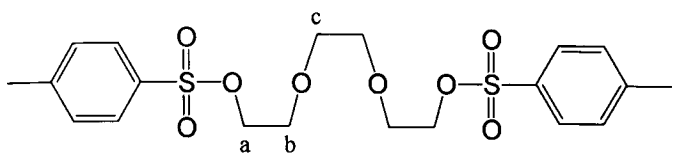

Tri(ethylene glycol) di-*p*-toluenesulfonate

Sodium hyrdroxide (5.60 g, 0.14 mol) was dissolved in water (30 mL) and cooled to 0 °C in a salt/ice bath. Tri(ethylene glycol) (6.68 mL, 50.0 mmol) was dissolved in a mixture of THF (40 mL) and water (10 mL) and added to the reaction, which was allowed to cool back to below 0°C. *p*-Toluenesulfonylchloride (10.8 g, 52.9 mmol) dissolved in THF (40 mL) was added dropwise to the reaction over 4 h. The mixture was then stirred for a further 3 h with the temperature maintained at 0°C, or below, for the entire reaction. The reaction was monitored by thin layer chromatography to confirm the complete consumption of the starting material *p*-toluenesulfonylchloride. The mixture was diluted with water (50 mL), ice (50 g) and toluene (50 mL) and the two phases were separated once the ice had thawed. The organic layer was washed with water (2 x 50 mL), dried over a large quantity of $CaCl_2$, stirred vigorously, filtered and dried *in vacuo* yielding a colourless solid (16.6 g, 73%). At this stage the product was observed to contain minor quantities (> 1%) of the mono-substituted tri(ethylene glycol product), which could easily be removed by chromatography on silica gel, elution gradient 100% hexane to 100% diethyl ether (R_f = 0.8 in diethyl ether).[221] ^{1}H NMR (200 MHz, $CDCl_3$): δ 7.79 (4H, d, ^3J 8.3, H^2-bn), 7.34 (4H, d, ^3J 8.3, H^3-bn), 4.14 (4H, t, ^3J 4.5, H_a), 3.65 (4H, t, ^3J 4.5, H_b), 3.52 (4H, s, H_c), 2.47 (6H, s, CH_3). MS (ES^+): *m/z* 481 $[M + Na]^+$. IR (cm^{-1}): 2926, 1604, 1359, 1190, 1020. Anal. Calcd. for $C_{20}H_{26}O_8S_2$: C, 52.39; H, 5.72. Found: C, 55.22; H 5.74%.

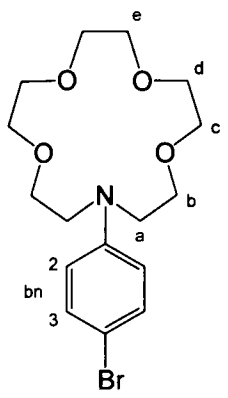

4-Bromo-phenyl-N-monoaza-15-crown-5

The reaction was based on literature procedures.[221] All glassware was dried in an oven for at least one day prior to the start of the reaction. While still hot from the oven the apparatus was evacuated under high vacuum and back-filled with dinitrogen three times. A large excess of sodium hydride (400 mg, 16.7 mmol) was suspended in anhydrous THF (20 mL) and treated with 4-bromo-N,N-bis(2-hydroxyethyl)aniline (525 mg, 2.02 mmol) in anhydrous THF (10 mL), transferred by cannular under positive pressure of dinitrogen. The mixture, stirred at room temperature, was then treated with tri(ethylene glycol)-di-*p*-tolylsulfonate (821 mg, 1.79 mmol) dissolved in anhydrous THF (15 mL), again transferred by cannular. The mixture was then stirred at 40°C for 3 d when complete consumption of the starting materials was observed by GC analysis. The reaction was then taken into DCM (100 mL) and any solid removed by filtration, and the organic solution was evaporated *in vacuo* to a light coloured oil. Purification was performed by chromatography on aluminium oxide; elution gradient 100% hexane to 50:50 hexane:ethyl acetate mix (R_f = 0.8 in ethyl acetate). The product was isolated as a colourless solid (256 mg, 34%). ^{1}H NMR (500 MHz, $CDCl_3$): δ 7.26 (2H, d, ^3J 9.0, H^3-ph), 6.53 (2H, d, ^3J 8.7, H^2-ph), 3.73 (4H, ^3J 6.2, H^b), 3.66 (8H, m, H^c, H^d), 3.63 (4H, s, H^e), 3.56 (4H, t, ^3J 6.2, H^a). ^{13}C NMR (126 MHz, $CDCl_3$): δ 146.65 (C^1-ph), 131.93 (C^3-ph), 113.17 (C^2-ph), 107.59 (C^4-ph), 71.39 (C^c or C^d), 70.29 (C^e), 70.18 (C^c or C^d), 68.39 (C^b), 52.68 (C^a). MS (ES^+): *m/z* 374 $[M + H]^+$, 396 $[M + Na]^+$. HRMS (ES^+): *m/z* 374.09626, $[C_{16}H_{25}O_4N^{79}Br]$ requires 374.09615. Anal. Calcd. for $C_{16}H_{24}NO_4Br$: C, 51.35; H, 6.46; N, 3.74. Found: C, 51.38; H 6.55; N, 3.59%.

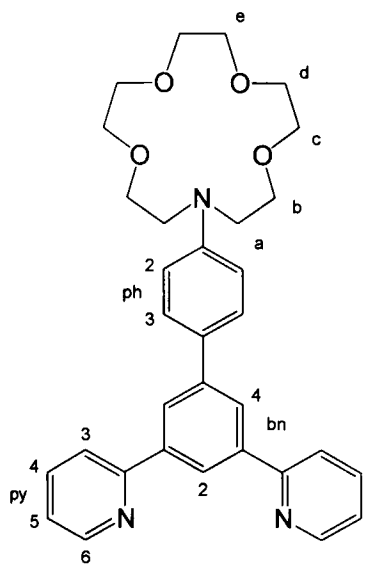

HL[18]: 4-(1,3-di(2-pyridyl)-5-phenyl)-phenyl-N-monoaza-15-crown-5

This compound was prepared *via* the Suzuki cross-coupling reaction using, 4-bromophenyl-N-monoaza-15-crown-5 (93 mg, 0.25 mmol), 3,5-di(2-pyridyl)-benzeneboronate ester (154 mg, 0.45 mmol), sodium carbonate (37 mg, 0.35 mmol) and tetrakis(triphenylphosphine)palladium(0) (34 mg, 0.029 mmol) in a mixture of toluene:ethanol:water (3:3:1 mL respectively). The mixture was heated at 80ºC for 3 d before work up. The product was purified by chromatography on aluminium oxide, gradient elution from hexane to 70:30 hexane:ethyl acetate (R_f = 0.8 in ethyl acetate) yielding a clear oil (122 mg, 88%). ^{1}H NMR (300 MHz, $CDCl_3$): δ 8.73 (2H, d, ^3J 4.6, H^6-py), 8.48 (1H, t, ^4J 1.6, H^2-bn), 8.23 (2H, d, ^4J 1.6, H^4-bn), 7.88 (2H, d, ^3J 7.9, H^3-py), 7.78 (2H, td, ^3J 7.9, ^4J 1.7, H^4-py), 7.65 (2H, d, ^3J 8.8, H^3-ph), 7.26 (2H, ddd, ^3J obscured, ^3J 5.0, ^4J 1.1, H^5-py), 6.76 (2H, d, ^3J 8.8, H^2-ph), 3.80 (4H, t, ^3J 6.0, H^b), 3.66 (16H, m, H^a, H^c, H^d, H^e). MS (ES^+): *m/z* 547 $[M + Na]^+$, 526 $[M + H]^+$.

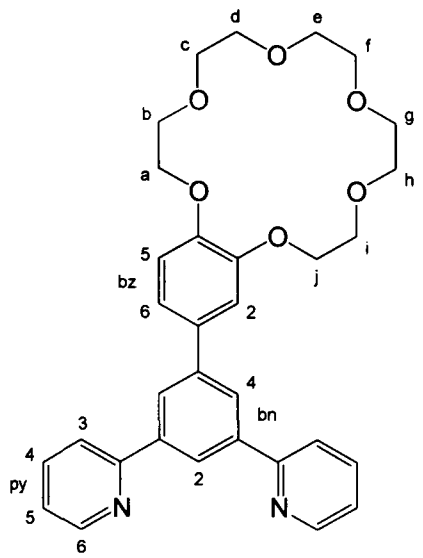

HL[19]: 1,3-Di(2-pyridyl)-benzene-5-(4'-benzo-18-crown-6)

This compound was prepared *via* the Suzuki cross-coupling reaction using 1,3-di(2-pyridyl)-5-phenylboronic acid, neopentyl ester (284 mg, 0.83 mmol), 4'-bromobenzo-18-crown-6 (337 mg, 0.86 mmol), sodium carbonate (119 mg, 1.12 mmol) and tetrkis(triphenylphosphine)palladium(0) (38 mg, 0.033 mmol) all suspended in a mixture of toluene:ethanol:water (6:6:1 mL). The mixture was heated at 80°C for 3½ days before work-up. Purification was performed by chromatography on aluminium oxide, gradient elution from hexane to ethyl acetate (R_f = 0.3 in ethyl acetate) yielding a clear, colourless oil (192 mg, 43%). ^{1}H NMR (500 MHz, $CDCl_3$): δ 8.74 (2H, d, ^3J 4.3, H^6-py), 8.53 (1H, t, ^4J 1.5, H^2-bn), 8.23 (2H, d, ^4J 1.5, H^4-bn), 7.89 (2H, d, ^3J 7.8, H^3-py), 7.79 (2H, td, ^3J 8.0, ^4J 1.7, H^4-py), 7.28 (4H, m, H^3-bz, H^5-bz, H^5-py), 6.98 (1H, d, ^3J 8.0, H^6-bz), 4.28 (2H, t, ^3J 4.3, H^j), 4.22 (2H, t, ^3J 4.3, H^a), 3.96 (4H, t, ^3J 4.3, H^b, H^i), 3.80 (4H, m, H^c, H^h), 3.74 (4H, m, H^d, H^g), 3.70 (4H, s, H^e, H^f). ^{13}C NMR (126 MHz, $CDCl_3$): δ 157.4, 149.8, 149.3, 149.0, 142.2, 140.5, 137.0, 134.6, 126.3 (C^4-bn), 124.2 (C^2-bn), 122.5 (C^5-py), 121.1 (C^3-py), 120.6, 114.5 (C^6-bz), 113.9 (C^3-bz), 71.0, 71.0, 70.9, 69.9, 69.8, 69.6 (C^J), 69.4 (C^A). HRMS (ES^+): *m/z* 543.24895 $[M + H]^+$, $[C_{32}H_{35}N_2O_6]$ requires 543.24896; *m/z* 565.23048 $[M + Na]^+$, $[C_{32}H_{34}O_6N_2{}^{23}Na]$ requires 565.23090.

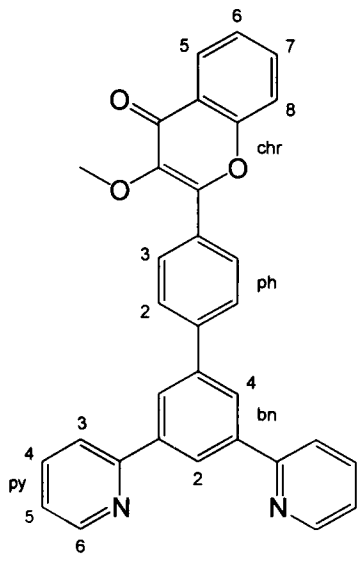

HL^{20}: 1,3-Di(2-pyridyl)-5-[4'-phenyl-(3"-methoxychrom-4"-one)]benzene

This compound was prepared *via* the Suzuki cross-coupling reaction using 1,3-di(2-pyridyl)-5-phenylboronic acid, pinacol ester (170 mg of crude material, estimated at 0.3 mmol by NMR analysis), 2-(4-bromophenyl)-3-methoxychrom-4-one (97 mg, 0.29 mmol), sodium carbonate (62 mg, 0.60 mmol) and tetrakis(triphenylphosphine)palladium(0) (54 mg, 0.047 mmol) all suspended in a mixture of toluene:ethanol:water (4:4:1 mL). Work-up was performed by dissolving the crude product in DCM (50 mL), washing with distilled water (3 x 30 mL), and removal of the solvent *in vacuo*. The crude material was purified by chromatography on silica gel, elution pentane to diethyl ether yielding a pale yellow solid (43 mg, 34%). Further purification by recrystallisation from acetonitrile yielded a white solid (30 mg, 24%). ^{1}H NMR (500 MHz, $CDCl_3$): δ 8.74 (2H, dd, ^{3}J 4.8, ^{4}J 1.6, H^{6}-py), 8.62 (1H, t, ^{4}J 1.6, H^{2}-bn), 8.38 (2H, d, ^{4}J 1.6, H^{4}-bn), 8.27 (1H, dd, ^{3}J 8.0, ^{4}J 1.5, H^{5}-chr), 8.23 (2H, d, ^{3}J 8.5, H^{2}-ph), 7.91 (4H, m, H^{3}-ph, H^{3}-py), 7.79 (2H, td, ^{3}J 7.8, ^{4}J 1.7, H^{4}-py), 7.67 (1H, ddd, ^{3}J 8.3, ^{3}J 7.0, ^{4}J 1.5, H^{7}-chr), 7.56 (1H, d, ^{3}J 8.3, H^{8}-chr), 7.39 (1H, td, ^{3}J 8.0, ^{4}J 0.9, H^{6}-chr), 7.27 (2H, ddd, ^{3}J 5.6, ^{3}J 4.8, ^{4}J 0.9, H^{5}-py), 3.93 (3H, s, CH_3). ^{13}C NMR (126 MHz, $CDCl_3$): δ 175.20 (quat), 157.07 (quat), 155.43 (quat), 155.41 (quat), 149.90 (C^{6}-py), 143.28 (quat), 141.79 (quat), 141.33 (quat), 140.78 (quat), 136.97 (C^{4}-py), 130.17 (quat), 129.08 (C^{2}-ph), 127.58 (C^{3}-ph), 126.49 (C^{4}-bn), 125.97 (C^{6}-chr), 125.20 (C_2-bn), 124.79 (C^{5}-chr), 124.40 (quat), 122.63 (C_5-py), 120.95 (C_3-py), 118.15 (C_3-chr), 60.22 (CH_3). MS (ES^+): *m/z* 483.2 $[M + H]^+$. HRMS (ES^+): *m/z* 483.16926 $[M + H]^+$; $[C_{32}H_{23}N_2O_3]$ requires 483.17032.

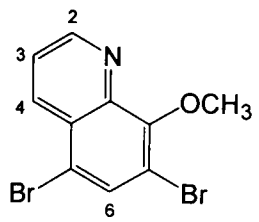

5,7-Dibromo-8-methoxyquinoline

5,7-Dibromo-8-hydroxyquinoline (1.43 g, 4.7 mmol) and tri-*n*-butyl ammonium bromide were suspended in DCM (25 mL) to give a colourless solution. Aqueous sodium hydroxide (610 mg, 15.3 mmol, 10 mL) was added to the DCM mixture and stirred for 1 h, producing a bright green colour. Dimethyl sulfate (902 mg, 7.2 mmol) was added to the reaction dropwise over 1 h and stirred for a further 3 h. The reaction was observed to change colour, from green through red to purple. Concentrated ammonia (4 mL) was added and stirred for 30 min to remove any excess dimethyl sulfate. The crude product was washed with aqueous $NaHCO_3$ (5% by mass, 50 mL) and passed through a small portion of aluminium oxide with DCM eluant (R_f = 0.6 in 50:50 hexane:diethyl ether). The product was isolated as a colourless solid (1.09 g, 73%). ^{1}H NMR (200 MHz, $CDCl_3$): δ 8.98 (1H, d, ^3J 4.0, H^2), 8.49 (1H, d, ^3J 8.6, H^4), 8.00 (1H, s, H^6), 7.55 (1H, dd, ^3J 8.5, ^4J 4.1, H^3), 4.17 (3H, s, CH_3). MS (EI^+): *m/z* 317 $[M]^+$, 288 $[M - OCH_3]^+$.

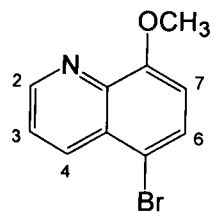

5-Bromo-8-methoxyquinoline

Based on literature precedent,[296] 5,7-dibromo-8-methoxyquinoline (1.64 g, 5.18 mmol) was dissolved in anhydrous diethyl ether (80 mL) and stirred at -75 °C. The mixture was treated dropwise with phenyl lithium (5.2 mL, 2.0 $mol.dm^{-3}$, 10.4 mmol). Maintaining reaction temperature at -75 °C, the mixture was stirred for a further 3 h, whereup it was then treated with 1 M HCl (10 mL) and stirred for a further 2 h at -75 °C. Concentrated HCl (12 M, 4 mL) was added to the mixture which was slowly allowed to warm to ambient temperature. The solvent was removed *in vacuo* yielding an orange solid, which was partitioned between DCM (50 mL) and water (50 mL). The aqueous phase was washed with additional quantities of DCM (2 x 50 mL), the organic layers were combined and the solvent evaporated *in vacuo*. Purification was performed by chromatography on silica gel,

gradient elution DCM to 98:2 DCM:methanol (R_f = 0.6 in diethyl ether). The product was isolated as a pale brown solid (639 mg, 52%). ^{1}H NMR (400 MHz, $CDCl_3$): δ 8.94 (1H, dd, ^3J 4.2, ^4J 1.5, H^2), 8.48 (1H, dd, ^3J 8.6, ^4J 1.5, H^4), 7.72 (1H, d, ^3J 8.4, H^6), 7.53 (1H, dd, ^3J 8.6, ^3J 4.2, H^3), 6.92 (1H, d, ^3J 8.4, H^7), 4.07 (3H, s, CH_3). MS (ES^+): 238 $[M + H]^+$.

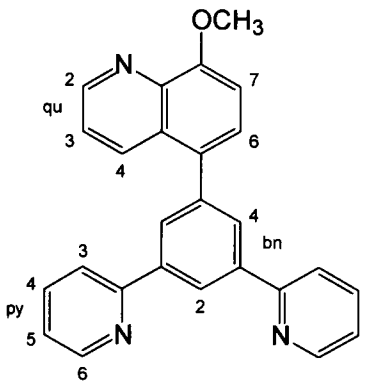

HL^{21}: 5-(1,3-Di(2-pyridyl)-5-phenyl)-8-methoxyquinoline

This compound was prepared *via* the Suzuki cross-coupling reaction using 1,3-di(2-pyridyl)-5-phenylboronic acid, neopentyl ester (245 mg, 0.71 mmol), 5-bromo-8-methoxyquinoline (162 mg, 0.68 mmol), sodium carbonate (121 mg, 1.14 mmol) and tetrakis(triphenylphosphine)palladium(0) (70 mg, 0.061 mmol) all suspended in a mixture of toluene:ethanol:water (6:6:1 mL respectively). The mixture was heated at 80°C for 24 h before work up. Purification was performed by chromatography on silica gel, elution gradient from DCM to 97:3 DCM:methanol followed by recrystallisation from ethanol yielding a white solid (73 mg, 26%). ^{1}H NMR (500 MHz, $CDCl_3$): δ 8.95 (1H, dd, ^3J 4.0, ^4J 1.3, H^2-qu), 8.72 (2H, d, ^3J 4.7, H^6-py), 8.67 (1H, t, ^4J 1.6, H^2-bn), 8.30 (1H, dd, ^3J 8.6, ^4J 1.4, H^4-qu), 8.12 (2H, d, ^4J 1.6, H^4-bn), 7.87 (2H, d, ^3J 7.9, H^3-py), 7.77 (2H, td, ^3J 7.8, ^4J 1.6, H^4-py), 7.56 (1H, d, ^3J 7.9, H^6-qu), 7.39 (1H, dd, ^3J 8.6, ^3J 4.0, H^3-qu), 7.26 (2H, obscured by $CHCl_3$ resonance, H^5-py), 7.13 (1H, d, ^3J 7.9, H^7-qu), 4.14 (3H, s, CH_3). ^{13}C NMR (126 MHz, $CDCl_3$): δ 157.0, 155.1, 149.8 (C^6-py), 149.2 (C^2-qu), 140.6, 140.3, 137.0 (C^4-py), 134.5, 132.0, 129.4, 127.8, 127.7 (C^6-qu), 124.7 (C^2-bn), 122.6 (C^5-py), 121.9 (C^3-qu), 121.1 (C^3-py), 107.2 (C^7-qu), 56.3 (CH_3). MS (ES^+): *m/z* 390 $[M + H]^+$. HRMS (ES^+): *m/z* 390.15992 $[M + H^+]$, $[C_{26}H_{20}N_3O]$ requires 390.16009; *m/z* 412.14177 $[M + Na]^+$, $[C_{26}H_{19}N_3O^{23}Na]$ requires 412.14203.

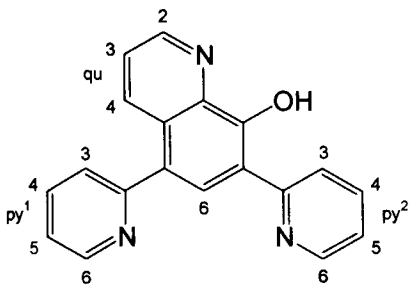

HL[22]: 8-Hydroxy-5,7-di(2-pyridyl)quinoline

This compound was prepared *via* the Stille cross-coupling reaction using 5,7-dibromo-8-hydroxyquinoline (303 mg, 1.00 mmol), 2-tri-*n*-butylstannyl-pyridine (1.466 g of 63% purity, equivalent to 2.50 mmol), lithium chloride (342 mg, 8.07 mmol), and bis(triphenylphosphine)palladium(II) chloride (51 mg, 0.073 mmol) all suspended in toluene (4 mL). The mixture was stirred at reflux for 30 h before work-up. Partial separation was performed by chromatography on silica gel, gradient elution from diethyl ether to 85:15 diethyl ether:methanol (R_f = 0.1 in 95:5 DCM:methanol), leading to the crude product, a brown oil (7 mg, 2%). Larger yields of this product could be obtained from reacting 5,7-dibromo-8-methoxyquinoline in a similar fashion, where deprotection yields this compound as a major product of the reaction. ^{1}H NMR (400 MHz, $CDCl_3$): δ 9.00 (1H, dd, ^3J 4.2, ^4J 1.7, H^2-qu), 8.80 (1H, ddd, ^3J 4.8, ^4J 1.7, ^5J 0.9, H^6-py^1), 8.65 (1H, ddd, ^3J 5.0, ^4J 1.8, ^5J 0.8, H^6-py^2), 8.55 (1H, dd, ^3J 8.6, ^4J 1.7, H^4-qu), 8.16 (1H, s, H^6-qu), 8.11 (1H, d, ^3J 8.5, H^3-py^1), 7.90 (1H, td, coupling obscured, H^4-py^1), 7.86 (1H, td, ^3J 8.1, ^4J 1.9, H^4-py^2), 7.62 (1H, d, ^3J 7.9, H^3-py^2), 7.46 (1H, dd, ^3J 8.6, ^3J 4.2, H^3-qu), 7.35 (1H, ddd, ^3J 7.6, ^3J 4.9, ^4J 1.1, H^5-py^1), 7.32 (1H, ddd, ^3J 7.6, ^3J 5.1, ^4J 1.0, H^5-py^2). MS (ES$^+$): *m/z* 300 [M + H]$^+$.

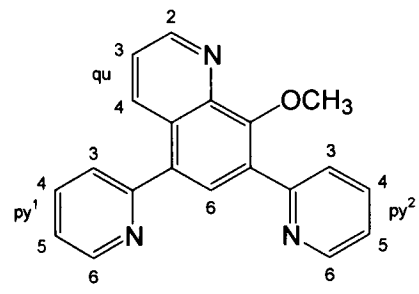

HL[23]: 8-Methoxy-5,6-di(2-pyridyl)-quinoline

Crude 8-hydroxy-5,7-di(2-pyridyl)quinoline (459 mg, 1.53 mmol) and phase transfer agent tri-*n*-butyl ammonium bromide (53 mg, 0.16 mmol) were suspended in DCM (10 mL). Aqueous sodium hydroxide (223 mg, 5.57 mmol, 5 mL) was added to the mixture and stirred for 1 h at RT. Dimethyl sulfate (471 mg, 3.74 mmol) was added

to the mixture dropwise over 1 h and stirred for a further 3 h, accompanied by a colour change. Concentrated ammonia (4 mL) was then added and stirred for 1 h. Purification was attempted by two separate chromatographic columns on silica gel, elution gradient DCM to 95:5 DCM:methanol (R_f = 0.9 in 95:5 DCM:methanol), yielding only the crude product as a dark solid (36 mg, 4%). No further product purification was attempted. ^{1}H NMR (400 MHz, $CDCl_3$): δ 9.01 (1H, dd, ^3J 4.0, ^4J 1.6 H^2-qu), 8.76 (2H, m, H^6-py^1, H^6-py^2), 8.63 (1H, dd, ^3J 8.6, ^4J 1.6, H^4-qu), 8.24 (1H, s, H^6-qu), 8.20 (1H, d, ^3J 8.0, H^3-py^1), 7.84 (1H, td, ^3J 7.6, ^4J 1.7, H^4-py^1), 7.81 (1H, td, ^3J 7.7, ^4J 1.9, H^4-py^2), 7.68 (1H, d, ^3J 8.0, H^3-py^2), 7.45 (1H, dd, ^3J 8.6, ^3J 4.0, H^3-qu), 7.33 (1H, ddd, ^3J 7.5, ^3J 4.8, ^4J 1.1, H^5-py^1), 7.28 (1H, ddd, ^3J 7.3, ^3J 4.8, ^4J 1.1, H^5-py^2), 4.02 (3H, s, CH_3).

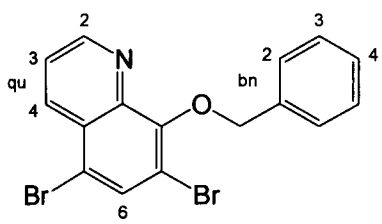

5,7-Dibromo-8-benzyloxyquinoline

5,7-Dibromo-8-hydroxyquinoline (1.00 g, 3.30 mmol) was dissolved in absolute ethanol (25 mL) and treated with potassium hydroxide pellets (205 mg, 3.66 mmol). The mixture was stirred at RT for 1 h creating a viscous suspension. Benzyl bromide (570 mg, 3.30 mmol) diluted in absolute ethanol (2 mL) was added and the mixture was stirred at reflux (78°C) for 15 h. After cooling to ambient temperature the solvent was removed *in vacuo*, the solid from which was taken into DCM (50 mL) and washed with $NaOH_{(aq)}$ (2 M, 2 x 25 mL). The organic layer was retained and the solvent evaporated *in vacuo*. Purification was performed by chromatography on silica gel, gradient elution from hexane to hexane:diethyl ether mix (75:25 hexane:diethyl ether). The product was isolated as a colourless solid (1.19 g, 92%). ^{1}H NMR (400 MHz, $CDCl_3$): δ 9.00 (1H, dd, ^3J 4.2, ^4J 1.6, H^2-qu), 8.51 (1H, dd, ^3J 8.5, ^4J 1.7, H^4-qu), 8.00 (1H, s, H^6-qu), 7.63 (2H, d, ^3J 7.3, H^2-bn), 7.57 (1H, dd, ^3J 8.5, ^3J 4.2, H^3-qu), 7.37 (3H, m, H^3 & H^4-bn), 5.48 (2H, s, -CH_2-). ^{13}C NMR (101 MHz, $CDCl_3$): δ 152.41, 150.83, 137.11, 136.48, 133.92, 128.96, 128.58, 128.46, 128.30, 122.74, 116.59. MS (ES^+): *m/z* 394 $[M + H]^+$.

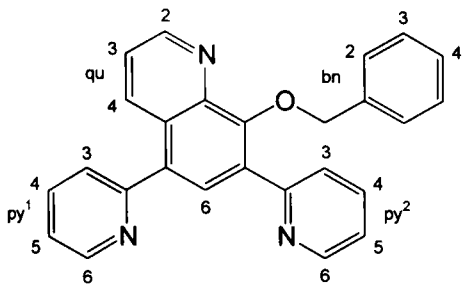

HL^{24}: 8-Benzyloxy-5,7-di(2-pyridyl)quinoline

Method A: This compound was prepared *via* the Stille cross-coupling using 8-benzyloxy-5,7-dibromoquinoline (938 mg, 2.39 mmol), 2-tri-*n*-butylstannylpyridine (2.88g of 73% purity, equivalent to 5.71 mmol), lithium chloride (811 mg, 19.1 mmol), and bis(triphenylphosphine)palladium(II) chloride (150 mg, 0.21 mmol) all suspended in toluene (20 mL). The mixture was stirred at 95°C for 24 h before work-up. Small samples (1 mL) were removed from the reaction under a positive flow of dinitrogen at regular intervals and analysed by GC. Heating was stopped when no trace of the starting material 8-benzyloxy-5,7-dibromoquinoline was detectable by GC. Addition of $KF_{(aq)}$ was omitted from the standard work-up, and purification was performed by chromatography on silica gel, gradient elution from hexane to 100% diethyl ether to diethyl ether:methanol mix (97:3 diethyl ether:methanol) yielding a light brown solid (203 mg, 29%; yield calculated with consideration for 5 mL of reaction removed for GC analysis). Among the side products was 8-benzyloxy-5-bromo-7-(2-pyridyl)quinoline (141 mg, 15%). ^{1}H NMR (500 MHz, $CDCl_3$): δ 9.08 (1H, dd, ^3J 3.9, ^4J 1.4, H^2-qu), 8.81 (1H, d, ^3J 4.9, H^6-py^1), 8.72 (1H, d, ^3J 5.0, H^6-py^2), 8.70 (1H, dd, ^3J 8.6, ^4J 1.4, H^4-qu), 8.21 (1H, s, H^6-qu), 8.15 (1H, d, ^3J 7.9, H^3-py^2), 7.88 (1H, td, ^3J 7.7, ^4J 1.8, H^4-py^1), 7.74 (2H, m, H^3-py^1, H^4-py^2), 7.51 (1H, dd, ^3J 8.5, ^4J 4.0, H^3-qu), 7.37 (1H, dd, ^3J 7.0, ^4J 4.8, H^5-py^1), 7.28 (6H, m, H^2-bn, H^3-bn, H^4-bn, H^5-py^2), 5.36 (2H, s, CH_2). ^{13}C NMR (126 MHz, $CDCl_3$): δ 157.2 (quat), 154.5 (quat), 152.0 (quat), 148.9 (C^2-qu), 148.5 (C^6-py^2), 148.4 (C^6-py^1), 142.8 (quat), 136.2 (quat), 136.0 (C^4-py^1), 135.0 (C^4-py^2), 133.9 (C^4-qu), 133.3 (quat), 131.4 (quat), 129.0 (C^6-qu), 127.8 (C^3-bn), 127.2 (C^2-bn), 127.1 (quat), 127.0 (C^4-bn), 125.6 (C^3-py^2), 124.1 (C^3-py^1), 121.3 (C^5-py^1), 121.3 (C^5-py^2), 121.0 (C^3-qu), 76.3 (CH_2). HRMS (ES^+): *m/z* 390.1629 $[M + H]^+$; $[C_{26}H_{20}N_3O]$ requires 390.1606.

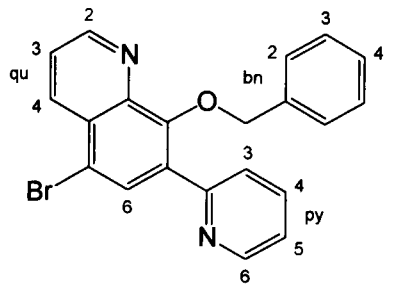

8-Benzyloxy-5-bromo-7-(2-pyridyl)quinoline

^{1}H NMR (500 MHz, $CDCl_3$): δ 9.01 (1H, d, ^{3}J 3.6, H^2-qu), 8.79 (1H, d, ^{3}J 4.9, H^6-py), 8.55 (1H, d, ^{3}J 8.6, H^4-qu), 7.88 (1H, td, ^{3}J 7.7, ^{4}J 0.8, H^4-py), 7.85 (1H, s, H^6-qu), 7.68 (1H, d, ^{3}J 7.6, H^2-bn), 7.59 (1H, d, ^{3}J 8.0, H^3-py), 7.46 (1H, dd, ^{3}J 8.6, ^{3}J 4.3, H^3-py), 7.36 (4H, m, H^3-bn, H^4-bn, H^5-py), 5.54 (2H, s, CH_2). ^{13}C NMR (126 MHz, $CDCl_3$): δ 156.8 (quat), 152.8 (quat), 150.1 (C^2-qu), 149.7 (C^6-py), 143.7 (quat), 137.3 (quat), 137.3 (C^4-py), 135.3 (C^4-qu), 135.0 (quat), 132.1 (C^6-qu), 128.9 (C^2-bn), 128.5 (C^4-bn), 128.3 (C^3-bn), 127.3 (quat), 125.1 (C^3-py), 122.8 (C^5-py), 121.9 (C^3-qu), 116.8 (quat). MS (ES^+): *m/z* 393 $[M + H]^+$.

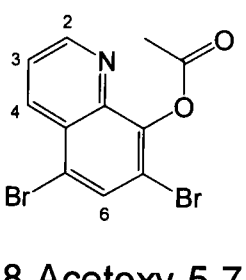

8-Acetoxy-5,7-dibromoquinoline

The overall reaction is known as the Schotten-Baumann reaction,[297,298] and was based on literature procedures.[299,300] 5,7-Dibromo-8-hydroxyquinoline (1.01 g, 3.30 mmol) was dissolved in DCM (20 mL) and treated with acetyl bromide (398 mg, 3.24 mmol). The mixture was stirred at RT for 13 h. The mixture was then washed with water (3 x 25 mL), the organic phase was retained, dried over anhydrous potassium carbonate, filtered and dried *in vacuo*. Purification was performed by chromatography on silica gel, gradient elution from hexane to 50:50 hexane:diethyl ether (R_f = 0.7 in diethyl ether) yielding a light yellow solid (560 mg, 49%). ^{1}H NMR (200 MHz, $CDCl_3$): δ 8.94 (1H, dd, ^{3}J 4.2, ^{4}J 1.2, H^2), 8.50 (1H, dd, ^{3}J 8.6, ^{4}J 1.3, H^4), 8.04 (1H, s, H^6), 7.56 (1H, dd, ^{3}J 8.6, ^{3}J 4.2, H^3), 2.54 (3H, s, CH_3). MS (ES^+): *m/z* 346 $[M^+]$. IR (cm^{-1}): 1777 C=O stretch, acetyl bromide 1790 cm-1.[301]

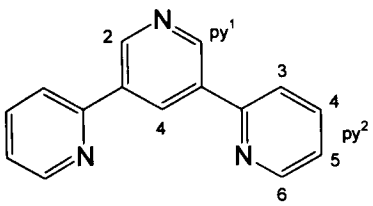

HL[26]: 4,6-Di(2-pyridyl)pyridine

This compound was prepared *via* the Stille cross-coupling reaction using 3,5-dibromopyridine (1.29 g, 5.43 mmol), 2-tri-*n*-butylstannylpyridine (6.40 g of 92% purity, equivalent to 13.6 mmol), lithium chloride (2.27 g, 53.5 mmol), and bis(triphenylphosphine)palladium(II) chloride (232 mg, 0.34 mmol) in toluene (20 mL). The mixture was heated at reflux for 3 d before work up. Purification was performed by chromatography on silica gel, gradient elution from hexane through 100% diethyl ether through 100% DCM and back to diethyl ether 100% (R_f = 0.2 in diethyl ether). The product was isolated as a pale light yellow solid (806 mg, 64%). ^{1}H NMR (400 MHz, $CDCl_3$): δ 9.25 (2H, d, ^4J 2.2, H^2-py^1), 8.94 (1H, t, ^4J 2.2, H^4-py^1), 8.75 (2H, dd, ^3J 4.8, ^4J 1.7, H^6-py^2), 7.86 (2H, d, ^3J 7.9, H^3-py^2), 7.81 (2H, td, ^3J 7.7, ^4J 1.7, H^4-py^2), 7.31 (2H, ddd, ^3J 7.3, ^3J 4.8, ^4J 1.4, H^5-py^2). ^{13}C NMR (101 MHz, $CDCl_3$): δ 154.7 (quat), 150.2 (C^6-py^2), 148.4 (C^2-py^1), 137.2 (C^4-py^2), 135.0 (quat), 132.8 (C^4-py^1), 123.1 (C^5-py^2), 121.0 (C^3-py^2). HRMS (ES^+): *m/z* 234.10265 $[M + H]^+$; $[C_{15}H_{12}N_3]$ requires 234.10257.

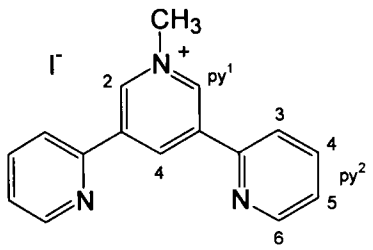

N-Methyl-3,5-di(2-pyridyl)pyridinium iodide

3,5-Di(2-pyridyl)pyridine (95 mg, 0.41 mmol) was dissolved in acetonitrile (1 mL), treated with iodomethane (26 µL, 0.42 mmol) and stirred at room temperature for 90 min, followed by 2½ d at 50°C. The precipitate was removed *via* centrifuge and dried *in vacuo*, yielding a cream solid (109 mg, 71%). ^{1}H NMR (500 MHz, $CDCl_3$): δ 9.99 (2H, d, ^4J 1.4, H^2-py^1), 9.74 (1H, t, ^4J 1.5, H^4-py^1), 8.77 (2H, ddd, ^3J 4.7, ^4J 1.7, ^5J 0.9, H^6-py^2), 8.51 (2H, dt, ^3J 8.0, ^4J 0.9, H^3-py^2), 8.00 (2H, td, ^3J 7.6, ^4J 1.7, H^4-py^2), 7.49 (2H, ddd, ^3J 7.6, ^3J 4.7, ^4J 1.0, H^5-py^2), 4.93 (3H, s, CH_3). ^{13}C NMR (126 MHz, $CDCl_3$): δ 150.5, 149.3, 142.8, 139.9, 139.3 (C^4-py^1), 138.4 (C^4-py^2), 125.7 (C^5-py^2), 122.8 (C^3-py^2), 50.0 (CH_3). MS (ES^+): *m/z* 248 $[M - I]^+$.

The hexafluorophosphate salt of this compound can be prepared by dissolving the compound in DCM (minimal amount) and adding dropwise to a saturated aqueous solution of potassium hexafluorophosphate. The product, a colourless solid, is isolated in quantitative yields by centrifugation.

8.2.2. Mercury(II) complexes

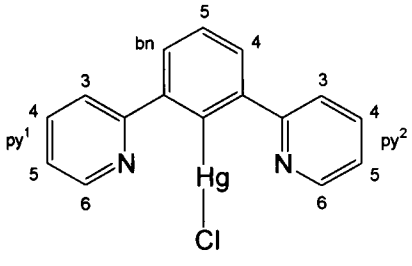

L^1HgCl: 1,3-Di(2-pyridyl)benzene-2-mercury(II) chloride

This compound was prepared according to literature methods.[252] 1,3-Di(2-pyridyl)-benzene (240 mg, 1.03 mmol) was added to absolute ethanol (20 mL) containing mercury(II) acetate (320 mg, 1.0 mmol). The mixture was degassed *via* the freeze-pump-thaw technique and placed under an atmosphere of dinitrogen before being heated at reflux (78°C) for 24 h. Afterwards, a degassed solution of lithium chloride (94 mg, 2.22 mmol) in methanol (15 mL) was added to the mixture, *via* cannular under positive pressure of dinitrogen, and the mixture was refluxed for a further 15 min. The solution was allowed to cool to ambient temperature before being added to water (100 mL), yielding a colourless precipitate. The solid was collected by filtration, washed with distilled water (2 x 20 mL) and ice cold methanol (2 x 5 mL). The solid was taken into DCM, filtered, and reduced *in vacuo* yielding a colourless solid (361 mg, 75%). Data were consistent with previously reported.[252] ^{1}H NMR (500 MHz, $CDCl_3$): δ 8.72 (2H, d, ^3J 4.8, H^6-py), 7.98 (2H, d, ^3J 7.7, $^4J(^{199}Hg)$ 69.2, H^4-bn), 7.87 (2H, d, ^3J 8.1, H^3-py), 7.80 (2H, td, ^3J 7.8, ^4J 1.7, H^4-py), 7.52 (1H, t, ^3J 7.7, H^5-bn), 7.35 (2H, ddd, ^3J 7.2, ^3J 4.8, ^3J 0.9, H^5-py). ^{13}C NMR (126 MHz, $CDCl_3$): δ 158.2 (quat), 149.2 (C^6-py), 143.9 (quat), 137.6 (C^4-py), 129.2 (C^5-bn), 128.3 (C^4-bn), 123.2 (C^5-py), 121.7 (C^3-py). Anal. Calcd for $C_{16}H_{11}N_2HgCl$: C, 41.12; H, 2.27; N, 5.99. Found: C, 40.51; H, 2.35; N, 5.95%.

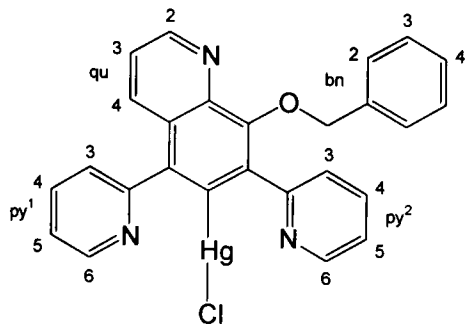

$L^{24}HgCl$: 5,7-Di(2-pyridyl)-8-benzyloxyquinoline-6-mercury(II) chloride

5,7-Di(2-pyridyl)-8-benzyloxyquinoline (39 mg, 0.10 mmol) was added to mercury(II) acetate (32 mg, 0.10 mmol) dissolved in absolute ethanol (10 mL) and degassed *via* the freeze-pump-thaw technique. The mixture was placed under an inert atmosphere of dinitrogen and stirred at reflux temperature (78°C) for 24 h. The mixture was then allowed to cool to ambient temperature and the solvent removed *in vacuo* yielding a yellow solid. The crude product was then washed *via* centrifuge using water (2 x 5 mL) and methanol (5 mL). The product was a pale yellow solid (18 mg, 29%). ^{1}H NMR (200 MHz, $CDCl_3$): δ 9.03 (1H, dd, ^3J 4.1, ^4J 1.6, H^2-qu), 8.83 (1H, d, ^3J 4.7, H^6-py^1), 8.70 (1H, d, ^3J 4.7, H^6-py^2), 8.37 (1H, d, ^3J 8.2, H^3-py^1), 8.25 (1H, d, ^3J 8.2, H^3-py^2), 7.87 (1H, td, ^3J 7.7, ^4J 1.8, H^4-py^1), 7.72 (1H, td, ^3J 7.7, ^4J 1.8, H^4-py^2), 7.63 (2H, d, ^3J 7.6, H^2-bn), 7.44 (2H, m, H^3-qu, H^4-bn), 7.31 (1H, m, H^5-py^1), 5.24 (2H, s, -OCH_2-), remaining peaks (H^3-bn, H^5-py^2) obscured by residual solvent resonance of $CHCl_3$. MS(ES^+): *m/z* 626 $[M + H]^+$.

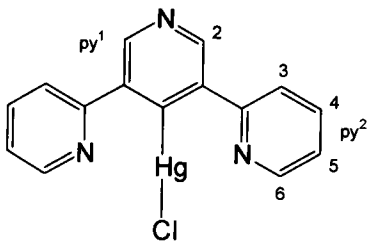

$L^{26}HgCl$: 3,5-Di(2-pyridyl)pyridine-4-mercury(II) chloride

3,5-di(2-pyridyl)pyridine (94 mg, 0.40 mmol) and mercury(II) acetate (122 mg, 0.38 mmol) were dissolved in absolute ethanol (10 mL) and degassed using the freeze-pump-thaw technique. The mixture was placed under an inert atmosphere of dinitrogen and stirred at reflux (78°C) for 72 h. Afterwards, a solution of lithium chloride (38 mg, 0.896 mmol) in methanol (5 mL), also deoxygenated, was added to the reaction, *via* cannular, and refluxed for a further 30 min. The solution was allowed to cool to ambient temperature before being added to distilled water (100 mL) yielding a colourless precipitate. The solid was separated by

centrifugation, washed with water (2 x 20 mL) and ice cold methanol (2 x 5 mL). The crude product was then suspended in successive quantities of chloroform (3 x 5 mL), sonicated and separated by centrifuge. The product was isolated as a colourless solid (79 mg, 44%). ^{1}H NMR (500 MHz, d_6-DMSO): δ 9.32 (2H, s, $^{4}J(^{199}Hg)$ 84.0, H^{2}-py^{1}), 8.69 (2H, dd, ^{3}J 4.8, ^{4}J 1.7, H^{6}-py^{2}), 8.27 (2H, d, ^{3}J 8.1, H^{3}-py^{2}), 8.02 (2H, td, ^{3}J 7.9, ^{4}J 1.9, H^{4}-py^{2}), 7.55 (2H, ddd, ^{3}J 7.5, ^{3}J 4.8, ^{4}J 0.9, H^{5}-py^{2}). From the chloroform used to wash the complex a small quantity of 3,5-di(2-pyridyl)pyridine-2-mercury chloride was obtained. ^{1}H NMR (300 MHz, $CDCl_3$): δ 9.37 (1H, s, $^{4}J(^{199}Hg)$ 63.4, H^{6}-py^{1}), 9.24 (1H, s, $^{4}J(^{199}Hg)$ too weak to distinguish, H^{4}-py^{1}), 8.82 (2H, m, H^{6}-py^{2}, H^{6}-py^{3}), 7.97 (4H, m, H^{3}-py^{2}, H^{3}-py^{3}, H^{4}-py^{2}, H^{4}-py^{3}), 7.53 (1H, m, H^{5}-py^{2}), 7.44 (1H, m, H^{5}-py^{3}).

8.2.3. Platinum(II) chloride complexes

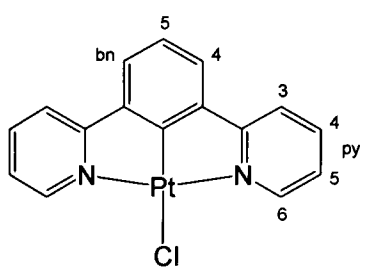

L^{1}PtCl: 1,3-Di(2-pyridyl)benzene-2-platinum(II) chloride

This compound was prepared using *Method A* described in Section 8.1.4.1, also as described previously in the literature.[66] A mixture of 1,3-di(2-pyridyl)benzene (138 mg, 0.59 mmol) and potassium tetrachloroplatinate (240 mg, 0.58 mmol) in glacial acetic acid (6 mL) was heated at reflux for 5 d. The product was isolated as a bright yellow solid (202 mg, 76%). Data were consistent with those previously reported.[66] ^{1}H NMR (500 MHz, $CDCl_3$): δ 9.36 (2H, dd, ^{3}J 5.7, ^{4}J 1.7, $^{3}J(^{195}Pt)$ 41.5, H^{6}-py), 7.95 (2H, td, ^{3}J 7.8, ^{4}J 1.7, H^{4}-py), 7.70 (2H, dd, ^{3}J 8.0, ^{4}J 1.4, H^{3}-py), 7.47 (2H, d, ^{3}J 7.7, H^{4}-bn), 7.30 (2H, ddd, ^{3}J 7.3, ^{3}J 5.6, ^{4}J 1.4, H^{5}-py), 7.24 (1H, t, ^{3}J 7.7, H^{5}-bn). ^{13}C NMR (126 MHz, $CDCl_3$): δ 167.5, 162.0, 152.4, 141.1, 139.2, 124.3 (C^{4}-bn), 123.4 (C^{5}-bn), 123.1 (C^{5}-py), 119.4 (C^{3}-py). MS (EI^{+}): *m/z* 462 $[M]^{+}$, 426 $[M - Cl]^{+}$.

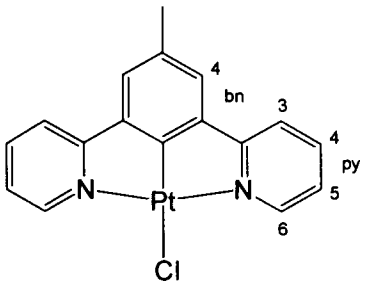

L^2PtCl: 1,3-di(2'-pyridyl)-5-methylbenzene-2-platinum(II) chloride

This compound was prepared by both Methods A and B, Section 8.1.4.

Method A: 1,3-di(2-pyridyl)-5-methylbenzene (101 mg, 0.42 mmol) and potassium tetrachloroplatinate (169 mg, 0.42 mmol) in glacial acetic acid (9 mL) were stirred at reflux for 3 d. The product was isolated as a bright yellow solid (145 mg, 75%).

Method B: Prepared *via* mixing degassed solutions of 1,3-di(2-pyridyl)-methylbenzene (51 mg, 0.21 mmol) in acetonitrile (15 mL) and potassium tetrachloroplatinate (85 mg, 0.21 mmol) in water (5 mL) and stirring at reflux for 3 d. The precipitate was washed by centrifuge with water and ethanol (3 x 5 mL of each), and then extracted into acetonitrile yielding a bright yellow solid (52 mg, 52%). ^{1}H NMR (400 MHz, $CDCl_3$): δ 9.33 (2H, d, ^3J 5.6, $^3J(^{195}Pt)$ 41.4, H^6-py), 7.93 (2H, td, ^3J 7.8, ^4J 1.6, H^4-py), 7.66 (2H, d, ^3J 8.0, H^3-py), 7.29 (2H, s, H-bn), 7.26 (2H, m, *J* not fully resolved due to overlap with former signal and solvent), 2.36 (3H, s, CH_3). ^{13}C NMR (101 MHz, $CDCl_3$): δ 167.3, 152.3, 140.9, 139.0, 132.5, 124.9, 123.1, 22.1 (CH_3). MS (EI^+): *m/z* 476 $[M]^+$, 440 $[M - Cl]^+$. Anal. Calcd for $C_{17}H_{13}N_2PtCl$: C, 42.91; H, 2.75; N, 5.89. Found: C, 42.41; H, 2.65; N, 5.41%.

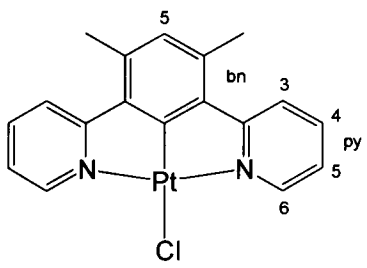

L^3PtCl: 1,3-Di(2-pyridyl)-4,6-dimethylbenzene-2-platinum(II) chloride

Prepared by *Method A* using 1,3-di(2-pyridyl)-4,6-dimethylbenzene (104 mg, 0.38 mmol) and potassium tetrachloroplatinate (161 mg, 0.38 mmol) in glacial acetic acid (9 mL). The mixture was heated at reflux for 2½ d. The product was isolated as a yellow solid (120 mg, 64%). ^{1}H NMR (500 MHz, $CDCl_3$): δ 9.51 (2H, d, ^3J 5.7, $^3J(^{195}Pt)$ 42.0, H^6-py), 7.92 (2H, td, ^3J 7.7, ^4J 1.8, H^4-py), 7.85 (2H, d,

^3J 7.8, H^3-py), 7.24 (2H, ddd, ^3J 7.3, ^3J 5.3, ^4J 1.7, H^5-py), 6.82 (1H, s, H^2-bn), 2.60 (6H, s, CH_3). MS (EI^+): *m/z* 491 $[M]^+$, 455 $[M - Cl]^+$.

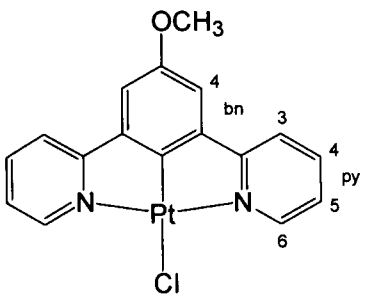

L^5PtCl: 1,3-Di(2-pyridyl)-5-methoxybenzene-2-platinum(II) chloride

Prepared *via Method A* using 1,3-di(2-pyridyl)-5-methoxybenzene (100 mg, 0.38 mmol) and potassium tetrachloroplatinate (154 mg, 0.37 mmol) in glacial acetic acid (5 mL). The mixture was stirred at reflux for 3½ d. The product was isolated from the standard work up (3 mg, 1%). Further quantities were extracted by combining the reaction solvent and methanol washings, evaporating the mixture to an orange solid, which was then washed *via* centrifuge with methanol (5 mL), yielding an orange solid (83 mg, 22%). ^1H NMR (500 MHz, $CDCl_3$): δ 9.23 (2H, d, ^3J 5.7, $^3J(^{195}Pt)$ 41.3, H^6-py), 7.89 (2H, td, ^3J 7.8, ^4J 1.2, H^4-py), 7.59 (2H, d, ^3J 7.8, H^3-py), 7.21 (2H, ddd, ^3J 7.3, ^3J 6.3, ^4J 1.2, H^5-py), 6.98 (2H, s, H^4-bn), 3.83 (3H, s, CH_3). ^{13}C NMR (126 MHz, $CDCl_3$): δ 167.2, 167.2, 157.1, 152.7, 152.2, 141.2, 139.1 (C^4-py), 123.5, 123.3 (C^5-py), 119.5 (C^3-py), 110.6 (C^4-bn), 56.1 (CH_3). Anal. Cald. for $C_{17}H_{13}N_2OPtCl$: C, 41.51; H, 2.66; N, 5.70. Found: C, 40.75; H, 2.61; N, 5.20%.

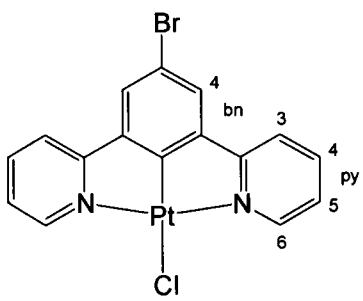

L^6PtCl: 1,3-di(2-pyridyl)-5-bromobenzene-2-platinum(II) chloride

Prepared by *Method A* using 1,3-di(2-pyridyl)-5-bromobenzene (61 mg, 0.197 mmol) and potassium tetrachloroplatinate (83 mg, 0.199 mmol) in glacial acetic acid (3 mL). The mixture was heated at reflux for 3 d. The product was isolated as a yellow/orange solid (55 mg, 52%). ^1H NMR (400 MHz, $CDCl_3$): δ 9.22 (2H, dd, ^3J 5.7, $^3J(^{195}Pt)$ 42.0, H^6-py), 7.95 (2H, td, ^3J 7.8, ^4J 1.6, H^4-py), 7.61 (2H,

d, ^{3}J 7.6, H^{3}-py), 7.44 (2H, s, H-bn), 7.28 (2H, ddd, ^{3}J 7.4, ^{3}J 5.6, ^{4}J 1.3, H^{5}-py). MS (ES^{+}): *m/z* 540 $[M^{+}]$, *m/z* 505 $[M - Cl]^{+}$.

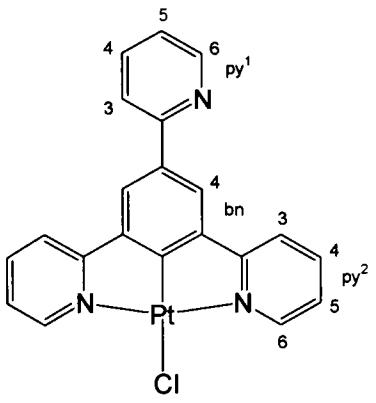

$L^{7}PtCl$: 1,3,5-Tri(2-pyridyl)benzene-2-platinum(II) chloride

Prepared *via Method A* using 1,3,5-tri(2-pyridyl)benzene (76 mg, 0.25 mmol) and potassium tetrachloroplatinate (95 mg, 0.23 mmol) in glacial acetic acid (7 mL). The mixture was heated at reflux for 3 d. The solvent volume was then reduced *in vacuo* to a yellow solid, which was taken into DCM (50 mL) and washed with a 10% aqueous solution of triethylamine. The organic layer was reduced to a yellow solid, which was suspended in methanol (5 mL) and sonicated for a few minutes. The solid was then isolated *via* centrifuge and washed with further quantities of methanol (3 x 5 mL) and diethyl ether (4 x 5 mL). The product was extracted into DCM and evaporated to dryness under reduced pressure, yielding a bright yellow solid (101 mg, 62%). ^{1}H NMR (500 MHz, $CDCl_3$): δ 9.31 (2H, d, ^{3}J 5.7, $^{3}J(^{195}Pt)$ 41.4, H^{6}-py^{2}), 8.69 (1H, d, ^{3}J 4.7, H^{6}-py^{1}), 8.06 (2H, s, H-bn), 7.94 (2H, td, ^{3}J 7.7, ^{4}J 1.3, H^{4}-py^{2}), 7.80 (4H, m, H^{3}-py^{1}, H^{4}-py^{1}, H^{3}-py^{2}), 7.27 (3H, m, H^{5}-py^{1}, H^{5}-py^{2}). ^{13}C NMR (126 MHz, $CDCl_3$): δ 167.2, 163.2, 157.7, 152.3, 149.8, 141.4, 139.3, 137.2, 134.8, 123.4 (C^{5}-py^{2}), 123.1 (C-bn), 122.1 (C^{5}-py^{1}), 120.2, 119.7. MS (EI^{+}): *m/z* 539 $[M]^{+}$, 503 $[M - Cl]^{+}$. HRMS (EI^{+}): *m/z* 539.050683; $C_{21}H_{14}N_3{}^{196}PtCl$ requires 539.052410. Anal. Calcd. for $C_{21}H_{14}N_3PtCl.H_2O$: C, 45.29; H, 2.90; N, 7.55. Found: C, 45.04; H, 2.88; N, 7.15%. The standard work-up procedure for this compound generates the complex protonated at the free pyridine site. ^{1}H NMR (500 MHz, $CDCl_3$): δ 9.15 (2H, d, ^{3}J 6.4, $^{3}J(^{195}Pt)$ 36.2, H^{6}-py^{2}), 8.72 (1H, d, ^{3}J 5.1, H^{6}-py^{1}), 8.51 (2H, s, H-bn), 8.32 (2H, d, ^{3}J 8.3, H^{3}-py^{2}), 8.26 (2H, td, ^{3}J 7.7, ^{4}J 1.6, H^{4}-py^{2}), 8.23 (1H, d, ^{3}J 8.1, H^{3}-py^{1}), 8.02 (1H, td, ^{3}J 8.1, ^{4}J 1.7, H^{4}-py^{1}), 7.61 (2H, ddd, ^{3}J 7.2, ^{3}J 5.8, ^{4}J 1.5, H^{5}-py^{2}), 7.47 (1H, ddd, ^{3}J 7.4, ^{3}J 5.3, ^{4}J 1.5, H^{5}-py^{1}).

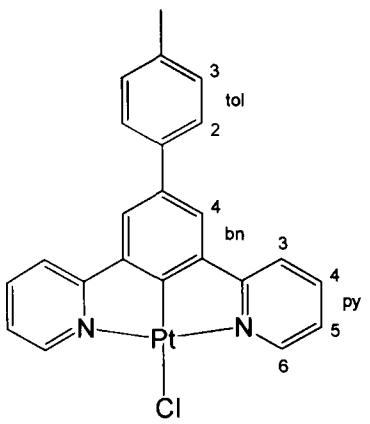

L[8]PtCl: 1,3-Di(2-pyridyl)-5-(*p*-tolyl)benzene-2-platinum(II) chloride

Prepared *via Method A* using 1,3-di(2-pyridyl)-5-(*p*-tolyl)benzene (73 mg, 0.27 mmol) and potassium tetrachloroplatinate (92 mg, 0.22 mmol) in glacial acetic acid (4 mL). The mixture was heated at reflux for 3½ d. The product was isolated as a yellow/orange solid (100 mg, 82%). ^{1}H NMR (400 MHz, $CDCl_3$): δ 9.35 (2H, d, ^{3}J 5.7, $^{3}J(^{195}Pt)$ 41.2, H^{6}-py), 7.96 (2H, td, ^{3}J 7.6, ^{4}J 1.6, H^{4}-py), 7.74 (2H, d, ^{3}J 8.0, H^{3}-py), 7.61 (2H, s, H^{4}-bn), 7.52 (2H, d, ^{3}J 8.2, H^{2}-tol), 7.29 (4H, m, H^{3}-tol, H^{5}-py), 2.41 (3H, s, CH_3). ^{13}C NMR (101 MHz, $CDCl_3$): δ 167.3, 152.5, 141.4, 139.3, 139.0, 137.2, 137.0, 129.8, 126.8, 126.9, 123.5, 123.3, 119.5, 109.9, 21.3 (CH_3). MS (LSIMS): *m/z* 516 $[M - Cl]^{+}$. Anal. Calcd. for $C_{23}H_{17}N_2PtCl$: C, 50.05; H, 3.10; N, 5.08. Found: C, 49.12; H, 3.13; N, 4.80%.

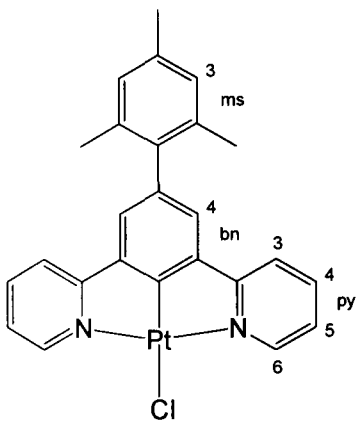

L[9]PtCl: 1,3-di(2-pyridyl)-5-mesitylbenzene-2-platinum(II) chloride

Prepared *via Method A* using 1,3-di(2-pyridyl)-5-mesitylbenzene (102 mg, 0.29 mmol) and potassium tetrachloroplatinate (92 mg, 0.22 mmol) in glacial acetic acid (5 mL). The mixture was stirred at reflux for 3 d. The product was isolated as a yellow solid (106 mg, 82%). ^{1}H NMR (400 MHz, $CDCl_3$): *δ* 9.38 (2H, dd, ^{3}J 5.8, ^{4}J 1.8, $^{3}J(^{195}Pt)$ 41.6, H^{6}-py), 7.94 (2H, td, ^{3}J 7.8, ^{4}J 1.8, H^{4}-py), 7.63 (2H, dd, ^{3}J 8.0, ^{4}J 1.4, $^{4}J(^{195}Pt)$ 19.8, H^{3}-py), 7.31 (2H, ddd, ^{3}J 7.5, ^{3}J 5.9, ^{4}J 1.7, H^{5}-py), 7.25 (2H, s, H-bn), 6.99 (2H, s, H-ms), 2.36 (3H, s, *p*-CH_3), 2.08 (6H, s, *m*-CH_3). Anal.

Calcd. for $C_{25}H_{21}N_2PtCl$: C, 51.77; H, 3.65; N, 4.83. Found: C, 51.04; H, 3.85; N, 4.49 %.

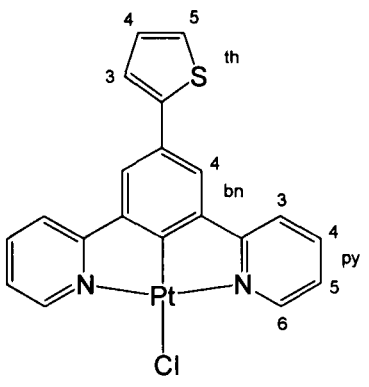

$L^{10}PtCl$: 1,3-Di(2-pyridyl)-5-(2-thienyl)benzene-2-platinum(II) chloride

Prepared *via Method A* using 1,3-di(2-pyridyl)-5-(2'-thiophenyl)benzene (39 mg, 0.12 mmol) and potassium tetrachloroplatinate (51 mg, 0.12 mmol) in glacial acetic acid (4 mL). The mixture was stirred at reflux for 3½ d. The product was isolated as an orange solid (20 mg, 30%). ^{1}H NMR (400 MHz, $CDCl_3$): δ 9.33 (2H, d, ^3J 5.9, $^3J(^{195}Pt)$ 41.0, H^6-py), 7.97 (2H, td, ^3J 7.9, ^4J 1.6, H^4-py), 7.75 (2H, d, ^3J 8.0, H^3-py), 7.64 (2H, s, H-bn), 7.35 (1H, d, ^3J 3.6, H^3-th), 7.30 (3H, m, H^5-py, H^5-th), 7.10 (1H, dd, ^3J 5.1, ^3J 3.6, H^4-th). ^{13}C NMR (101 MHz, $CDCl_3$): δ 167.0, 152.4 (C^6-py), 139.3 (C^4-py), 128.4 (C^4-th), 124.5 (C^5-th), 123.6 (C^3-th), 122.8 (C^4-bn), 119.6 (C^3-py). MS (LSIMS): *m/z* 508 $[M - Cl]^+$

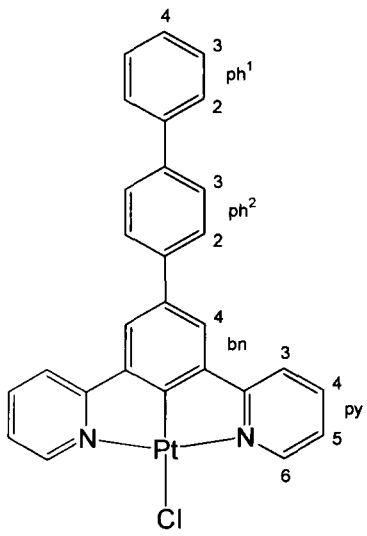

$L^{11}PtCl$: 5-(4-Biphenyl)-1,3-di(2'-pyridyl)benzene-2-platinum(II) chloride

Prepared *via Method A* using 5-(4-biphenyl)-1,3-di(2-pyridyl)benzene (55 mg, 0.14 mmol) and potassium tetrachloroplatinate (59 mg, 0.14 mmol) in glacial acetic acid (3 mL). The mixture was heated at reflux for 3 d. The product was isolated as

a yellow/orange solid (58 mg, 66%). ^{1}H NMR (500 MHz, $CDCl_3$): 9.35 (2H, dd, ^{3}J 5.7, ^{4}J 1.8, $^{3}J(^{195}Pt)$ 39.0, H^{6}-py), 7.96 (2H, td, ^{3}J 7.8, ^{4}J 1.5, H^{4}-py), 7.76 (2H, d, ^{3}J 8.1, H^{3}-py), 7.71 (4H, m, H-bn, H^{2}-ph^{1}), 7.67 (4H, m, H^{2}-ph^{2}, H^{3}-ph^{2}), 7.49 (2H, t, ^{3}J 7.8, H^{3}-ph^{1}), 7.39 (1H, tt, ^{3}J 7.5, ^{4}J 1.8, H^{4}-ph^{1}), 7.29 (2H, ddd, ^{3}J 7.5, ^{4}J 1.8, H^{5}-py). ^{13}C NMR (126 MHz, $CDCl_3$): δ 167.3, 152.5, 141.5, 140.7, 140.2, 139.3 (C^{4}-py), 129.1 (C^{3}-ph^{1}), 127.9 (C^{4}-ph^{1}), 127.6, 127.4 (C-bn), 127.2 (C^{2}-ph^{2}), 123.5 (C^{5}-py), 123.3 (C^{3}-ph^{2}), 199.5 (C^{3}-py). MS (EI^{+}): *m/z* 614.089 $[M]^{+}$, $[C_{28}H_{19}N_2PtCl]$ requires 613.995.

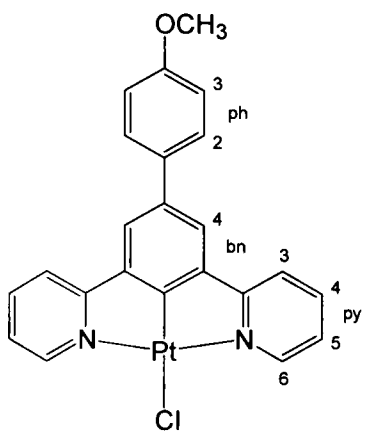

L^{12}PtCl: 1,3-Di(2-pyridyl)-5-(*p*-methoxy)-benzene-2-platinum(II) chloride

Prepared *via Method A* using 1,3-di(2-pyridyl)-5-(*p*-methoxyphenyl)benzene (48 mg, 0.14 mmol) and potassium tetrachloroplatinate (56 mg, 0.14 mmol) in glacial acetic acid (4 mL). The mixture was stirred at reflux for 3d. The product was isolated as a bright yellow solid (55 mg, 72%). ^{1}H NMR (500 MHz, $CDCl_3$): *δ* 9.33 (2H, d, ^{3}J 5.5, $^{3}J(^{195}Pt)$ 40.1, H^{6}-py), 7.94 (2H, t, ^{3}J 7.9, H^{4}-py), 7.73 (2H, d, ^{3}J 7.6, H^{3}-py), 7.56 (2H, s, H^{4}-bn), 7.55 (2H, s, signal obscured, H^{2}-ph), 7.27 (2H, t, ^{3}J 6.3, H^{5}-py), 7.07 (2H, d, ^{3}J 8.1, H^{3}-ph), 3.88 (3H, s, CH_3). ^{13}C NMR (126 MHz, $CDCl_3$): *δ* 167.4, 160.2, 159.2, 152.5 (C^{6}-py), 141.3, 139.2 (C^{4}-py), 136.7, 134.5, 128.1 (C^{2}-ph), 123.4 (C^{5}-py), 123.2 (C^{4}-bn), 119.5 (C^{3}-py), 114.5 (C^{3}-ph), 55.6 (CH_3). Anal. Calcd. for $C_{23}H_{17}N_2OPtCl.¼CH_2Cl_2$: C 47.40, H 2.99, N 4.75. Found: C 47.88, H 2.93, N 4.76%. IR ($^{cm-1}$): 1262, 1178 Ph-O-CH_3.

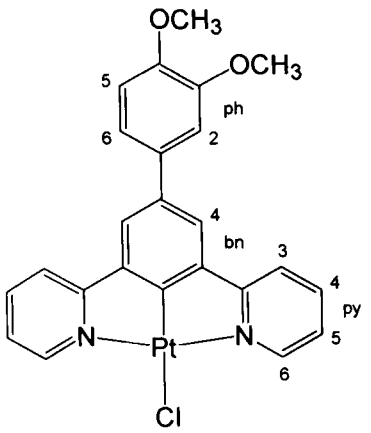

$L^{13}PtCl$: 1,3-Di(2-pyridyl)-5-(3,4-dimethoxyphenyl)benzene-2-platinum(II) chloride

Prepared *via Method A* using 1,3-di(2-pyridyl)-5-(3,4-dimethoxyphenyl)benzene (64 mg, 0.17 mmol) and potassium tetrachloroplatinate (68 mg, 0.16 mmol) in glacial acetic acid (4 mL). The mixture was stirred at reflux for 3 d. The product was isolated as a yellow solid (64 mg, 65%). ^{1}H NMR (500 MHz, $CDCl_3$): δ 9.28 (2H, d, ^3J 5.6, $^3J(^{195}Pt)$ 40.4, H^6-py), 7.92 (2H, td, ^3J 7.7, ^4J 1.2, H^4-py), 7.72 (2H, d, ^3J 8.0, H^3-py), 7.52 (2H, s, H-bn), 7.23 (2H, ddd, ^3J 7.1, ^3J 6.0, ^4J 1.2, H^5-py), 7.16 (2H, m, H^2-ph, H^6-ph), 6.97 (1H, d, ^3J 8.7, H^5-ph), 4.01 (3H, s, *m*-CH_3), 3.96 (3H, s, *p*-CH_3). ^{13}C NMR (126 MHz, $CDCl_3$): δ 167.2, 160.4, 152.4 (C^6-py), 149.5, 148.7, 141.2, 139.1 (C^4-py), 136.8, 135.0, 123.3 (C^5-py), 123.3 (C^4-bn), 119.5 (C^3-py), 119.4 (C^6-ph), 111.7 (C^5-ph), 110.5 (C^2-ph), 56.4 (*m*-CH_3), 56.2 (*p*-CH_3). Anal. Calcd for $C_{24}H_{19}N_2O_2PtCl.\frac{2}{3}CH_2Cl_2$: C, 45.26; H, 3.13; N, 4.28. Found: C, 45.12; H, 3.30; N, 4.16%.

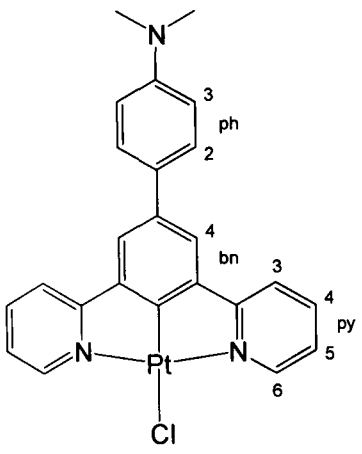

$L^{16}PtCl$:1,3-Di(2-pyridyl)-5-phenyl-(4-N,N-dimethylaniline)-2-platinum(II) chloride

Prepared *via Method B* using 1,3-di(2-pyridyl)-5-[4-N,N-dimethylaniline]benzene (67 mg, 0.19 mmol) in acetonitrile (4 mL) and potassium tetrachloroplatinate (75 mg, 0.18 mmol) in water (2.5 mL). The mixture was stirred at reflux for 2 d. The product was isolated as an orange solid (39 mg, 37%). ^{1}H NMR (400 MHz,

$CDCl_3$): δ 9.33 (2H, d, ^3J 5.7, $^3J(^{195}Pt)$ 41.2, H^6-py), 7.94 (2H, td, ^3J 7.8, ^4J 1.7, H^4-py), 7.73 (2H, d, ^3J 8.0, H^3-py), 7.58 (2H, s, H-bn), 7.52 (2H, d, ^3J 8.6, H^2-ph), 7.27 (2H, t, ^3J 7.4, H^5-py), 6.83 (2H, d, ^3J 8.6, H^3-ph), 3.02 (6H, s, CH_3). ^{13}C NMR (101 MHz, $CDCl_3$): δ 167.5, 159.5, 152.4, 150.0, 141.3, 139.2, 137.2, 129.9, 127.7 (C^2-ph), 123.3 (C^5-py), 122.8 (C^4-bn), 119.4 (C^3-py), 113.0 (C^3-ph), 40.8 (CH_3). MS (ES^+): *m/z* 577 $[M - Cl]^+$. Anal. Calcd. for $C_{24}H_{20}N_3PtCl.½H_2O$: C, 48.86; H, 3.59; N, 7.12. Found: C, 48.92; H, 3.33; N, 6.73%.

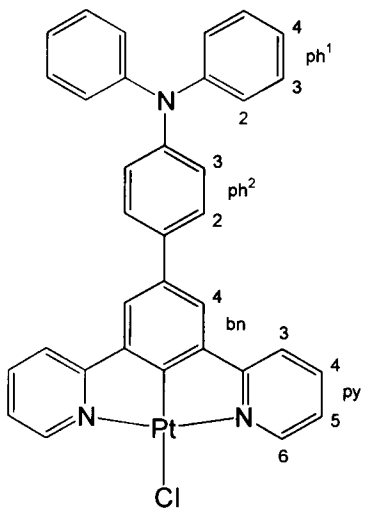

$L^{17}PtCl$:1,3-Di(2-pyridyl)-5-phenyl-[4-N,N-diphenylaniline]-2-platinum(II) chloride

Prepared *via Method A* using 1,3-di(2-pyridyl)-5-phenyl-(4-N,N-dimethylaniline) (76 mg, 0.16 mmol) and potassium tetrachloroplatinate (65 mg, 0.16 mmol) in glacial acetic acid (3 mL). The mixture was stirred at reflux for 2 d. The product was isolated as a yellow solid (97 mg, 88%). ^1H NMR (400 MHz, $CDCl_3$): δ 9.35 (2H, d, ^3J 5.8, $^3J(^{195}Pt)$ 39.1, H^6-py), 7.96 (2H, td, ^3J 7.7, ^4J 1.7, H^4-py), 7.74 (2H, dd, ^3J 8.0, ^4J 1.4, H^3-py), 7.61 (2H, s, H-bn), 7.50 (2H, d, ^3J 8.8, H^2-ph^2), 7.29 (6H, m, H^3-ph, H^5-py), 7.16 (6H, m, H^2-ph, H^3-ph^2), 7.05 (2H, tt, ^3J 7.3, ^4J 1.2, H^4-ph). ^{13}C NMR (101 MHz, $CDCl_3$): δ 167.3, 152.5, 147.7, 147.3, 141.4, 139.3 (C^4-py), 136.6, 135.8, 129.5, 127.7 (C^2-ph^2), 124.5, 124.2, 123.5, 123.2 (C^4-ph), 123.1 (C^4-bn), 119.4 (C^3-py). Anal. Calcd. for $C_{34}H_{24}N_3PtCl.\frac{1}{10}CH_2Cl_2$: C, 57.39; H, 3.42; N, 5.89. Found C, 57.09; H, 3.38; N, 5.87%.

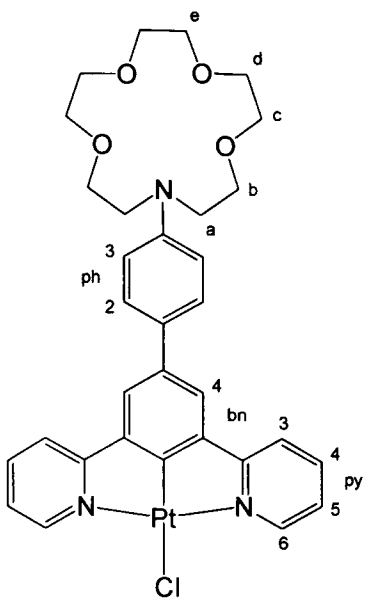

$L^{18}PtCl$: (1,3-Di(2-pyridyl)-5-phenyl-2-platinum(II) chloride)-phenyl-4-N-monoaza-15-crown-5

Prepared *via Method B* using 1,3-di(2-pyridyl)-5-(4-monoaza-15-crown-5-phenyl)benzene (112 mg, 0.21 mmol) in acetonitrile (7 mL) and potassium tetrachloroplatinate (81 mg, 0.20 mmol) in water (3 mL). The mixture was stirred at reflux for 3 d before work-up which slightly differed from the standard procedure. The mixture was reduced in volume *in vacuo*, the residue of which was dissolved in DCM (30 mL) and washed with water (2 x 10 mL). The organic layer was reduced down to a minimal amount (*ca.* 5 mL) and added dropwise to diethyl ether (25 mL). An orange precipitate was collected by filtration and washed, *via* centrifuge, by successive amonts of ethanol (3 x 5 mL), diethyl ether (3 x 5 mL) and DCM (1 mL). The product, an orange solid, was then dried under reduced pressure, (100 mg, 68%). ^{1}H NMR (500 MHz, $CDCl_3$): δ 9.28 (2H, d, ^{3}J 5.6, $^{3}J(^{195}Pt)$ 36.5, H^{6}-py), 7.91 (2H, t, ^{3}J 7.8, H^{4}-py), 7.69 (2H, d, ^{3}J 7.7, H^{3}-py), 7.51 (2H, s, H^{4}-bn), 7.46 (2H, d, ^{3}J 8.7, H^{3}-ph), 7.23 (2H, t, ^{3}J 6.7, H^{5}-py), 6.74 (2H, d, ^{3}J 8.7, H^{2}-ph), 3.81 (4H, t, ^{3}J 6.1, *b*-CH_2-), 3.71 (8H, m, *c,e*-CH_2-), 3.67 (8H, m, *a,d*-CH_2-). ^{13}C NMR (126 MHz, $CDCl_3$): δ 167.5, 159.7, 152.3, 147.0, 141.2, 139.1 (C^{4}-py), 137.0, 129.1, 127.8 (C^{2}-ph), 123.2 (C^{5}-py), 122.6 (C^{4}-bn), 119.4 (C^{3}-py), 111.9 (C^{3}-ph), 71.5, 70.4, 70.3, 68.7 (*b*-CH_2), 52.7 (*a*-CH_2). MS (ES^+): *m/z* 778.2 [M + Na^+], 719.4 [M – Cl]$^+$. HRMS (ES^+): 777.17832 [M + Na]$^+$; [$C_{32}H_{34}N_3O_4PtCl^{23}Na$] requires 777.17778.

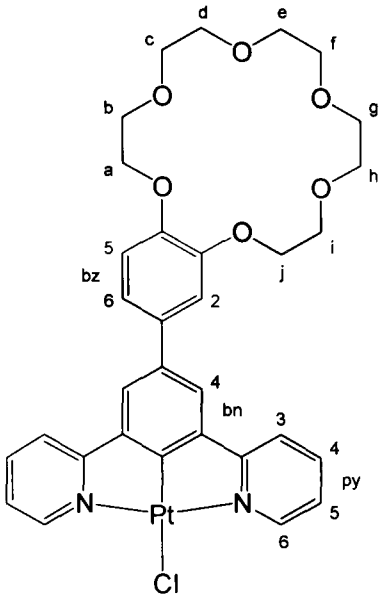

$L^{19}PtCl$: 5-[phenyl-18-crown-6]-1,3-di(2-pyridyl)benzene-2-platinum(II) chloride

Method A: Prepared *via Method A* using 5-[phenyl-18-crown-6]-1,3-di(2-pyridyl)benzene (86 mg, 0.16 mmol) and potassium tetrachloroplatinate (32 mg, 0.16 mmol) in glacial acetic acid (5 mL). The mixture was stirred at reflux for 4 d. The product was purified as specified in the standard procedure, Section 8.1.4.1, but with smaller quantities of solvent. The product was isolated as a yellow solid (26 mg, 21%).

Method B: Prepared *via Method B* using 5-[phenyl-18-crown-6]-1,3-di(2-pyridyl)benzene (84 mg, 0.16 mmol) in acetonitrile (7 mL) and potassium tetrachloroplatinate (63 mg, 0.15 mmol) in water (3 mL). The mixture was stirred at reflux for 1 d. The solvent was removed *in vacuo*, and the residue sonicated in water (2 x 2 mL) and the solid collected by centrifuge. From this point the work-up followed that of the standard procedure, Section 8.1.4.2. The product was isolated as a yellow solid (33 mg, 28%). ^{1}H NMR (400 MHz, $CDCl_3$): δ 9.31 (2H, dd, ^3J 5.7, ^4J 1.2, ^3J(195Pt) 39.8, H^6-py), 7.94 (2H, td, ^3J 7.7, ^4J 1.4, H^4-py), 7.72 (2H, d, ^3J 7.9, H^3-py), 7.53 (2H, s, H-bn), 7.26 (2H, obscured by $CHCl_3$ signal, H^5-py), 7.16 (1H, s, H^2-ph), 7.15 (1H, *J* couplings obscured, H^6-ph), 6.97 (1H, d, ^3J 8.4, H^5-ph), 4.29 (1H, t, ^3J 4.3, H^j), 4.23 (1H, t, ^3J 4.6, H^a), 3.98 (2H, m, H^b, H^i), 3.81 (2H, m, H^c, H^h), 3.75 (2H, m, H^d, H^g), 3.71 (2H, s, H^e, H^f). MS (ES^+): *m/z* 794.2 $[M + Na]^+$, *m/z* 768.3 $[M - Cl + MeOH]^+$.

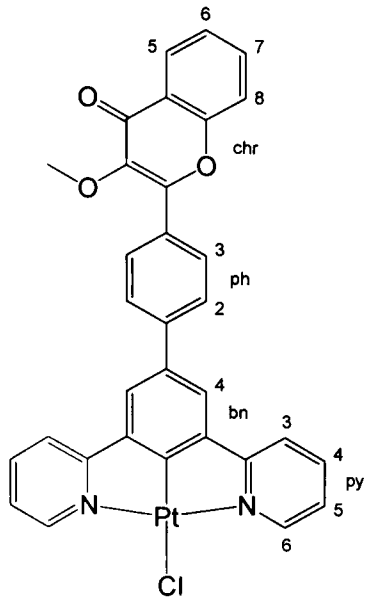

$L^{20}PtCl$: 1,3-Di(2-pyridyl)-5-[phenyl-4-(3-methoxychrom-4-one)]benzene-2-platinum(II) chloride

Prepared *via Method B* using:1,3-di(2-pyridyl)-5-[4'-phenyl-(3-methoxychrom-4-one)]benzene (30 mg, 0.06 mmol) in acetonitrile (7 mL) and potassium tetrachloroplatinate (27 mg, 0.07 mL) in water (3 mL). The mixture was stirred at reflux for 3 d. The product was isolated as a yellow solid (20 mg, 45%). ^{1}H NMR (500 MHz, $CDCl_3$): δ 9.38 (2H, d, ^3J 5.7, $^3J(^{195}Pt)$ 38.9, H^6-py), 8.30 (1H, dd, ^3J 8.0, ^4J 1.5, H^6-chr), 8.25 (2H, d, ^3J 8.4, H^2-ph), 7.99 (2H, td, ^3J 7.8, ^4J 1.0, H^4-py), 7.81 (4H, m, H^3-ph, H^3-py), 7.72 (3H, m, H^4-bn, H^4-chr), 7.59 (1H, d, ^3J 8.3, H^3-chr), 7.44 (1H, t, ^3J 7.3, H^5-chr), 7.33 (2H, t, ^3J 6.8, H^5-py), 3.97 (3H, s, CH_3). ^{13}C NMR (126 MHz, $CDCl_3$): δ 175.2, 167.1, 155.4, 155.4, 152.6, 144.1, 141.8, 141.7, 139.4, 135.8, 133.7, 129.3, 127.1, 126.0, 125.0, 124.4, 123.7, 123.7, 123.4, 119.6, 118.2, 60.3. Anal: Calcd for $C_{32}H_{21}N_2O_3PtCl$: C, 53.98; H, 2.97; N 3.93. Found: C, 53.46; H, 3.51; N, 3.38%.

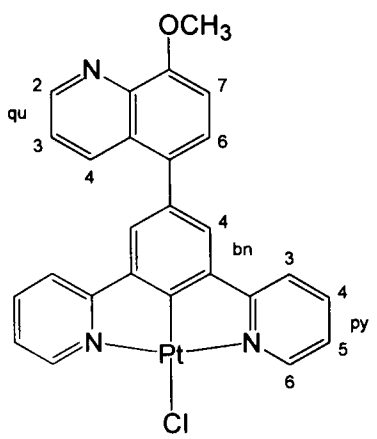

$L^{25}PtCl$: 1,3-di(2-pyridyl)-5-[5-(8-methoxyquinoline)]benzene-2-platinum(II) chloride

Prepared *via Method B* using 1,3-di(2-pyridyl)-5-[5-(8-methoxyquinoline)]-benzene (73 mg, 0.19 mmol) in acetonitrile (5 mL) and potassium tetrachloroplatinate (77 mg, 0.19 mmol) in water (2 mL). The mixture was stirred at 100°C for 5½ d. The reaction was reduced *in vacuo* yielding an orange/brown solid, which was taken into DCM (50 mL) and washed with $NaHCO_{3(aq)}$ (2 x 50 mL of 5% by mass). The organic layer was retained and reduced *in vacuo* to an orange solid. The product was then purified by successive washings, *via* centrifuge, with ethanol (2 x 5 mL), diethyl ether (2 x 5mL) and extracted into DCM, and evaporated to dryness. Product was isolated as an orange solid (27 mg, 24%). ^{1}H NMR (500 MHz, $CDCl_3$): δ 9.41 (2H, d, ^3J 5.7, $^3J(^{195}Pt)$ 40.0, H^6-py), 8.98 (1H, dd, ^3J 4.1, ^4J 1.7, H^2-qu), 8.24 (1H, dd, ^3J 8.5, ^4J 1.6, H^4-qu), 7.96 (2H, td, ^3J 7.8, ^4J 1.6, H^4-py), 7.70 (2H, d, ^3J 8.0, H^3-py), 7.52 (1H, d, ^3J 8.0, H^6-qu), 7.50 (2H, s, H-bn), 7.43 (1H, dd, ^3J 8.5, ^3J 4.1, H^3-qu), 7.34 (2H, ddd, ^3J 7.4, ^3J 6.0, ^4J 1.7, H^5-py), 7.15 (1H, d, ^3J 8.0, H^7-qu), 4.17 (3H, s, CH_3). ^{13}C NMR (126 MHz, $CDCl_3$): δ 167.2 (C^2-py), 160.9 (C^2-bn), 155.1 (C^8-qu), 152.6 (C^6-py), 149.4, 141.3, 140.5, 139.4 (C^4-py), 134.6, 134.3 (C^4-qu), 132.4 (C^5-qu), 127.8, 127.3 (C^6-qu), 126.1 (C^4-bn), 123.7 (C^5-py), 122.0 (C^3-qu), 119.5 (C^3-py), 107.2 (C^7-qu), 56.3 (CH_3). MS (ES^+): *m/z* 619 $[M]^+$.

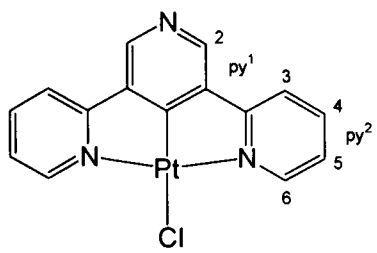

$L^{26}PtCl$: 3,5-Di(2-pyridyl)pyridine-4-platinum(II) chloride

Tetrakis(triphenylphosphine)platinum (724 mg, 80%) was prepared from K_2PtCl_4 (301 mg, 0.725 mmol) and triphenylphosphine (1.50 g, 5.72 mmol) in an alkaline ethanol solution according to a standard literature procedure.[260] The desired platinum(II) complex was prepared *via* a method based on published literature.[252] 3,5-Di(2-pyridyl)pyridine-4-mercury(II) chloride (75 mg, 0.16 mmol) and tetrakis(triphenylphosphine)platinum(0) (199 mg, 0.16 mmol) were placed under inert atmosphere and dissolved in anhydrous toluene (15 mL). The mixture was stirred at reflux (116°C) for 40 h, during which the mixture was observed to change colour from orange to a dark red suspension. Lithium chloride (710 mg, 16.8 mmol) in degassed methanol (4 mL) was added and the reaction was stirred at 85°C, for a further 40 mins. The mixture was then reduced in volume (to *ca.* 2 mL) and partitioned between water (100 mL) and DCM (50 mL). The organic layer was evaporated *in vacuo* yielding an orange, oily solid. The crude product was then washed and separated, *via* centrifuge, with methanol (4 x 3 mL) and diethyl ether (8 x 5 mL) yielding a bright yellow solid (8 mg, 11%). ^{1}H NMR (400 MHz, $CDCl_3$): δ 9.38 (2H, ddd, ^3J 5.8, ^4J 1.6, ^5J 0.8, $^3J(^{195}Pt)$ 41.1, H^6-py^2), 8.58 (2H, s, H^2-py^1), 8.04 (2H, td, ^3J 7.8, ^4J 1.6, H^4-py^2), 7.83 (2H, d, ^3J 7.9, $^3J(^{195}Pt)$ 19.8, H^3-py^2), 7.40 (2H, ddd, ^3J 7.4, ^3J 5.9, ^4J 1.6, H^5-py^2). ^{13}C NMR (101 MHz, $CDCl_3$): δ 152.9, 139.8, 124.2, 119.9, sample too weak to identify further signals. MS (ES^+): *m/z* 463 $[M + H]^+$.

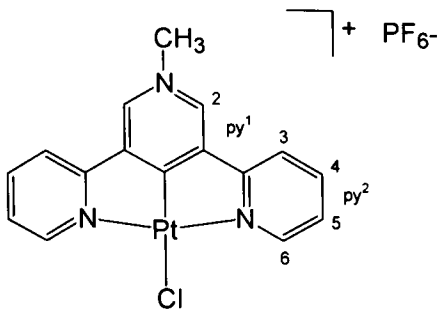

[N-MeL^{26}PtCl]PF$_6$: N-Methyl-3,5-di(2-pyridyl)pyrinium-4-platinum(II) chloride

Prepared *via Method A* using N-methyl-3,5-di(2-pyridyl)pyrinium hexafluorophosphate (141 mg, 0.36 mmol) and potassium tetrachloroplatinate (146 mg, 0.35 mmol) in glacial acetic acid (5 mL). The mixture was stirred at reflux for 3 d. Work-up in this case used only 3 washings with each solvent before the crude product was dissolved in DMSO, and any insoluble residue was removed by centrifuge. The DMSO solution was added dropwise to saturated $KPF_{6(aq)}$ yielding a dark red/brown solid (88 mg, 39%). ^{1}H NMR (300 MHz, d_6-DMSO): δ 9.27 (2H, s, H^2-py^1), 9.21 (2H, d, ^3J 5.2, ^3J(^{195}Pt) obscured, H^6-py^2), 8.46 (2H, t, ^3J 7.9, H^4-py^2), 8.30 (2H, d, ^3J 7.6, H^3-py^2), 7.84 (2H, t, ^3J 6.9, H^5-py^2), 4.15 (3H, s, CH_3). HRMS (ES$^+$): *m/z* 477.04609, $C_{16}H_{13}N_3{}^{35}Cl^{195}Pt$ requires 477.04404; *m/z* 476.04382, $C_{16}H_{13}N_3{}^{35}Cl^{194}Pt$ requires 476.04193. N-Methyl-3,5-di(2-pyridyl)pyridine platinum(II) iodide hexafluorophosphate can be acquired by a similar method simply by using N-methyl-3,5-di(2-pyridyl)pyridine iodide as the starting ligand. Product isolated as an orange solid (20 mg, 16%). ^{1}H NMR (300 MHz, CD_3CN): δ 9.80 (2H, d, ^3J 5.2, ^3J(^{195}Pt) obscured, H^6-py^2), 8.68 (2H, s, H^2-py^1), 8.23 (2H, t, ^3J 7.5, H^4-py^2), 7.99 (2H, d, ^3J 7.8, H^3-py^2), 7.61 (2H, d, ^3J 7.4, H^5-py^2). MS (ES$^+$): *m/z* 568.9857 [M – PF$_6$]$^+$; $C_{16}H_{13}N_3PtI$ requires 568.9802.

8.2.4. Platinum ligand exchange products

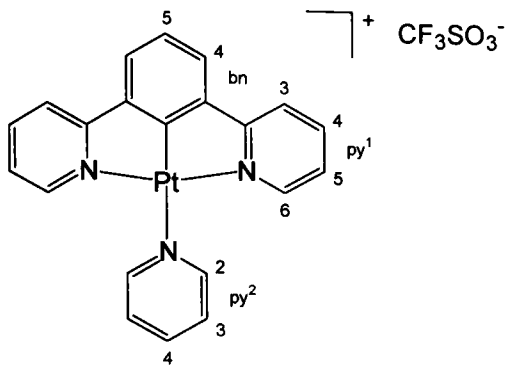

[L[1]Ptpy]SO_3CF_3:1,3-Di(2-pyridyl)benzene-2-platinum(II)-N-pyridine trifluoromethanesulfonate

Prepared by chloride metathesis as described in Section 8.1.6, using 1,3-di(2-pyridyl)benzene-2-platinum(II) chloride (103 mg, 0.22 mmol), silver trifluoromethanesulfonate (62 mg, 0.24 mmol), and pyridine (0.2 mL, 2.5 mmol) in acetone (20 mL). The mixture was stirred at RT for 1 h before the removal of silver chloride, and a further 16 h after treatment with pyridine. The solvent was reduced in volume (~ 1 mL) prior to work up, washing with acetone (4 x 1 mL), yielding a pale yellow solid (38 mg, 26%). ^{1}H NMR (500 MHz, d_6-acetone): δ 9.23 (2H, dd, ^3J 4.8, ^4J 1.2, $^3J(^{195}Pt)$ 19.6, H^2-py^2), 8.37 (1H, t, ^3J 7.9, H^4-py^2), 8.29 (2H, td, ^3J 7.7, ^4J 1.3, H^4-py^1), 8.21 (2H, d, ^3J 7.9, H^3-py^1), 8.02 (2H, ddd, ^3J 7.6, ^3J 5.0, ^4J 1.2, H^3-py^2), 8.00 (2H, d, ^3J 5.7, $^3J(^{195}Pt)$ 41.0, H^6-py^1), 7.83 (2H, d, ^3J 7.7, H^4-bn), 7.47 (2H, ddd, ^3J 7.3, ^3J 5.7, ^4J 1.5, H^5-py^1), 7.42 (1H, t, ^3J 7.7, H^5-bn). MS (ES^+): *m/z* 505 $[M - CF_3SO_3]^+$; *m/z* 426 $[M - C5H5NCF_3SO_3]^+$. HRMS (ES^+): *m/z* 505.0985; $C_{21}H_{16}N_3Pt$ requires 505.0986.

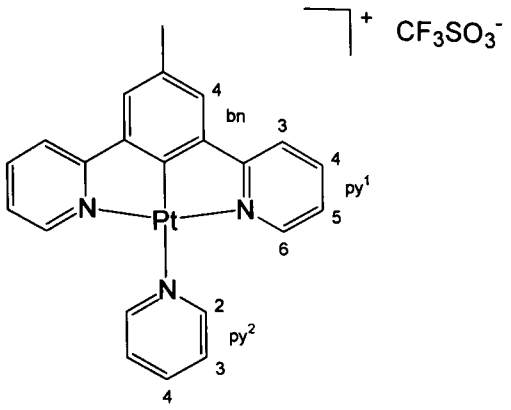

3,5-Di(2-pyridyl)-5-methylbenzene-2-platinum(II)-N-pyridine trifluoromethanesulfonate

Prepared *via* chloride metathesis using L^2PtCl (68 mg, 0.14 mmol), silver trifluoromethanesulfonate (36 mg, 0.14 mmol) and pyridine (0.5 mL, 6.25 mmol) in acetone (12 mL). The mixture was stirred at RT for 1 h before removal of silver chloride, followed by another 3 h after treatment with pyridine. Work-up (4 x 1 mL acetone) yielded the product as a yellow powder (49 mg, 50%). ^{1}H NMR (300 MHz, d_6-acetone): δ 9.20 (2H, dd, ^3J 6.2, ^4J 1.6, H^2-py^2), 8.35 (1H, tt, ^3J 8.0, ^4J 1.5, H^4-py^2), 8.26 (2H, td, ^3J 7.7, ^4J 1.5, H^4-py^1), 8.16 (2H, d, ^3J 8.0, H^3-py^1), 7.99 (4H, m, $^3J(^{195}Pt)$ obscured, H^6-py^1, H^3-py^2), 7.67 (2H, s, H-bn), 7.43 (2H, ddd, ^3J 7.3, ^3J 5.8, ^4J 1.5, H^5-py^1), 2.44 (3H, s, CH_3).

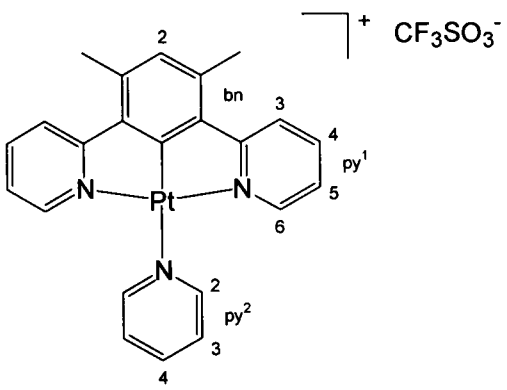

$[L^3Pt(DMAP)]SO_3CF_3$: 3,5-Di(2-pyridyl)-m-xylene-4-platinum(II)-N-pyridine trifluoromethanesulfonate

Prepared *via* chloride metathesis using L^3PtCl (80 mg, 0.163 mmol), silver trifluoromethanesulfonate (43 mg, 0.168 mmol) and pyridine (148 mg, 0.187 mml) in acetone (5 mL). The product was isolated as a yellow solid. ^{1}H NMR (200 MHz, d_6-acetone): δ 9.21 (2H, d, ^3J 5.8, H^2-py^2), 8.37 (1H, t, ^3J 7.7, H^4-py^2), 8.23 (4H, m, H^3-py^1, H^4-py^1), 8.01 (2H, t, ^3J 6.5, H^3-py^2), 7.94 (2H, d, ^3J 5.8, $^3J(^{195}Pt)$ obscured, H^6-py^1), 7.39 (2H, t, ^3J 5.7, H^5-py^1), 7.06 (1H, s, H-xy), 2.75 (6H, s, CH_3).

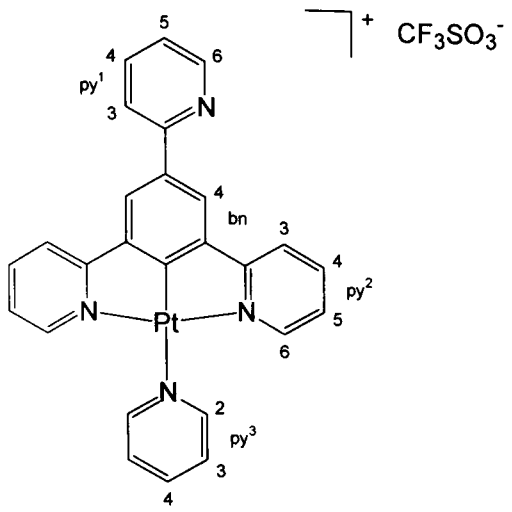

[L^{7}Ptpy]SO$_3$CF$_3$: 1,3,5-Tri(2-pyridyl)benzene-2-platinum(II)-N-pyridine trifluoromethanesulfonate

Prepared *via* chloride metathesis using L^{7}PtCl (42 mg, 0.078 mmol), silver trifluoromethanesulfonate (25 mg, 0.097 mmol) and pyridine (1 mL, 12.5 mmol) in acetone (12 mL). The mixture was stirred at RT for 2 h before removal of silver chloride, followed by another 2 h after treatment with pyridine. Work-up (5 x 1 mL acetone) yielded the product as a yellow powder (38 mg, 66%). ^{1}H NMR (400 MHz, d_6-acetone): δ 9.26 (2H, d, ^3J 3.6, H^2-py^3), 8.75 (1H, m, H^4-py^3), 8.58 (2H, s, H-bn), 8.40 (3H, m, H^6-py^1, H^3-py^2), 8.33 (2H, t, ^3J 7.4, H^4-py^2), 8.16 (1H, d, ^3J 7.3, H^3-py^1), 8.03 (4H, m, H^6-py^2, H^3-py^3), 7.94 (1H, m, H^4-py^1), 7.50 (2H, t, ^3J 4.9, H^5-py^2), 7.41 (1H, m, H^5-py^1). ^{13}C NMR (101 MHz, d_6-acetone): δ 152.7, 152.0, 142.3, 128.7, 125.8, 124.2, 120.9. MS (ES$^+$): *m/z* 582 [M – CF_3SO_3]$^+$; *m/z* 503 [M – $C_5H_5NCF_3SO_3$]$^+$.

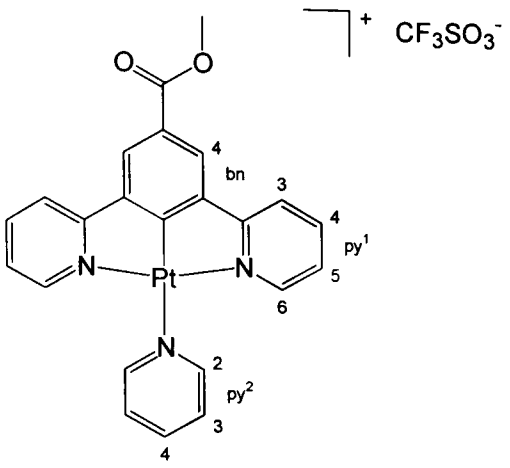

3,5-Di(2-pyridyl)methylbenzoate-4-platinum(II)-N-pyridine trifluoromethanesulfonate

Prepared *via* chloride metathesis using 3,5-di(2-pyridyl)methylbenzoate-4-platinum(II) chloride (22 mg, 0.04 mmol), silver trifluoromethanesulfonate (12 mg, 0.04 mmol), and an excess of pyridine (1 mL, 12.5 mmol) in acetone (10 mL). The mixture was stirred at RT for 2½ h before removal of silver chloride, followed by a further 4 h after treatment with pyridine. The work-up (3 x 1 mL of acetone) yielded the product as a pale yellow solid (6 mg, 20%). ^{1}H NMR (400 MHz, d_6-acetone): δ 9.25 (2H, d, ^3J 5.0, H^2-py^2), 8.37 (7H, m, H-bn, H^3-py^1, H^4-py^1, H^4-py^2), 8.05 (4H, m, H^6-py^1, H^3-py^2), 7.54 (2H, ddd, ^3J 7.4, ^3J 6.0, ^4J 1.6, H^5-py), 4.0 (3H, s, CH_3). MS (ES^+): *m/z* 563 $[M - CF_3SO_3]^+$; *m/z* 484 $[M - C_5H_5NF_3SO_3]^+$. HRMS (ES^+): *m/z* 563.1036 $[M - CF_3SO_3]^+$; $C_{23}H_{18}O_2N_3Pt$ requires 563.1041.

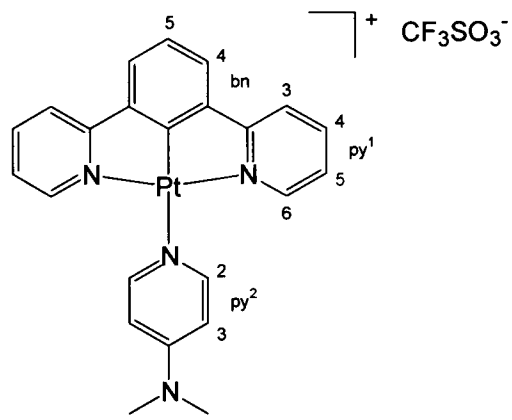

$[L^1Pt((DMAP))]SO_3CF_3$: 1,3-Di(2-pyridyl)benzene-2-platinum(II)-N-pyridyl-4-(N,N-dimethylamine) trifluoromethanesulfonate

Prepared *via* chloride metathesis using L^1PtCl (42 mg, 0.091 mmol), silver trifluoromethanesulfonate (33 mg, 0.13 mmol) and 4-N,N-dimethylaminopyridine (28 mg, 0.23 mmol) in acetone (15 mL). The mixture was stirred at room temperature for 2 h before removal of silver chloride, followed by a further 2 h after

treatment with 4-N,N-dimethylaminopyridine. The product was isolated as a yellow solid. ^{1}H NMR (400 MHz, d^6-acetone): δ 8.55 (2H, ^3J 5.4, ^3J(^{195}Pt) 17.5, H^2-py^2), 8.27 (2H, td, ^3J 7.9, ^4J 1.5, H^4-py^1), 8.18 (2H, d, ^3J 8.0, ^4J(^{195}Pt) 18.8, H^3-py^1), 8.06 (2H, dd, ^3J 5.6, ^4J 1.5, ^3J(^{195}Pt) 41.2, H^6-py^1), 7.80 (2H, d, ^3J 8.0, H^4-bn), 7.49 (2H, ddd, ^3J 7.3, ^3J 5.9, ^4J 1.5, H^5-py^1), 7.37 (1H, t, ^3J 7.5, H^5-bn), 7.01 (2H, d, ^3J 5.6, H^3-py^2), 3.26 (6H, s, CH_3). MS (ES$^+$): *m/z* 548 [M – CF_3SO_3]$^+$.

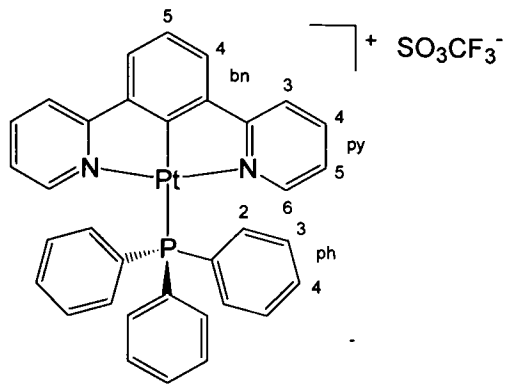

[L^{1}Pt(PPh$_3$)]SO$_3$CF$_3$:1,3-Di(2-pyridyl)benzene-2-platinum(II) triphenylphosphine trifluoromethanesulfonate

Prepared *via* chloride metathesis using 1,3-di(2-pyridyl)benzene-2-platinum(II) chloride (34 mg, 0.073 mmol), silver trifluoromethanesulfonate (25 mg, 0.097 mmol), and triphenylphosphine (22 mg, 0.084 mmol) in acetone (5 mL). The mixture was stirred at RT for 1 h before the removal of silver chloride, and a further hour after treatment with triphenylphosphine. The solvent was completely evaporated prior to work-up, followed by washing with acetone (4 x 2 mL), yielding a pale yellow solid (23 mg, 37%). ^{1}H NMR (400 MHz, d$_6$-acetone): δ 8.17 (3H, td, ^3J 8.1, ^4J 2.1, H^4-ph), 8.15 (2H, td, ^3J 8.0, ^4J 1.5, H^4-py), 8.04 (6H, m, H^2-ph), 7.91 (2H, d, ^3J 7.7, H^4-bn), 7.73 (2H, d, ^3J 6.0, ^{195}Pt coupling masked by neighbouring peaks, H^6-py), 7.66 (10H, m, H^3-ph, H^3-py, H^4-py), 7.50 (1H, t, ^3J 7.7, H^5-bn), 6.95 (2H, ddd, ^3J 8.0, ^3J 5.0, ^4J 2.2, H^5-py). MS (ES$^+$): *m/z* 688.1 [M]$^+$. HRMS (ES$^+$): *m/z* 688.14799 [M]$^+$; [$C_{34}H_{26}N_2PPt$] requires 688.14759. Anal: Calcd for $C_{35}H_{26}F_3N_2O_3PPtS_1.H_2O$: C, 49.13; H, 3.30; N 3.27. Found: C, 48.99; H, 3.04; N, 3.26%.

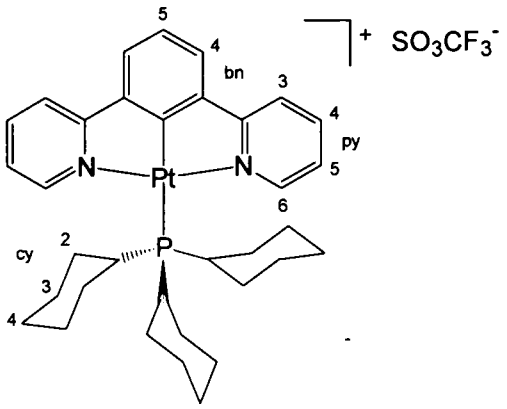

[$L^1Pt(PCy_3)$]SO_3CF_3: 1,3-Di(2-pyridyl)benzene-2-platinum(II) tricyclohexylphosphine trifluoromethane-sulfonate

Prepared *via* chloride metathesis using 1,3-di(2-pyridyl)benzene-2-platinum(II) chloride (36 mg, 0.078 mmol), silver trifluoromethanesulfonate (30 mg, 0.116 mmol), and tricyclohexylphosphine (24 mg, 0.086 mmol) in acetone (5 mL). The mixture was stirred at RT for 1½ h before the removal of silver chloride, and a further 3½ h after treatment with tricyclohexylphosphine. The solvent was completely evaporated prior to work-up, followed by washing with acetone (4 x 2 mL), yielding a pale yellow solid (31 mg, 45%). ^{1}H NMR (400 MHz, d_6-acetone): δ 8.99 (2H, d, ^3J 5.9, $^3J(^{195}Pt)$ 42.4, H^6-py), 8.33 (2H, td, ^3J 7.5, ^4J 1.4, H^4-py), 8.23 (2H, d, ^3J 8.0, H^3-py), 7.89 (2H, d, ^3J 7.8, H^4-bn), 7.72 (2H, ddd, ^3J 7.5, ^3J 5.9, ^4J 1.5, H^5-py), 7.47 (1H, t, ^3J 7.7, H^5-bn), 2.63 (3H, m, H^1-cy), 1.73 (18H, m, H^2-cy, H^4-cy), 1.27 (12H, m, H^3-cy). ^{13}C NMR (101 MHz, d_6-acetone): 156.7, 143.4, 142.1, 126.9 (C^5-bn), 126.2 (C^5-py), 126.0 (C^4-bn), 122.1 (C^3-py), 30.9, 30.6, 28.3, 28.2, 26.9. MS (ES^+): *m/z* 704.8 $[M]^+$. Anal: Calcd for $C_{35}H_{41}F_3N_2O_3P_1Pt_1S_1$: C, 49.29; H, 4.85; N 3.28. Found: C, 49.15; H, 5.29; N, 3.09%.

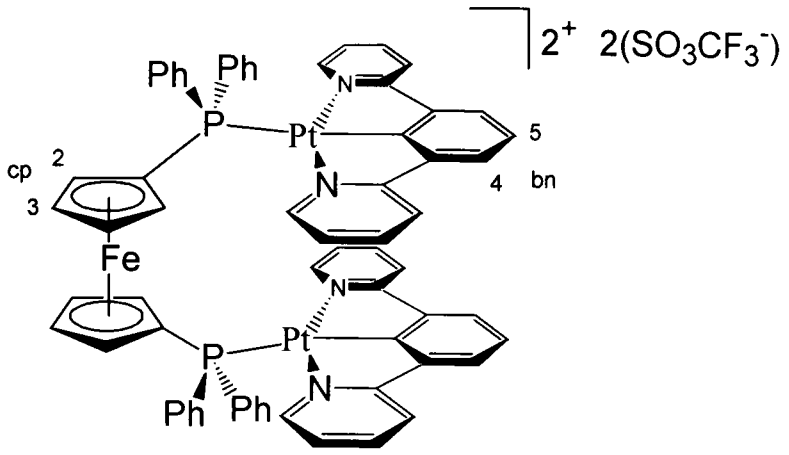

[L^{1}Pt]$_2$(dppf): 1,1'-Bis(diphenylphosphino-[1,3-di(2-pyridyl)benzene-2-platinum-(II)])-ferrocene bis(trifluoromethanesulfonate)

Prepared *via* chloride metathesis using 1,3-di(2-pyridyl)benzene-2-platinum(II) chloride (30 mg, 0.065 mmol), silver trifluoromethanesulfonate (17 mg, 0.066 mol), and 1,1'-bis(diphenylphosphino) ferrocene (18 mg, 0.032 mmol) in acetone (5 mL). The mixture was stirred at RT for 1 h before the removal of silver chloride, and overnight after treatment with the new bisphosphine ligand. The reaction solvent was completely evaporated prior to work-up, followed by washing with acetone (4 x 2 mL), yielding a yellow solid (12 mg, 22%). ^{1}H NMR (200 MHz, d_6-acetone): δ 8.10 (14H, m), 7.81 (4H, d, ^3J 7.7, H^4-bn), 7.65 (16H, m), 7.46 (4H, t, ^3J 7.7, H^5-bn), 6.88 (4H, m, H^4-ph), 4.79 (4H, m, H^2-cp), 4.53 (4H, m, H^3-cp). Anal: Calcd for $C_{68}H_{50}F_6FeN_4O_6P_2Pt_2S_2$: C, 47.90; H, 2.96; N 3.29. Found: C, 48.04; H, 3.05; N, 3.23%.

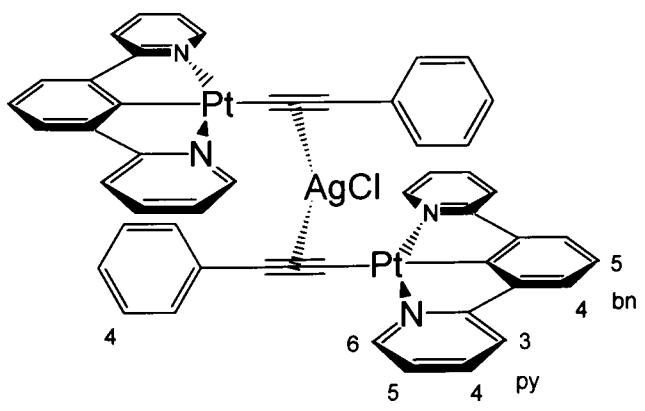

[L^{2}PtC$_2$Ph]$_2$AgCl: Bis[1,3-di(2-pyridyl)benzene-2-platinum(II) phenylacetylide]-η^2,η^2-silver chloride

Silver acetylide was prepared by treating ammoniacal solutions of $AgNO_3$ with phenylaceylene (**Caution!** Silver acetylides are potentially explosive and should be handled with care and in small quanitities).[290] 1,3-Di(2-pyridly)benzene-2-

platinum(II) chloride (84 mg, 0.182 mmol) was suspended in anhydrous acetone (10 mL), treated with silver phenylacetylide (50 mg, 0.239 mmol) and stirred at RT for 3 d. The reaction was formed a yellow solution accompanied by a dark red precipitate. The precipitate was isolated *via* centrifuge and washed with acetone (10 x 1 mL), yielding a deep red solid (24 mg, 11%). ^{1}H NMR (500 MHz, d_6-acetone): δ 9.09 (2H, d, ^{3}J 5.4, $^{3}J(^{195}Pt)^{t}$ 44.7, H^{6}-py), 7.93 (2H, td, ^{3}J 7.8, ^{4}J 1.1, H^{4}-py), 7.65 (2H, d, ^{3}J 7.8, H^{3}-py), 7.57 (2H, dd, ^{3}J 7.6, ^{4}J 1.6, H^{2}-ac), 7.39 (2H, d, ^{3}J 7.6, H^{4}-bn), 7.33 (3H, m, H^{4}-ac, H^{5}-py), 7.14 (1H, t, ^{3}J 7.8, H^{5}-bn), 7.08 (2H, t, ^{3}J 6.2, H^{3}-ac). ^{13}C NMR (126 MHz, d_6-Acetone): δ 169.7, 167.5, 155.3, 143.5, 140.5, 132.9, 129.2, 128.2, 125.3, 124.7, 124.6, 121.1. MS(EI^{+}): 527.1 $[C_{16}H_{11}N_2PtC_2C_6H_5]^{+}$; 426.0 $[M - C_2C_6H_5]^{+}$.

8.2.5. Palladium complexes

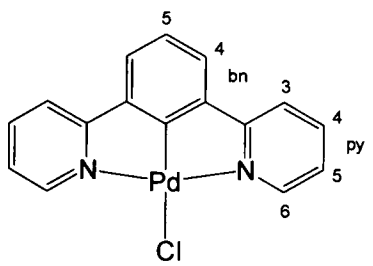

L^{1}PdCl: 1,3-Di(2-pyridyl)benzene-2-palladium(II) chloride

This compound was prepared according to the method outlined in the literature.[252] Palladium(II) acetate (58 mg, 0.26 mmol) in DCM (8 mL) was degassed *via* the freeze-pump-thaw technique. Meanwhile, 1,3-di(2-pyridyl)benzene-2-mercury(II) chloride (120 mg, 0.26 mmol) in absolute ethanol (20 mL) was degassed *via* the freeze-pump-thaw technique. The palladium acetate solution was transferred into the reaction vessel containing the mercury compound, *via* cannular, under positive pressure of dinitrogen, and the mixture stirred at reflux temperature (78°C) for 4 h. The mixture was filtered through celite, before being reduced *in vacuo* yielding a bright orange solid. This solid was then taken into methanol (50 mL), degassed and treating with an excess of lithium chloride (735mg, 17.33 mmol). This mixture was then stirred at RT for 1 h, before being reduced *in vacuo* yielding a beige solid. The crude product was washed repeatedly with hot methanol (10 x 5 mL), isolated by centrifugation and air dried yielding a grey solid (14 mg, 15%). ^{1}H NMR (500 MHz, $CDCl_3$): δ 8.84 (2H, d, ^{3}J 5.5, H^{6}-py), 7.79 (2H, td, ^{3}J 7.7, ^{4}J 1.3, H^{4}-py), 7.56 (2H, d, ^{3}J 7.9, H^{3}-py), 7.23 (2H, d, ^{3}J 7.7, H^{4}-bn), 7.15 (2H, t, ^{3}J 6.4, H^{5} py), 7.00 (1H, t, ^{3}J 7.7, H^{5}-bn). ^{13}C NMR (126 MHz, $CDCl_3$): δ 172.5 (C^{2}-bn), 164.9

(C^2-py), 152.2 (C^6-py), 143.2 (C^1-bn), 139.1 (C^4-py), 124.5 (C^5-bn), 124.0 (C^4-bn), 123.2 (C^5-py), 119.1 (C^3-py). Anal: Calcd for $C_{16}H_{11}N_2PdCl$: C, 51.50; H, 2.97; N 7.51. Found: C, 53.15; H, 3.98; N, 6.28%.

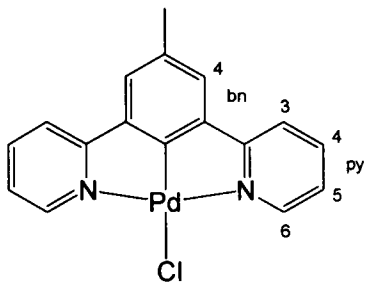

L^2PdCl: 1,3-Di(2-pyridyl)-5-methylbenzene-2-palladium(II) chloride

This compound was prepared using the methodology for palladium complexation outlined in Section 8.1.5 above, using palladium(II) dichloride (79 mg, 0.45 mmol), lithium chloride (60 mg, 1.42 mmol) and 1,3-di(2-pyridyl)-5-methylbenzene (116 mg, 0.47 mmol). The mixture was stirred at reflux for 16 h before work-up. The product isolated as a pale beige solid (40 mg, 23%). ^{1}H NMR (500 MHz, $CDCl_3$): δ 9.13 (2H, dd, ^3J 5.5, ^4J 1.1, H^6-py), 7.90 (2H, td, ^3J 7.9, ^4J 1.4, H^4-py), 7.67 (2H, d, ^3J 7.9, H^3-py), 7.29 (2H, s, H-bn), 7.28 (2H, obscured by residual solvent peak, H^5-py), 2.42 (3H, s, CH_3). ^{13}C NMR (126 MHz, $CDCl_3$): δ 169.6, 165.2, 152.9, 143.3, 139.1 (C^4-py), 134.2, 124.8 (C^5-py), 123.28 (C^4-bn), 118.83 (C^3-py). MS (EI^+): 388 $[M]^+$; 351 $[M - Cl]^+$. Anal: Calcd for $C_{17}H_{13}N_2PdCl$: C, 52.74; H, 3.38; N, 7.24. Found: C, 52.74; H, 3.65; N, 7.04%.

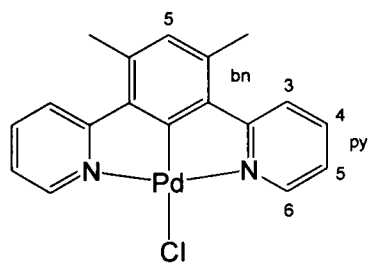

L^3PdCl: 1,3-Di(2-pyridyl)-4,6-dimethylbenzene-2-palladium(II) chloride

Prepared from palladium(II) dichloride (80 mg, 0.45 mmol), lithium chloride (60 mg, 1.42 mmol) and 1,3-di(2-pyridyl)-4,6-dimethylbenzene (117 mg, 0.45 mmol) in a reduced amount of glacial acetic acid (5 mL). The mixture was stirred at reflux for 1½ d before work-up. The product was isolated as a beige/grey solid (114 mg, 63%). ^{1}H NMR: (500 MHz, $CDCl_3$): δ 9.24 (2H, dd, ^3J 5.6, ^4J 1.3, H^6-py), 7.85 (2H, td, ^3J 7.2, ^4J 1.8, H^4-py), 7.80 (2H, d, ^3J 8.1, H^3-py), 7.19 (2H, ddd, ^3J 7.2, ^3J 5.7, ^4J 1.5, H^5-py), 6.72 (1H, s, H-bn), 2.60 (6H, s, CH_3). ^{13}C NMR (126 MHz, $CDCl_3$):

δ 175.0 (C^3-xy), 166.0 (C^5-xy), 152.9 (C^6-py), 139.7 (C^4-xy), 138.8 (C^4-py), 136.1 (C^1-xy), 132.3 (C^2-xy), 122.3 (C^5-py), 122.2 (C^3-py), 22.5 (CH_3). Anal. Calcd for $C_{18}H_{15}N_2PdCl$: C, 53.89; H, 3.77; N, 6.98. Found: C, 53.86; H, 3.77; N, 7.06%.

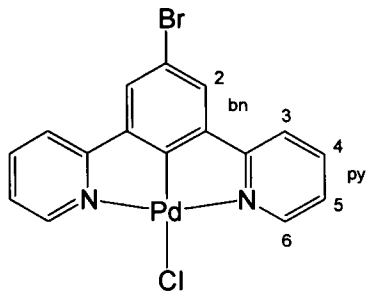

L^6PdCl: 1,3-Di(2-pyridyl)-5-benzene-2-palladium(II) chloride

Prepared using palladium(II) dichloride (76 mg, 0.43 mmol), lithium chloride (59 mg, 1.39 mmol) and 1-bromo-3,5-(2-pyridyl)benzene (148 mg, 0.48 mmol). The mixture was stirred at reflux for 3 d before work-up. The product was isolated as a beige/yellow solid (78 mg, 40%). ^{1}H NMR (400 MHz, $CDCl_3$) δ 9.08 (2H, d, ^3J 5.7, H^6-py), 7.93 (2H, t, ^3J 7.9, H^4-py), 7.63 (2H, d, ^3J 7.8, H^3-py), 7.48 (2H, s, H-bn), 7.30 (2H, t, ^3J 7.5, H^5 py). ^{13}C NMR (101 MHz, $CDCl_3$) δ 170.7 (C^2-bn), 164.0 (C^2-py), 153.1 (C^6-py), 145.0, 139.5 (C^4-py), 126.7 (C^4-bn), 124.1 (C^5-py), 119.4 (C^3-py), 117.9. MS (EI^+): *m/z* 452 $[M]^+$; *m/z* 417 $[M - Cl]^+$; *m/z* 373 $[M - Br]^+$. Anal: Calcd for $C_{16}H_{10}N_2BrPdCl$: C, 42.51; H, 2.23; N, 6.20. Found: C, 42.23; H, 2.19; N, 5.90%.

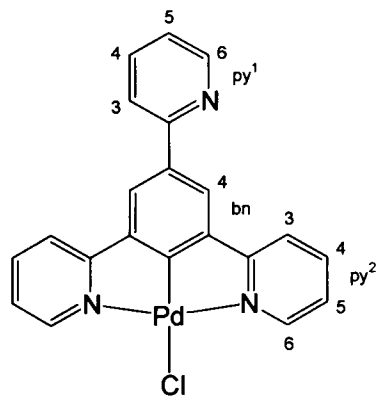

L^7PdCl: 1,3,5-Tri(2-pyridyl)benzene-2-palladium(II) chloride

Prepared using palladium(II) dichloride (80 mg, 0.45 mmol), lithium chloride (61 mg, 1.44 mmol) and 1,3,5-tri(2-pyridyl)benzene (136 mg, 0.44 mmol). The mixture was stirred at reflux for 2 d before work-up. The work-up was slightly different for this compound, requiring the use of $Na_2CO_{3(aq)}$ as the aqueous washing part of the work-up, yielding a beige solid (113 mg, 57%). ^{1}H NMR

(500 MHz, $CDCl_3$): δ 9.06 (2H, dd, ^3J 5.5, ^4J 1.0, H^6-py^2), 8.69 (1H, dt, ^3J 4.9, ^4J 2.4, H^6-py^1), 8.01 (2H, s, H-bn), 7.87 (2H, td, ^3J 7.8, ^4J 1.6, H^4-py^2), 7.79 (4H, m, H^3-py^1, H^4-py^1, H^3-py^2), 7.28 (1H, m, H^5-py^1), 7.21 (2H, ddd, ^3J 7.1, ^3J 5.1, ^4J 1.4, H^5-py^2). ^{13}C NMR (126 MHz, $CDCl_3$): 174.3 (C^2-bn), 164.9 (C^1-bn), 156.9 (C^2-py^2), 152.8 (C^6-py^2), 149.8, 143.7, 139.2 (C^4-py^2), 137.2 (C^4-py^1), 136.3, 123.5 (C^5-py^2), 122.6, 122.4, 120.4 (C^3-py^1), 119.3 (C^3-py^2). MS (ES^+): *m/z* 865 $[2M - Cl]^+$.

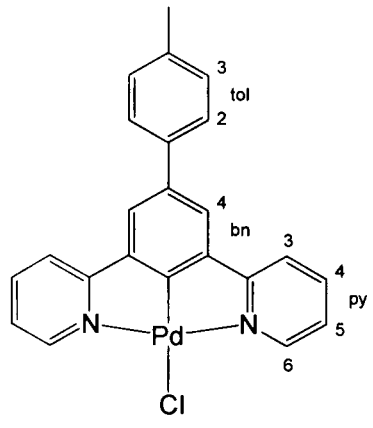

L^8PdCl: 5-(*p*-Tolyl)-1,3-di(2-pyridyl)benzene-2-palladium(II) chloride

Prepared using palladium(II) dichloride (80 mg, 0.45 mmol), lithium chloride (61 mg, 1.44 mmol) and 1,3-di(2-pyridyl)-5-(*p*-tolyl)benzene (102 mg, 0.32 mmol). The mixture was stirred at reflux for 16 h before work-up. Further purification in this case involved successive washings of the crude product *via* centrifuge with diethyl ether (10 x 10 mL), acetone (3 x 3 mL) and again with diethyl ether (3 x 5 mL). Product was isolated as a pale yellow solid (43 mg, 29%). ^1H NMR (500 MHz, $CDCl_3$): δ 9.02 (2H, d, ^3J 5.5, H^6-py), 7.85 (2H, t, ^3J 7.7, H^4-py), 7.68 (2H, d, ^3J 7.8, H^3-py), 7.47 (4H, m, H^4-bn, H^2-tol), 7.26 (2H, obscured by $CHCl_3$ peak, H^3-tol), 7.18 (2H, t, ^3J 6.7, H^5-py), 2.42 (3H, s, CH_3). ^{13}C NMR (126 MHz, $CDCl_3$): δ 171.6 (C^2-bn), 164.9 (C^2-py), 152.7 (C^6-py), 143.6 (C^5-bn), 139.1 (C^4-py), 138.1 (quat), 138.1 (quat), 137.4 (quat), 129.8 (C^3-tol), 126.9 (C^2-tol), 123.3 (C^5-py), 122.7 (C^4-bn), 119.1 (C^3-py), 21.3 (CH_3). Anal. Calcd. for $C_{23}H_{17}N_2PdCl$: C, 59.63; H, 3.70; N, 6.05. Found: C, 54.64; H, 3.46; N, 5.43%.

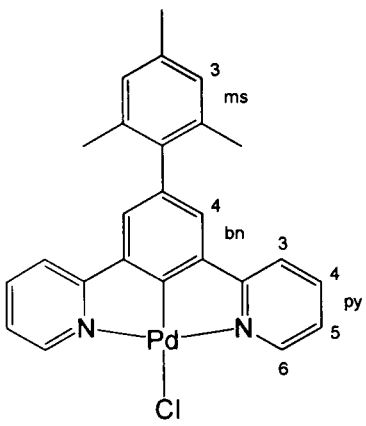

L^9PdCl: 1,3-Di(2-pyridyl)-5-mesitylbenzene-2-palladium(II) chloride

Prepared using palladium(II) dichloride (79 mg, 0.45 mmol), lithium chloride (60 mg, 1.42 mmol) and 1,3-di(2-pyridyl)-5-mesitylbenzene (161 mg, 0.46 mmol). The mixture was stirred at reflux for 2½ d before work-up. Extra washings with diethyl ether (4 x 5 mL) were required, to remove persistent aromatic signals in the ^{1}H NMR. The product was isolated as an off-white solid (68 mg, 31%). ^{1}H NMR (500 MHz, $CDCl_3$): δ 9.15 (2H, d, ^3J 5.5, ^4J 0.9, H^6-py), 7.89 (2H, td, ^3J 7.8, ^4J 1.6, H^4-py), 7.61 (2H, d, ^3J 7.8, H^3-py), 7.28 (2H, ddd, ^3J 7.1, ^3J 5.9, ^4J 1.5, H^5-py), 7.21 (2H, s, H-bn), 6.99 (2H, s, H-ms), 2.36 (3H, s, *p*-CH_3), 2.08 (6H, s, *o*-CH_3). ^{13}C NMR (126 MHz, $CDCl_3$): δ 171.0, 165.1, 152.9, 143.6, 139.2 (C^4-py), 138.2, 137.7, 137.3, 136.2, 128.3 (C^3-ms), 124.8 (C^4-bn), 123.4 (C^5-py), 119.0 (C^3-py), 21.1 (*p*-CH_3), 21.0 (*o*-CH_3). MS (EI^+): *m/z* 492 $[M]^+$; *m/z* 455 $[M - Cl]^+$. Anal: Calcd for $C_{25}H_{21}N_2PdCl$: C, 61.11; H, 4.31; N 5.70. Found: C, 54.42; H, 3.97; N, 6.24%.

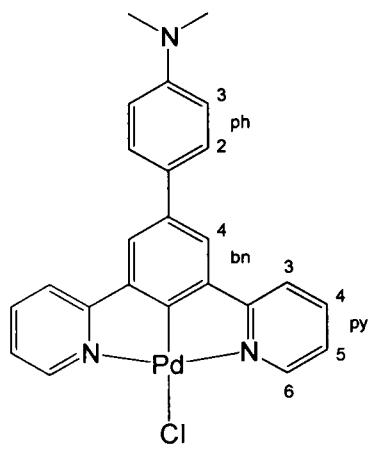

$L^{16}PdCl$: 1,3-Di(2-pyridyl)-5-phenyl-(4-N,N-dimethylaniline)-2-palladium(II) chloride

Prepared using palladium(II) dichloride (33 mg, 0.19 mmol), lithium chloride (4 mg, 0.09 mmol) and 1,3-di(2-pyridyl)-5-phenyl-(4-N,N-dimethylaniline) (55 mg, 0.157 mmol). The mixture was stirred at reflux for 19 h before work-up. The

mixture was allowed to cool to ambient temperature before being evaporated to dryness *in vacuo* to an off-yellow solid. This solid was then diluted in DCM (75 mL) and washed with $NaHCO_{3(aq)}$ (5% by mass, 2 x 100 mL). The organic phase was retained, and the solvent evaporated to afford a yellow solid before washing with diethyl ether (10 x 10 mL) by sonication, and separation *via* centrifugation, yielding a bright yellow solid (31 mg, 40%). ^{1}H NMR (400 MHz, $CDCl_3$): δ 9.07 (2H, d, ^3J 5.6, H^6-py), 7.87 (2H, td, ^3J 7.8, ^4J 1.6, H^4-py), 7.69 (2H, d, ^3J 7.8, H^3-py), 7.51 (2H, s, H^4-bn), 7.48 (2H, d, ^3J 8.7, H^2-ph), 7.22 (2H, ddd, ^3J 7.4, ^3J 5.6, ^4J 1.2, H^5-py), 6.82 (2H, d, ^3J 8.7, H^3-ph), 3.02 (6H, s, CH_3). ^{13}C NMR (126 MHz, $CDCl_3$): δ 170.6 (C^2-bn), 165.2 (C^2-py), 152.8 (C^6-py), 150.2 (C^4-ph), 143.5, 139.1 (C^4-py), 138.5, 129.0, 127.8 (C^2-ph), 123.3 (C^5-py), 122.3 (C^4-bn), 119.0 (C^3-py), 112.9 (C^3-ph), 40.7 (CH_3). MS (ES^+): *m/z* 514 [M + Na^+]. Anal. Calcd for $C_{24}H_{20}N_3PdCl$: C, 58.55; H, 4.09; N, 8.54. Found: C, 57.96; H, 4.10; N, 8.15%.

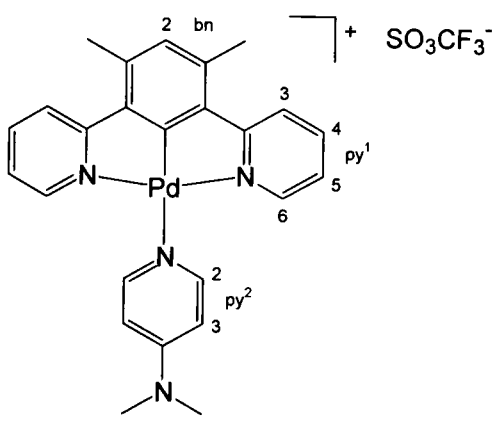

[L^3Pd(DMAP)]SO_3CF_3: 1,3-Di(2-pyridyl)-4,6-dimethylbenzene-2-palladium(II)-N-pyridyl-4-(N',N'-dimethylamine) trifluoromethanesulfonate

Prepared *via* chloride metathesis using L3PdCl (40 mg, 0.10 mmol), silver trifluoromethanesulfonate (37 mg, 0.15 mmol) and N,N-dimethylamino-4-pyridine (26 mg, 0.21 mmol) in acetone (4 mL). The mixture was stirred at RT for 1 h before removal of silver chloride, followed by a further hour after treatment with N,N-dimethylamino-4-pyridine. After work-up (3 x 3 mL acetone) the product isolated as a beige solid (45 mg, 70%). ^{1}H NMR (400 MHz, d_6-acetone): δ 8.54 (2H, d, ^{3}J 6.4, H^2-py^2), 8.18 (4H, m, H^3-py^1, H^4-py^1), 7.90 (2H, d, ^{3}J 4.8, H^6-py^1), 7.40 (2H, m, H^5-py), 7.01 (3H, m, H-xy, H^3-py^2), 3.23 (6H, s, CH_3-xy), 2.72 (6H, s, CH_3-py^2). MS (ES^+): *m/z* 395 [M – $NC_5H_4NC_2H_6$ + CH_3O]$^+$.

9. Conclusions and future work

A series of platinum(II) and palladium(II) complexes have been synthesised based on the coordination geometry of 1,3-di(2-pyridyl)benzene, HL^1. The luminescence properties of these new complexes show a significant development in the application of these metal complexes in photophysical applications. The platinum(II) complexes have shown that the dramatically increased quantum yields associated with the coordination geometry can be maintained whilst being able to tune the emission colour through changes in the ligand, $\Phi = 0.45 - 0.60$.

The terdentate coordination of the ligands, important for preventing metal centre distortion, and the high ligand-field induced by cyclometalation are both critical in preventing excited-state deactivation of square-planar platinum and palladium complexes. Expansion on this theory for future work could be around the synthesis and coordination of a currently unexplored N^C^C coordinating geometry. The target complexes would be doubly cyclometalated, and predicted to be achievable through modification of recent high yielding synthesis of C^N^C systems, Equation 1; Page 17.[56,60] Ligands of such design shown in Scheme 24 are ideal primiary targets and are expected to offer blue shifted emission compared to their N^C^N equivalent, whilst maintaining high quantum yields.

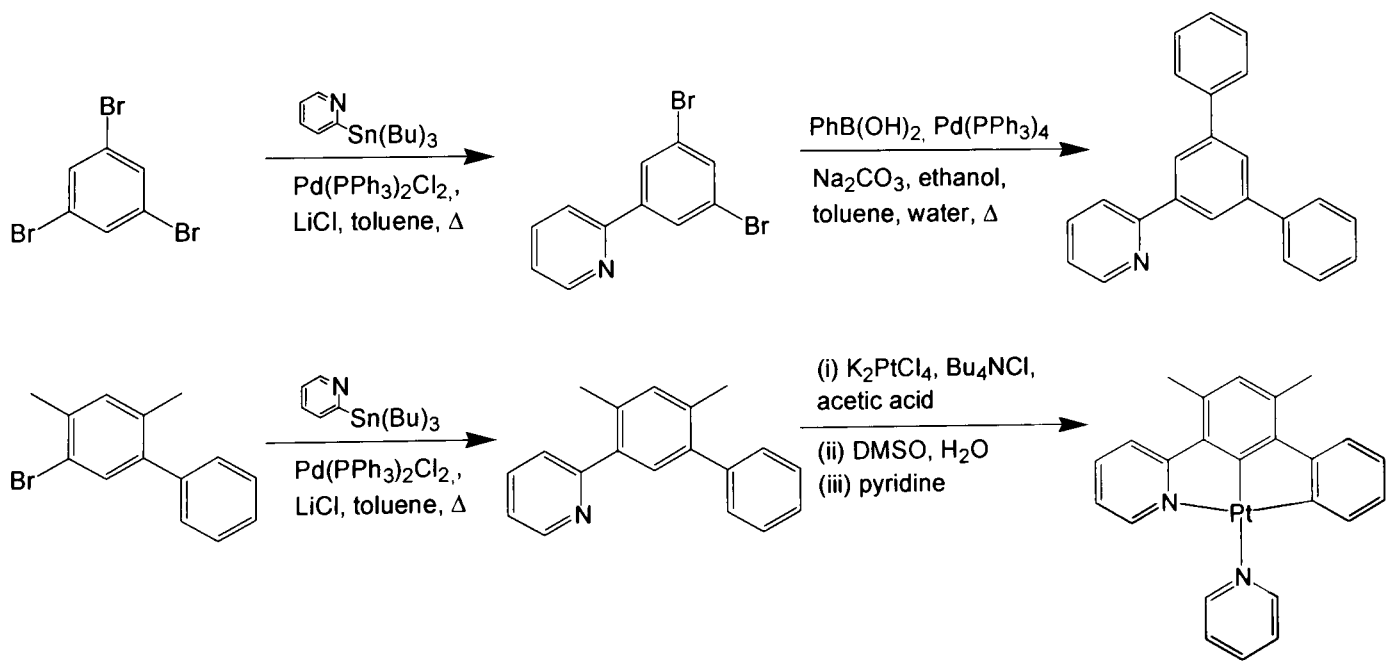

Scheme 24: Synthetic strategy for a series of N^C^C coordinated complexes. The method is based on the site directing synthesis of palladium(II) N^C^N complexes, Section 7.1. The peripheral aryl donor is expected to be a viable site for facile substitution, as could be envisaged through a series of ligands based on mono-pyridyl versions of HL^n (n = 8, 10 – 13, 16 – 20).

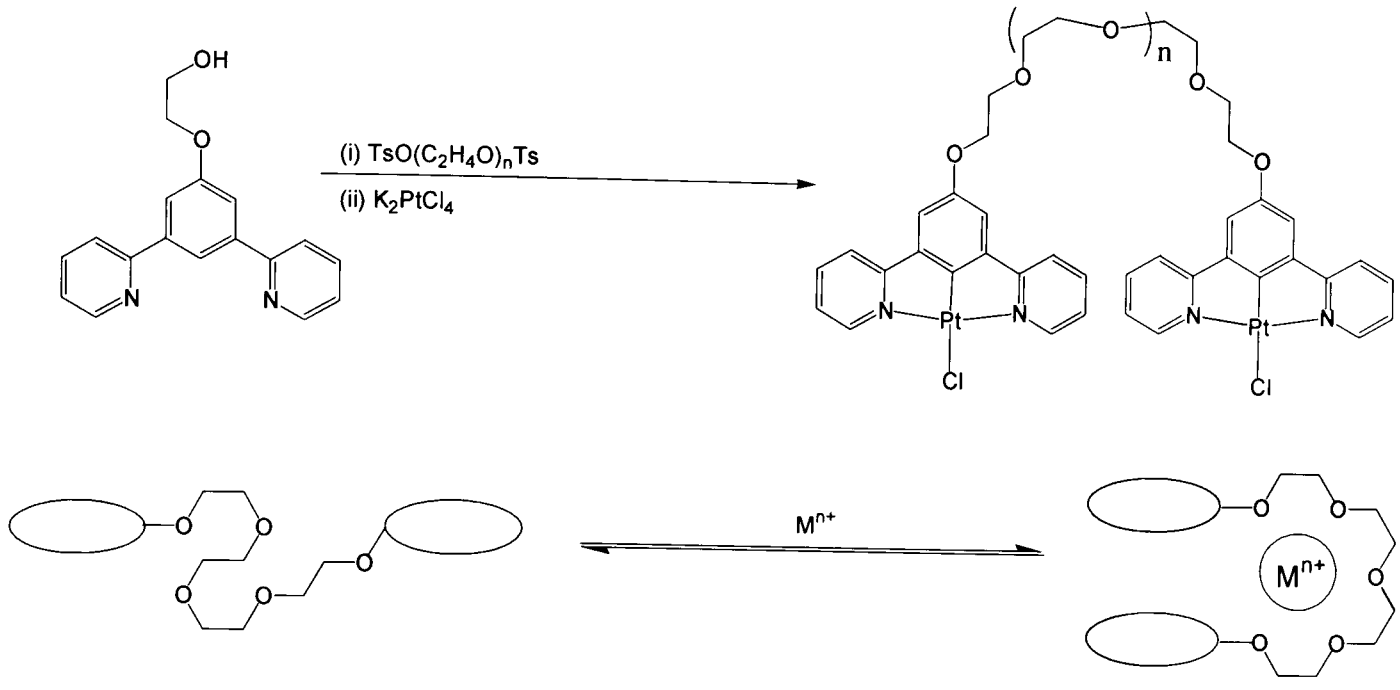

Scheme 25: The extention of the ether complex L^5PtCl to contain bridging polyether units could incorporate a small ion recognition centre capable of exerting daramatic photophysical changes in the luminescence spectra as excimeric behaviour is induced through physical reorganisation of the system as well as an increase in favourable electronic interactions.

The ability to modify the electron-donating properties allowed the induction of excited-state switching through small ion recognition events (L^nPtCl n = 16, 18, 25 and 26). The interesting luminescence properties of L^5PtCl developed interest in the synthesis of target molecules outlined in Scheme 25. The tendency for L^5PtCl to resist excimer formation and emission could be controlled by removing the electron donating effects of phenyl bound oxygen through small ion binding events in the polyether chain. The act of binding is then predicted to reorientate the molecule so that the two aromatic metal-complexes are now positioned favourably for a dinuclear excited-state species to form, be they either excimeric or oligomeric (as described for solid-state interactions observed in crystals of L^6PtCl, Section 4). The synthesis of L^5PtCl derivatives were abandoned mid-synthesis due to time restrictions.

Multiple crystal structures of L^6PtCl highlighted the polymorphic crystalline-behaviour of these square-planar complexes. The luminescent changes observed in the polymorphs, apparently induced by the presence of solvent disrupting the intermolecular interactions between neighbouring complexes, points towards the use of these complexes as luminescent-signalling vapochromic sensors, however, a large amount of further work would be required. In the same

vien the application as luminescent luquid crystalline materials could be a fruitful endeavour due to the exploitation of similar systems in this field.[12]

Some work has been performed on the involvement of these complexes as luminescent probes for *in vivo* applications. Some preliminary results had been obtained but were not described in this report.

The series of luminescent palladium(II) complexes shows progress in their application as room temperature luminescent materials required for OLEDs and sensors (as has been demonstrated for the platinum complexes, Section 5). Further development of the plalladium species as luminescent systems may require the synthesis of systems with low lying MLCT states such as those described by McMillan et al.[42] Ligands such as HL^1 substituted at the 5-position of the benzene ring with large electron rich groups such as pyrene could display such photophysical properties.

Additionally, further investigation into the excimeric behaviour observed in these complexes holds particular interest, as it is to our best understanding that this type of behaviour in palladium complexes is yet to be explored.

References

[1] W. B. Connick, D. Geiger, R. Eisenberg, *Inorg. Chem.* **1999**, *38*, 3264.

[2] V. W.-W. Yam, K. M.-C. Wong, N. Zhu, *J. Am. Chem. Soc.* **2002**, *124*, 6506.

[3] T. K. Aldridge, E. M. Stacy, D. R. McMillin, *Inorg. Chem.* **1994**, *33*, 722.

[4] K.-T. Wan, C.-M. Che, K.-C. Cho, *Dalton Trans.* **1991**, 1077.

[5] P. Du, J. Schneider, P. Jarosz, R. Eisenberg, *J. Am. Chem. Soc.* **2006**, *128*, 7726.

[6] L. Chassot, A. von Zelewsky, D. Sandrini, M. Maestri, V. Balzani, *J. Am. Chem. Soc.* **1986**, *108*, 6084.

[7] W. B. Connick, H. B. Gray, *J. Am. Chem. Soc.* **1997**, *119*, 11620.

[8] W. Paw, S. D. Cummings, M. A. Mansour, W. B. Connick, D. K. Geiger, R. Eisenberg, *Coord. Chem. Rev.* **1998**, *171*, 125.

[9] L. J. Grove, J. M. Rennekamp, H. Jude, W. B. Connick, *J. Am. Chem. Soc.* **2004**, *126*, 1594.

[10] T. J. Waddas, Q.-M. Wang, Y.-J. Kim, C. Flaschenreim, T. N. Blanton, R. Eisenberg, *J. Am. Chem. Soc.* **2004**, *126*, 16841.

[11] Y. Kunugi, K. R. Mann, L. L. Miller, C. L. Exstrom, *J. Am. Chem. Soc.* **1998**, *120*, 589.

[12] C. P. Newman, G. W. V. Cave, M. Wong, W. Errington, N. W. Alcock, J. P. Rourke, *Dalton Trans.* **2001**, 2678.

[13] S. J. Lippard, *Acc. Chem. Res.* **1978**, *11*, 211.

[14] M. Howe-Grant, S. J. Lippard, *Biochemistry* **1979**, *18*, 5762.

[15] M. Albercht, G. Rodriguez, J. Schoemaker, G. van Koten, *Org. Lett.* **2000**, *2*, 3461.

[16] P. S. Pregosin, *Coord. Chem. Rev.* **1982**, *44*, 247.

[17] C. S. Peyratout, T. K. Aldridge, D. K. Crites, D. R. McMillin, *Inorg. Chem.* **1995**, *34*, 4484.

[18] B. Rosenberg, L. Vancamp, T. Krigas, *Nature* **1965**, *205*, 698.

[19] R. A. Alberden, M. D. Hall, T. W. Hambley, *J. Chem. Ed.* **2006**, *83*, 728.

[20] G. Lowe, A. S. Droz, T. Vilaivan, G. W. Weaver, J. J. Park, J. M. Pratt, L. Tweedale, L. R. Kelland, *J. Med. Chem.* **1999**, *42*, 3167.

[21] W. J. Finkenzeller, T. Hofbeck, M. E. Thompson, H. Yersin, *Inorg. Chem.* **2007**, *46*, 5076.

[22] F. A. Castro, G. B. Silva, F. Nüesch, L. Zuppiroli, C. F. O. Graeff, *Org. Electron.* **2007**, *8*, 249.
[23] Z. Guijiang, W.-Y. Wong, B. Yao, Z. Xie, L. Wang, *Ang. Chem. Int. Ed.* **2007**, *46*, 1149.
[24] www.universaldisplay.com and en.wikipedia.org/wiki/Organic_light-emitting diode. contain interesting overviews of the subject at the date of publication of this report.
[25] C. Adachi, M. A. Baldo, S. R. Forrest, S. Lamansky, M. E. Thompson, R. C. Kwong, *Appl. Phys. Lett.* **2001**, *78*, 1622.
[26] B. W. D'Andrade, J. Brooks, V. Adamovich, M. E. Thompson, S. R. Forrest, *Adv. Mater.* **2002**, *14*, 1032.
[27] F. G. Gao, A. J. Bard, *J. Am. Chem. Soc.* **2000**, *122*, 7426.
[28] J. V. Caspar, T. D. Westmoreland, G. H. Allen, P. G. Bradley, T. J. Meyer, W. H. Woodruff, *J. Am. Chem. Soc.* **1984**, *106*, 3492.
[29] J. N. Demas, B. A. DeGraff, *Coord. Chem. Rev.* **2001**, *211*, 317.
[30] C. J. Ballhausen, N. Bjerrum, R. Dingle, K. Eriks, C. R. Hare, *Inorg. Chem.* **1965**, *4*, 514.
[31] L. J. Andrews, *J. Phys. Chem.* **1979**, *83*, 3203.
[32] V. Balzani, V. Carassiti, *J. Phys. Chem.* **1968**, *72*, 383.
[33] V. M. Miskowski, V. H. Houlding, C.-M. Che, Y. Wang, *Inorg. Chem.* **1993**, *32*, 2518.
[34] V. M. Miskowski, V. H. Houlding, *Inorg. Chem.* **1989**, *28*, 1529.
[35] J. A. Zuleta, J. M. Bevilacqua, R. Eisenberg, *Coord. Chem. Rev.* **1991**, *111*, 237.
[36] G. Arena, G. Calogero, S. Campagna, L. M. Scolaro, V. Ricevuto, R. Romeo, *Inorg. Chem.* **1998**, *37*, 2763.
[37] M. G. Hill, J. A. Bailey, V. M. Miskowski, H. B. Gray, *Inorg. Chem.* **1996**, *35*, 4585.
[38] H.-K. Yip, L.-K. Cheng, K.-K. Cheung, C.-M. Che, *Dalton Trans* **1993**, 2933.
[39] J. A. Bailey, M. G. Hill, R. E. Marsh, V. Miskowski, W. P. Schaefer, H. B. Gray, *Inorg. Chem.* **1995**, *34*, 4591.
[40] T. C. Cheung, K. K. Cheung, S. M. Peng, C. M. Che, *Dalton Trans.* **1996**, 1645.
[41] E. C. Constable, R. P. G. Henney, T. A. Leese, D. A. Tocher, *Chem. Commun.* **1990**, 513.
[42] J. F. Michalec, S. A. Bejune, D. R. McMillan, *Inorg. Chem.* **2000**, *39*, 2708.

[43] J. S. Field, J-A. Gertenbach, R. J. Haines, L. P. Lebwaba, N. T. Mashapa, D. R. McMillin, O. Q. Munro, G. C. Summerton, *Dalton Trans.* **2003**, 1176.
[44] S. C. Chan, M. C. W. Chan, C.-M. Che, Y. Wang, K.-K. Cheung, N. Y. Zhu, *Chem. Eur. J.* **2001**, *7*, 4180.
[45] M. Hissler, W. B. Connick, D. K. Geiger, J. E. McGarrah, D. Lipa, R. J. Lachicotte, R. Eisenberg, *Inorg. Chem.* **2000**, *39*, 447.
[46] J. Brooks, Y. Babayan, S. Lamansky, P. I. Djurovich, I. Tsyba, R. Bau, M. E. Thompson, *Inorg. Chem.* **2002**, *41*, 3055.
[47] L. Chassot, E. Muller, A. von Zelewsky, *Inorg. Chem.* **1984**, *23*, 4249.
[48] P. Jolliet, M. Gianini, A. von Zelewsky, G. Bernardinelli, H. Stoeckli-Evans, *Inorg. Chem.* **1996**, *35*, 4883.
[49] P.-I. Kvam, J. Songstad, *Acta Chem. Scand.* **1995**, *49*, 313.
[50] M. M. Mdleleni, J. S. Bridgewater, R. J. Watts, P. C. Ford, *Inorg. Chem.* **1995**, *34*, 2334.
[51] C. W. Chan, T. F. Lai, C.-M. Che, S. M. Peng, *J. Am. Chem. Soc.* **1993**, *115*, 11245.
[52] F. Neve, M. Ghendini, A. Crispini, *Chem. Commun.* **1996**, 2463.
[53] S.-W. Lai, M. C.-W. Chan, T.-C. Cheung, S.-M. Peng, C.-M. Che, *Inorg. Chem.* **1999**, *38*, 4046.
[54] J. H. K. Yip, Suwarno, J. J. Vital, *Inorg. Chem.* **2000**, *39*, 3537.
[55] W. Lu, B.-X. Mi, M. C. W. Chan, Z. Hui, C.-M. Che, N. Zhu, S.-T. Lee, *J. Am. Chem. Soc.* **2004**, *126*, 4958.
[56] W. Lu, M. C. W. Chan, K.-K. Cheung, C.-M. Che, *Organometallics* **2001**, *20*, 2477.
[57] M. Maestri, C. Deuschel-Cornioley, A. von Zelewsky, *Coord. Chem. Rev.* **1991**, *111*, 117.
[58] C. Deuschel-Cornioley, T. Ward, A. von Zelewsky, *Helv. Chim. Acta* **1988**, *71*, 130.
[59] G. W. V. Cave, F. P. Fanizzi, R. J. Deeth, W. Errington, J. P. Rourke, *Organometallics* **2000**, *19*, 1355.
[60] G. W. V. Cave, N. W. Alcock, J. P. Rourke, *Organometallics* **1999**, *18*, 1801.
[61] E. Peris, J. A. Loch, J. Mata, R. H. Crabtree, *Chem. Commun.* **2001**, 201.
[62] M. Gupta, C. Hagen, R. J. Flesher, W. C. Kaska, C. M. Jensen, *Chem. Commun.* 1996, 2083.

[63] H. P. Dijkstra, M. Albrecht, G. van Koten, *Chem. Commun.* 2002, 126.
[64] T. Kanbara, K. Okada, T. Yamamoto, H. Ogawa, T. Inoue, *J. Organomet. Chem.* **2004**, *689*, 1860.
[65] M. Crespo, J. Sales, X. Solans, M. F. Altaba, *Dalton Trans.* **1988**. 1617 and references therein.
[66] D. J. Cárdenas, A. M. Echavarren, M. C. Ramírez de Arellano, *Organometallics* **1999**, *18*, 3337.
[67] M. Albrecht, G. van Koten, *Angew. Chem. Int. Ed.* **2001**, *40*, 3750.
[68] G. Guillena, C. A. Kruithof, M. A. Casado, M. R. Egmond, G. van Koten, *J. Organomet. Chem.* **2003**, *668*, 3.
[69] S. Köcher, G. P. M. van Klink, G. van Koten, H. Lang, *J. Organomet. Chem.* **2003**, *684*, 230.
[70] J. S. Fossey, C. J. Richards *Organometallics*, **2002**, *21*, 5259.
[71] H. Jude, J. A. Krause Bauer, W. B. Connick, *Inorg. Chem.* **2002**, *41*, 2275.
[72] H. Jude, J. A. Krause Bauer, W. B. Connick, *Inorg. Chem.* **2004**, *43*, 725.
[73] M. Q. Slagt, H. P. Dijkstra, A. McDonald, R. J. M. Klein Gebbink, M. Lutz, D. D. Ellis, A. M. Mills, A. L. Spek, G. van Koten, *Organometallics* **2003**, *22*, 27.
[74] J. A. G. Williams, A. Beeby, E. S. Davies, J. A. Weinstein, C. Wilson, *Inorg. Chem.* **2003**, *42*, 8609.
[75] S.-W. Lai, T.-C. Cheung, M. C. W. Chan, K.-K. Cheung, S.-M. Peng, C.-M. Che, *Inorg. Chem.* **2000**, *39*, 255.
[76] K. M.-C. Wong, W.-S. Tang, X.-X. Lu, N. Zhu, V. W.-W. Yam, *Inorg. Chem.* **2005**, *44*, 1492.
[77] J. E. McGarrah, R. Eisenberg, *Inorg. Chem.* **2003**, *42*, 4355.
[78] S. Chakraborty, T. J. Waddas, H. Hester, C. Flaschenreim, R. Schmehl, R. Eisenberg, *Inorg. Chem.* **2005**, *44*, 6284.
[79] C. W. Chan, L. K. Cheng, C.-M. Che, *Coord. Chem. Rev.* **1994**, *132*, 87.
[80] J. E. McGarrah, Y-J. Kim, M. Hissler, R. Eisenberg, *Inorg. Chem.* **2001**, *40*, 4510.
[81] W. Lu, B.-X. Mi, M. C. W. Chan, Z. Hui, N. Zhu, S.-T. Lee, C.-M. Che, *Chem. Commun.* **2002**, 206.
[82] V. W.-W. Yam, R. P.-L. Tang, K. Man-Chung, C.-C. Ko, K.-K. Cheung, *Inorg. Chem.* **2001**, *40*, 571.
[83] J. A. Zeluta, C. A. Chesta, R. Eisenberg, *J. Am. Chem. Soc.* **1989**, *111*, 8916.

[84] M. Albrecht, P. Dani, M. Lutz, A. L. Speck, G. van Koten, *J. Am. Chem. Soc.* **2000**, *122*, 11822.
[85] W. B. Connick, R. E. Marsh, W. P. Schaefer, H. B. Gray, *Inorg. Chem.* **1997**, *36*, 913.
[86] V. Miskowski, V. H. Houlding, *Inorg. Chem.* **1991**, *30*, 4446.
[87] H.-Q. Liu, T.-C. Cheung, C.-M. Che, *Chem. Commun.* **1996**, 1039.
[88] N. Rifai, G. Cohen, M. Wolf, L. Cohen, C. Fraser, J. Savory, L. DePalma, *Ther. Drug Monit.* **1993**, *15*, 71.
[89] M. Licini, J. A. G. Williams, *Chem. Commun.* **1999**, 1943.
[90] F. Barigelletti, L. Flamigni, M. Guardigli, J.-P. Sauvage, J.-P. Collin, A. Sour, *Chem. Commun.* **1996**, 1329.
[91] F. Barigelleti, L. Flamigni, G. Calogero, L. Hammarström, J.-P. Sauvage, J.-P. Collin, *Chem. Commun.* **1998**, 2333.
[92] W. Goodall, J. A. G. Williams, *Chem. Commun.* **2001**, 2514.
[93] S. C. Burdette, S. J. Lippard, *Coord. Chem. Rev.* **2001**, *216*, 333.
[94] W. Goodall, J. A. G. Williams, *Dalton Trans.* **2000**, 2893.
[95] A. P. de Silva, D. B. Fox, A. J. M. Huxley, T. S. Moody, *Coord. Chem. Rev.* **2000**, *205*, 41.
[96] A. P. de Silva, H. Q. N. Gunaratne, T. Gunnalaugsson, A. J. M. Huxley, C. P. McCoy, J. T. Rademacher, T. E. Rice, *Chem. Rev.* **1997**, *97*, 1515.
[97] C.-M. Che, M. Yang, K.-H. Wong, H.-L. Chan, W. Lam, *Chem. Eur. J.* **1999**, *5*, 3350.
[98] M. H. Keefe, K. D. Benkstein, J. T. Hupp, *Coord. Chem. Rev.* **2000**, *205*, 201.
[99] Q.-Z. Yang, Q.-X. Tong, L.-Z. Wu, Z.-X. Wu, L.-P. Zhang, C.-H. Tung, *Eur. J. Inorg. Chem.* **2004**, 1948.
[100] C. J. Pedersen, *J. Am. Chem. Soc.* **1967**, *89*, 7017.
[101] C. J. Pedersen, *Angew. Chem. Int. Ed.* **1988**, *27*, 1021.
[102] J. M. Lehn, *Angew. Chem. Int. Ed.* **1988**, *27*, 89.
[103] D. J. Cram, *Angew. Chem. Int. Ed.* **1988**, *27*, 1009.
[104] C. E. Anson, C. S. Creaser, G. R. Stephenson, *Chem. Commun.* **1994**, 2175.
[105] V. W.-W. Yam, K. K. W. Lo, *Coord. Chem. Rev.* **1999**, *184*, 157.
[106] V. W.-W. Yam, K. K. W. Lo, K. K. Cheung, *Inorg. Chem.* **1995**, *34*, 4013.
[107] V. W.-W. Yam, V. W. M. Lee, F. Ke, K.-W. M. Siu, *Inorg. Chem.* **1997**, *36*, 2124.
[108] V. W.-W. Yam, C. K. Li, C. L. Chan, *Angew. Chem. Int. Ed.* **1998**, *37*, 2857.

[109] V. W.-W. Yam, Y.-L. Pui, W.-P. Li, K. K.-W. Lo, K.-K. Cheung, *Dalton Trans.* **1998**, 3615.
[110] Y. Shen, B. P. Sullivan, *J. Chem. Educ.* **1997**, *74*, 685.
[111] A. P. de Silva, S. A. de Silva, *Chem. Commun.* **1986**, 1709.
[112] W.-S. Tang, X.-X. lu, K. M.-C. Wong, V. W.-W. Yam, *J. Mater. Chem.* **2005**, *15*, 2714.
[113] V. W.-W. Yam, R. P. L. Tang, K. M. C. Wong, K.-K. Cheung, *Organometallics* **2001**, *20*, 4476.
[114] V. W.-W. Yam, R. P. L. Tang, K. M. C. Wong, X. X. Lu, K.-K. Cheung, N. Zhu, *Chem. Eur. J.* **2002**, *8*, 4066.
[115] A. Gül, O. Berkâroğlu, *Dalton Trans.* **1983**, 2537.
[116] C.-T. Chen, W.-P. Huang, *J. Am. Chem. Soc.* **2002**, *124*, 6246.
[117] M. Smiddy, M. Firzgerald, J. P. Kerry, D. B. Papkovsky, C. K. O'Sullivan, G. G. Guilbault, *Meat Science* **2002**, *61*, 285.
[118] M. Gouterman, *J. Chem. Ed.* **1997**, *74*, 697.
[119] R. N. Gillanders, M. C. Tedford, P. J. Crilly, R. T. Bailey, *Anal. Chim. Acta* **2004**, *502*, 1.
[120] A. Beeby, R. S. Dickens, S. FitzGerald, L. J. Govenlock, C. L. Maupin, D. Parker, J. P. Riehl, G. Siligardi, J. A. G. Williams, *Chem. Commun.* **2000**, 1183.
[121] B. Witulski, Y. Zimmermann, V. Darcos, J.-P. Desvergne, D. M. Bassani, H. Bouas-Laurent, *Tet. Lett.* **1998**, *39*, 4807.
[122] K. H. Wong, M. C.-W. Chan, C.-M. Che, *Chem. Eur. J.* **1999**, *5*, 2845.
[123] M. Cusumano, M. L. Di Pietro, A. Giannetto, *Inorg. Chem.* **2006**, *45*, 230.
[124] R. C. Kwong, S. Lamansky, M. E. Thompson, *Adv. Mater.* **2000**, *12*, 1134.
[125] M. A. Baldo, M. E. Thompson, S. R. Forrest, *Nature* **2000**, *403*, 750.
[126] J. K. Borchardt, *Mater. Today* **2004**, *7*, 42.
[127] R. C. Kwong, M. R. Nugent, L. Michalski, T. Ngo, K. Rajan, Y.-J. Tung, M. S. Weaver, T. X. Zhou, M. Hack, M. E. Thompson, S. R. Forrest, I. J. Brown, *Appl. Phys. Lett.* **2002**, *81*, 162.
[128] M. Ikai, S. Tokito, Y. Sakamoto, T. Suzuki, Y. Taga, *Appl. Phys. Lett.* **2001**, *79*, 156.
[129] C. Adachi, M. A. Baldo, M. E. Thompson, S. R. Forrest, *J. Appl. Phys.* **2001**, *90*, 5048.

[130] F. Li, M. Zhang, G. Cheng, J. Feng, Y. Zhao, Y. G. Ma, S. Y. Lui, J. C. Shen, *Appl. Phys. Lett.* **2004**, *84*, 148.
[131] M. A. Baldo, D. F. O'Brien, Y. You, A. Shoustikov, S. Sibley, M. E. Thompson, S. R. Forrest, *Nature* **1998**, *395*, 151.
[132] V. Grove, G. Yahioglu, P. Le Barny, R. H. Friend, N. Tessler, *Adv. Mater.* **1999**, *11*, 285.
[133] M. A. Baldo, S. Lamansky, P. E. Burrows, M. E. Thompson, S. R. Forrest, *Appl. Phys. Lett.* **1999**, *75*, 4.
[134] C. Adachi, M. A. Baldo, S. R. Forrest, M. E. Thompson, *Appl. Phys. Lett.* **2000**, *77*, 904.
[135] K. Mullen "Organic light emitting devices" Chapter 11, Wiley-VCH Press (2006).
[136] R. C. Evans, P. Douglas, C. J. Winsom, *Coord. Chem. Rev.* **2006**, *250*, 2093.
[137] R. C. Kwong, S. Sibley, T. Dubovoy, M. Baldo, S. R. Forrest, M. E. Thompson, *Chem. Mater.* **1999**, *11*, 3709.
[138] D. F. O'Brien, M. A. Baldo, M. E. Thompson, S. R. Forrest, *Appl. Phys. Lett.* **1999**, *74*, 442.
[139] V. V. Grushin, N. Herron, D. D. LeCloux, W. J. Marshall, V. A. Petrov, Y. Wang, *Chem. Commun.* **2001**, 1494.
[140] H. Z. Xie, M. W. Liu, O. Y. Wang, X. H. Zhang, C. S. Lee, L. S. Hung, S. T. Lee, P. F. Teng, H. L. Kwong, Z. Hui, C.-M. Che, *Adv. Mater.* **2001**, *13*, 1245.
[141] M. Ghendini, I. Aiello, A. Crispini, A. Golemme, M. La Deda, D. Pucci, *Coord. Chem. Rev.* **2006**, *250*, 1373.
[142] E. G. Rodriguez, L. S. Silva, D. M. Fausto, M. S. Hayashi, S. Dreher, E. L. Santos, J. B. Pesquero, L. R. Travessos, A. C. F. Caires, *Int. J. Cancer* **2003**, *107*, 498.
[143] W. A. Herrmann, M. Elison, J. Fischer, C. Koecher, G. R. J. Artus, *Angew. Chem. Int. Ed.* **1995**, *34*, 2371.
[144] A. C. Hillier, G. A. Grasa, M. S. Viciu, H. M. Lee, C. Yang, S. P. Nolan, *J. Organomet. Chem.* **2002**, *653*, 69.
[145] D. S. McGuinness, K. J. Cavell, *Organometallics* **2000**, *19*, 741.
[146] J. A. Loch, M. Albrecht, E. Peris, J. Mata, J. W. Faller, R. H. Crabtree, *Organometallics* **2002**, *21*, 700.
[147] C. S. Consorti, G. Ebeling, F. Rodembusch, V. Stefani, P. R. Livotto, F. Rominger, F. H. Quina, C. Yihwa, J. Dupont, *Inorg. Chem.* **2004**, *43*, 530.

[148] J. Dupont, C. S. Consorti, J. Spencer, *Chem. Rev.* **2005**, *105*, 2527.
[149] Y. Wakatsuki, H. Yamazaki, P. A. Grutsch, M. Santhanam, C. Kutal, *J. Am. Chem. Soc.* **1985**, *107*, 8153.
[150] B. C. Tzeng, S. C. Chan, M. C. W. Chan, C. M. Che, K. K. Cheung, S. M. Peng, *Inorg. Chem.* **2001**, *40*, 6699.
[151] F. Neve, A. Crispini, C. Di Pietro, S. Campagna, *Organometallics* **2002**, *21*, 3511.
[152] D. Pucci, G. Barberio, A. Crispini, O. Francescangeli, M. Ghedini, M. La Deda, *Eur. J. Inorg. Chem.* **2003**, 3649.
[153] Y. Nojima, M. Nonoyama, K. Nakajima, *Polyhedron*, **1996**, *15*, 3795.
[154] M. Akaiwa, T. Kanbara, H. Fukumoto, T. Yamamoto, *J. Organomet. Chem.* **2005**, *690*, 4192.
[155] F. Neve, A. Crispini, S. Campagna, *Inorg. Chem.* **1997**, *36*, 6150.
[156] P. Steenwinkel, R. A. Gossage, G. van Koten, Chem. Eur. J. 1998, 4, 759.
[157] M. Gagliardo, G. Rodriguez, H. H. Dam, M. Lutz, A. L. Spek, R. W. A. Havenith, P. Coppo, L. De Cola, F. Hartl, G. P. M. van Klink, G. van Koten, *Inorg. Chem.* **2006**, *45*, 2143.
[158] B. Neumann, T. Hegmann, R. Wolf, C. Tscheirske, *Chem. Commun.* **1998**, 105.
[159] Q. Wu, A. Hook, S. Wang, *Angew. Chem. Int. Ed.* **2000**, *39*, 3933.
[160] G. R. Crosby, *Acc. Chem. Res.* **1975**, *8*, 231.
[161] N. Armaroli, L. De Cola, V. Balzani, J.-P. Sauvage, C. O. Dietrich-Buchecker, J.-M. Kern, A. Bailal, *Dalton Trans.* **1993**, 3241.
[162] L. Mao, T. Moriuchi, H. Sakurai, H. Fujii, T. Hirao, *Tet. Lett.* **2005**, *46*, 8419.
[163] M. La Deda, M. Ghedini, I. Aiello, T. Pugliese, F. Barigelletti, G. Accorsi, *J. Organomet. Chem.* **2005**, *690*, 857.
[164] M. Maestri, D. Sandrini, V. Balzani, A. von Zelewsky, C. Deuschel-Cornioley, J. Polliet, *Helv. Chim. Acta* **1988**, *71*, 1053.
[165] K. Endo, S. Igarashi, T. Yotsuyanagi, *Chem. Lett.* **1986**, 1711.
[166] D. Song, Q. Wu, A. Hook, I. Kozin, S. Wang, *Organometallics*, **2001**, *20*, 4683.
[167] H. Yersin, D. Donges, J. K. Nagle, R. Sitters, M. Glasbeek, *Inorg. Chem.* **2000**, *39*, 770.
[168] Md. A. Hossain, S. Lucarini, D. Powell, K. Bowman-James, *Inorg. Chem.* **2004**, *43*, 7275.
[169] J. Kjellgren, H. Sunden, K. J. Szabo, *J. Am. Chem. Soc.* **2004**, *126*, 474.

[170] J. Kjellgren, H. Sunden, K. J. Szabo, *J. Am. Chem. Soc.* **2005**, *127*, 1787.
[171] A. Suzuki, *Chem. Commun.* **2005**, 4759.
[172] R. F. Heck, J. P. Nolley Jr., *J. Org. Chem.* **1972**, *37*, 2320.
[173] J. Zhao, X. Yang, X. Jia, S. Luo, H. Zhai, *Tetrahedron*, **2003**, *59*, 9379
[174] W. Cabri, I. Candiani, *Acc. Chem. Res.* **1995**, *28*, 2.
[175] V. V. Grushin, H. Alper, *Chem. Rev.* **1994**, *94*, 1047.
[176] G. C. Fu, A. F. Littke, *Angew Chem. Int. Ed.* **2002**, *41*, 4176.
[177] D. J. Cardenas, *Angew. Chem. Int. Ed.* **2003**, *42*, 384.
[178] V. Farina, *Adv. Synth. Catal.* **2004**, *346*, 1553.
[179] W. A. Herrmann, C. Brossmer, K. Oefele, C.-P. Reisinger, T. Priermeier, M. Beller, H. Fischer, *Angew. Chem. Int. Ed.* **1995**, *34*, 1844.
[180] J. Dupont, M. Pfeffer, J. Spencer, *Eur. J. Inorg. Chem.* **2001**, 1917.
[181] M. S. Yoon, D. Ryu, J. Kim, K. H. Ahn, *Organometallics* 2006, *25*, 2409.
[182] M. Poyatos, F. Marquez, E. Peris, C. Claver, E. Fernandez, *New. J. Chem.* **2003**, *27*, 425.
[183] C. Amatore, A. Jutand, *Acc. Chem. Res.* **2000**, *33*, 314.
[184] A. H. M. de Vries, J. M. C. A. Mulders, J. H. M. Mommers, H. J. W. Henderickx, J. G. de Vries, *Org. Lett.* **2003**, *5*, 3285.
[185] I. P. Beletskaya, *J. Organomet. Chem.* **1983**, *250*, 551.
[186] I. P. Beletskaya, *Pure Appl. Chem.* **1997**, *69*, 471.
[187] T. Jeffery, *Tetrahedron* **1996**, *52*, 10113.
[188] M. Ohff, A. Ohff, M. E. van der Boom, D. Milstein, *J. Am. Chem. Soc.* **1997**, *119*, 11687.
[189] M. Nowotny, U. Hanefeld, H. van Koningsveld, T. Mschmeyer, *Chem. Commun.* **2000**, 1877.
[190] J. Louie, J. F. Hartwig, *Angew. Chem. Int. Ed.* **1996**, *35*, 2359.
[191] T. Nishimura, T. Onoue, K. Che, S. Uermira, *J. Org. Chem.* **1999**, *64*, 6750.
[192] B. A. Steinhoff, S. S. Stahl, *Org. Lett.* **2002** *4*, 4179.
[193] Y. Tsuji, T. Fujihara, *Inorg. Chem.* **2007**, *46*, 1895.
[194] D. R. Anton, R. H. Crabtree, *Organometallics* **1983**, *2*, 855.
[195] B. L. Shaw, *New J. Chem.* **1998**, *22*, 77.
[196] M.-H. Huang, L.-C. Liang, *Organometallics* **2004**, *23*, 2813.
[197] B. Soro, S. Stoccoro, G. Minghetti, A. Zucca, M. A. Cinellu, M. Manassero, S. Gladiali, *Inorg. Chim. Acta* **2006**, *359*, 1879.

[198] T. Hayashi, K. Hayashizaki, T. Kiyoi, Y. Ito, *J. Am. Chem. Soc.* **1988**, *110*, 8153.
[199] T. Hayashi, K. Hayashizaki, Y. Ito, *Tet. Lett.* **1989**, *30*, 215.
[200] B. L. Shaw, S. D. Perera, E. A. Staley, *Chem. Commun.* **1998**, 1361.
[201] S. Ramdeehul, L. Barloy, J. A. Osborn, A. De Cian, J. Fischer, *Organometallics* **1996**, *15*, 5442.
[202] L. Barloy, R. M. Gauvin, J. A. Osborn, C. Sizun, R. Graff, N. Kyritsakas, *Eur. J. Inorg. Chem.* **2001**, 1699.
[203] P. W. N. M. van Leeuwen, *Applied Catalysis* **2001**, *212*, 61.
[204] D. J. Cardenas, J.-P. Sauvage, *Synlett* **1996**, 916.
[205] M. Benaglia, S. Toyota, C. R. Woods, J. S. Siegel, *Tet. Lett.* **1997**, *38*, 4737.
[206] J. K. Stille, *Angew. Chem. Int. Ed.* **1986**, *25*, 508.
[207] H. Bönnemann, *Angew. Chem. Int. Ed.* **1978**, *17*, 505.
[208] The use of tri-n-butylstannylpyridine over other alkyl sources presents reduced toxicity of the reagents, for examples see http://en.wikipedia.org/wiki/-Stille_reaction and http://en.wikipedia.org/wiki/acetylene for some basic safety features representing these chemicals and processes.
[209] M. Chavarot, Z. Pikremenou, *Tet. Lett.* **1999**, *40*, 6865.
[210] A. Jouaiti, M. Geoffrey, J.-P. Collin, *Inorg. Chim. Acta* **1996**, *245*, 69.
[211] M. Beley, S. Chodorowski, J.-P. Collin, J.-P Sauvage, *Tet. Lett.* **1993**, *34*, 2933.
[212] A.-S. Castanet, F. Colobert, P.-E. Broutin, M. Obringer, *Tetrahedron: Asym.* **2002**, *13*, 659.
[213] T. Watanabe, N. Miyaura, A. Suzuki, *Synlett*, **1992**, 207.
[214] J. M. McKenna, J. Moliterni, Y. Qiao, *Tet. Lett.* **2001**, *42*, 5797.
[215] T. Ishiyama, M. Murata, N. Miyaura, *J. Org. Chem.* **1995**, *60*, 7508.
[216] The intermediate [4'-phenyl-(3-methoxychrom-4-one)]bromobenzene was kindly provided by Dr. J.-L. Fillaut.
[217] S. Wagaw, R. A. Rennels, S. L. Buchwald, *J. Am. Chem. Soc.* **1997**, *119*, 8451.
[218] J. F. Hartwig, *Synlett* **1997**, 329.
[219] H. Adkins, R. M. Simington, *J. Am. Chem. Soc.* **1925**, *47*, 1688.
[220] G. L. Baker, Y. Chen, *J. Org. Chem.* **1999**, *64*, 6870.
[221] Parker, D.; Harwood, L. M.; Moody, C. J. 'Macrocycle Synthesis A Practical Approach'; Oxford University Press (1996)
[222] S. J. Farley, D. L. Rochester, A. L. Thompson, J. A. K. Howard, J. A. G. Williams, *Inorg. Chem.* **2005**, *44*, 9690.

[223] E. C. Constable, J. Lewis, M. C. Liptrot, P. R. Raithby, *Inorg. Chim. Acta* **1990**, *178*, 47.
[224] E. C. Constable, F. A. Khan, P. R. Raithby, V. E. Marquez, *Acta Crystallogr., Sect. C* **1992**, *C48*, 932.
[225] W. Leslie, A. S. Batsanov, J. A. K. Howard, J. A. G. Williams, *Dalton Trans.* **2004**, 623.
[226] P. Nilsson, F. Plamper, O. F. Wendt, *Organometallics* **2003**, *22*, 5235.
[227] S. I. Pombrik, V. M. Pachevskaya, L. S. Golovchenko, A. S. Peregudov, D. N. Kravtsov, A. S. Batsanov, Y. T. Struchkov, *Metalloorganicheskaya Khimiya*, **1988**, *1*, 379.
[228] E. Forsellini, G. Bombieri, B. Crociani, T. Boschi, *Chem. Commun.* **1970**, 1203.
[229] R. Buchner, J. S. Field, R. J. Haines, C. T. Cunningham, D. R. McMillin, *Inorg. Chem.* **1997**, *36*, 3952.
[230] J. S. Field, R. J. Haines, D. R. McMillin, G. C. Summerton, *Dalton Trans.* **2002**, 1369.
[231] R. Bardi, A. Del Pra, A. M. Piazzesi, M. Trozzi, *Cryst. Struct. Commun.* **1981**, *10*, 301.
[232] N. W. Alcock, P. R. Barker, J. M. Haider, C. L. Painting, Z. Pikramenou, E. A. Plummer, K. Rissanen, P. Saarenketo, *Dalton Trans.* **2000**, 1447.
[233] F.-M. Hwang, H.-Y. Chen, P.-S. Chen, C.-S. Liu, Y. Chi, C. F. Shu, F.-L. Wu, P.-T. Chou, S.-M. Peng, G.-H. Lee, *Inorg. Chem.* **2005**, *44*, 1344.
[234] A. J. Wilkinson, H. Puschmann, J. A. K. Howard, C. E. Foster, J. A. G. Williams, *Inorg. Chem.* **2005**, *45*, 8685.
[235] A. Horvath, K. L. Stevenson, *Coord. Chem. Rev.* **1996**, *153*, 57.
[236] C. M. Pettijohn, E. B. Jochnowitz, B. Choung, J. K. Nagle, A. Vogler, *Coord. Chem. Rev.* **1998**, *171*, 85 *and references therein.*
[237] M. Maestri, D. Sandrini, A. von Zelewsky, C. Deuschel-Cornioley, *Inorg. Chem.* **1991**, *30*, 2476.
[238] K. E. Dungey, B. D. Thompson, N. A. P. Kane-Maguire, L. L. Wright, *Inorg Chem.* **2000**, *39*, 5192.
[239] B. J. Basu, A. Thirumurugan, A. R. Dinesh, C. Anandan, K. S. Rajam. *Sens. Actuators B: Chem* **2005**, *104*, 15.
[240] B. J. Basu, K. S. Rajam, *Sens. Actuators* **2004**, *B99*, 459.

[241] J. F. Michalec, S. A. Bejune, D. G. Cuttell, G. C. Summerton, J. A. Gertenbach, J. S. Field, R. J. Haines, D. R. McMillan, *Inorg. Chem.* **2001**, *40*, 2193.
[242] D. K. Crites, D. R. McMillan, *Coord. Chem. Rev.* **2001**, *211*, 195.
[243] J. P. Phillips, *Chem. Rev.* **1956**, *56*, 271.
[244] A. G. Maslakov, E. Gresham, T. A. Hamor, W. R. McWhinnie, M. C. Perry, N. Shaikh, *J. Organomet. Chem.* **1994**, 480, 261.
[245] M. K. Nayak, A. K. Chakraborti, *Chem. Lett.* **1998**, 297.
[246] A. K. Chakraborti, L. Sharma, M. K. Nayak, *J. Org. Chem.* **2002**, *67*, 2541.
[247] S. Takahashi, M. Kita, M. Nonoyama, *Trans. Met. Chem.* **1995**, *20*, 528.
[248] F. Trécourt, M. Mallet, F. Mongin, G. Quéguiner, *Synthesis* **1995**, 1159.
[249] J. F. W. McOmie, M. L. Watts, D. E. West, *Tetrahedron* **1968**, *24*, 2289.
[250] S. Punna, S. Meunier, M. G. Finn, *Org. Lett.* **2004**, *6*, 2777.
[251] I. Ryu, H. Matsubara, S. Yasuda, H. Nakamura, D. P. Curran, *J. Am. Chem. Soc.* **2002**, *124*, 12946.
[252] B. Soro, S. Stoccoro, G. Minghetti, A. Zucca, M. A. Cinellu, S. Gladiali, M. Manasseo, M. Sansoni, *Organometallics* **2005**, *24*, 53.
[253] D. St. C. Black, G. B. Deacon, G. L. Edwards, B. M. Gatehouse, *Aust. J. Chem.* **1993**, *46*, 1323.
[254] K. Takenaka, M. Minakawa, Y. Uozumi, *J. Am. Chem. Soc.* **2005**, *127*, 12273.
[255] A. Berger, A. de Cian, J.-P. Djukic, J. Fischer, M. Pfeffer, *Organometallics* **2001**, *20*, 3230.
[256] P. Peringer, P.-P. Winkler, *J. Organomet. Chem.* **1980**, *195*, 249.
[257] M. Ali, W. R. McWhinnie, *J. Organomet. Chem.* **1989**, *371*, C37.
[258] E. C. Constable, T. A. Leese, D. A. Tocher, *Chem. Commun.* **1989**, 570.
[259] R. Ugo, F. Cariati, G. La Monica, *Inorg. Synth.* **1968**, *11*, 105.
[260] P. J. Stang, A. K. Datta, *Organometallics*, **1989**, *8*, 1024.
[261] K. J. Arm, J. A. G. Williams, *Chem. Commun.* **2005**, 230.
[262] L. A. van de Kuil, H. Luitjes, D. M. Grove, J. W. Zwikker, J. G. M. van der Linden, A. M. Roelofsen, L. W. Jenneskens, W. Drenth, G. van Koeten, *Organometallics*, **1994**, *13*, 468.
[263] J. Biedermann, G. Gliemann, U. Klement, K.-J. Range, M. Zabel, *Inorg. Chem.* **1990**, *29*, 1884.
[264] W. B. Connick, L. M. Henling, R. E. Marsh, H. B. Gray, *Inorg. Chem.* **1996**, *35*, 6261.

[265] R. Buchner, C. T. Cunningham, J. S. Field, R. J. Haines, D. R. McMillin, G. C. Summerton, *Dalton Trans.* **1999**, 711.
[266] V. M. Miskowski, V. H. Holding, *Coord. Chem. Rev.* **1991**, *111*, 145.
[267] J. A. Bailey, M. V. Miskowski, H. B. Gray, *Inorg. Chem.* **1993**, *32*, 369.
[268] C. A. Hunter, N. Meah, J. K. M. Sanders, *J. Am. Chem. Soc.* **1990**, *112*, 5773.
[269] C. A. Hunter, J. K. M. Sanders, *J. Am. Chem. Soc.* **1990**, *112*, 5525.
[270] Statistically a reduced deviation is expected from reducing the number of atoms involved in the calculation. However, the reduction observed here is greatly beyond the effects expected through simple statistical treatment.
[271] R. H. Herber, M. Croft, M. T. Coyer, B. Bilash, A. Sahiner, *Inorg. Chem.* **1994**, *33*, 2422.
[272] P. M. Kiernan, A. Ludi, *Dalton Trans.* **1978**, 1127.
[273] C. E. Buss, K. R. Mann, *J. Am. Chem. Soc.* **2002**, *124*, 1031.
[274] H.-K. Yip, C.-M. Che, Z.-Y. Zhou, T. C. W. Mak, *Chem. Commun.* **1992**, 1369.
[275] S.-W.Lai, M. C. W. Chan, K.-K Cheung, C.-M. Che, *Inorg. Chem.* **1999**, *38*, 4262.
[276] M. Cocchi, D. Virgili, V. Fattori, D. L. Rochester, J. A. G. Williams, *Adv. Funct. Mater.* **2006**, *17*,
[277] A. S. Ionkin, W. J. Marshall, Y. Wang, *Organometallics*, **2005**, *24*, 619.
[278] J. Kalinowski, W. Stampor, J. Mezyk, M. Cocchi, D. Virgili, V. Fattori, P. DiMarco, *Phys. Rev. B* **2002**, *66*, 235321.
[279] M. A. Baldo, C. Adachi, S. R. Forrest, *Phys. Rev. B* **2000**, *62*, 10967
[280] D. P. Papkovsky, G. E. Ponomarev, W. Trettnak, P. O'Leary, *Anal. Chem.* **1995**, *67*, 4112.
[281] A. Beeby, S. Faulkner, *Chem. Phys. Lett.* **1997**, *266*, 116.
[282] P. K. Byers, A. J. Canty, *Organometallics* **1990**, *9*, 210.
[283] P. Colamarino, P. L. Orioli, *Dalton Trans.* 1975, 16, 1656.
[284] Interestingly the angle observed between the two planes inversely correlates with the platinum-ancillary-pyridine bond length.
[285] A. Díez, J. Forniés, A. García, E. Lalinde, T. Moreno, *Inorg. Chem.* **2005**, *44*, 2443.
[286] M. Janka, G. K. Anderson, N. P. Rath, *Organometallics* **2004**, *23*, 4382.
[287] R. D'Amato, I. Fratoddi, A. Cappotto, P. Altamura, M. Delfini, C. Bianchetti, A. Bolasco, G. Polzonetti, M. V. Russo, *Organometallics* **2004**, *23*, 2860.

[288] K. Sonogashira, Y. Fujikura, T. Yatake, N. Toyoshima, S. Takahashi, N. Hagihara, *J. Organomet. Chem.* **1978**, *145*, 101.

[289] Silver acetylides are dangerous and are heat and shock sensitive high explosives. Great care is needed when preparing and utilising such materials, information can be found at http://en.wikipedia.org/wiki/Silver_acetylide and http://www.poerlabs.org/chemlabs/acetylide.htm

[290] O. M. Abu-Saiah, A. R. A. Al-Ohlay, *Dalton Trans.* **1988**, 2297.

[291] A. J. Wilkinsons, A. E. Goeta, C. E. Foster, J. A. G. Williams, *Inorg. Chem.* **2004**, *43*, 6513.

[292] N. A. Bumagin, P. Androkovan, I. P. Beletskaya, *Metalloorg. Chim.* **1989**, *2*, 911.

[293] L. A. van de Kuil, D. M. Grove, R. A. Gossage, J. W. Zwikker, L. W. Jenneskens, W. Drenth, G. van Koten, *Organometallics* **1997**, *16*, 4985.

[294] Wakatsuki, Y; Yoshimura, H.; Yamazaki, H. *J. Organomet. Chem.* **1989** *366*, 215.

[295] I. Goldberg, *Ber.* **1906**, *39*, 1691.

[296] F. Trecourt, M. Mallet, F. Mongin, G. Queguiner, *Synthesis* **1995**, *9*, 1159

[297] C. Schotten, *Ber.* **1884**, *17*, 2544.

[298] E. Baumann, *ibid.* **1886**, *19*, 3218.

[299] N. O. V. Sonntag, *Chem. Rev.* **1953**, *52*, 272.

[300] G. I. Georg, *Bioorg. Med. Chem. Lett.* **1994**, *4*, 335.

[301] Pouchet, C. J.; "The Aldrich Library of Infrared Spectra; Third Edition" © 1981 by Aldrich Chemical Company Inc.